

River bank erosion rates and the case for willow spiling as a bank stabilisation solution

Lenka Anstead MSc

Submitted for the degree of Doctor of Philosophy

**School of Environmental Sciences
University of East Anglia, UK**

April 2012

© This copy of the thesis has been supplied on condition that anyone who consults it is understood to recognise that its copyright rests with the author and that use of any information derived there-from must be in accordance with current UK Copyright Law. In addition, any quotation or extract must include full attribution.

*We shall not cease from exploration
And the end of all our exploring
Will be to arrive where we started
And know the place for the first time.*

T. S. Elliot (1974)

To Roxana

ABSTRACT

River bank retreat is an essential part of a river's natural function, but if progressing fast the cause may be human activity. A study was undertaken to explore the rates and causes of river bank erosion on the River Stour in East Anglia, UK. Flows in this river are enhanced by the Ely Ouse to Essex Water Transfer Scheme and the river channel was modified in order to carry these additional flows. A four-year field study that commenced in 2006 employed a unique combination of four geomorphologic methods at nine field sites which revealed a river bank retreat of up to 1.32 m per year. This was considerably higher than the maximum annual retreat of 0.23 m obtained from an analysis of historical maps dating back to 1886, but the rates were similar to those reported in other field studies from similar streams in the UK. The complexity of river processes presented a major challenge in researching the causes of river bank erosion and retreat. While bank material showed some causality, properties such as bank angles, channel planform, water surface slopes and river discharges were found to have a weak correlation with the field erosion rates. However, some morphological evidence was found which demonstrated the effect that additional flows of constant discharge have had on the river channel.

A solution to human-induced river bank instability could be vegetation-based engineering approaches, but limited research on these represents a major barrier to their wider application. Willow spiling, one of the most common of these methods used in the UK, was chosen and reviewed to obtain fundamental knowledge on its successful application. The principle conditions needed to apply the technique were listed, together with a review of project successes and failures. It was found that at least 47 km of UK river banks have been protected by willow spiling over the last 20 years. Out of 139 projects, only in 37 cases was the result recorded. One third of these had failed, most commonly due to scouring of the bank foot, floods, poor quality willow material or shading from other vegetation.

To apply what was found in the review and to examine the method further, two willow spiling revetments were established at eroding field sites on the River Stour in March 2009. The post-project monitoring during the first 12 months reported on biological survival rates and geomorphological changes to the river bank and the bed adjacent to the spiling. Both projects reduced river bank retreat during the post-project monitoring period, but the future of one revetment is questionable because part of the willow structure did not survive and started to disintegrate. To draw on these findings, further recommendations are summarised for situations experienced at the project sites when spiling is exposed to stress conditions such as extreme droughts, floods or grazing.

ACKNOWLEDGEMENTS

First and most of all, I would like to thank my primary supervisor Dr N. Keith Tovey who guided me on the whole research journey. Also Dr Rosalind R. Boar who was always keen to help, and gave crucial feedback and personal support, and Dr Victor Bense for willingly joining my supervisory panel at the later stage and for giving important hydrological advice. My thanks also go to Professor Richard Hey, who helped during the initial stages of my PhD.

Secondly, I am deeply grateful to the landowners Colin Clifton-Brown, Charles Ryder, Hugh Craig and Hector Bunting, and ranger Adrian Walters. Without their help and stamina, this research would not have been possible. Equally, I am grateful to my friend, Roger Kistruck, for his funny but thoughtful advice in the field and for critically reading my work. I am also grateful to my brother, Juraj Milon, for constructing the photo electronic erosion pins and my friend, George Millins, for donating over one hundred steel offcuts from his factory for measurement pins.

A number of other people working on the river were very sympathetic and helpful, especially at the starting stages, to name just a few: Peter Ennis from the Stour Valley and Dedham Vale Project, and James Carr, Tim Barritt, Irena Novakova and Andrew Baker from the Environment Agency. Thank you, Irena, for taking up the challenge of wading through the infinite Agency's archives for me! Also my gratitude goes to The River Restoration Centre, UK county councils, national park authorities and the many individuals in the UK and overseas who were extremely helpful in collating information for the willow spiling review.

I would also like to thank, of course, UEA staff, mainly Jenny Stevenson and Rick Bryant for their help with field equipment and in the lab. Special acknowledgments also to The University of East Anglia, The River Restoration Centre, British Ecological Society, The British Society for Geomorphology and King's College London for the financial support towards my presentations at various events. I am also very grateful to my colleagues at Green Light Trust, who allowed me to work flexibly during the last few months of my research.

Finally, sincere thanks go to my husband Alan and daughter Roxy for putting up with me and for giving me a hand whenever it was needed. You may be pleased to know: no more weekends to be spent by the muddy riverside, carrying heavy boxes; well at least for a next few months!

CONTENTS

Abstract	iii
Acknowledgements	iv
Contents	v
List of figures	ix
List of tables	xv
List of research acronyms	xvii
List of notations	xviii
1. INTRODUCTION	1
1.1. Research context	1
1.2. Thesis aims, objectives and justification	3
1.3. Thesis structure	6
2. RIVER BANK EROSION CONCEPTS	9
2.1. Geomorphologic status of rivers	9
2.2. River bank erosion processes	14
2.2.1. Subaerial erosion processes	15
2.2.2. Fluvial erosion processes	17
2.2.2(A) A comparison of fluvial processes on cohesive and non-cohesive banks	18
2.2.3. Mass failure	18
2.2.3(A) Critical bank height	21
2.3. Concept of the Factor of Safety	24
2.3.1. Shear strength	25
2.3.2. Shear stress	26
2.4. Effects of vegetation on river bank stability	28
2.5. River bank erosion management	33
2.5.1. River bank erosion management approaches	33
2.5.1(A) Allowing for natural channel adjustment	34
2.5.1(B) Ground bioengineering	34
2.5.1(C) Biotechnical solutions	36
2.5.1(D) Structural engineering	36
3. RIVER BANK EROSION RATES	39
3.1. Study area	39
3.1.1. Geographic, climatic and hydrologic characteristics of the catchment studied	39
3.1.2. Long profile and river sinuosity	40
3.1.3. Land use	43
3.1.4. History of river management on the River Stour	43
3.1.5. Ely Ouse to Essex Water Transfer Scheme	45
3.1.5(A) The impact of transferred flows on the river's natural flows	49
3.1.5(B) Possible influence of the scheme on the geomorphology of the River Stour	56
3.2. Properties of field sites	58
3.2.1. Site selection criteria	58
3.2.2. Geometric properties	63
3.2.3. Soil associations	66
3.2.4. Soil textures	68
3.2.4(A) Sampling strategy and particle size distribution procedure	70
3.2.4(B) Results of particle size distribution	71
3.2.5. Shear strength of soils and variability with moisture content	79
3.2.5(A) Shear strength testing	80
3.2.5(B) Soil moisture and specific gravity	81
3.2.5(C) Saturated and unsaturated shear strength parameters at some chosen profiles	82

3.3. Historical erosion rates	87
3.3.1. <i>Methodology of historical analysis</i>	87
3.3.1(A) Ordnance survey maps	87
3.3.1(B) Vertical aerial photographs.....	89
3.3.2. <i>Results of historical changes</i>	91
3.3.2(A) Changes to the river channel as identified from ordnance survey maps since 1886	91
3.3.2(B) Changes observed from vertical aerial photographs since 2000	97
3.3.3. <i>Challenges in analysing historical resources</i>	100
3.3.3(A) Assumption of continuity and linearity of change	100
3.3.3(B) Accuracy of maps and aerial photographs.....	100
3.3.3(C) Change in channel definition over time	101
3.3.3(D) Digitizing errors.....	101
3.3.3(E) Georeferencing challenges.....	101
3.3.3(F) Level of intervention	102
3.4. Field erosion rates.....	103
3.4.1. <i>Field methods for quantifying the rate of erosion</i>	103
3.4.1(A) Erosion pins.....	103
3.4.1(B) Repeated vertical bank profiling	106
3.4.1(C) Repeated bank top surveys	107
3.4.1(D) Photo-Electronic Erosion Pins (PEEPS).....	111
3.4.2. <i>Results</i>	113
3.4.2(A) Erosion pin readings.....	113
3.4.2(B) Changes in cross-sectional profiles	115
3.4.2(C) Bank top retreat	122
3.4.2(D) Continuous erosion monitoring using PEEPS	127
3.4.3. <i>A discussion on the magnitude of river bank retreat and some observations on the measurement methods used</i>	132
3.4.3(A) The variability of erosion pin readings.....	132
3.4.3(B) Observations from repeated vertical profiles	134
3.4.3(C) Observations from repeated bank top surveys.....	136
3.4.3(D) Notes on experience of using Photo-Electronic Erosion Pins	138
3.4.3(E) Summary characteristics of erosion monitoring methods	138
3.4.3(F) The relationship between long-term historical and short-term field erosion rates.....	140
3.4.3(G) Field erosion rates in the context of other British and world river bank erosion studies ..	142
3.5. Erosion rates and site properties correlations.....	144
3.5.1. <i>The influence of bank material properties on erosion rates</i>	145
3.5.1(A) An examination of soil texture.....	145
3.5.1(B) Shear strength effect.....	148
3.5.2. <i>The influence of bank and channel geometry</i>	150
3.5.2(A) Bank height and slope.....	151
3.5.2(B) Water surface slope and channel planform.....	153
3.5.3. <i>The effects of natural and transferred flows</i>	155
3.5.4. <i>Relating stability indexes to bank erosion rates</i>	162
4. WILLOW SPILING IN THE UK.....	165
4.1. Review of the method.....	165
4.1.1. <i>History and recent research</i>	165
4.1.2. <i>Principles of willow spiling</i>	166
4.1.3. <i>Project planning considerations</i>	168
4.1.3(A) Hydrological character of the stream	168
4.1.3(B) Species selection	169
4.1.3(C) Site conditions.....	170

4.1.3(D) Dimensions	172
4.1.3(E) Timing	172
4.1.3(F) Cost	173
4.1.3(G) Maintenance	173
4.1.3(H) Monitoring	174
4.2. Project experience	175
4.2.1. <i>Inventory of willow spiling projects in the UK</i>	175
4.2.2. <i>UK project performance and case studies</i>	178
4.2.3. <i>Willow spiling outside UK</i>	181
4.2.4. <i>Proposals to improve success rates based on the review</i>	182
5. TWO APPLICATIONS OF WILLOW SPILING ON THE RIVER STOUR, EAST ANGLIA.....	183
5.1. Introduction and justification.....	183
5.2. Design and implementation	185
5.3. Biological Performance	189
5.3.1. <i>Introduction to post-construction evaluation</i>	189
5.3.2. <i>Methods of sampling and data analysis</i>	189
5.3.3. <i>Results</i>	192
5.3.3(A) Stake survival	192
5.3.3(B) Shoot extension	193
5.3.3(C) Number of live shoots	198
5.3.3(D) Frequency size distribution	201
5.3.4. <i>Discussion on biological performance</i>	207
5.3.4(A) Stake survival	207
5.3.4(B) Shoot extension and number of live shoots	208
5.3.4(C) Net seasonal shoot extension	210
5.4. Geomorphologic performance	215
5.4.1. <i>Methods</i>	215
5.4.1(A) Data gridding	215
5.4.1(B) Cross-sectional plots of river bed	216
5.4.1(C) Three-dimensional analysis	219
5.4.1(D) Measurements from stake tops	219
5.4.2. <i>Results and interpretation</i>	220
5.4.2(A) Cross-sectional plots of the river bed	220
5.4.2(B) Three-dimensional analysis of the river bed	224
5.4.2(C) Three-dimensional analysis of the backfill	229
5.4.2(D) Measurements from stake tops	231
5.5 Project performance factors and recommendations	234
5.5.1. <i>Abiotic factors</i>	234
5.5.1(A) River flows	234
5.5.1(B) Bed and bank material properties	239
5.5.1(C) Light conditions	241
5.5.2. <i>Biotic factors</i>	241
5.5.2(A) Invertebrates and fungi	241
5.5.3. <i>Anthropogenic factors</i>	243
5.5.3(A) Grazing and mechanical damage	243
5.5.4. <i>Recommendations based on experience from the two willow spiling projects</i>	244
6. CONCLUSION.....	247
6.1. Summary of the main concept	247
6.2. Summary of results	249
6.2.1 <i>River bank erosion rates</i>	250

6.2.2 Willow spiling review	256
6.2.3 Practical applications and post-project monitoring of two willow spiling projects	256
6.3 Lessons learned and further research directions	259
7. FOLLOW UP TO THE TWO WILLOW SPILING PROJECTS THREE YEARS AFTER INSTALLATION	263
References.....	267
Appendix	285

LIST OF FIGURES

CHAPTER 1

Fig. 1.1.1 The location of the River Stour's catchment area between Suffolk and Essex in East Anglia.

CHAPTER 2

Fig. 2.1.1 Six channel evolution stages for unstable streams (Simon 1989a).

Fig. 2.2.1 Ped fabric structure of dried bank face with desiccation cracks.

Fig. 2.2.2 Signs of fluvial erosion on monitored bank with pins.

Fig. 2.2.3 Types of mass wasting on river banks (Hey & Tovey 1989).

Fig. 2.2.4 Culman's stability analysis for plane slip failure on the river bank and the stability analysis modified to account for effects of tension crack (Thorne 1982).

Fig. 2.2.5 Forces of weight, shear, compression and tension acting on a cantilever with regard to the three modes of failure (Thorne & Tovey 1981).

Fig. 2.2.6 Recently failed cantilever, research field site on the River Stour, evening in February 2009.

Fig. 2.3.1 Relationship between shear stress and strength of soils (Hemphill & Bramley 1989).

Fig. 2.3.2 Patterns of secondary flows and boundary shear stresses in meandering channels (Hey 1986).

Fig. 2.4.1 Contribution to soil cohesion through the presence of root systems (Coppin & Richards 1990).

Fig. 2.4.2 Bank scour caused by back eddies scouring around the solitary tree trunk.

Fig. 2.5.1 Revetment using willow stakes, hazel faggots and reeds for river narrowing and habitat improvement.

Fig. 2.5.2 Two-tiered gabion revetment on the River Stour on a flood relief channel, 400 m upstream of the N1 site.

Fig. 2.5.3 Gabion revetment on a channel upstream of LB2 site.

CHAPTER 3

Fig. 3.1.1 The River Stour catchment with the locations of the nine field sites.

Fig. 3.1.2 Long profile of the River Stour showing positions of the field sites.

Fig. 3.1.3 River sinuosity versus distance and elevation based on 10m elevation contour intervals.

Fig. 3.1.4 John Constable's 'Haywain' from 1821.

Fig. 3.1.5 The Denver Complex.

Fig. 3.1.6 Schematic map of the Ely Ouse to Essex Water Transfer Scheme (Entec 2007).

Fig. 3.1.7 The Stour part of the Ely Ouse to Essex Water Transfer Scheme.

Fig. 3.1.8 The River Stour catchment divided into four stretches depending on the amount of water transfer.

Fig. 3.1.9 Schematic contribution of the water transfer to each sub-catchment.

Fig. 3.1.10 Contribution of transferred flows to the overall flows.

Fig 3.1.11 Transferred flows and natural river flows (represented as mean daily discharge) at Keddington and Westmill stations.

Fig. 3.1.12 Transferred flows and natural river flows (represented as mean daily discharge) at Lamarsh and Langham stations.

Fig. 3.2.1 Water slope versus distance from the nearest upstream weir, based on nine field sites.

Fig. 3.2.2 Meander geometry variables.

Fig. 3.2.3 Example samples from field sites in Clare (C1), left and Great Bradley (GB1), right illustrating the variability in texture and colour between the Thames and Ludford Associations.

Fig. 3.2.4 Soil texture triangle (Burton 2006).

Fig. 3.2.5 Soil triangle for each of the soil samples taken from the bank top, middle and bank foot sections based on volumetric percentage of soil, silt and sand particles in the sample.

Fig. 3.2.6 Volumetric content of clay, silt and sand across the field sites.

Fig. 3.2.7 The relationship between the site specific surface area (logarithmic scale) and the% of clay in the soil sample.

Fig. 3.2.8 Cumulative volumetric percentage of particle size fractions for two sites GB1 and GB2 for particles below 2 mm.

Fig. 3.2.9 Cumulative volumetric percentage of particle size fractions for three sections of banks at sites GB3 and LB1 for particles below 2 mm.

Fig. 3.2.10 Cumulative volumetric percentage of particle size fractions for three sections of banks at sites LB2 and C1 for particles below 2 mm.

Fig. 3.2.11 Cumulative volumetric percentage of particle size fractions for three sections of banks at sites C2 and S1 for particles below 2 mm.

Fig. 3.2.12 In situ soil shear strength testing using the Field Vane at the S1 site.

Fig. 3.2.13 Comparison of the undrained shear strength measured at the S1 site on 24 June 2008 and at N1 site on 25 January.2008.

Fig. 3.2.14 Sample shear strength values with a given water content for some chosen gravel, loamy sand and sandy silt loam samples during unsaturated conditions.

Fig. 3.3.1 Identical reach near Great Bradley in 1945 and in 2007.

Fig. 3.3.2 The channel of the River Stour with the GB1 site in 1886, 1981 and 2008.

Fig. 3.3.3 The channel of the River Stour showing GB2 and GB3 sites in 1886, 1981 and 2008.

Fig. 3.3.4 The channel of the River Stour with the LB1 site in 1886, 1981 and 2008.

Fig. 3.3.5 The channel of the River Stour with the LB2 site in 1886, 1981 and 2008.

Fig. 3.3.6 The channel of the River Stour showing C1 and C2 sites in 1886, 1968 and 2008.

Fig. 3.3.7 Position of the channel of the Rive Stour showing the S1 site in 1886, 1966 and 2008.

Fig. 3.3.8 River channel with the N1 site in 1904, 1962 and 2008.

Fig. 3.3.9 Aerial imagery sequence for the C2 field site in Clare.

Fig. 3.3.10 Aerial imagery sequence for the S1 field site in Sudbury.

Fig. 3.3.11 Aerial imagery sequence for the N1 field site.

Fig. 3.4.1 Detail of erosion pins on field site LB1 in Little Bradley.

Fig. 3.4.2 Frequency and timing of field readings of erosion pins, vertical bank sections and bank edge surveys.

Fig. 3.4.3 Channel cross section surveying using Nikon automatic level at GB2 site in Great Bradley.

Fig. 3.4.4 Total station positioned in the centre of the meander with the surveyed bank line in the background at C2 site in Clare.

Fig. 3.4.5 Example data interpolation of bank line survey in MatLab (LB1 site).

Fig. 3.4.6 Subtracted bank lines shown as retreat in m along the bank.

Fig. 3.4.7 Circuit design for the PEEP system.

Fig. 3.4.8 Schematic installation of PEEPs sensors in river bank Lawler (2002).

Fig. 3.4.9 Site-specific and bank section-specific summaries based on field readings of 95 erosion pins.

Fig. 3.4.10 Timeline showing the mean cumulative erosion in mm at each of the field sites. Vertical bars are the standard error.

Fig. 3.4.11 Bank profiles at GB1.

Fig. 3.4.12 Bank profiles at the GB2 and GB3 sites.

Fig. 3.4.13 Bank profiles at the LB1 site, Section 1.

Fig. 3.4.14 Bank profiles at the LB1 sites, Sections 2-5.

Fig. 3.4.15 Bank profiles at the LB2 sites, Sections 1-2.

Fig. 3.4.16 Bank profiles at site C1 in Clare.

Fig. 3.4.17 Plan of bank top line at the LB1 site surveyed in 2007, 2009 and 2010.

Fig. 3.4.18 Area of eroded bank expressed as the overall difference between June 2007 and April 2010 and the intermediate difference between June 2007 and May 2009.

Fig. 3.4.19 The position of the bank top at the C2 site surveyed on five occasions in 2007, 2008 and 2010.

Fig. 3.4.20 Area of eroded bank at C2 site expressed as the overall difference between May 2007 and March 2010 and the intermediate difference between May 2007 and April 2008.

Fig. 3.4.21 The position of the bank top at the N1 site surveyed in 2007, 2008 and 2009.

Fig. 3.4.22 Area of eroded bank at the N1 site expressed as a difference between the interpolated coordinates between 2.6.2007 and the two dates shown.

Fig. 3.4.23 Mean daily discharge as m^3 per second as gauged at Westmill and the output current from upper and lower PEEPs between 28 November and 5 December 2009.

Fig. 3.4.24 Mean daily discharge as m^3 per second as gauged at Westmill and the output current from upper and lower PEEPs between 25 January and 22 February 2010.

Fig. 3.4.25 Mean daily discharge as m^3 per second as gauged at Westmill and the output current from upper and lower PEEPs between 22 February 2011 and 19 March 2010.

Fig. 3.4.26 Slumped piece of the right bank at GB1 site with the uprooted tall herbal vegetation, June 2007. Failed material is covering the lower pin.

Fig. 3.4.27 A large cavity formed around the pin on left bank at LB1 site near Little Bradley, January 2008.

Fig. 3.4.28 Relationship between the retreat calculated from the cross-sectional area and retreat recorded on erosion pins.

Fig. 3.4.29 Two instances of slumped bank at the upstream end of the surveyed bank at LB1 site.

Fig. 3.4.30 Two instances of slumped bank at the downstream section of C2 site in November 2006 and October 2007.

Fig. 3.4.31. Maximum retreat per year during the three historic intervals and maximum readings recorded in the field.

Fig. 3.4.32 Maximum retreat versus time interval over which this retreat was measured.

Fig. 3.4.33 Relationship between the erosion rates and the catchment area on a logarithmic scale from worldwide and British rivers (data from reviews by Hooke 1980 and from Lawler 1993) and from this research on the River Stour.

Fig. 3.5.1 Vertical process dominance zones applied to the study sites with the formation of a 'step' on the boundary between where fluvial processes and subaerial processes dominate.

Fig. 3.5.2 Clay content and silt-clay content (as volumetric %) versus annual erosion rate recorded on pins (cm of retreat/year) for three vertical bank zones: top (A), middle (B) and bank foot (C).

Fig. 3.5.3 Shear strength (kPa) versus erosion rate (cm/year) for loamy sand and sandy silt loam during unsaturated and saturated conditions.

Fig. 3.5.4 Mean shear strength (\pm standard error) of saturated soil (kPa) and corresponding erosion rates, as recorded on the individual pins and expressed as cm retreat per year.

Fig. 3.5.5 Bank heights (in m) and angles (in radians) with the corresponding retreat rates (m/year) recorded between June 2007 and April 2010 at site LB1.

Fig. 3.5.6 Bank heights (in m) and angles (in radians) with the corresponding retreat rates (m/year) recorded between December 2007 and March 2009 at site N1.

Fig. 3.5.7 Maximum erosion rate recorded on pins (cm/year) versus site water slope (left) and site sinuosity (right) at the research sites shown.

Fig. 3.5.8 Hydrograph for the study period (2006 until 2010) based on mean daily flows as gauged at Keddington station (Q_{Kedd}), overlaid with transferred discharges (in grey).

Fig. 3.5.9 Hydrograph for the study period (2006 until 2010) based on mean daily flows as gauged at Westmill station (Q_{West}), overlaid with transferred discharges from the Ely Ouse minus the amounts taken out to Chelmer.

Fig. 3.5.10 Proportion of days with flows above Q_{10} to the specific pin reading period against the mean annual erosion rate (cm/year) for the pins at the bank top (A), bank middle (B) and bank foot zone (C).

Fig. 3.5.11 Proportion of days with flows above effective discharge (Q_{Eff}) between the individual pin readings against erosion rate, expressed as the site mean and the site maximum on a single pin (cm/day).

Fig. 3.5.12 Flow-specific summaries of the erosion rates.

CHAPTER 4

Fig. 4.1.1 Installation of willow spiling at N1 site in Nayland, March 2009 and the completed willow spiling wall with the initial growth, May 2009.

Fig. 4.1.2 Cross-sectional view of a two-staged willow spiling revetment with incorporated erosion control blanket made of coir (natural fibre extracted from the husk of coconut).

Fig. 4.1.3 Distribution of inventoried willow spiling projects in Great Britain carried out since 1989.

Fig. 4.1.4 Project cost in relation to project length, based on 26 projects.

Fig. 4.1.5 Disintegrating spiling structure two years after installation.

Fig. 4.1.6 Successful willow spiling, approximately 15 years old on the River Ives in Bedfordshire (October 2008).

Fig. 4.1.7 Shoots growing on a willow stake installed one year ago.

CHAPTER 5

Fig. 5.1.1 Aerial maps of the project sites.

Fig. 5.2.1 Snapshot from the project diary: Cohesive site in Sudbury.

Fig. 5.2.2 Project diary: Non-cohesive site in Nayland.

Fig. 5.3.1 Number of samples versus the cumulative mean.

Fig. 5.3.2 Adventitious roots growing from submerged parts of stems.

Fig. 5.3.3 Mean shoot length based on stake means.

Fig. 5.3.4 Mean shoot lengths at the cohesive site on the upper tier (S1-UT) and lower tier (S1-LT).

Fig. 5.3.5 Mean shoot lengths at the Non-cohesive site on the upper tier (N1-UT) and lower tier (N1-LT).

Fig. 5.3.6 Appearance of new shoots from a willow stake and dead shoots on a stake.

Fig. 5.3.7 Mean number of shoots per stake at individual sampling dates at cohesive and non-cohesive sites between May and October 2009.

Fig. 5.3.8 Number of live shoots on sampled stakes in upper (S1-UT) and lower tier (S1-LT) at the cohesive site.

Fig. 5.3.9 Number of live shoots on sampled stakes in upper (N1-UT) and lower tier (N1-LT) at non-cohesive site.

Fig. 5.3.10 Frequency distributions for the cohesive site – upper tier (S1-UT) showing shoot length size classes against number of shoots.

Fig. 5.3.11 Frequency distributions for the cohesive site – lower tier (S1-LT) showing shoot length size classes against number of shoots.

Fig. 5.3.12 Frequency distributions for the non-cohesive site – upper tier (N1-UT) showing shoot length size classes against number of shoots.

Fig. 5.3.13 Frequency distributions for the non-cohesive site – lower tier (N1-LT) showing shoot length size classes against number of shoots.

Fig. 5.3.14 Plots of mean and median values for each cohort for mean shoot length and number of shoots per stake.

Fig. 5.3.15 Net seasonal shoot extension (NSSE) at cohesive (S1) and non-cohesive (N1) site.

Fig. 5.3.16 Summed shoot length per stake at the sampling dates for each cohort.

Fig. 5.4.1 Contour plots with three gridding methods overlain, XY coordinates are in m, elevations are displayed in m AOD.

Fig. 5.4.2 Illustration of intersecting points of cross section through a grid file showing locations where data points are created.

Fig. 5.4.3 Contour plot of full and blanked grid file with location of the surveyed elevation points.

Fig. 5.4.4 The network of surveyed data points in November 2009 and in March 2010 with eight plotted cross sections.

Fig. 5.4.5 Cross-sectional plots of the river bed adjacent to the spiling at the cohesive site S1..

Fig. 5.4.6 Cross-sectional plots of the river bed adjacent to the spiling at the non-cohesive site N1.

Fig. 5.4.7 Percentage difference of cross-sectional areas at the cohesive (S1) and non-cohesive (N1) site that occurred between November 2009 and March 2010.

Fig. 5.4.8 Erosion of the river bed underneath the spiling that occurred between November 2009 and March 2010.

Fig. 5.4.9 Percentile distribution of river bed elevation before and after high flow events at cohesive and non-cohesive site.

Fig. 5.4.10 Image map of the river bed at cohesive site before and after high flow events.

Fig. 5.4.11 Image map of the river bed at non-cohesive site before and after high flow events.

Fig. 5.4.12 Percentile distribution of backfill elevation before and after high flow events at cohesive (S1) and non-cohesive site (N1).

Fig. 5.4.13 Image map of the backfill at the cohesive (S1) and non-cohesive (N1) sites before and after high flow events.

Fig. 5.4.14 Erosion on backfill that occurred on stakes in the upper (UT) and lower tiers (LT) at the cohesive and at the non-cohesive site (N1) recorded between November 2009 and January 2010.

Fig. 5.4.15 Eroded backfill on the lower tier, non-cohesive site.

Fig. 5.5.1 Mean daily flows at Lamarsh gauging station between 1 April 2009 and 31 March 2010.

Fig. 5.5.2 High flow events during January and February 2010.

Fig. 5.5.3 River flows during the winter period November 2009-March 2010 and rainfall data.

Fig. 5.5.4 Near bank flow velocities at the cohesive site S1 during two bankfull events before and after coppicing.

Fig. 5.5.5 Volumetric water content (VWC) and available water content (AWC) in% of soil volume estimated by Time Domain Reflectometry (TDR) on 8 and 9 August 2009.

Fig. 5.5.6 Larvae of Willow Redgall Sawfly (*Pontania proxima* LEPELETIER) and Brown Tail Moth caterpillar (*Euproctis Chrysorrhoea* L.).

Fig. 5.5.7 Fungi and aphids and mosses on dead willow withies.

Fig. 5.5.8 Stake damaged by grazing at the non-cohesive site and a recovery node created in the breakage zone on the stem.

CHAPTER 7

Fig. 7.1 Willow spiling in Sudbury at the S1 site on the River Stour, during a high flow event, looking upstream in March 2012. The spiling acts as a flow deflector and a trap for small floating debris and sediment.

Fig. 7.2 Willow spiling at N1 site in Nayland on the River Stour in June 2012, looking upstream. Some dead stakes and scouring are visible on the left (right bank) and there is no growth from the revetment in the upper tier. On the other hand, a vigorous growth is seen from the shorter lower tier, in the top middle of the picture.

LIST OF TABLES

CHAPTER 2

Table 2.1.1 Channel evolution stages (Hupp & Simon 1986; Simon 1989a; 1992).

Table 2.1.2 Geomorphic impacts on channel changes in flow and sediment metamorphosis (Schumm 1977).

Table 2.4.1 Root tensile strength for selected plant species (Schiechtl & Horstmann 1980).

Table 2.4.2 Contribution of vegetation to erosion control and bank stability (Coppin and Richards 1990).

CHAPTER 3

Table 3.1.1 Main geographic, climatic and hydrologic data for five gauging stations on the River Stour ordered from upstream to the estuary near Stratford St Mary.

Table 3.1.2 Equations describing the relationship of the discharges at gauging stations to estimate the discharge at the field sites with how these will change after 2015.

Table 3.1.3 Transferred amounts from the Ely Ouse at Kirtling and extraction taken at Wixoe into Chelmer since 1996.

Table 3.2.1 Description of field sites with photograph and geographic position. OS x is the geographic easting and OS y is the northing.

Table 3.2.2 The distance of the study site locations from the source, elevation, water slope and distance from the nearest weir.

Table 3.2.3 Meander geometry, channel and bank properties at the field sites.

Table 3.2.4 Soil associations, hydrology types, parent material and texture characteristics for the floodplain soil at research field sites

Table 3.2.5 British Soils Classification of soils based on particle size (in mm), BS 5930 (British Standards Institution 1999).

Table 3.2.6 Soil texture parameter means for each bank section across eight sampled sites.

Table 3.2.7 Wet and dry sample weights, gravimetric water content and the specific gravity for sample locations.

Table 3.2.8 Mean shear strength taken during unsaturated conditions.

Table 3.2.9 Mean shear strength during saturated conditions.

Table 3.3.1 Historical maps and aerial photographs available for the research area.

Table 3.3.2 Historical maps used for bank retreat measurement in GIS.

Table 3.3.3 Bank retreat at each field site.

Table 3.3.4 Evolution of channel sinuosity.

Table 3.4.1 Number of pins installed on each field site.

Table 3.4.2 Sample pin readings.

Table 3.4.3 Erosion data delivered from repeated cross-profiling.

Table 3.4.4 Summary bank top retreat data for sites LB1, C2 and N1.

Table 3.4.5 Length of the Photoelectronic Erosions Pins (PEEPs) protruding at the C1 site between May 2009 and March 2010.

Table 3.4.6 Statistical summary of PEEPs outputs.

Table 3.4.7 Summary characteristics of applied methods: advantages, drawbacks and recommendations.

Table 3.4.8 Maximum retreat derived from historic map sources and as recorded in the field between 2006-2010.

CHAPTER 4

Table 4.1.1 Tolerance thresholds for flow velocity and shear stress for different stream banks stabilization methods (modified from Fischenich, 2001; Sotir & Fischenich, 2007).

Table 4.1.2 Frequency of various causes of failure in willow spiling projects in the UK carried out between 1989 and 2009, based on documentation from four failed and 11 partially failed projects.

CHAPTER 5

Table 5.2.1 Technical comparisons between willow spiling projects.

Table 5.3.1 Values for mean shoot length.

Table 5.3.2 Percentage of stakes with at least one living shoots between May and October 2009.

Table 5.3.3 Mean and median shoot lengths at individual sampling dates.

Table 5.3.4 Probability of difference with 95% confidence for mean shoot length and number of shoots obtained from Kruskal-Wallis (Mann -Whitney) test.

Table 5.3.5 Values for Net seasonal shoot extension (NSSE) of *Salix* sp. cohorts at S1-UT, S1-LT, N1-UT and N1-LT.

Table 5.3.6 Final values for shoot extension by instantaneous growth (P_G) and by increment summation (P_S) for all the stakes and the values per stake.

Table 5.4.1 Bed areas of eight random cross-sectional plots for cohesive S1 and non-cohesive N1 site and the percentage of difference in the cross-sectional area between November 2009 and March 2010.

Table 5.4.2 Statistical comparison of river bed elevation changes at cohesive (S1) and non-cohesive (N1) sites, including cut off planes and volumes of river bed.

Table 5.4.3 Statistical comparison of backfill elevations.

LIST OF RESEARCH ACRONYMS

GB1	<i>Great Bradley site 1</i>
GB2	<i>Great Bradley site 2</i>
GB3	<i>Great Bradley site 3</i>
LB1	<i>Little Bradley site 1</i>
LB2	<i>Little Bradley site 2</i>
C1	<i>Clare site 1</i>
C2	<i>Clare site 2</i>
S1	<i>Sudbury (cohesive) site 1</i>
N1	<i>Nayland (non-cohesive) site 1</i>
GB1-A	<i>Bank top section at GB1</i>
GB1-B	<i>Bank middle section at GB1</i>
GB1-C	<i>Bank lower section at GB1</i>
GB1-1	<i>Bank profile 1 (upstream) at GB1</i>
GB1-2	<i>Bank profile 2 (middle) at GB1</i>
GB1-3	<i>Bank profile 3 (downstream) at GB1</i>
GB1-1A	<i>Erosion pin/soil sampling location at the top section (A) of vertical profile 1 at GB1 site</i>
UT	<i>Upper tier</i>
LT	<i>Lower tier</i>

LIST OF NOTATIONS

Q_s	<i>Sediment discharge</i>
Q_w	<i>Water discharge</i>
H_c	<i>The critical bank height</i>
C	<i>Soil cohesion</i>
c'	<i>The effective soil cohesion</i>
c_a	<i>Apparent cohesion due to matrix suction</i>
Γ	<i>Unit weight of material</i>
A	<i>The angle of the potential failure plane to the horizontal</i>
Φ	<i>The friction angle of the bank material</i>
τ	<i>Shear stress</i>
τ_{max}	<i>Maximum shear stress</i>
τ_0	<i>Mean boundary shear stress</i>
F_s	<i>Factor of Safety</i>
S_r	<i>Shear strength</i>
Σ	<i>Normal stress</i>
μ_w	<i>Pore water pressure</i>
$\mu_a - \mu_w$	<i>Matric suction</i>
μ_a	<i>Air pressure</i>
γ_w	<i>Unit weight of the water</i>
d	<i>Depth</i>
ϕ	<i>Friction angle</i>
ϕ'	<i>Effective friction angle</i>
S_w	<i>Water surface slope</i>
c_r	<i>Additional apparent cohesion due to roots</i>
t_r	<i>Mobilised root tensile strength per soil unit area</i>
K	<i>Factor taking into account that roots are randomly orientated with respect to the failure plane</i>
T_E	<i>Transfer from Ely Ouse</i>
T_C	<i>Transfer to Chelmer</i>
T_A	<i>Transfer to Abberton</i>
c_1	<i>Net contribution to flow from catchment Q1</i>
c_{Kedd}	<i>Net contribution to flow from catchment q_{kedd} (to the Keddington gauge)</i>
c_{West}	<i>Net contribution to flow from catchment q_{west}</i>
c_{Lam}	<i>Net contribution to flow from catchment q_{lam}</i>
c_{Lang}	<i>Net contribution to flow from catchment q_{lang}</i>
c_{Strat}	<i>Net contribution to flow from catchment q_{strat}</i>
T_{AE}	<i>Second column indicates the contribution from Abberton scheme</i>
T_W	<i>The flow through an additional extraction point that will be built at Wormingford</i>
R_c	<i>Meander radius</i>
θ	<i>Meander arc angle</i>
B	<i>Meander width/amplitude x 2</i>
L	<i>Wavelength</i>
Z	<i>Riffle spacing</i>
M	<i>Gravimetric water content</i>
m_w	<i>Mass of water in a sample</i>
m_s	<i>Mass of dry solids</i>

<i>G_s</i>	<i>Specific gravity of soil</i>
<i>m_{cw}</i>	<i>Mass of cylinder with 100 ml of water</i>
<i>m_{cws}</i>	<i>The mass of cylinder with soil and topped up with water</i>
<i>VA</i>	<i>Vertical angle</i>
<i>HA</i>	<i>Horizontal angle</i>
<i>SD_x</i>	<i>Slope distance between the total station and the target</i>
<i>HD</i>	<i>Horizontal distance</i>
<i>A</i>	<i>Angle of rotation in radians</i>
<i>x_{trans}</i>	<i>Transformed x coordinate</i>
<i>y_{trans}</i>	<i>Transformed y coordinate</i>
<i>E_s</i>	<i>Error of sampling</i>
<i>S</i>	<i>Sample standard deviation</i>
<i>N</i>	<i>Size of population</i>
<i>N</i>	<i>Size of sample</i>
<i>m, μ</i>	<i>Sample, population mean</i>
<i>σ_x</i>	<i>Standard error</i>
<i>N_{ave}</i>	<i>Mean number of shoots for two consecutive time intervals</i>
<i>ΔL</i>	<i>Change in individual length ($L_2 - L_1$)</i>
<i>L_{tot}</i>	<i>Total length of a shoot (L.N)</i>
<i>L_{tot,ave}</i>	<i>Average total length for two consecutive time intervals</i>
<i>G</i>	<i>Growth rate over time interval ($\ln(L_1/L_0)$)</i>
<i>P_s</i>	<i>Shoot extension by Increment Summation ($n_{ave} \cdot \delta l$)</i>
<i>P_G</i>	<i>Shoot extension by Instantaneous Growth ($G \cdot L_{tot, ave}$)</i>

1. INTRODUCTION

1.1. RESEARCH CONTEXT

River processes are extremely complex, especially in natural meandering or braided channels (Leopold & Wolman 1957; Schumm 1977). Bank erosion fulfils an integral role amongst river processes, but it is one that has been in conflict with human needs for centuries (Thorne 1982; Coppin & Richards 1990; Thorne *et al.* 1996a). A shifting bank is seen as a negative, isolated phenomenon that presents a threat to land, settlement or infrastructure.

The majority of British streams do not pose an erosion 'problem'. Apart from situations where the banks are highly erodible, most instances of fast progressing erosion rates are a result of human activity (Thorne *et al.* 1996a). In East Anglia, a region of the UK, engineering interventions mainly during the 1960s and 70s (such as dredging, straightening of river channels, putting in weirs or sluices and the removal of riparian vegetation) caused the banks to become higher and therefore more prone to instability (Hey 2006).

River engineers were frequently required to 'repair' a failing length of river bank. The commonly used hard engineering solutions had little consideration for the critical causes of this instability. Thorne (1978) stated that it is crucial to establish the mode of failure when selecting the optimum approach to the management of river bank erosion to ensure it is sustainable in the long term. Indeed, some hard bank stabilisation schemes installed along the River Stour in East Anglia (Fig. 1.1) that were researched for this study have either collapsed, caused significant erosion at both ends of the structure or increased the stream energy only to move the problem downstream. Therefore the problems caused by universally applied hard engineering and its high installation costs have made a strong case in favour of alternative methods that 'work with nature' rather than against it. According to Hey (2006), the widespread application of structural engineering methods is unjustified not only on ecological grounds but also on economic ones.

An important aspect in terms of river bank erosion is the effect of climate change. Proving a link between climate change and river stability is one of the most difficult and contentious problems that researchers and engineers face at the moment. Significant fluctuations in precipitation and run off as a result of climate change and land use have

affected the flow regime in the last few decades, as demonstrated by Knox (1985; 1988) and Starkel *et al.* (1991) through comparing the data from recent floods to paleofloods.

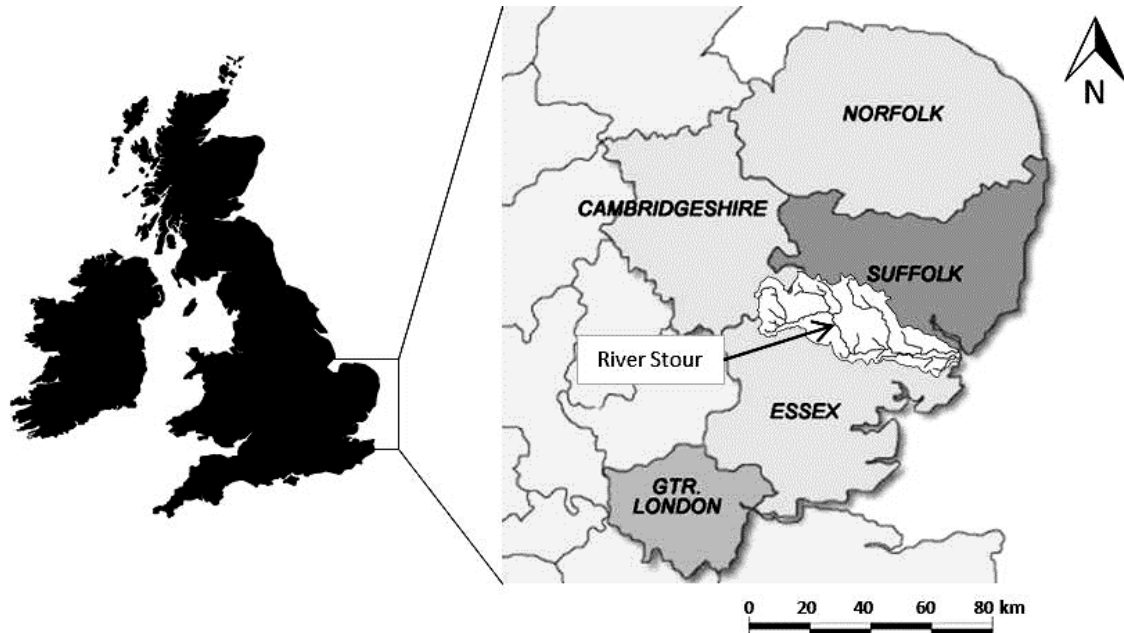


Fig. 1.1.1 The location of the River Stour's catchment area between Suffolk and Essex in East Anglia.

In East Anglia particularly, climate change is prominently acting on either side of the scale of hydrological extremes: floods and droughts. Adaptation is absolutely crucial or the region will face serious water shortages. East Anglia is the driest region in the UK with an effective annual rainfall of only 147 mm. Long, dry summers with evaporation rates greater than rainfall are typical for the region. East Anglia has less water available per person than many hotter and drier countries (EA 2009). The UKCIP02 scenarios (Hulme *et al.* 2002) predict that by 2050, the annual winter rainfall in East Anglia will increase between 15 and 20% (for low to high carbon emissions scenarios) and summer rainfall will decrease by between minus 20 and minus 40%. Heavy winter precipitation will become more frequent and so will summer droughts. Any further decrease in spring and summer flows due to climate change will intensify drought conditions (EERA SDRT 2004) and increase pressure on the already overstretched water supply in the region (EA 2009). Increases in the amount of transferred water during winter and less natural water in rivers during dry summer months would thus put more strain on the ecology and hydromorphology of aquatic ecosystems.

The UK has adopted the EU Water Framework Directive (WFD) that compels signatory countries to classify the ecological status of their rivers and prepare management plans that would lead towards fulfilling improvement targets. Currently in East Anglia, only

12.3% of rivers have a good ecological status, 72.7% fall under moderate and 12.3% are of poor or bad status. No rivers have been classified as having a high ecological status (EA 2011).

The WFD defines water bodies as having a high ecological status when '*there are no, or only very minor, anthropogenic alterations to the values of the physicochemical and hydromorphological quality elements from those normally associated with that type under undisturbed conditions.*' A stream can be considered to have a good status when '*the values of the biological quality elements show low levels of distortion resulting from human activity, but deviate only slightly from those normally associated with the surface water body type under undisturbed conditions*' (UK TAG WFD 2008).

Furthermore, based on the WFD criteria for intervention, all major rivers and many tributaries in East Anglia are regarded as heavily modified, modified or artificial. The Water Framework Directive sets a target to prevent deterioration of the status of all surface water and groundwater bodies and to protect, enhance and restore them with the aim of achieving a good ecological status by 2015 (UK TAG WFD 2008). Considering the recent state of rivers in East Anglia, achieving this target seems unrealistic. However, alternative objectives can be set if the measures required for achieving a good status by 2015 would be technically unfeasible or disproportionately expensive. The Directive allows for an extension to the timetable for achieving a good status by up to 12 years (UK TAG WFD 2008). The current classification of the ecological status of East Anglia's rivers and the high level of modification should cause concern, especially with a context where climate change has increased in its impact over the last few decades.

1.2. THESIS AIMS, OBJECTIVES AND JUSTIFICATION

The purpose of this research was two-fold. Firstly, it aimed to explore the magnitude of river bank erosion and retreat rates on the River Stour, an engineered river used for water transfers, and what where the main factors driving the river bank erosion processes.

Secondly, this work aimed to review and test ecological river bank management approaches, focusing on the soil bioengineering method of willow spiling. Two pilot projects on the River Stour were implemented to test whether willow walls made of local live materials can work effectively in reducing erosion and whether they might be proposed as an ecological management alternative to hard engineering options.

The context to these aims and a justification of the importance of researching river bank erosion rates on the River Stour in East Anglia is the increasing water demand due to population growth (*e.g.* Thames Gateway by the River Thames estuary, east of London, with a proposed development of 160,000 new homes) and increasing climate change extremes make it more difficult to meet this demand. It is expected that the amount of water transferred via the River Stour to reservoirs will increase in the future. This will have an influence on river bank stability in two ways: (1) directly – as a consequence of the banks being subjected to prolonged periods of transferred flows and (2) indirectly – through related channel engineering and maintenance. Although a number of studies have been undertaken on artificial water releases from dams and reservoirs (*e.g.* Williams & Wolman 1984; Hupp *et al.* 2009), limited research is available on the impact of water transfer schemes on a river channel. Some studies speculate, as part of the water transfer project appraisal process, that there are possible impacts that the water transfer can have on the channel geomorphology (Entec 1998a; Newson & Block 2002; EA 1998). The main assumptions for these are presented in Chapter 3.1. However, none of them quantified and described river bank erosion and retreat in such detail and over such a long period of time as presented in this study.

Furthermore, a lack of robust post-project monitoring of river bank stabilisation schemes is generally the norm with most bioengineering methods. There is no reference to a study of project monitoring in the literature specifically on willow spiling. The UK-wide review of willow spiling carried out as part of this research (Chapter 4) revealed that, despite the wide application of this method in the UK, limited evidence exists on how well this approach performs. Some photographs and observations exist for a small proportion of the projects, but there are no quantitative data on biological or geomorphological performance.

The interactions between vegetation, water and soil processes are not well understood by practitioners, and there appears to be little scientific basis for the way in which vegetation is applied in river management projects (Thorne *et al.* 1998). The reason for this is the complexity of the many life forms and growth stages of plants and in the ways they function on the bank. Their effects can be both beneficial and adverse to river bank stability (Rowntree & Dollar 1999; Simon & Collison 2002).

There are serious gaps between the type of fundamental research being conducted on vegetation-soil-water interactions and the needs of practitioners working in river management agencies and consultancy companies. Specifically, many design engineers

and river managers have found that existing research does not address key problems or produce results that can be applied in practice. Coppin and Richards (1990) raised four questions that future research should tackle:

- (1) To what extent can the role of vegetation be quantified?
- (2) Is the level of quantification sufficient for engineering application?
- (3) Can vegetation provide economic and environmental advantages over conventional materials?
- (4) How much engineering experience is there on which to base designs using vegetation?

The second aim of the thesis, stated above, contributes to answering these questions, both by reviewing the existing engineering practice of willow spiling and by studying two project sites prior, during and after project implementation. Biological and geomorphological performance is related to some critical factors that have been identified. Based on the findings, and to further build on the review of existing project experience, recommendations are made for future engineering applications. These do not apply solely to willow spiling, but may be useful also in the application of other soil bioengineering methods that utilise willows.

The following research hypotheses were therefore proposed:

- (1) The magnitude of river bank erosion and retreat on an engineered river used for water transfers is substantially higher than on a lowland stream of size and climate similar to the one in the UK. The combination of engineering intervention and artificially enhanced flows in a river increases the rates of river bank erosion.
- (2) Willow spiling, if implemented correctly, can be an effective option in reducing river bank erosion of lowland rivers, even on sections with steeper water surface slopes than the typical mean water surface slope of the river reach.

To test these hypotheses, the objectives of this research were:

- (1) To measure the magnitude of river bank erosion and retreat on a modified river (River Stour, site location map in Fig. 3.1.1) that is also used as part of a water transfer scheme and to assess the effectiveness of the methods used for identifying the river bank retreat.
- (2) To compare river bank erosion rates measured in the field as part of this research between 2006 and 2010 with those derived from historical maps since the 1880s

and to evaluate this using field data from other field studies on similar rivers in the UK.

- (3) To assess the relative influence of river bank and channel properties such as bank material textures, shear strengths, bank heights and angles, water surface slopes or channel planform on river bank erosion rates on the field sites between 2006 and 2010.
- (4) To assess whether, and to what extent, transferred flows (that increase discharge artificially) are increasing river bank erosion rates at the research sites.
- (5) To review project experience of willow spiling across the UK and determine what can be learnt from this for the successful implementation of similar projects.
- (6) To implement willow spiling on two eroding, high stream power sites on the River Stour and to evaluate, biologically and geomorphologically, whether these projects were successful in reducing erosion during the first 12 months after installation.
- (7) To use the observations from (6) to establish the advantages, disadvantages and the preferred procedures for willow spiling and whether this approach can be recommended for wider application as a substitute to commonly used hard engineering methods.

1.3. THESIS STRUCTURE

The thesis is divided into two thematic parts and consists of six main chapters. Chapters 2 and 3 review and quantify streambank erosion processes, Chapters 4 and 5 are related to bank erosion management and present a national review as well as a practical application of willow spiling on the river. Chapter 6 concludes the main findings and presents areas that are worth exploring with further research. After the research was completed, a final Chapter 7 has been added which reflects on the performance of willow spiling three years after installation.

Chapter 2 introduces the fundamentals of river bank erosion as a review of key literature and research. It refers to mechanisms of erosion, stability analysis and key factors influencing river bank stability with a particular focus on vegetation. Furthermore, it reviews bank erosion management approaches including soil bioengineering methods.

Chapter 3 is a study of river bank erosion rates on the River Stour in East Anglia composed of three sub-themes. First, it introduces the study area and the key properties of the field sites. Second, the methods and results for bank erosion rates are shown, both from an

analysis of historical resources and from a field-based research. In the third part, these results are correlated with the field site properties and river flows.

Chapter 4 forms an introduction to the soil bioengineering method piloted in this study on the River Stour - willow spiling. It covers the history of the approach, benefits and factors to be considered, and information about the distribution and experience using this method within the UK. This review has been published (Anstead & Boar 2010).

Chapter 5 is a description of the practical application of willow spiling on two fast-eroding river sites and a narrative review of performance. As this is a living method and success depends on its survival, the review covers biological performance in detail. To show whether the approach has effectively eliminated bank erosion and what the success prognosis could be for the future, a detailed mapping of the river bed and any erosion signs is presented. Lastly, the factors that could have influenced the success of the method are discussed and further recommendations are listed, based on the experience from these two projects.

Finally, Chapter 6 concludes the findings from the previous chapters and relates them to the main research hypotheses. The research outcomes are presented in a form applicable to both research and river management.

2. RIVER BANK EROSION CONCEPTS

2.1. GEOMORPHOLOGIC STATUS OF RIVERS

An understanding of the causes and the spatial extent of processes affecting river bank erosion is necessary for the identification of stabilisation approaches and the management of bank erosion problems (Thorne *et al.* 1996a; 1998). Projects involving river bank stabilisation and mitigation measures should incorporate, as a core part, a prediction of stable bank geometry (Thorne *et al.* 1996a; Hey 2006; Dapporto *et al.* 2003). An evaluation of this stability status is a form of assessment that provides an understanding of the river's past, present and future processes and therefore helps river management.

The geomorphologic status of a river system may be classified as (1) unstable; (2) stable - dynamic or (3) stable - moribund (HR Wallingford 1992).

- (1) Unstable channels are ones that are, in time and space, actively changing their form and tend to exhibit evidence of serious, constant aggradation, degradation or lateral channel change (Thorne *et al.* 1996a). Although channel change and evolution is regarded as normal in alluvial systems, if there is no equilibrium, uncontrolled instability can lead to the destruction of valuable river habitats (Thorne *et al.* 1996a).
- (2) Dynamic stable channels occur where the morphology is adjusted to the hydrological regime and the supply of sediment from the catchment area, boundary materials and valley topography. The characteristic features of this type of channel do not change over engineering timescales (Hey & Thorne 1986). Any disturbance is likely to trigger dynamic process-response mechanisms that will, eventually, lead towards the re-establishment of a stable state in a new form (Simon & Thorne 1996; Hey 1994).
- (3) Moribund channels are ones that are not precisely alluvial because they were not formed by the present flow regime. Geometry and morphological features are relics of a fluvial environment that no longer exists. These types of channels are characterised by low flow energy and erosion resistant bank and bed materials (Thorne *et al.* 1996a).

Based on management status, river channels may be classified as:

- (1) Pristine and vulnerable (either in pristine condition or fully recovered from a past engineering intervention);
- (2) Engineered and recovering naturally (geomorphologically active while getting over the process of past engineering interventions); or
- (3) Terminally engineered (geomorphologically moribund and unable to recover or prevented from recovery by engineering interventions) (Thorne *et al.* 1996b).

Because river channels undergo a systematic series of morphological changes over time, historical, current and future channel processes can be described according to the phases of channel evolution that lead towards self-stabilisation (Hupp & Simon 1986; Simon 1989a; Rosgen 2001). Six stages have been identified by Simon (1989a) for unstable channels: (1) Premodified; (2) Constructed; (3) Degradation; (4) Threshold; (5) Aggradation and (6) Restabilisation stages (Fig. 2.1.1 & Table 2.1.1).

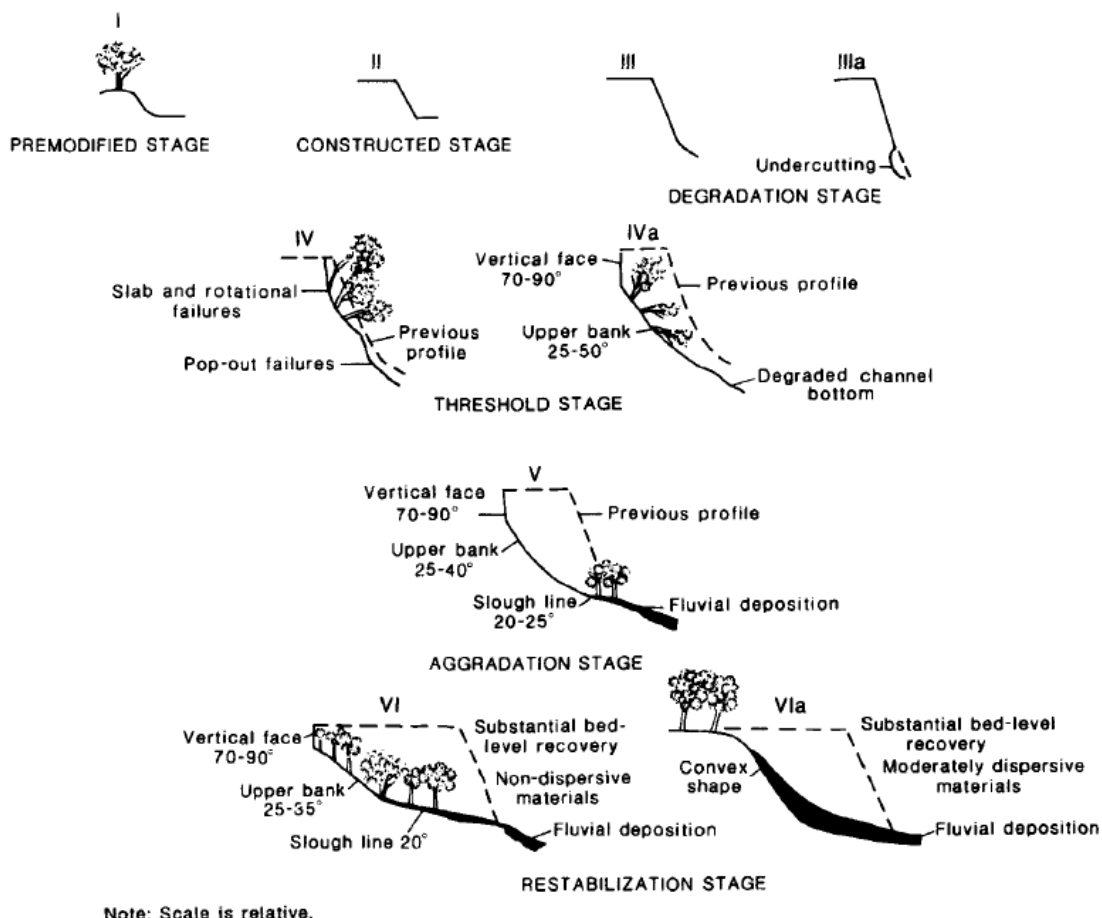


Fig. 2.1.1 Six channel evolution stages for unstable streams (Simon 1989a).

Table 2.1.1 Channel evolution stages (Hupp & Simon 1986; Simon 1989a; 1992).

Stage	Dominant processes	Forms	Vegetation
I. PREMODIFIED	Mild aggradation, basal erosion on outside and deposition on inside bends.	Stable, alternate channel bars; convex top bank shape; flow line high relative to top bank; channel straight or meandering.	Vegetated banks to mean summer water level.
II. CONSTRUCTED	Artificially reshaped or relocated channel.	Trapezoidal cross-section; linear bank surfaces; flow line lower relative to top bank.	Normally removed to increase conveyance.
III. DEGRADATION	Rapid basal erosion on banks.	Heightening and steepening of banks; alternate bars eroded; flow line lower relative to the bank top.	Riparian vegetation high relative to the flow line and may lean towards the channel.
IV. THRESHOLD	Basal erosion on banks, slab, rotational and pop-out failures.	Large scallops and bank retreat; vertical face, upper bank surfaces; failure blocks on upper bank; some reduction in bank angles; flow line very low relative to top bank.	Tilted and fallen riparian vegetation.
Va. AGGRADATION	Development of meandering thalweg; initial deposition of alternate bars; reworking of failed material on lower banks.	Slab, rotational and pop-out failures, low angle slides of previously failed material. Large scallops and bank retreat; vertical face, upper bank, and slough line; flattening of bank angles; flow line low relative to top of the bank, development of new floodplain.	Tilted and fallen riparian vegetation; re-establishing vegetation on slough line; deposition of material above root collars of slough-line vegetation.
Vb. AGGRADATION	Further development of meandering thalweg, deposition of alternate bars; reworking of failed material; some basal erosion on outside bends and deposition on flood plain and bank surfaces.	Low angle slides, some pop-out failures near the flow line. Stable, alternate channel bars; convex-short vertical face on top of the bank; flattening of bank angles; development of new floodplain; flow-line high relative to the bank top.	Re-establishing vegetation extends up slough line and upper bank; deposition of material above root collars of slough-line and upper-bank vegetation; some vegetation establishing on bars.
VI. RESTABILISATION	Significant reduction of bank heights; fluvial deposition on the upper bank and slough line surfaces.	Bank retreat along the vertical face by intense mass wasting processes subsides because bank heights no longer exceed critical heights.	Woody vegetation extends upslope towards the base of the vertical face and the former floodplain surface becomes a terrace

For example, successive reaches of a river could be in different evolution stages going upstream. A reach in a threshold stage will begin to cease degrading, stabilise and then begin to aggrade as the degradation upstream continues to supply sediment. An upstream reach in the degradation stage will continue to degrade until the banks reach critical heights and enter the threshold stage through mass wasting and channel widening (Thorne *et al.* 1996a).

According to Simon (1989a), it takes up to 40 years for a sand-bed channel to undergo the primary five stages of the evolution model. Between 50 to 100 years is anticipated as necessary for the re-stabilisation of channel banks (stage VI) and for the development of early meanders in these channels. However, much longer timescales are required for unstable channels of silt-clay alluvium (Simon 1989a).

Whether or not a channel is stable depends primarily on the sediment supply and flow regime (Werritty 1997). Using possible combinations of changes in water and sediment supply, Schumm (1977) pioneered eight conceptual treatments of river metamorphosis (Table 2.1.2). In some instances, the river accommodates the change as part of its natural characteristic variability. In some cases, change will not automatically result in sustained river instability and irreversible channel change due to negative feedback. In other cases, the change will exceed the natural inherent variability of the river. In such circumstances, the disturbance will result in the channel becoming unstable (positive feedback). Under such conditions, for example as a result of severe storms, channel change will occur (Werritty 1997) and this will exceed a natural threshold and the river will enter a new stable state.

Table 2.1.2 *Geomorphologic impacts on channel changes in flow and sediment metamorphosis (Schumm 1977). Q_s is sediment discharge, Q_w – water discharge, (+) stands for increase, (-) for decrease and (=) remains constant.*

Change	River Bed Morphology	Change	River Bed Morphology
$Q_s + Q_w =$	Aggradation, channel Instability, wider and shallower channel	$Q_s + Q_w -$	Aggradation
$Q_s - Q_w =$	Incision, channel instability, narrower and deeper channel	$Q_s + Q_w +$	Processes increased in intensity
$Q_s = Q_w +$	Incision, channel instability, wider and deeper channel	$Q_s - Q_w -$	Processes decreased in intensity
$Q_s = Q_w -$	Aggradation, channel instability, narrower and shallower channel	$Q_s - Q_w =$	Incision, channel instability, deeper and possibly wider channel

The flow responsible for having the most significant impact on channel form is known as the dominant discharge (Wolman & Miller 1960; Pickup & Warner 1976; Ashmore & Day 1988, Soar & Thorne 2001; Copeland *et al.* 2005) while the effective discharge is the minimum discharge necessary for the entrainment of boundary material. Although much of this theory is still challenged, the dominant discharge is one that yields the maximum sediment transport (Wolman & Miller 1960). In typical natural channels in a temperate climate, the dominant discharge occurs when there is a bankfull flow. However, in most engineered incised rivers the dominant discharge is less than the bankfull stage (Benson & Thomas 1966). In the UK, the return period for the dominant discharge can be around one year for gravel bed streams, but it is much less for sand-bedded streams (Hey 1975). However, Wolman and Miller (1960) concluded that low magnitude, high frequency events carrying flows equal or higher than the effective discharges are more important in some cases than rare floods in terms of their cumulative sediment transport.

2.2. RIVER BANK EROSION PROCESSES

Bank erosion occurs primarily through a combination of three mechanisms:

- (1) mass failure,
- (2) fluvial entrainment and
- (3) subaerial weakening and weathering (Couper & Maddock 2001).

'Subaerial events are the smallest in magnitude but the most frequent ones, while mass failures are the rarest but of the highest magnitude, and fluvial erosion is operating between these two' (Couper & Maddock 2001).

Over the past two decades, research has looked at all three aspects of river bank erosion. Preparatory processes have been recognized and researched as a mechanism enhancing fluvial bank erosion (Lawler 1993b; Prosser *et al.* 2000; Couper & Maddock 2001). In particular, frost and needle ice processes have been investigated by Lawler (1986; 1993b). Progress has also been made in understanding and quantifying mass failures and the influence of pore water pressures (Casagli *et al.* 1999; Rinaldi & Casagli 1999; Rinaldi *et al.* 2004; Simon *et al.* 2000; Dapporto *et al.* 2003), progress was made in research of seepage erosion (Chu-Agor *et al.* 2008a; 2008b; Fox *et al.* 2007; Wilson *et al.* 2007) and in understanding the role of riparian vegetation on river bank stability (Abernethy & Rutherford 1998; 2000a; 2000b; 2001; Simon & Collison 2002).

Some researchers have characterized downstream sequences based on the relative dominance of bank erosion processes in relation to channel dimensions, slope, stream power, erosion, sediment transport, deposition and downstream fining of sediments (Lawler 1992b; Lawler 1993b; Hooke 1980; Abernethy & Rutherford 1998). Lawler (1992b) suggested that a river channel can be divided downstream into 'process domains' according to the three mechanisms of erosion prevailing in each domain. In the upper reaches, where stream power is relatively weak and sediments are coarser, subaerial erosion may dominate. In middle reaches, stream power is at a peak and fluvial erosion may dominate (Lewin 1987; Graf 1984; Hooke 1995). Going downstream, the depth is increasing and so where the critical bank height is exceeded, mass failure dominates. Although there is some evidence that 'erosion domain thresholds' exist in the field (Abernethy & Rutherford 1998), these processes are by no means exclusive to any particular river section (Goodson 2002).

Hooke (1980) and Lewin (1987) among others also discovered that on the scale of a river's whole reach, change in one part of the system appeared to initiate or accelerate change in adjacent reaches. This emphasises the need to adopt an integrated approach to river management.

Whether bank material might be eroded by fluvial erosion, mass wasted or weathered through sub aerial processes, depends on a range of factors that could be grouped as follows:

- (1) climatic (e.g. basin scale water balance, climate conditions and weather),
- (2) hydrological (e.g. groundwater levels, precipitation, flows, soil moisture),
- (3) geomorphological (e.g. river channel planform, bank geometry, channel slope, physical and chemical properties of materials),
- (4) biological (e.g. vegetation, grazing and wild animals, humans) and
- (5) chemical (e.g. nutrients, pH, salinity, chemical structure of soil), (Goodson 2002).

These factors are closely dependent on each other and not only can the combinations be complex, the individual factors can also vary on a seasonal or even daily scale (Lawler *et al.* 1997). Taking an example, climate and weather conditions influence the hydrology that would have an effect on the river system but will also impact the biology and chemistry and *vice versa*. Goodson (2002) compares the factors to a complex matrix that could be understood by analogy with the concept of an ecological food web (Begon *et al.* 1996) where a change to one function could lead to a further response by another function in the system or lead to a whole series of changes. In dealing with river restoration and conservation schemes, it is important to understand which characteristics play the most vital roles in maintaining a 'natural' balance (Goodson 2002).

2.2.1. SUBAERIAL EROSION PROCESSES

Subaerial processes loosen the bank prior to fluvial erosion. They can occur in many ways, but all are associated with the moisture condition of the bank material (Thorne & Osman 1988; Dietrich & Gallinatti 1991; Thorne 1992). The higher the moisture content, the weaker the inter-particle forces within the bank material (Wolman 1959; Knighton 1973; Hooke 1979). Increasing moisture in the bank, also known as 'pre-wetting', reduces the ability of the soil to resist the shear forces associated with river flow. Thus, late winter flows in a temperate climate such as that found in the UK are more erosive than similar flows earlier in the season (Wolman 1959; Hooke 1979).

However, low soil moisture can also weaken the bank. Drying cohesive soil shrinks and this results in 'ped fabric' (Fig. 2.2.1) where columns or blocks of soil are separated by desiccation cracks (Thorne & Lewin 1979; Osman & Thorne 1988; Dietrich & Gallinatti 1991). These cracks are planes of weakness in the bank, because cohesion is greater within the peds than between them (Thorne 1990). This process is also referred to as 'fretting'. Less cohesive banks form smaller prismatic or columnar shapes, while more cohesive banks typically generate large thin 'flakes'.



Fig. 2.2.1 An example of river bank with ped fabric structure that has numerous desiccation cracks, on the River Stour in East Anglia (Chapter 1, Fig. 1.1.1). The actual size of peds will be an indication of the mechanical properties of the material (e.g. larger peds would normally be associated with higher cohesive strength).

Temperature extremes can also contribute towards the creation of cracks in the river bank (Lawler 1992b; Thorne 1982). Freeze-thaw processes can be the dominant source of bank retreat in some smaller catchments (Hill 1973; Leopold 1973) with needle ice effect being the most significant. Needle ice crystals grow in the direction of nocturnal cooling whilst lifting or incorporating bank material. During ablation, the incorporated sediment is transported downslope by freeze-thaw action and removed by the flow (Leopold 1973; Lawler 1993b). On a larger scale during melting, cantilevers of ice or floating ice can also cause serious damage to the river banks (Lawler 1993b).

2.2.2. FLUVIAL EROSION PROCESSES

All river banks are controlled by the river flow because the nature and magnitude of erosion processes are determined by the degree of fluvial activity on the channel boundary (Thorne 1978). Fluvial erosion can occur with the detachment and entrainment of boundary particles or by the entrainment of particles that have already been detached through subaerial processes, especially in cohesive banks. Entrainment occurs when the motivating forces applied to a stream bank by flowing water exceed the resistance of the bank surface to withstand these forces (Lawler *et al.* 1997), (Chapter 2.3). This often happens on the toe of the bank (at the water's edge), where the suspended particles scour away the bank soil (Fig. 2.2.2). Bank protection and flow speed are important factors and vegetation can greatly reduce the scour by dissipating the flow velocities adjacent to the bank (Thorne *et al.* 1998).

There are two components of flow on which the erosion of the bank depends: (1) the magnitude of velocity and (2) the tractive force. The velocity necessary to initiate a particle movement is known as the critical velocity (Chapter 3.3). One of the early studies which identified critical velocities for particles of different sizes was by Hjulstrom (1935). He found that critical velocity increased with size in the case of coarse particles (>0.5 mm), but decreased with increasing size in finer particles (<0.5 mm). This anomaly is caused by the strong bonding interparticle forces in a bank composed of cohesive materials. Partly, this is also due to the sheltering of particles finer than 0.5 mm in the viscous sub-layer under hydrodynamically smooth flows (C. Thorne, personal communication 2012).



Fig. 2.2.2 Signs of fluvial erosion illustrated by the exposed erosion pins, research site on the River Stour in East Anglia (Fig. 1.1.1), May 2009.

2.2.2(A) A COMPARISON OF FLUVIAL PROCESSES ON COHESIVE AND NON-COHESIVE BANKS

There are two types of river banks examined in this study: (1) cohesive and (2) non-cohesive. Cohesive banks are generally more resistant to erosion and the erosion rates are lower as the bank material is supported by complex physical-chemical inter-granular forces that depend on mineralogy, dispersivity, moisture, particle size, temperature, pH or electrical conductivity (Thorne 1978; Osman & Thorne 1988). In banks consisting of non-cohesive material, such forces are often very small and thus can be neglected. If no pore pressure or external forces act, the stability of a non-cohesive bank depends on the angles of slope and internal friction (Taylor 1948).

Cohesive materials are seldom well drained and therefore pore water pressure can be an important factor in bank stability (Thorne & Tovey 1981). Rapid drawdown in the channel followed by a high flow event may cause a build-up of positive pore water pressure that acts within the bank to reduce the bank's cohesion. In extreme circumstances, this can lead to complete loss of strength (Lawler *et al.* 1997).

Non-cohesive material is eroded grain by grain. The entrainment depends on the forces acting on the channel boundary: the motivating (erosive) forces are composed of the flow force acting in the direction of flow and the gravitational force. Resisting forces are the interparticle forces of friction and interlocking. Imbrication (overlapping) and packing of non-cohesive materials can greatly increase their resistance to being eroded (Chapter 2.3).

On the other hand, in the case of banks composed primarily of cohesive materials, the cohesive forces are often more significant and the gravity force component causing the particles to roll down can be neglected (Chow 1959).

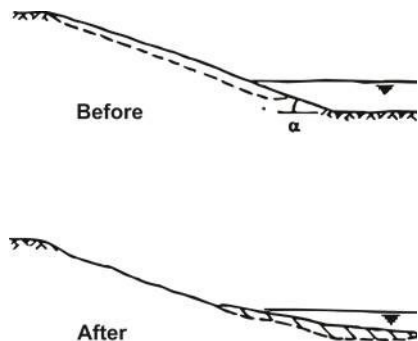
2.2.3. MASS FAILURE

Failure of the bank takes place when the motivating forces exceed the resisting forces of the bank material (Simon *et al.* 1999). These forces are dependent on critical factors that differ with the type of erosion mechanism. These include cantilever failures in undercut banks, shallow slides, rotational slumping or other mechanisms (Fig. 2.2.3).

Fig. 2.2.3 Types of mass wasting on river banks (Hey & Tovey 1989).

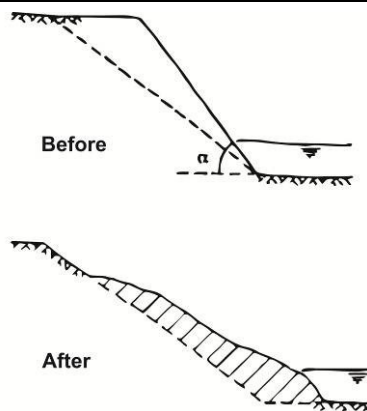
SHALLOW FAILURE

- Shallow bank angle
- Typical for non-cohesive banks
- Failure nearly parallel to slope ($\phi' = \alpha$)
- Water seepage from bank can substantially reduce stable α
- Vegetation will normally be effective to stabilize against failure



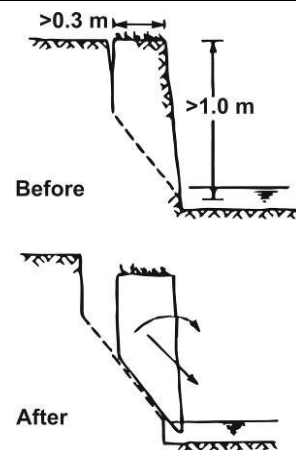
PLANAR FAILURE

- Steep or vertical bank angle
- Typical (with exceptions) in non-cohesive banks
- Water table and channel water usually low relative to bank height



PLANAR/SLAB FAILURE

- Steep or near vertical banks
- Deep tension cracks
- Failure occurs by sliding and/or toppling
- Failure more likely if cracks fill with water
- Little impact from the water table



ROTATIONAL FAILURE IN HOMOGENOUS MATERIAL

- Usually on moderately high and steep banks
- Typical for cohesive bank material
- Tension cracks reduce stability practically when water filled
- Significantly affected by the position of water table
- Failure may extend beyond the toe

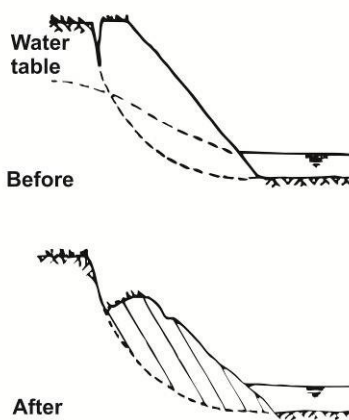
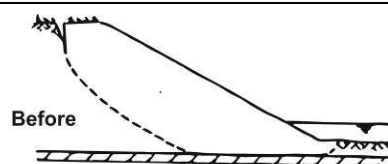


Fig. 2.2.3 Types of mass wasting – continued.

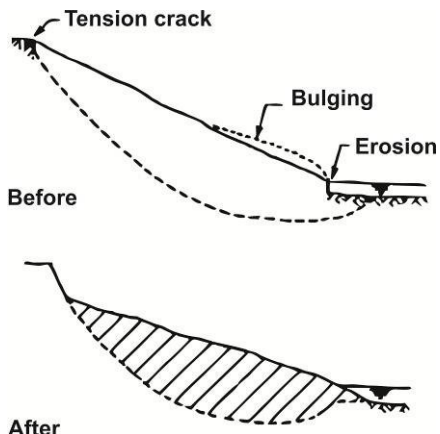
ROTATIONAL FAILURE WITH WEAK ZONE

- Failure surface dictated by position of the weak zone
- Similar to type IV.



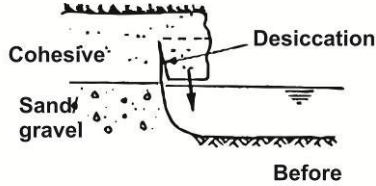
MASSIVE ROTATION FAILURE/LANDSLIDE

- Erosion of river bank threatens the stability of whole valley side
- Very large volume of slipped material
- Tension cracks up valley side with bulging above the bank toe, or noticeable movement are signs of potential failure



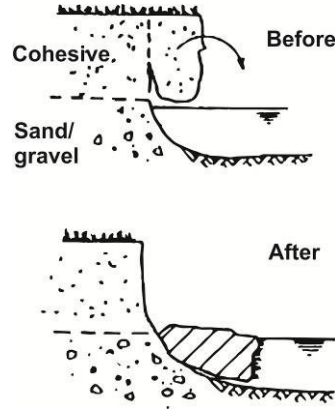
TENSILE FAILURE OF COMPOSITE BANK

- Failure surface dictated by position of the weak zone
- Similar to type IV.



FAILURE OF COMPOSITE BANK AS BEAM

- Occurs as type VII
- Failure with upper soil in tension, followed by rotation
- After failure, block usually remains intact with vegetation towards river
- Failure can also be shear



Resisting forces are a complex function of river geometry, the structure of the bank and its geotechnical properties, the channel flow hydraulics and also climatic conditions (Thorne & Tovey 1981). On the other hand, driving forces are controlled by the bank height and slope, the unit weight of soil and the moisture content (Chapter 3.3). Any surcharge imposed by an object on the bank top, on the surface of the bank or within the bank such as trees, also needs to be considered (Simon & Collison 2002).

2.2.3(A) CRITICAL BANK HEIGHT

When erosion of the bank toe and the river bed adjacent to the bank exceeds the bank height and angle to the level that the components of gravitational force exceed the shear force along a potential failure plane, bank failure is likely to happen (Wolman 1959; Simon 1989b). Banks of various heights will have different types of failure mechanisms. For shallow failures, the critical bank height (H_c) depends on the cohesion (c), unit weight of material (γ), the angle of the potential failure plane to the horizontal (α) and on the friction angle of the bank material (φ). The friction angle varies with soil type and moisture content and it can be determined empirically (Lawler *et al.* 1997):

$$H_c = \frac{4c}{\gamma} \cdot \frac{\sin \alpha \cdot \cos \varphi}{(1 - \cos(\alpha - \varphi))}$$

The parameters of this equation are shown graphically in Fig. 2.2.4.

Tension and desiccation cracks will reduce the effective length of the potential failure surface and thus decrease bank stability (Fig. 2.2.4). The depth of tension cracks is dependent on the material properties of cohesion and unit weight: $\sim 2c/\gamma$. The critical bank height, where a tension crack may extend into around half of the bank height, can be obtained as (Thorne 1982):

$$H_c' = \frac{2c}{\gamma} \cdot \tan(45 + \frac{\varphi}{2})$$

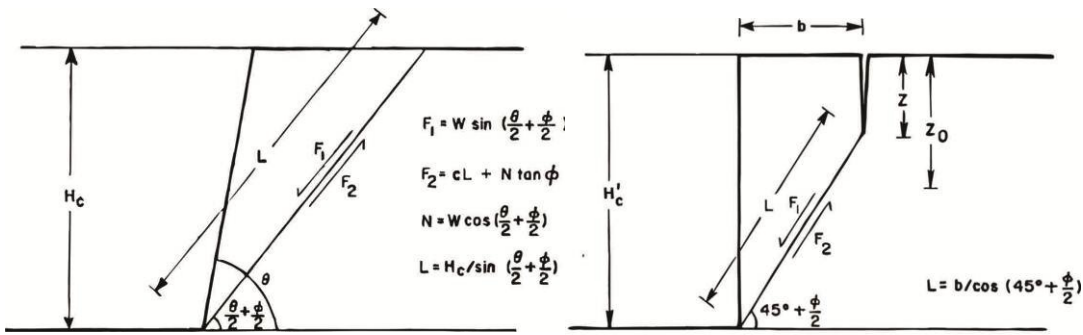


Fig. 2.2.4 Culman's stability analysis for plane slip failure on the river bank (left) and the stability analysis modified to account for effects of tension crack (right), (Thorne 1982).

Tension cracks behind overhanging blocks, where the material below has been removed by fluvial or subaerial processes, will usually result in a cantilever failure. This can occur by three mechanisms: (a) shear (downward failure along a vertical plane) (b) beam (forward rotation of the block about a horizontal axis, in tension above the axis and compression below the axis) and (c) tensile failure (across a horizontal plane), (Thorne & Tovey 1981), Fig. 2.2.5.

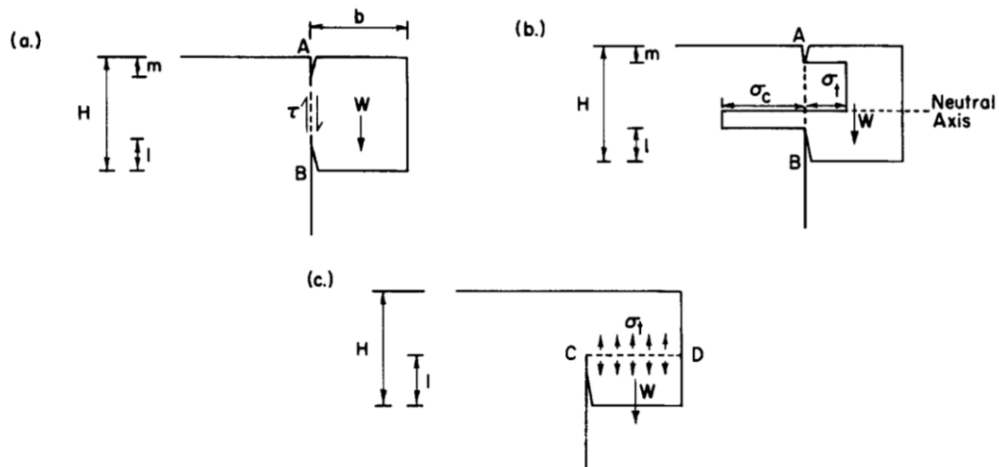


Fig. 2.2.5 Forces of weight, shear, compression and tension acting on a cantilever with regard to the three modes of failure: (a) shear failure (b) beam and (c) tensile failure. Individual stability equations apply for each type of cantilever failure (Thorne & Tovey 1981).

Numerous failed blocks of bank material at the base of the bank and/or tension cracking on the floodplain indicate that mass failure is important and retreat may be rapid (Fig. 2.2.6). Development of cantilevers from the bank indicates that the flow at less than the bankfull level is effective in producing erosion (Hupp & Simon 1986).



Fig. 2.2.6 An example of a recently failed cantilever on the River Stour in East Anglia (Chapter 1, Fig. 1.1.1), February 2009.

If undercutting and cantilever formation is to continue, the fallen blocks of soil must be first removed by fluvial entrainment. Therefore, the rate of bank erosion is controlled by fluvial processes, despite the fact that the failure mechanism of the upper bank is not directly fluvial in nature. This cycle of bank erosion is also referred to as the 'concept of basal endpoint control' (Carson & Kirkby 1972): undermining, cantilever failure and fluvial scour of the toe, operates over several flood events (Thorne & Tovey 1981).

2.3. CONCEPT OF THE FACTOR OF SAFETY

The ratio of driving and resistive forces acting on the potential failure plane is defined as the Factor of Safety (F_s). A F_s value greater than one indicates stability, whilst if it is less than one, failure had already occurred (Thorne & Tovey 1981).

The model for calculating the Factor of Safety for a river bank comes from Thorne and Osman (1988), in which the Factor of Safety varies directly with the cohesion and friction angle and inversely with the soil bulk density, bank slope and bank height. For example, an increase in bank height from 1.0 m to 1.5 m would decrease the Factor of Safety approximately by one third (Micheli & Kirchner 2002).

Mobilising forces of erosion are a function of the maximum shear stresses (τ_{\max}) and the resisting forces relate to the ultimate shear strength (S_r) of the material. At the threshold state, mobilised shear force (which is equal to the relevant shear stress multiplied by the area over which it acts) is equal to the material shear strength over that area. The Factor of Safety (F_s) is then equal to 1. Theoretically, values of less than one should not exist as the bank should have already failed (Hemphill & Bramley 1989).

$$F_s = \frac{\text{soil shear strength } (s)}{\text{shear stress acting on the soil } (\tau)}$$

Variations in bulk density and material saturation can influence the assumption of the Factor of Safety. Ideally, a Factor of Safety largely above the value of unity should guarantee that a failure will not occur. According to Hemphill and Bramley (1989), a value of 1.4 or higher is necessary in some critical situations, for example where a life or property is at risk, however civil engineers use much higher values (R. Kistruck, personal communication 2012).

2.3.1. SHEAR STRENGTH

Shear strength could be described by the Coulomb equation for saturated soils (Craig 2004):

$$S_r = c' + (\sigma - \mu_w) \tan \varphi'$$

Where S_r is the shear strength (kPa), c' is the effective cohesion (kPa), σ is the normal stress (kPa), μ_w is the pore water pressure (kPa) and φ' is the effective friction angle as the maximum friction angle under saturated conditions (degrees). Failure will occur at any point in the soil where a critical combination of shear stress and effective normal stress develops. c' and φ' are normal mathematical constants that describe the relationship between the shear strength and effective normal stress (Fischenich 2001).

For cohesive soils during saturated conditions, the friction angle is reduced to zero and therefore the shear strength is equal to undrained cohesion. For cohesionless soils, the effective cohesion can be regarded as zero, therefore the shear strength is given by (Craig 2004):

$$s = \sigma' \tan \varphi'$$

The undrained shear strength can be estimated *in situ* by shear vane testing, pocket penetrometer or triaxial compression tests (Tengbeh 1989). The effective cohesion and normal stress are obtained from triaxial or shear box testing (Chapter 3.2). Shear stress-strength relationships are shown on Fig. 2.3.1.

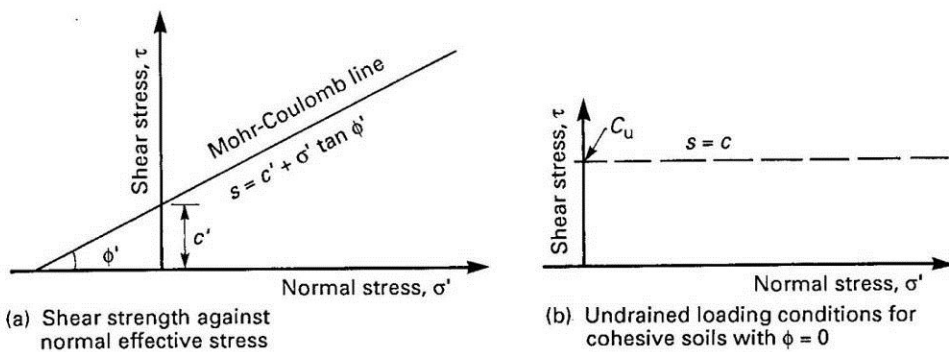


Fig. 2.3.1 Relationship for shear stress and strength of soils (Hemphill & Bramley 1989).

For unsaturated soils, the stabilising effect of negative pore-water pressures, the matric suction ($\mu_a - \mu_w$), needs to be included as suggested by Freudlund *et al.* (1987).

$$S_r = c' + (\sigma - \mu_a) \tan \varphi' + (\mu_a - \mu_w) \tan \varphi^b$$

Where μ_a is the air pressure and φ^b is the rate of increase in shear strength resulting from increasing matric suction. The term 'apparent cohesion' has been introduced to account for effective cohesion as well as for the cohesion due to matric suction:

$$c_a = c' + (\mu_a - \mu_w) \tan \varphi^b$$

Cohesion resulting from matric suction can be envisaged as the attraction of water molecules towards each other in the void space between unsaturated soil particles, generating a suction or negative pore-water pressure that binds the attached soil particles together (Ward & Robinson, 1990). The size of this force varies with the degree of saturation, pore characteristics and other material properties (Chapter 3.2).

2.3.2. SHEAR STRESS

On the other hand, the removal of bank material depends on the driving hydraulic forces. The mean boundary stress caused by the flow can be defined as:

$$\tau_0 = \gamma_w d S_w$$

Where τ_0 is the mean boundary shear stress (Pa), γ_w is the unit weight of the water (N/m^3), d is depth (m) and S_w is water surface slope. However, this is only the case in straight channels with uniform two-dimensional flow (Hemphill & Bramley 1989).

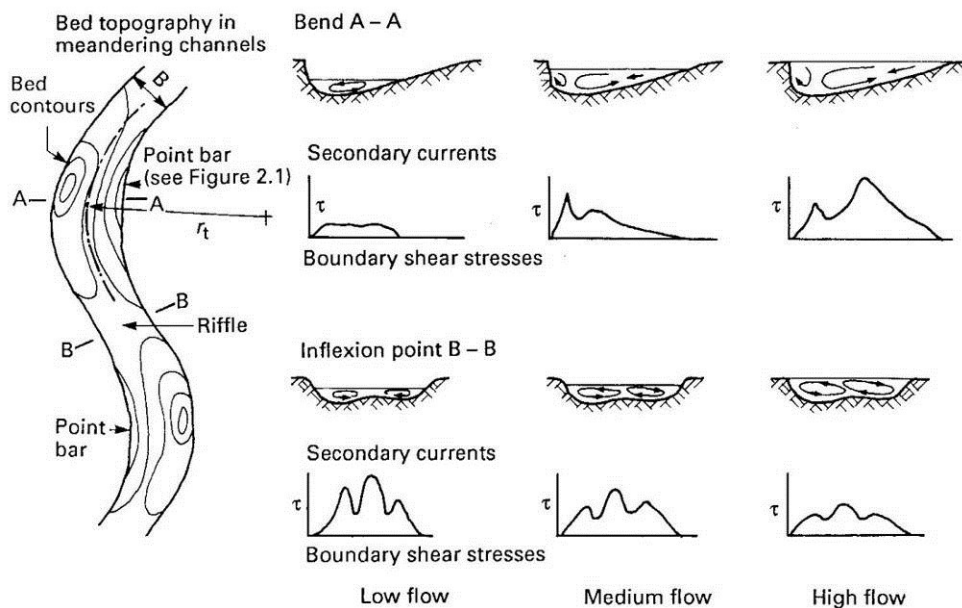


Fig. 2.3.2 Patterns of secondary flows and boundary shear stresses in meandering channels (Hey 1986).

In natural channels, secondary flows produce complex variations of boundary shear stress (Hemphill & Bramley 1989; Thorne 1978). Boundary shear stress is, at any point, proportional to the velocity gradient but this relationship is influenced by water slope or backwater (Thorne 1978). As a result, it is not possible to theoretically predict the shear stress distribution (Hemphill & Bramley 1989).

Within one stretch of a river, shear stresses would vary significantly between the riffle and pools sections and along meanders. In meanders, secondary flows operate in upwelling (away from the bed) or downwelling (towards the bed) directions (Bathurst *et al.* 1979). Scouring occurs on the outside bank of the meander bends (Fig. 2.3.2). Highest shear stresses occur at the bankfull discharge. During overbank flows, shear stresses are reduced due to flow separation (Hey 1986).

2.4. EFFECTS OF VEGETATION ON RIVER BANK STABILITY

Vegetation is believed to increase the stability of riverbanks (e.g. Coppin & Richards 1990; Thorne 1990; Abernethy & Rutherford 1998; Simon & Collison 2002) and empirical research has demonstrated that alluvial channels supporting well-developed riparian vegetation are deeper, narrower and are migrating more slowly than their cleared equivalents (Graf 1978; Hickin 1984; Andrews 1984; Hey & Thorne 1986).

The stabilising effects of plants include the reinforcement of soil by root systems and the reduction of soil moisture content through canopy interception and evapotranspiration (Greenway 1987, Coppin & Richards 1990; Simon & Collison 2002). Vegetation stems and foliage will also reduce near bank velocities and shear stresses thus reducing fluvial erosion (Gray & Sotir 1996; Li & Eddleman 2002). Even low root densities can provide substantial increases in shear strength compared to non-root-permeated soils. Unfortunately, the precise role that vegetation plays is often elusive and complicated, making it difficult to separate and quantify its effect (Thorne 1990; Abernethy & Rutherford 1998; Gregory & Gurnell 1988; Hupp 1986) and as a result, this makes vegetation a less trusted method amongst some river engineers (Chapter 1).

Soil is strong in compression but weak in tension. Conversely, the fibrous roots of trees and herbs are strong in tension but weak in compression (Thorne 1990). Therefore soil penetrated with roots makes a composite material that has enhanced strength (Gray & Leiser 1982; Bischetti *et al.* 2005), Fig. 2.4.1.

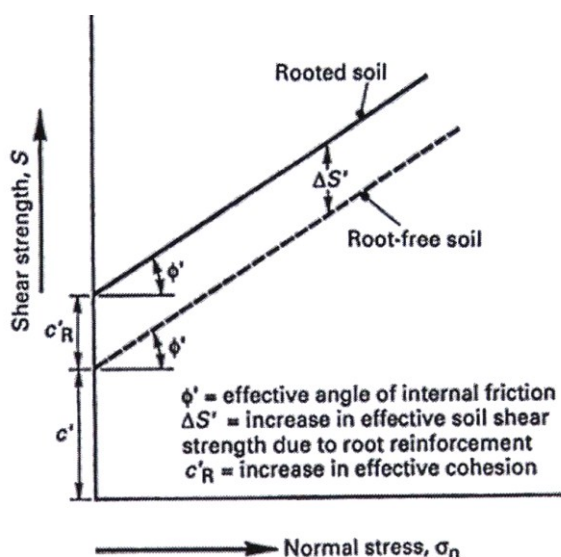


Fig. 2.4.1 Contribution to soil cohesion through the presence of root systems. Soil with roots has similar values for the angle of friction (ϕ) as soil without roots (Coppin & Richards 1990).

To estimate the additional strength of soil due to roots, Wu (1976) developed an equation where the contribution of roots can be considered as the additional apparent cohesion c_r that is a function of a root tensile strength, areal density and root distortion during shear:

$$c_r = K \cdot t_r$$

Where t_r is the mobilised root tensile strength per soil unit area and K is the factor taking into account that roots are randomly orientated with respect to the failure plane and it generally varies between 1.0 and 1.3 (Waldron 1977; Wu *et al.* 1979). However, Wu's perpendicular model (1976) has been criticised by Waldron and Dakessian (1981), Pollen (2004) and Pollen *et al.* (2004) on the basis that it overestimated the effect of roots. It assumed that the full tensile strength of each root is mobilised during soil shearing and that all roots break at the same time (Pollen 2007; Tosi 2007). To correct this, the fibre-bundle model (RipRoot) was developed by Pollen and Simon (2005) to incorporate the progressive processes that take place during bank failure.

When water is present in the soil and a steady downslope seepage condition prevails, the soil shear strength aided by the roots can be described as (Freudlund *et al.* 1987):

$$S_r = c' + c_r + (\sigma - \mu_w) \tan \varphi$$

Where total normal stress (Chapter 2.3.1) is replaced by an effective stress $(\sigma - \mu_w)$, where μ_w is the pore water pressure.

Fibrous roots are more important in increasing soil strength than thick roots (Thorne *et al.* 1998). A non-linear, inverse relationship between root diameter and strength per unit area is commonly used. Optimum species for root stabilisation are therefore considered to be grasses and shrubs which combine large numbers of small strong roots with little surcharge (Thorne *et al.* 1998).

On the other hand, main roots intersect the shear plane and act as anchors (Coppin & Richards 1990). The effects vary with vegetation types and species but in general, the higher the bank, the less effective is the vegetation on top in reducing collapse. Tree roots can anchor the soil to a depth of at least two metres and to a distance equivalent to the canopy dripline. However, roots in well drained soils will go deeper but roots directly above ground water level will spread laterally (Coppin & Richards 1990), which is important to consider with regards to the potential failure plane. Roots need to reach

down at least to the average low water level to minimise the undercutting (Rowntree 1991).

Vegetation serves as a buffer between the water and underlying soil. While it increases the effective roughness of the boundary it also increases the flow resistance and displaces the velocity away from the soil. As the boundary shear stress is proportional to the square of the near bank velocity, reduced velocity thus means greater reduction in the boundary forces responsible for erosion. Large strands of vegetation may also act to suppress small scale eddies which will further reduce the erosive attack of the flow on the bank (Coppin & Richards 1990; Thorne *et al.* 1998).

Grasses and other herbaceous plants are effective in protecting the soil surface for certain velocities but their impact decreases as velocity increases. Stiff woody stems can, on the other hand, retard the flow up to high velocities (Chapter 5.5) but they can also cause local scour through convective acceleration around their trunks (Thorne *et al.* 1998), Fig. 2.4.2. Dense enough spacing of tree trunks or shrub vegetation with flexible stems may prevent this from happening.



Fig. 2.4.2 Bank scour caused by back eddies scouring around the solitary tree trunk upstream of research site on the River Stour in East Anglia (Chapter 1, Fig. 1.1.1), May 2009.

Flexible woody stems offer much greater bank protection than herbaceous bank colonisers near the water margin. Particularly when the above and below ground effects are combined and thus the density of vegetation and its distance and continuity from the water margin to the top of the bank are likely to be important (Thorne *et al.* 1998).

Different vegetation type may vary in its rooting depths and forms and in root tensile strengths. Table 2.4.1 shows examples of tensile strengths for some common UK species.

Table 2.4.1 Root tensile strength for selected plant species.

Vegetation type	Species	Tensile strength (MN/m ²)
Grasses and herbs	<i>Elytrigia repens</i> (L.) Desv. ex Nevski. (Couch Grass)	7 – 25 ⁽¹⁾
	<i>Convolvulus arvensis</i> L. (Field Bindweed)	5 – 21 ⁽¹⁾
	<i>Plantago lanceolata</i> L. (Ribwort Plantain)	4 – 8 ⁽¹⁾
	<i>Trifolium pratense</i> L. (Red Clover)	11 – 19 ⁽¹⁾
Trees and shrubs	<i>Alnus incana</i> (L.) Moench (Grey Alder)	32 ^(1,2)
	<i>Betula pendula</i> Roth. (Silver Birch)	37 ⁽¹⁾
	<i>Populus nigra</i> L. (Black Poplar)	5 – 12 ⁽¹⁾
	<i>Rosa canina</i> L. (Dog Rose)	19-25 ⁽³⁾
	<i>Quercus robur</i> L. (Pendunculate Oak)	32 ^(1,2)
	<i>Salix purpurea</i> L. (Purple Osier)	36 ⁽¹⁾
	<i>Salix fragilis</i> L. (Crack Willow)	18 ⁽²⁾
	<i>Salix cinerea</i> L. (Grey Willow)	11 ^(1,2)

Schiechtl & Horstmann (1980)¹, Greenway (1987)², Tosi (2007)³

In terms of flood protection, many engineers believe that vegetation significantly reduces channel capacity. Therefore it is cleared away despite the fact that the vegetation will dissipate the flow energy and will also trap floating debris and prevent it from accumulating at more vulnerable constructions such as bridge piers (Thorne *et al.* 1998). Removal of vegetation also causes other sediment related issues and because of the lack of vegetation, frequent desilting or dredging is required. The contribution of vegetation to bank stability, both positive and negative, is summarised in Table 2.4.2.

Table 2.4.2 Contribution of vegetation to erosion control and bank stability. Adverse effect -; beneficial effect: +; occasional effect under conditions described in the table: (+/-), (Coppin & Richards 1990).

Hydrological effect	
Rainfall interception reducing amount of water available for infiltration	+
Greater roughness to flow, reducing its velocity. Flexible stems may lay prone in the flow and protect the soil surface	+
Isolated trees may cause local eddying and higher flow velocities	-
Roots open up the soil and increase infiltration; beneficial if banks are desiccated	-/(+)
Roots extract moisture which is lost to the atmosphere by transpiration, thereby lowering pore water pressures; may lead to instability if pore water pressures are already low	+/-
Roots accentuate desiccation cracks but their tensile strength may reduce potential for cracking	-/+
Mechanical effects	
Roots increase the strength of the soil through a matrix of tensile fibres	+
Roots increase the shear strength of the soil through a matrix of tensile fibres	+
Roots penetrate deep strata to anchor the soil mantle to subsoil and bedrock	+
Root support the upslope mantle through buttressing and arching	+
Weight of tall trees may surcharge the bank, increasing downslope and normal force components	-/+
When exposed to wind, dynamic forces of air movement are transmitted to the ground	-
Root development may be limited by the water table to the upper bank; undermining the lower bank where no roots have developed leads to slab or Cantilever failure	-

2.5. RIVER BANK EROSION MANAGEMENT

River maintenance is frequently undertaken to preserve the river channel's capacity to convey floods, increase visual aesthetics, conservation value and geomorphic stability. Maintenance includes the removal of channel and bank vegetation, and dredging (Darby & Thorne 1995). However, routine maintenance is often unnecessary and in many cases counter-productive to the river habitat and channel stability. As an example, dredged materials are often dumped on top of the river bank, which makes the banks higher and therefore more prone to failure. There are many alternative approaches available that would reduce the impact of routine maintenance but could still keep the river channel up to standard with regards to flood protection and land drainage. Reviews by Darby & Thorne (1995) and Sear & Newson (2003) suggest that economic and environmental impacts associated with fluvial maintenance can be reduced by (a) improving the efficiency of maintenance tasks, (b) reducing the intensity of maintenance and (c) considering future maintenance requirements at the design stage of new projects in order to reduce the overall need for fluvial maintenance. The Water Framework Directive places a legislative requirement on EU Member States to monitor the physical condition of the country's river network and make changes to meet given targets (EC 2000). The improvement of a river's ecological status needs to be incorporated into river channel management plans. This section of the thesis presents the types of river bank erosion management generally used, including those approaches that could contribute towards the improvement of the ecological status of rivers.

2.5.1. RIVER BANK EROSION MANAGEMENT APPROACHES

Before a specific strategy for bank protection is chosen, the preferred solution should be weighed against the competing priorities and interests for the given river stretch. For example, flood defence or minimal channel properties for navigation, or improving the ground water level and protection of the infrastructure. At the same time, the solution should contribute to habitat enhancement and help to preserve the river as an amenity for angling or other leisure pursuits. The final approach should also be compatible with natural processes and complement or enhance geomorphological processes, contributing to a dynamically stable river channel (Morgan *et al.* 1999). It is rarely possible to satisfy all interests, although the author believes that alternative, vegetation-based approaches provide more benefits than hard engineering. Thorne *et al.* (1996a) argue that engineering

design and management approaches that work with, rather than against, natural processes, provide more successful solutions to river instability problems. These are also cheaper in the long term and result in fewer unwanted side effects somewhere else in the fluvial system.

In this section, four main approaches are summarised in the order that they should be considered when assessing a river bank erosion problem. Detailed methodological approaches for selecting the most suitable solution were published by Hemphill and Bramley (1989), Coppin and Richards (1990) and Morgan *et al.* (1999). Specific references to the preliminary conditions for applications using the ground bioengineering method known as willow spiling are made in Chapter 4.

2.5.1(A) ALLOWING FOR NATURAL CHANNEL ADJUSTMENT

Natural adjustment should be the first option considered in the management of river bank erosion (Morgan *et al.* 1999). This approach is particularly important when the investment in engineering cannot be justified on financial or environmental grounds, or where the bank modification could cause instability upstream or downstream. The tendency of a bank to meander and therefore to erode, transport and deposit sediment is a natural process for river channels. And eroding banks will stabilise over time. Even heavily modified rivers have a tendency to restore their natural dynamic stability and the author observed a number of straightened rivers across East Anglia which had subsequently developed a tendency to meander. This dynamic is important as it increases the flow variability which would in turn increase the diversity of habitats. If the dynamism within a river environment is reduced, for example by stabilising a river bank, the quality and diversity of habitats will also be reduced (Sear *et al.* 2004). If the erosion is caused by artificial processes (e.g. boat wash, cattle trampling, fishing etc.) an approach to manage these causes should be implemented (by either restriction or relocation of the problematic activity). This approach is also referred to as a 'positive management of the bank' (Morgan *et al.* 1999).

2.5.1(B) GROUND BIOENGINEERING

The second consideration is ground (or soil) bioengineering, which utilises the positive effects of vegetation to aid river bank stability (see Chapter 2.4). A bioengineering approach to water engineering has been carried out for centuries and is becoming

gradually popular in modern civil river engineering in the UK, but this is not solely because of its geotechnical functionality. Living structures are more pleasing to the human eye than hard engineering and enhance stream habitats (Li & Eddleman 2002). A range of vegetation-based methods exist and are grouped by Gray and Sotir (1996) under the term 'soil bioengineering'.

There are numerous guidelines and methodologies for soil bioengineering that refer to the use of willows in civil engineering projects (*e.g.* Brooks & Agate 1981; Hemphill & Bramley 1989; Coppin & Richards 1990; Gray & Sotir 1996; Schiechtl & Stern 1996, 1997; Allen & Leech 1997; Bentrup & Hoag 1998; Morgan *et al.* 1999).

Ecologically, soil bioengineering methods offer a natural restoration solution (Gray & Sotir 1996; Schiechtl & Stern 1997) and enhance the aesthetic value of a stream (Ree & Palmer 1949; Parsons *et al.* 1963; Schiechtl & Horstmann 1980), (Fig 2.5.1). The most commonly used ground bioengineering methods are described by Schiechtl and Stern (1997) and Hemphill and Bramley (1989). Schiechtl and Stern (1997) used their experience of observing vegetative protection measures on banks of rapidly flowing watercourses in an Alpine region. Vegetation measures that can withstand the erosion forces of torrent streams were more likely to be effective for most erosive situations, including those stretches along spillways and below weirs. Gerstgraser (2000) built and tested common bioengineering methods on an artificial flume in the Austrian Alps, observing them fail or succeed.



Fig. 2.5.1 Revetment using willow stakes, hazel faggots and reeds for river narrowing and habitat improvement, the River Shep, Cambridgeshire (TL384473), April 2008.

Schiechtl and Stern (1997) grouped water bioengineering systems by type of bank protection into: (1) soil protection measures (turf establishment, grass seeding, direct shrub and tree seeding, seed matts or live brush matts) and (2) ground stabilisation (live cuttings, wattle fence and wattles, live willow spiling, hedge or brush layers).

2.5.1(C) BIOTECHNICAL SOLUTIONS

This approach combines the stabilising function of vegetation with some inert material. A range of materials is often used, from geotextiles to gabions, rip-rap or cellular concrete blocks, which provide additional strength which is necessary, for example, during the vegetation establishment period. Hybrid solutions have been used with great success (Allen & Leech 1997; Watson *et al.* 1997; Li & Eddleman 2002) and some further references to this approach are made in Chapter 4. Schiechtl and Stern (1997) call these 'combined construction techniques' and review a range of strategies to implement them, such as live deflectors, reed rolls, stone revetments reinforced by cuttings etc.

2.5.1(D) STRUCTURAL ENGINEERING

Also referred to as 'hard' engineering, structural engineering was widely applied during the 20th century. It relied heavily on hard structures such as concrete walls, rock, sheet piling, rip-rap, gabion mattresses etc. (Simon & Steinemann 2000). Many government agencies favoured these because this type of intervention provided a high degree of precision and reliability during planning and construction, but increasing failures of these methods, notably during the 1980s and 1990s, started to raise questions about their appropriateness in every setting (Li & Eddleman, 2002; Hoag & Fripp 2005).

Structural engineering should be viewed as the last resort, only to be used when the other strategies have been ruled out and there is a serious risk to property or safety. Implementation of hard engineering on a grazed floodplain, for example, is unjustified. Gabion baskets (Fig. 2.5.2) are, by far, the most popular method for protecting river banks on the River Stour in East Anglia, with the aim of preventing loss of riparian land.



Fig. 2.5.2 Example of a two-tiered gabion revetment, flood relief channel upstream on the River Stour in East Anglia (Chapter 1, Fig. 1.1.1).

However, an increasing number of observed failures of these and other hard engineering revetments (Fig. 2.5.3), together with their relatively high financial cost and environmental impact, started to raise questions about the suitability of these solutions not only in a rural setting, but also overall.



Fig. 2.5.3 Gabion revetment on the River Stour (Chapter 1, Fig 1.1.1). The arrow points to the location of a large scour at the end of the revetment. Note also the sliding tree that is falling into the channel.

This chapter has presented the main concepts in channel stability, outlined the role of vegetation and featured four types of river management approaches for river bank erosion control. It set the scope for the field study of river bank erosion rates (Chapter 3) and conceptualised one particular approach to bank protection, willow spiling (Chapters 4 & 5), an ecological approach to managing river bank erosion.

3. RIVER BANK EROSION RATES

3.1. STUDY AREA

3.1.1. GEOGRAPHIC, CLIMATIC AND HYDROLOGIC CHARACTERISTICS OF THE CATCHMENT STUDIED

The River Stour is located in East Anglia, England. It rises in eastern Cambridgeshire, passes through Suffolk to Sudbury and eventually joins the North Sea in Essex. It forms most of the county boundary between Suffolk to the north and Essex to the south (Fig. 3.1.1 and Fig. 3.1.A in the Appendix). The name 'Stour' comes from the Celtic 'Sturr' meaning strong (Mills 2003).

The river is 108.5 km long and drains an area of 1,044 km². Geology is represented by Cretaceous chalk covered with boulder clay, fluvial sands and gravels. Maximum discharges and prolonged wet periods usually occur during winter months. During dry months, flows are enhanced by a water transfer scheme to fill Essex reservoirs, providing up to 3.8 m³/s of additional water into the river. This amount indicates that in such conditions the flow may be over double the natural flow and is much higher than the average flow of 0.83 m³/s. The annual rainfall in the catchment area over the last 20 years is between 550 to 600 mm. Annually, around 40% of rainfall in the catchment enters the river and aquifer system and 60% is lost by evapotranspiration. The Base Flow Index (BFI), which describes the contribution of ground water to the river flow, varies between 52 and 43%. Table 3.1.1 illustrates the main geographic, climatic and hydrologic data for the five river's gauging stations.

Table 3.1.1 Main geographic, climatic and hydrologic data for five gauging stations on the River Stour ordered from upstream to the estuary near Stratford St Mary. The rainfall and flow data are long-term averages (Based on National River Flows Archive data, 2010).

Flow gauging station	Drainage area (km ²)	Station altitude (m AOD)	Maximum altitude in drainage area (m AOD)	Annual rainfall (mm)	Q_{mean} (m ³ /s)	Q_{95} (m ³ /s)	Q_{10} (m ³ /s)
Keddington	76.2	52.5	122	599	0.83	0.047	2.317
Westmill	224.5	33.2	126	589	1.34	0.137	2.725
Lamarshe	480.7	17.5	128	583	2.51	0.587	4.664
Langham	578.0	6.4	128	580	3.05	0.571	6.443
Stratford	844.3	5.4	128	578	3.1	0.566	7.644

Nine research sites were selected along the River Stour in East Anglia and monitored for erosion over a period of five years 2006 – 2010 (Fig. 3.1.1).

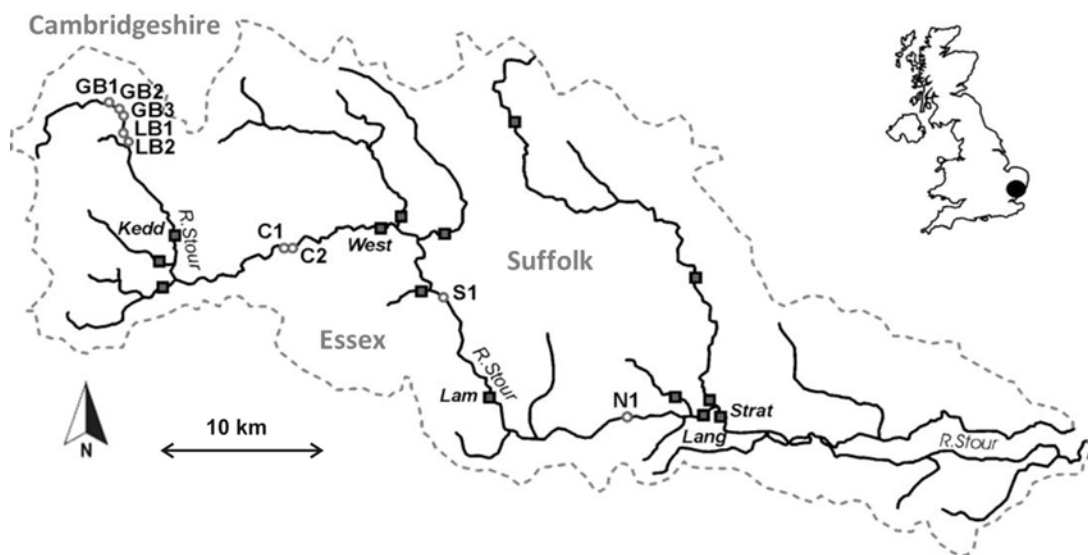


Fig. 3.1.1 The River Stour catchment with the locations of the nine field sites (Great Bradley: GB1, GB2, GB3, Little Bradley: LB1, LB2, Clare: C1 and C2, Sudbury: S1, Nayland: N1) and network of gauging stations. The gauging stations on the main river are marked with an abbreviation of their location (Keddington (Kedd); Westmill (West); Lamarsh (Lam); Langham (Lang) and Stratford St Mary (Strat)). The dotted line represents the surface drainage watershed of the river.

3.1.2. LONG PROFILE AND RIVER SINUOSITY

The river's headwaters rise at 109 m AOD and the river bed slope drops 50 metres during the first 14.5 km. The maximum gradient changes from 6.7 to 0.53 m/km and there is a near zero gradient in the last 22 km before the river enters the estuary. A long profile of the river with the locations of the field sites is shown on Fig. 3.1.2. The distances and elevations have been obtained from a contour plot of the area at the scale of 1:10 000 (OS Map 2010) in ArcGIS. This method is described in more detail in Chapter 3.2.

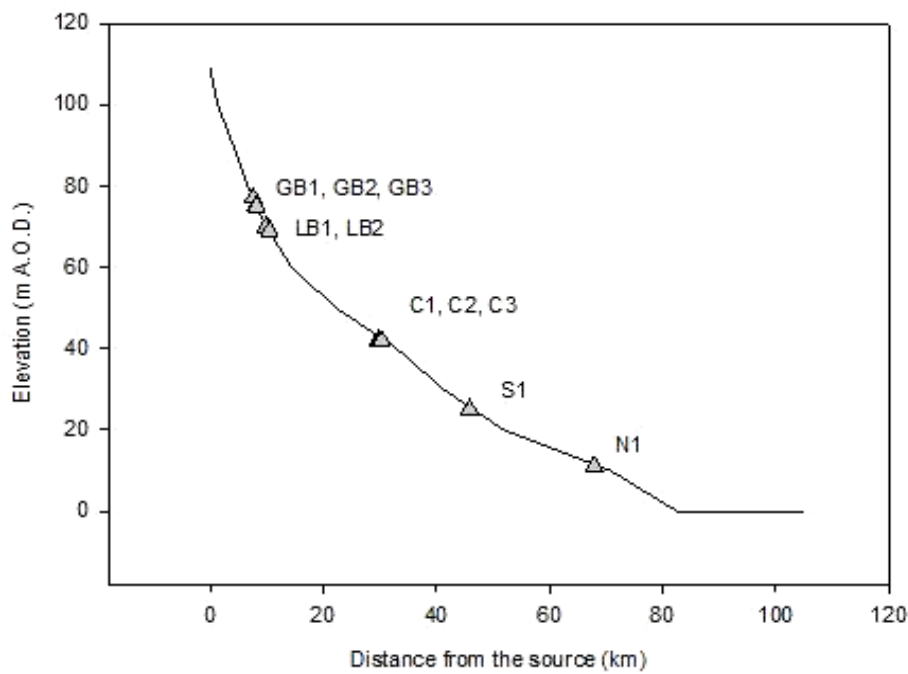


Fig. 3.1.2 Long profile of the River Stour showing positions of the field sites. (Based on data from the analysis of OS 1:10 000 maps.)

The reach-specific sinuosity of the main river channel has been calculated as a ratio of channel length to the length of adjacent floodplain for each 10 metres of elevation. In the upper reaches, sinuosity was as low as 1.0 while in the lower reaches sinuosity was at its maximum of 1.33 (Fig. 3.1.2). The relationships between increasing sinuosity with distance from the source, decrease in elevation and relationship with the river gradient are illustrated in Fig. 3.1.3. Sinuosity grows linearly with increasing distance downstream ($R^2=0.778$) but there is an exponential decay with increasing elevation ($R^2=0.764$) and river bed gradient ($R^2=0.448$). The river bed gradient is also related to elevation and it decreases with distance going downstream (see slope of curve on Fig. 3.1.2). This is a typical pattern for UK rivers, where the gradient gradually drops from the upper reaches down to the confluence or sea as the valley gradient also drops, the floodplain becomes wider and the river meanders. Both the gradient and the sinuosity of the studied river channel were, and continue to be, altered by human interventions. Historical mill channels, weirs, sluices, flood relief channels and straightened sections influenced the river gradient. The relationship between the distance from weirs, slopes and site-specific sinuosity (calculated as a ratio of the site's bend length to valley distance) is presented in Chapter 3.2.

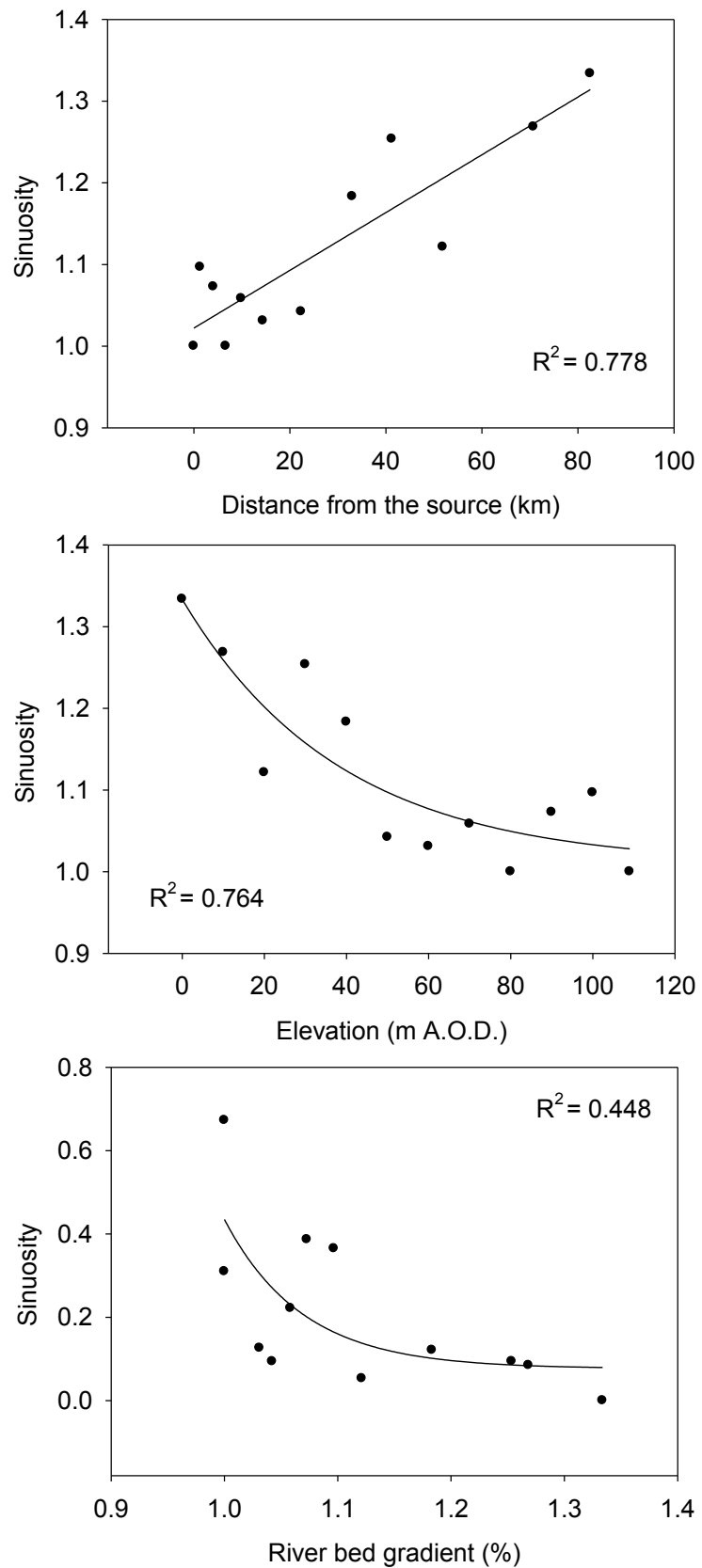


Fig. 3.1.3 River sinuosity versus distance, elevation and river bed gradient based on 10 m elevation contour intervals. (Based on data from analysis of Ordnance Survey 1:10 000 maps).

3.1.3. LAND USE

The upper reaches of the river are arable and the lower reaches are used mostly for grazing by cattle and sheep. As recorded in 2005, the catchment land use was mainly arable (75.5%) with the remaining part created by grassland (13.9%), woodland (6.1%) and built-up areas (1.7%), (CEH 2005). Agriculture is the largest source of diffuse pollution in the catchment and the river floodplain is a Nitrate Vulnerable Zone (EA 2011).

The river has been extensively modified and together with a straightened and re-profiled channel, the lack of riparian cover, low rainfall and intensive agriculture result in poor water quality. The whole river is classified as eutrophic, with a 10 km long reach downstream of Keddington (Fig. 3.1.1) classified as hypertrophic with high concentrations of nitrates and phosphates in the water (EA 2011). Typical fish found are dace, roach, chub and bream. Species important for their conservation value also occur here, for example brown trout, brook lamprey and bullhead (EA 2011).

Part of the Stour valley is designated as an Area of Outstanding Natural Beauty (AONB) with numerous Sites of Special Scientific Interest (SSSI) and local wildlife sites (Fig. 3.1.A in Appendix). In particular, the estuary saltmarshes, heathland and water meadows are rich in rare flora and fauna. Species-targeted conservation work to protect barn owls, bats, water voles, otters and other declining species is starting to pay off, as is evident from more frequent sightings of these animals (N. Oliver, A. Walters, personal communication 2010).

3.1.4. HISTORY OF RIVER MANAGEMENT ON THE RIVER STOUR

The River Stour was one of the first modified rivers or canals in England. In 1705, Parliament passed an act to make the river navigable from the tidal reach to Sudbury. The 1795 canalisation of the Stour added 15 locks and the towpath crossed the river 33 times. Barges were drawn by two horses going upstream and by one horse going down. The 40 km long journey took 14 hours upstream and 12 hours down. The horses were trained to jump on and off the barges and were ferried across the river when the towpath changed sides. In the early days of navigation, they had also to jump stiles between fields. Later, the stiles were replaced by gates (Marriage 2001).

Although partly replaced by railway, lighters (the type of barges used on the river) were still working on the Stour almost until World War II. Today, the river is only navigable by motor craft for a few kilometres downstream from Sudbury, but canoes and other small

boats that can be lifted over the sluices can continue on a 37 km route to Cattawade near the river's estuary (RST 2012).

The Stour used to have 23 water mills on it, some dating back to Roman times, with the first located along the river in Keddington. The painting by John Constable 'The Haywain' (Fig. 3.1.4) has become an icon of the English countryside, and with it, the actual landscape it represented. One hundred and sixty four years later, in 1984, the Anglian Water Authority applied for permission to carry out a land drainage scheme on the Stour near Flatford Mill (Stratford St Mary) with the aim of turning the picturesque riverside pasture to oil-seed rape. Mr Constable, the painter's great grandson, protested in *The Times* newspaper: 'Believe me, rape is what we are talking about.' (Purseglove 1988).



Fig. 3.1.4 John Constable's 'Haywain' from 1821 from a site in Suffolk, near Flatford (Stratford St Mary) on the River Stour. The hay wain is a type of horse-drawn cart.

The largest impact on the river channel in present times has been the result of river management associated with land drainage, flood protection and water supply. The River Stour is part of the Ely Ouse to Essex Water Transfer Scheme which brings water from the northerly flowing River Great Ouse southwards. The impact of the water transfer scheme has, in part, led to the present study. The transfer scheme is therefore described in more detail in the Section 3.1.5 and its possible effects on river banks are discussed in Chapter 3.5.

3.1.5. ELY OUSE TO ESSEX WATER TRANSFER SCHEME

Essex is the driest county in the UK. It receives only 50% of the national average annual rainfall in a normal year (EA 2011). This means that the amount of available water is low and only half the water supplied to households in the Essex area is sourced from within the county. In a dry year, up to one third of the required water is derived from the Ely Ouse to Essex Water Transfer Scheme (EOETS), which has transferred water from Denver in Norfolk, *via* pipelines and pumping stations to the River Stour and then to the River Blackwater in Essex since 1972 (ESW 2005), Fig. 3.1.6. As outlined in Chapter 1, low average rainfall and rising demand for water creates significant challenges to fulfil the needs of a growing population. The East Anglian region had the UK's highest percentage increase in population between 2001 and 2009 at 6.8% with a projected increase to 6.9 million residents by 2028 - 20% more than in 2008 (ONS 2011).

The water that supplies the scheme comes from the River Great Ouse. It is transferred to the flood protection scheme 'Cut-off Channel' at Denver *via* a complex that sends water in the opposite direction (Fig. 3.1.5).



Fig. 3.1.5 Aerial view of the Denver Complex in Norfolk (ESW 2011).

From there, the water is sent 25 km south in a reverse direction to Blackdyke, Feltwell (Fig. 3.1.6). Here it is transferred into a 20 km long tunnel to Kennet pumping station and then it is pumped uphill along a 14 km pipeline to Kirtling Green and into the Kirtling Brook which takes the water to the River Stour near Great Bradley (Fig. 3.1.6).

At Wixoe, part of the water can be abstracted from the River Stour for transfer into the River Chelmer. The rest of the transferred water travels from Wixoe down the River Stour to abstraction points at Langham, Stratford St Mary and Branham Mill (Cattawade). Here

it is taken for treatment at Langham Water Treatment Works (WTW) or travels through pipelines to the Abberton reservoir before it is treated at WTW there (Entec 2007), see photographs on Fig. 3.1.7.

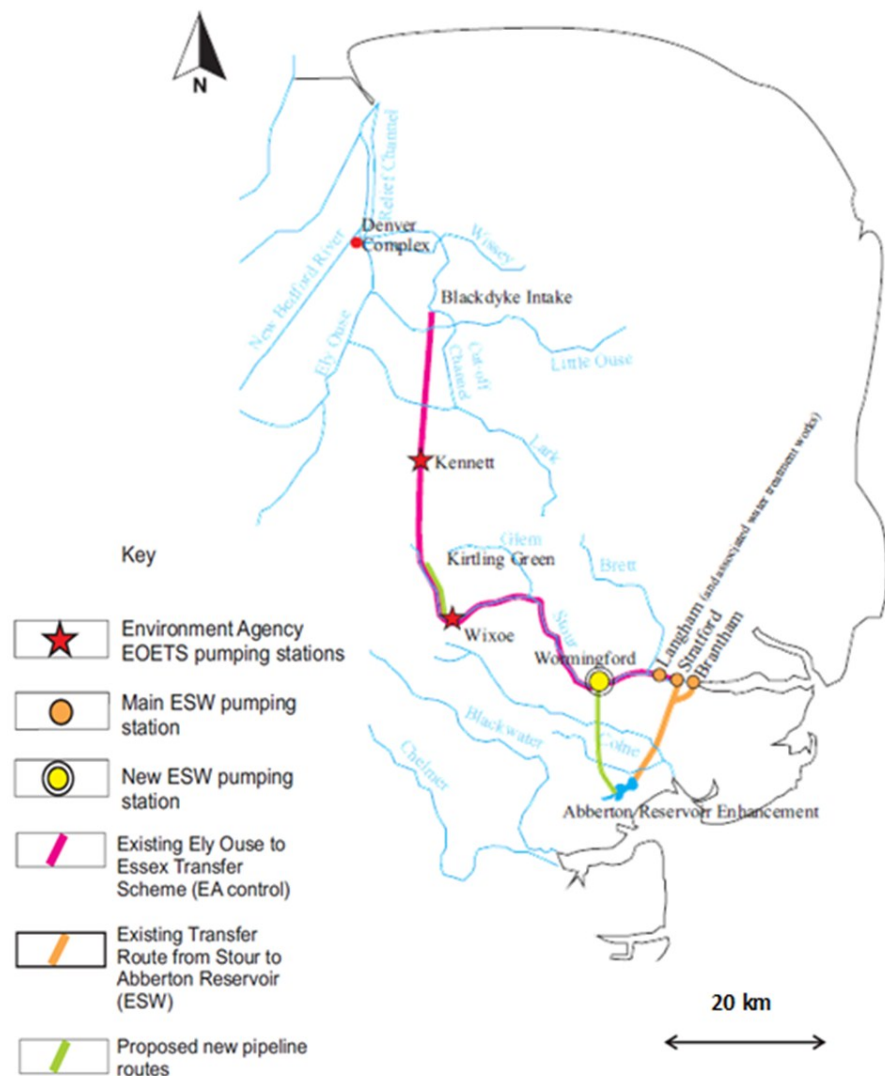


Fig. 3.1.6 Schematic map of the Ely Ouse to Essex Water Transfer Scheme (Entec 2007).

Additionally, flows are supplemented by the Environment Agency's Stour Augmentation Groundwater Scheme (SAGS). This uses pumping stations along the upper stretches of the river to abstract water from the underground chalk aquifers and put it into the river to be taken to the Essex reservoirs.



Fig. 3.1.7 The Stour part of the Ely Ouse to Essex Water Transfer Scheme (EOETS): (A) Outfall from the Kirtling pumping station, looking upstream; (B) Kirtling channel with weirs taking the water down to the River Stour, looking downstream, (C) Wixoe pumping station hexagonal reservoir and (D) The Abberton reservoir.

The current licensed water transfer capacity is 455 ML/day (5.27 m³/s). Although the full capacity of the tunnel from Blackdyke is 700 ML/day, the pumped amount is limited by the capacity of the River Stour between Great Bradley and Wixoe and by electricity supply to power the pumping (Entec 2007). On average, 5-15% of water supplied in Essex is transferred *via* the EOETS: in dry years this may reach 35%. However, in very dry years, water is needed also at Denver to satisfy the minimal flow requirements (called a 'Hands-Off Flow'); therefore the capacity to transfer water to Essex can be limited.

Under the licences, the maximum volume of water that can be transported to Essex in an 18 month period, starting on 1 April each year, is currently 79,555 ML, which will be increased in 2015 to 90,000 ML under a new licence. The Abberton Scheme is being put in place with two pipelines to take additional water to the Abberton reservoir. The present licensed amount for the period from September to February, that is given by 'hands off flow' left in The Great Ouse, is 318 ML/day (3.68 m³/s), while from March to August it is 114 ML/day (1.32m³/s), (Saynor 2005). As the licensed 'hands off flow' during spring and summer is only a third of the winter transfer, the Abberton and Hanningfield reservoirs have to cope with consumer demand during the dry months and the purpose of the increased winter transfer is to ensure the reservoirs are full at the end of February. An

amendment to the 'hands off flow', namely the Denver variation, was applied for. Under a new licence, less water can be extracted at Denver during March and April, but an increased amount can be taken in October-December when water is plentiful.

The additional water for the Abberton reservoir will come from the River Ely-Ouse *via* a new 15.4 km gravitational pipeline from Kirtling to Wixoe (Entec 2007). The pipeline has a diameter of 1.2 m and a capacity of 1.68 m³/s. The pipeline was proposed because the corresponding stretch of the River Stour cannot be used to carry any additional flows, since these might increase existing problems of channel scour along this stretch during periods of high flow. Channel scour is a feature of the study sites and one of the reasons why they have been chosen in particular.

The pipeline will not be used to take flood water from the Stour because it does not bypass any areas of significant flood risk. Also, as its capacity is limited it would have little impact on a flood event. However, it does have some flood function in that it is designed to reduce the time it takes for the transfer water to be switched off. In principle, the transfer water can be diverted down the pipe and this reduces the time it takes for a drop in flow by approximately four hours (Mark Andrews, personal communication 2010).

At Wixoe, the additional water will discharge into the River Stour and flow along the river to Wormingford, where it will be abstracted into a second pipeline, which runs to Abberton Reservoir. The Abberton Scheme should be completed by 2015 and should satisfy the regional water demand forecast for the next 25 years (Saynor 2005).

3.1.5(A) THE IMPACT OF TRANSFERRED FLOWS ON THE RIVER'S NATURAL FLOWS

Depending on the amount of water transferred, the River Stour can be divided into four stretches (Fig. 3.1.8).

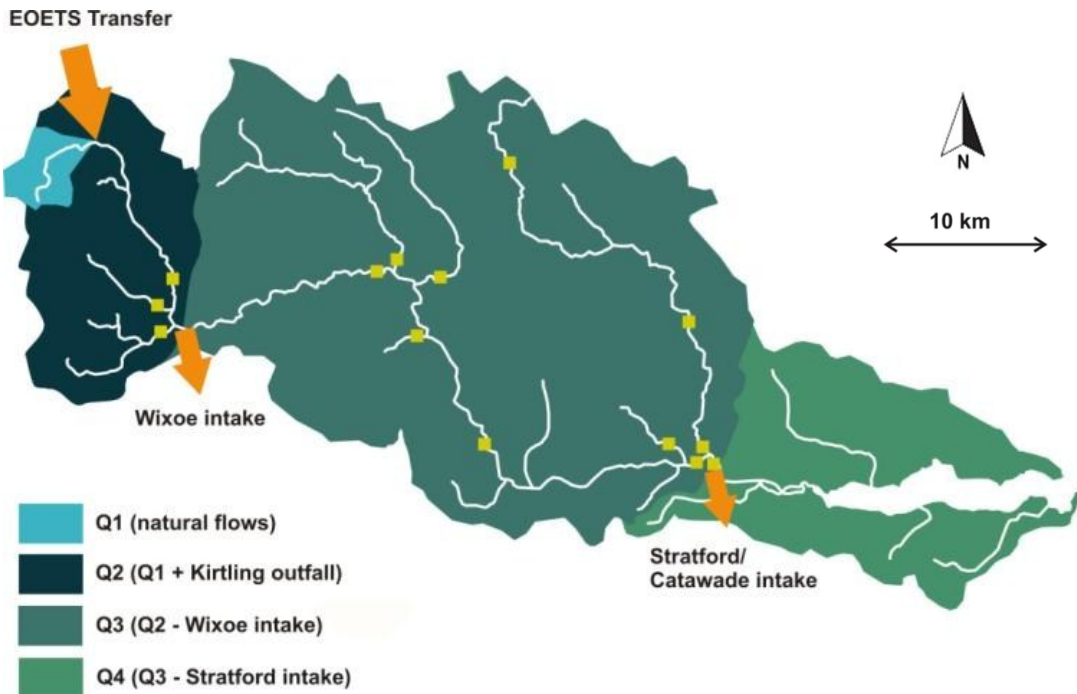


Fig. 3.1.8 The River Stour watershed divided into four stretches depending on the amount of water transfer. The yellow points indicate the location of gauging stations and the orange arrows indicate the intake and off-take points for the transfer scheme. The Ely Ouse to Essex Water Transfer Scheme (EOETS) enters the River through Kirtling outfall (top left).

(1) River flows (Q1): Headwaters to Kirtling Brook

This reach, upstream from the Kirtling Brook outfall carries river flows not enhanced through the scheme. It is characterised by its relatively high mean bed gradient of 1.6 m/km. The river bed is composed of fine gravel, sandy bars and silted pools. Chalk bedrock is visible in places. Apart from the flow regime, erosion processes are influenced by dredging or cattle trampling. Steep and high banks with no vegetation are subject to failures such as shallow slides, slab block failures and rotational failures.

(2) Flows enhanced by Ely Ouse (Q2): Kirtling Brook mouth to Wixoe intake

In addition to the natural river flows, this reach carries all the water pumped from the River Great Ouse. This reach has a mean gradient of 1.8 m/km, falling locally to 0.7 m/km, with a substratum of fine gravel to clay. Rapid erosion in some places is a cause of concern to landowners. A number of cantilever failures, slumping and rotational slides were recorded along this reach during the study period. To accommodate increased flows due to pumping, engineering was required in this reach. The approximate dredged volume has

been estimated to be 4,130 m³ with 60% of the dredging carried out between Great Bradley (sites GB2 & 3) and Little Bradley (site LB1, Fig. 3.1.1), (T. Barrett, personal communication 2006).

(3) Flows reduced by extraction to Chelmer (Q3): Wixoe to Stratford St Mary

This reach transports the transferred flows minus the amount of water abstracted into the River Chelmer at Wixoe pumping station. Sometimes, the abstraction rate can be relatively high, greatly reducing the flows downstream of Wixoe (Table 3.1.2). Although transferred flows have a lesser impact in this river stretch, high, unstable banks and over-wide, silted channels are common and are the result of bank vegetation removal due to land drainage and flood defence schemes (for example downstream of C1 & C2 sites, Fig. 3.1.1). A variety of mass failures and fluvial scouring occurs along the stretch and that is typical for such steep cohesive banks. Under the enhanced transfer scheme, an additional flow of 145 ML/d (1.68 m³/s) will take place in this stretch. Four field sites are located in this section: C1, C2, S1 and N1 (Fig. 3.1.1).

(4) Flows reduced by abstraction to Abberton reservoir (Q4): Stratford St Mary to the River Stour estuary

This is largely a tidal reach that carries natural flows minus the amount extracted at Wixoe and Stratford/Cattawade intakes. The sea level changing with the tidal cycle has an impact on the river flows in this reach and flood control is ensured by flood gates approximately 6 km downstream of Stratford. No field sites have been selected on this stretch.

There are five gauging stations on the main river and a further nine on seven major tributaries (Fig. 3.1.8). In order to estimate the discharges at field sites at any given time, simple equations have been developed in this research (Table 3.1.2). The discharge relationships for each field site have been derived based on the impact of water transfer flows. Furthermore the expected situation after the enhanced scheme has been implemented in 2015 is outlined.

For example, the discharge at the C1 site is made up of the composite of the natural flow (Q_{GB1}), the net contribution from the catchments Q_1 and catchment for the Keddington gauging station (c_{Kedd}) and the amount of water transferred from the Ely Ouse (T_E) minus the transfer extracted at Wixoe (T_c). The 2015 enhanced scheme will bring additional transfer (T_{AE}).

Table 3.1.2 Equations describing the relationship between the discharges at gauging stations to estimate the discharge at the field sites with how these will change after 2015.

Gauging station	Field sites	Section type	Discharge	Discharge after 2015
Keddington	GB1, GB2, GB3, LB1, LB2	Q1	Q_{GB1}	Q_{GB1}
		Q2	$Q_{GB1} + c_1 + T_E$	$Q_{GB1} + c_1 + T_E$
Westmill	C1, C2	Q3	$Q_{GB1} + c_1 + c_{Kedd} + T_E - T_c$	$Q_{GB1} + c_1 + c_{Kedd} + T_E - T_c + T_{AE}$
Lamarsh	S1	Q3	$Q_{GB1} + c_1 + c_{Kedd} + c_{West} + T_E - T_c$	$Q_{GB1} + c_1 + c_{Kedd} + c_{West} + T_E - T_c + T_{AE}$
Langham	N1	Q3	$Q_{GB1} + c_1 + c_{Kedd} + c_{West} + c_{Lam} + T_E - T_c - T_A$	$Q_{GB1} + c_1 + c_{Kedd} + c_{West} + c_{Lam} + T_E - T_c - T_A + T_{AE} - T_W$
Stratford St Mary		Q4	$Q_{GB1} + c_1 + c_{Kedd} + c_{West} + c_{Lam} + c_{Strat} + T_E - T_c - T_A$	$Q_{GB1} + c_1 + c_{Kedd} + c_{West} + c_{Lam} + c_{Strat} + T_E - T_c - T_A + T_{AE} - T_W$

T_E - transfer from Ely Ouse, T_c - transfer to Chelmer, T_A - transfer to Abberton;
 c_1 - net contribution to flow from catchment Q1;
 c_{Kedd} - net contribution to flow from catchment Q_{Kedd} (to the Keddington gauge);
 c_{West} - net contribution to flow from catchment Q_{West} ;
 c_{Lam} - net contribution to flow from catchment Q_{Lam} ;
 c_{Lang} - net contribution to flow from catchment Q_{Lang} ;
 c_{Strat} - net contribution to flow from catchment Q_{Strat} ;
 T_{AE} in second column indicates the contribution from Abberton scheme and T_W is the flow through an additional extraction point that will be built at Wormingford.

The equations in Table 3.1.2 can be used to estimate the net discharges in critical reaches derived from hydrological data. A map illustrating the river flows for each of the sub-catchments to the flow gauge on the main river is shown on Fig. 3.1.9.

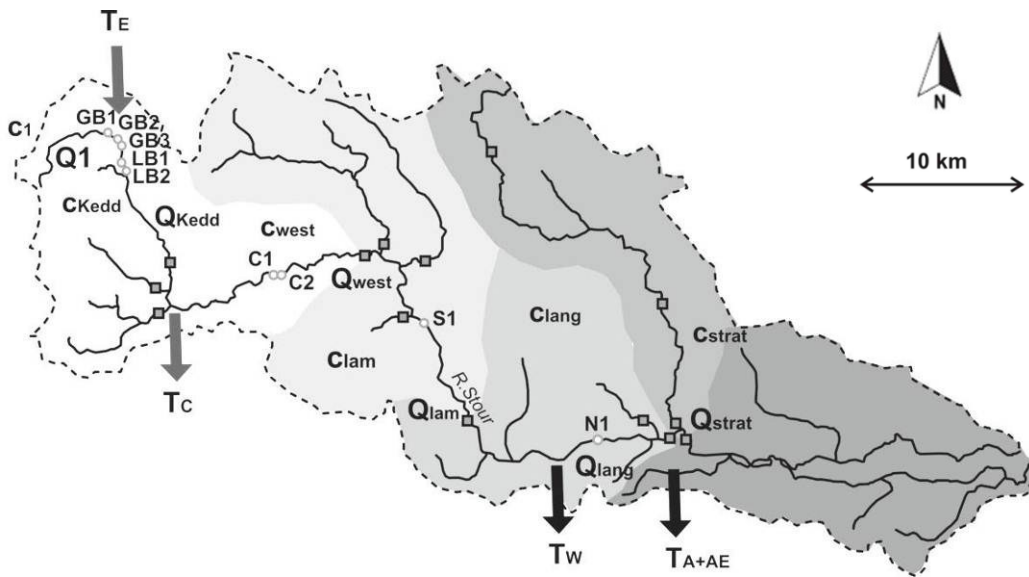


Fig. 3.1.9 Schematic contribution of the water transfer to each sub-catchment (for legend see Table 3.1.2).

The effect of water transfer differs between years, depending on rainfall conditions and reservoir levels. Since 1972, when the EOETS scheme came into operation, there have been several years when only relatively small amounts of water were transferred (less than 10,000 ML). Generally, the 1970s and 1980s were decades of low transfer amounts but demand for transferred water increased in the 1990s and 2000s. The highest amount of water transfer from the Ely Ouse occurred in 1997 (60,145 ML). During the bank erosion study between 2006 and 2010, 42,086 ML was transferred *via* the scheme to the Stour in total. Almost 50% of this occurred in 2006, while transfers in 2007 and 2008 were low. Table 3.1.3 shows amounts transferred annually since 1996.

Table 3.1.3 Transferred amounts from the Ely Ouse at Kirtling (T_E) and extraction taken at Wixoe into Chelmer and Hanningfield (T_C) in ML/year since 1996 (Based on data provided by the Environment Agency).

Year	T_E	T_C	Year	T_E	T_C
1996	43,162	20,251	2004	1,196	2,157
1997	60,145	26,949	2005	14,284	7,823
1998	25,110	9,862	2006	22,051	5,795
1999	10,837	4,034	2007	387	0
2000	2,708	467	2008	1,455	735
2001	979	662	2009	14,919	7,590
2002	4,196	1,294	2010	3,274	1,045
2003	20,995	15,210	2011	9,984*	2,176*

*as on 5th September 2011

During wet periods, transfers are kept to a minimum to avoid exacerbating flood flows. Paradoxically, during a very dry period such as in spring 2011, the amount of transferable

water is limited by the amount of minimum residual flow (also known as 'hands-off flow') at Denver. No water can be extracted unless there is extra water available on top of these flows (M. Andrews, personal communication 2011).

When in full operation, the scheme has a significant effect on river flows. Fig. 3.1.10 shows the proportion of transferred water as a percentage of total river flow as measured at four gauging stations, going downstream. It is clear that the scheme has the strongest impact on the gauged flows at Keddington and in some years at Westmill. Negative values in 2004 occurred when more water was taken out of the river at Wixoe than was transferred from The Great Ouse.

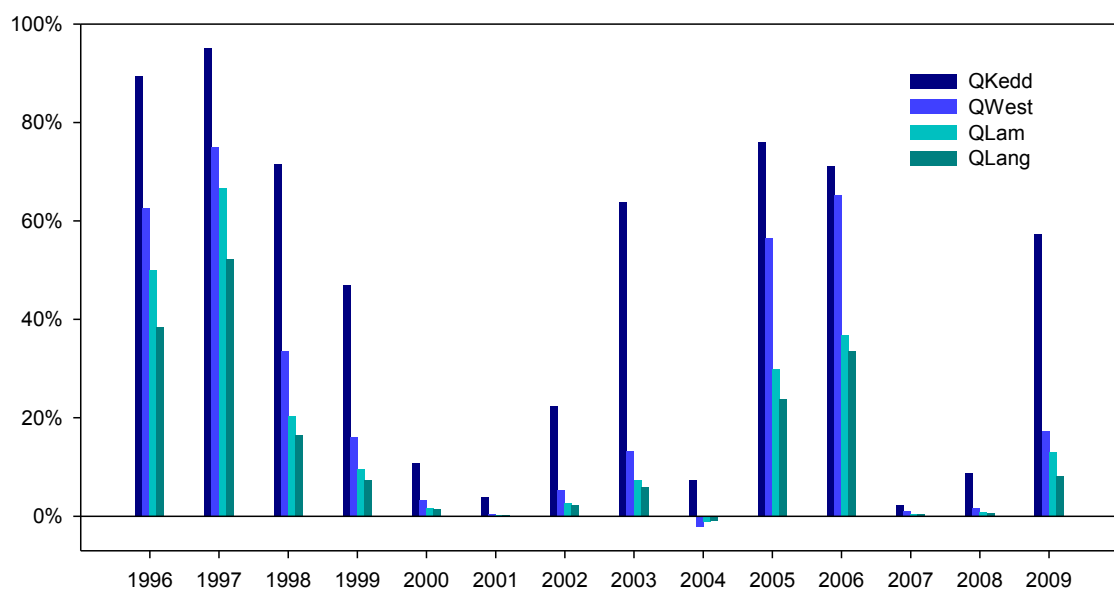


Fig. 3.1.10 Contribution of transferred flows to the overall flows, based on total amounts in ML/year. Q_{Kedd} is the annual discharge at Keddington, Q_{West} at Westmill, Q_{Lam} at Lamarsh and Q_{Lang} at Langham gauging stations (Data were derived from raw mean daily discharges provided by the Environment Agency).

As can be noted on Fig. 3.1.10, the effect of the transferred water decreases downstream as some water is taken out of the river at Wixoe (T_C) and the contribution from tributaries, run-off and base flow increases. Figs 3.1.11 & 12 present the overall flows versus transferred flows at each of the gauging stations up to Langham during 2006, in more detail.

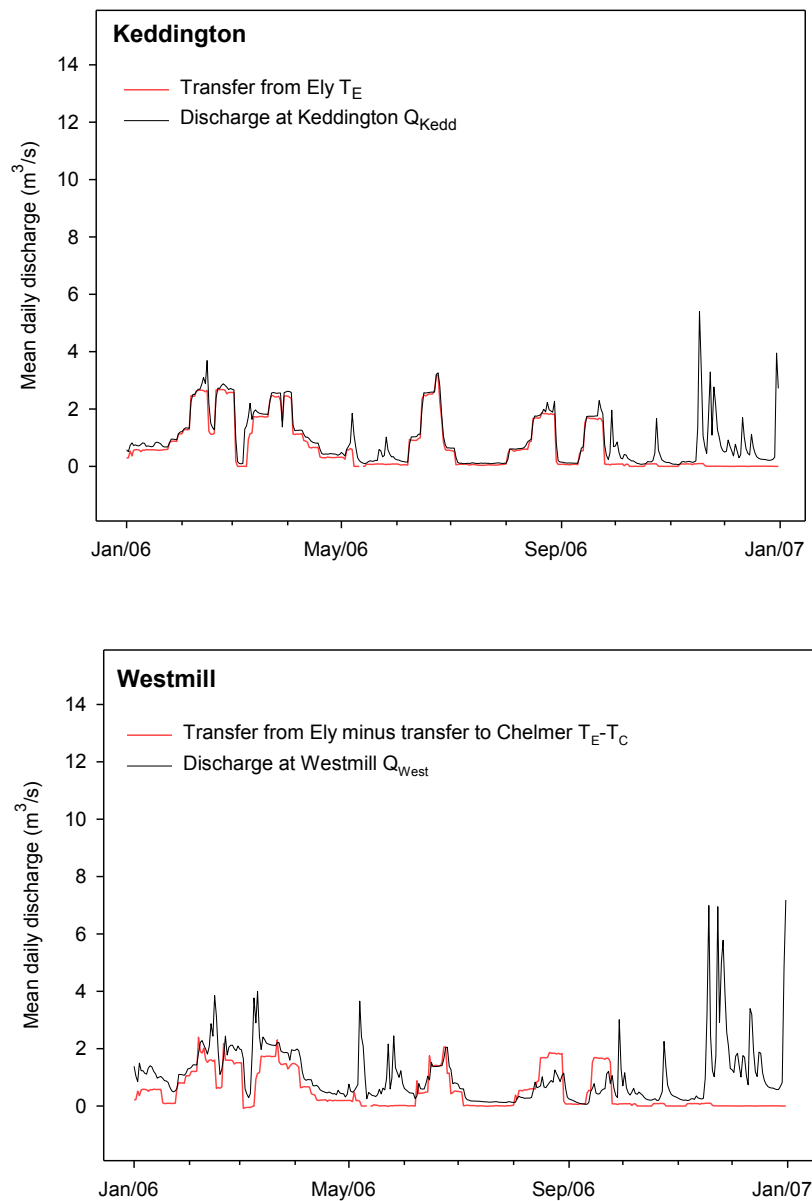


Fig 3.1.11 Transferred flows and natural river flows (represented as mean daily discharge) at Keddington and Westmill stations. (Plots based on data for mean daily discharge provided by the Environment Agency).

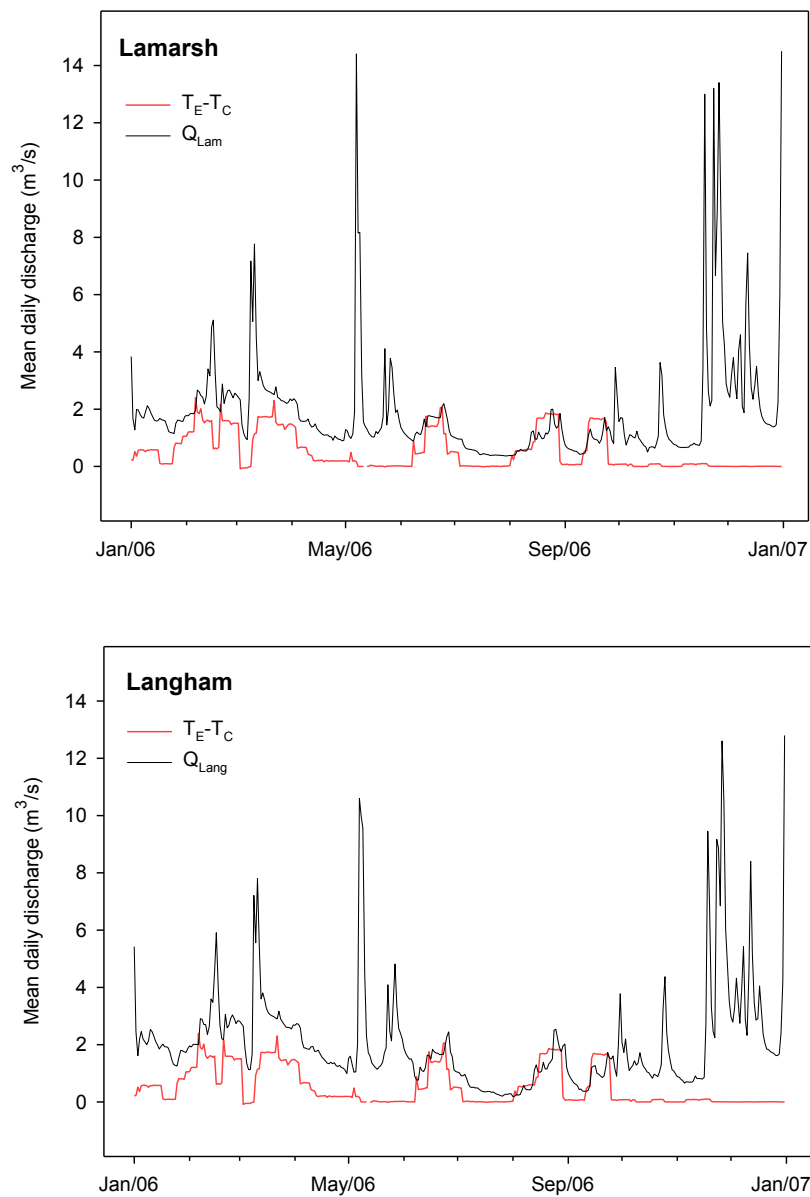


Fig 3.1.12 Transferred flows and natural river flows (represented as mean daily discharge) at Lamarsh and Langham stations. (Plots based on data for mean daily discharge provided by the Environment Agency).

3.1.5(B) POSSIBLE INFLUENCE OF THE SCHEME ON THE GEOMORPHOLOGY OF THE RIVER STOUR

When in operation, transferred water makes a considerable contribution to the natural river flow. However, it is not clear what impact these additional flows have on the channel's geomorphology and what the predicted impact will be after 2015 when the licence will allow increased flows. Although some reports are available (Entec 1998a,b; Atkins 2000; Newson & Block 2002), it is not clear to what extent the transferred flows influence the rate of bank retreat.

Engineering aspects of the Scheme were described by Huntington and Armstrong (1974). Some detailed drawings of the engineering work on the river channel have been discovered, including control structures and longitudinal profiles but with no cross sections (Newson & Block 2002). Observations of the upper River Stour were made during River Corridor Surveys undertaken in 1995 that briefly reported on the geomorphologic situation and identified locations of significant erosion. Various studies on the impact of the EOETS have been carried out by Entec (1998a,b) and Atkins (2000). Although these have no direct relevance to fluvial geomorphology, they provide some information about the flow and sediment conditions of the upper River Stour (Newson & Block 2002).

Newson and Block (2002) in their fluvial audit of the upper Stour presented observations on the impact of flows on occasions with and without water transfer. Newson and Block (2002) concluded that a major role of the transferred flows was to continuously 'freshen' the bank face by basal removal of weathered or failed material. These authors also suggested that the weathering of the bare loamy alluvial banks of the upper Stour is evidence that the engineering works to accommodate the water transfer, channel maintenance and riparian land management are key contributors to bank instability. Major dredging and sectioning works were undertaken between Kirtling outfall and Wixoe pumping station (Q₂ section of flows). The river along this 13.7 km long stretch was widened, deepened, existing weirs were improved and ten new structures were installed (EA 1998). Newson and Block (2002) found that the longest stretches of eroding banks were located on reaches that were straightened, re-sectioned and deepened for land drainage or the EOETS scheme. Based on information collected by Newson and Block (2002), approximately 4130 m³ of bed material was dredged between the Kirtling Brook outfall and Wixoe with the aim of designing the channel to accommodate flows of up to 3.68 m³/s. The altered channel dimensions were calculated to allow for 0.91m 'free board' before the designed flow reached bank top and for a Manning's coefficient of flow resistance (*n*) = 0.04. A report by Entec (1998a) suggests that although the scheme's

potential capacity is $5.27 \text{ m}^3/\text{s}$, the dimensions of the channel makes $4 \text{ m}^3/\text{s}$ a safe upper transfer rate. Although this is less than the channel's bankfull discharge, a sustained $4 \text{ m}^3/\text{s}$ in the upper Stour can still be effective in transporting the surface bed and bank materials. Chapter 3.5 explores the correlation of this transferred discharge to the erosion rates. Secondly, Entec (1998a) suggests that the scheme operates in on-off extremes. As shown on Fig 3.1.7, the changes to the flow caused by the scheme are rapid. Wetting and drying cycles influenced by the transferred flows are important in bank erosion and, as mentioned in Chapter 2, the highest erosion rates usually occur after prolonged wet periods, such as those caused by transferred flows. Additionally, the presence of transferred flows during the growth season inhibits colonization by vegetation on the lower reaches of the bank.

Further to this, a study by the Environment Agency (EA 1998) suggests that erosion is likely to occur in the upper Stour when mean flow velocities reach 1m/s . This is based on an estimate made by Chow (1959). More recently and following on the velocity threshold, a study by Essex and Suffolk Water (ESW 2011) predicted that river discharges in excess of $0.58 \text{ m}^3/\text{s}$ would cause mean velocity to reach 1 m/s somewhere within the test site (near Great Bradley). Based on the future scenario, the transfer scheme will produce around 85 days of velocities above 1m/s on average per year (based on the situation for the next 25 years). However, if the pipeline is used effectively, then this could be reduced to around 42 days. Downstream of the C1 site, near Westmill gauge, discharges of $2.31 \text{ m}^3/\text{s}$ will produce velocities of 1m/s . This is predicted to occur on around 19 of the scheme days in a year but will increase to around 21 days under the enhanced scheme.

Further examination of the effect that the transferred flows are having on the bank erosion and retreat rates found in this research are presented in Chapter 3.5.3. This is a key issue to confirm part of the first research hypothesis that the transferred flows contribute to increased erosion rates on the river.

3.2. PROPERTIES OF FIELD SITES

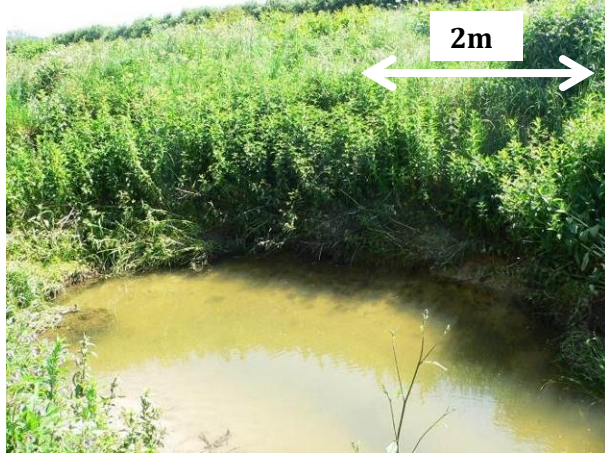
This chapter describes some of the most important geomorphic, geometric and geotechnical properties of the nine chosen field sites. Firstly, it introduces the individual field sites and the basis on which these were selected. Secondly, it describes some of the most important geometric characteristics such as water surface slopes, sinuosity and channel width, data which were obtained from field surveys and maps. Thirdly, it describes the material from which the banks are composed. Here, the soil associations for each site are described and the results of soil texture analysis are presented. Lastly, the shear strength of some banks under saturated and unsaturated conditions, alongside the water content, is shown. Particular parameters discussed in this chapter are later analysed against observed field erosion rates (Chapter 3.5) and this directly relates to the first hypothesis and Objective 3 that examines the importance of the bank parameters, some of which were altered by river engineering.

3.2.1. SITE SELECTION CRITERIA

In a natural environment, it is difficult to find similar field sites. Within the semi-natural reaches on the River Stour, the variability between sites was great. To make the selection, and to minimise the number of variables, the following criteria were applied when choosing the sites: (1) steep, high and nearly vertical banks; (2) no woody bank vegetation and (3) signs of erosion on banks.

Actively eroding banks were chosen in order to record a geomorphological change over the short timescale available for this research, thus these are not a representative random sample of bank processes in general. The selection was restricted by limited access to private land. An effort was made to choose sites that occurred at each of the three types of reach in which the flows are influenced by the water transfer scheme (Section 3.1.5). Within the chosen sites, erosion occurred on the outside of bends (concave banks). Due to past engineering interventions, these were not all typical meander bends and the channel planform type and development stage differed within the sites (Table 3.2.1). Sites were composed of cohesive material with the exception of a gravel site in Nayland (N1). This site was added later in the project; firstly, as a comparison to observe erosion rates on a bank made of non-cohesive material. Secondly, because a hard engineering scheme had been proposed to stabilise the river bank at this site, it was therefore ideal as a proposition for a soil bioengineering solution.

Table 3.2.1 Descriptions of field sites with photographs and grid references on OS map (x, y coordinates). The position of field sites along the river was shown on Fig. 3.1.1. The scales on pictures are approximate.

<p style="text-align: center;">GB1 (OS GR 566959, 253835)</p> <ul style="list-style-type: none"> Site is situated on a sharp bend taking river flows not enhanced by the transfer scheme (Q1 zone), upstream from Kirtling outfall. Located north-east of village Great Bradley. Despite of the high sinuosity, channel planform appears engineered, consisting of long straight reaches and ninety degree corners, copying land boundaries. Outer bank is set to water meadow, inner bank is arable land with a buffer zone. Flows in summer can be extremely low. Bed is varied with shallow riffles on meander flex points and deep silted pool by the outer bank and sand point bar by the inside bank. Chalk bed is visible in places. Banks on both sides are steep and high, disconnected from the floodplain. Shrubby and tree vegetation grows upstream and downstream of the site. Monitored bank has tall herb vegetation with shallow root systems that is of limited aid to bank stability. Typical are shallow slides and slumping. 	
<p style="text-align: center;">GB2 (OS GR 567386, 253528)</p> <ul style="list-style-type: none"> Site is situated around 400 m downstream from Kirtling outfall and 100 m downstream from a weir. Located north-east of Great Bradley. Straightened in the past (prior to 1886) but now recovering some sinuosity through early-stage meandering. Both banks are arable with narrow buffer zone. Reach is subjected to full water transfer (Q2 zone). Bed is uniform, composed of sand and fine gravel with chalk bedrock visible along the left bank. Right bank is shallow and stable, connected to floodplain, while the left bank is nearly vertical. Bank material is silty with no vegetation. Cantilever failures, weathering and fluvial entrainment are the most common causes of bank retreat. 	

GB3
(OS GR 567442, 253472)

- Site is situated 70 m downstream of GB2 on a slight bend north-east of Great Bradley.
- Subject to impact of full water transfers.
- Planform geometry similar to the GB2.
- Land on both banks arable, footpath on the edge of outer bank, narrow buffer zone.
- Right bank is nearly vertical.
- Cantilever failures are the most typical.
- Bed is varied in depth and type of substrate, narrow riffle section at entry of site changes into pool section.
- Outer bank foot is heavily silted. Inner bank is less steep with large herbaceous vegetation.
- Land on both banks is arable but with narrow buffer strip.



LB1
(OS GR 567928, 252034)

- Site situated 200 m upstream of a weir close to the village of Little Bradley.
- Signs of straightening in the past (prior to 1886) but now starting to meander.
- Wide channel with large gravel bar and >2 m deep pool at the entry section of the site.
- Bed profile changes from pool into narrow step alongside a bar and a riffle.
- Bare banks are exposed to weathering and fluvial entrainment.
- Prolonged water transfers have possibly created a 'dent' in the outer bank.
- Outer bank is arable close to the edge, inner bank is set to mixed tree plantation.



LB2**(OS GR 568028, 251468)**

- Site located on a narrower stretch 400 m downstream of a weir south of Little Bradley and close to Little Thurlow to the south.
- Channel planform appears artificial, similar to LB1.
- Left bank is naturally steep and high supported by woody vegetation.
- Right bank (monitored) low but nearly vertical and less stable with common occurrence of cantilever failures.
- Riffle at the entry section of the site.
- Large gravel bar in the channel is possibly a result from accumulation of materials used for restoring some spawning gravels upstream of the site (T. Barratt, personal communication 2006).
- Gabion baskets installed on two stretches upstream of the site.
- Right bank is grassland and left bank is steep with bushy and tree vegetation.

**C1****(OS GR 577571, 244979)**

- Growing meander bend 350 m located downstream of flood gate situated south of the village of Clare.
- Section of river that carries flows reduced by extraction at Wixoe (Q3).
- High and steep cohesive banks.
- No signs of overhangs or significant weathering.
- Bed varied with riffle at the entry section composed of fine gravel that transforms to deep pool section downstream.
- Large number of signal crayfish burrowing at this site.
- Inner bank is grassland and outside bank is arable but with 10 m strong buffer strip.



C2
(OS GR 577682, 244968)

- Site situated 220 m downstream of C1 on a large meander bend.
- Migrating meander approaching the stage of meander cut off and termination.
- Steep bare banks with signs of weathering and cantilevers.
- Fallen blocks of silty material visible at bank foot and on the riffle at the downstream part of the site.
- Bed is varied in depth but largely silted and no point bars are present.
- Entry and points of the meander are shallow while the middle reach is very deep and silted, therefore unsafe for wading any time of the year.
- Right bank is arable land with a 10 m wide buffer and left bank is grassland.



S1
(OS GR 586791, 241843)

- Site situated in the conservation area of water meadows near Sudbury.
- The flows are the natural and transferred flows minus the extraction at Wixoe (Q3).
- Channel straightened in the past, now recovering sinuosity by lateral erosion.
- Located on the main channel, about 100 m downstream of a weir.
- Banks made of layers of silt with varying clay content.
- Typical are cantilever failures and slumping.
- Bed varied with deeper stretch in the upstream section.
- Bed silted near the bank, otherwise chalk bedrock and gravel.
- Large gravel bar at the right inner bank. The gravel was introduced to river as part of the restoration project to support barbel (*Barbus Barbus L.*).
- Both banks used as grassland.
- Site taken on later in the project because of the ranger's interest and used as a willow spiling demonstration site (referred to as the 'cohesive site', Chapter 5).



N1
(OS GR 597428, 233740)

- Site situated approximately 200 metres downstream from a confluence of the flood alleviation channel built in 1968 and the old Stour near the village of Nayland.
- Situated on a downstream end of large migrating meander.
- The only site with non-cohesive bank material seen on the river.
- Recent erosion rates very high (up to 1.3 m/year).
- High but less steep banks.
- Gravel bed varied in form and depth.
- Both banks are grassland.
- The site was taken on later in the project at landowner's suggestion and was used as the second willow spiling demonstration site (in Chapter 5 referred to as the 'non-cohesive site').



3.2.2. GEOMETRIC PROPERTIES

Attributes such as long stream gradient, bank and meander geometry or distances from any engineering structure will have an effect on erosion rates (Chapter 3.5). The distance of the site from the source and from the nearest upstream weir, elevation and surface water slope are shown in Table 3.2.2.

River distances have been acquired from the relevant OS maps in GIS. Elevations corresponding to bankfull were obtained from the field survey using geodetic reference points with known elevations. Site water surface slope was the mean water surface slope along the thalweg within the field site. Because this was obtained from a fixed point on the bank perpendicular to the thalweg, the partial distances along the long profile between the readings were calculated using the trigonometric \cos rule of a triangle, where α is the horizontal angle and b, c are the horizontal distances:

$$a^2 = b^2 + c^2 - 2bc \cos \alpha$$

The approximate distance from the nearest weir was measured in Google Earth 5.1 (Google Inc. 2009).

Table 3.2.2 The distance of the study site locations from the source, elevation, water surface slope and distance from the nearest weir.

Field site code	River km downstream	Elevation based on bankfull (m AOD)	Site water surface slope (m/km)	Distance from nearest upstream weir (m)
GB1	7.6	76.97	7.032	50*
GB2	8.1	75.50	6.117	110
GB3	8.2	75.15	3.864	170
LB1	9.9	69.75	1.956	350
LB2	10.5	66.20	1.553	400
C1	29.7	40.23	1.351	350
C2	30.0	39.99	0.990	570
S1	45.8	23.98	6.041	125
N1	67.9	11.16	2.279	250**

*small drop from ford, **distance from major confluence

A common characteristic for the field sites is that a weir is situated within at most 600 m upstream of each site. GB1, GB2 and S1 are located nearest to drop structures upstream. Within the nine field sites, there is a hyperbolic correlation ($R^2=0.956$) that demonstrates that with decreasing distance from an upstream weir the water surface slope increases (Fig. 3.2.1). Because stream power is proportional to the water surface slope and the bankfull discharge (Simons *et al.* 1965), an increase in slope will increase the stream power and thus the erosive forces of the stream. Furthermore, an increase in bankfull discharge will increase the stream power. Hydraulic geometry equations indicate that the slope decreases but the velocity increases with increasing discharge or distance downstream.

Considering this on the scale of the river reach (tens of kilometres), the slope and velocity are inversely related. However, on a site specific scale (metres), they correspond (for example, faster flowing water occurs over a steeper riffle section). At the bankfull stage, velocities become approximately similar across the site since there is less variation in cross-sectional areas of pools or riffles (Hey & Thorne 1986) and the water surface slope along the long profile is smoothed.

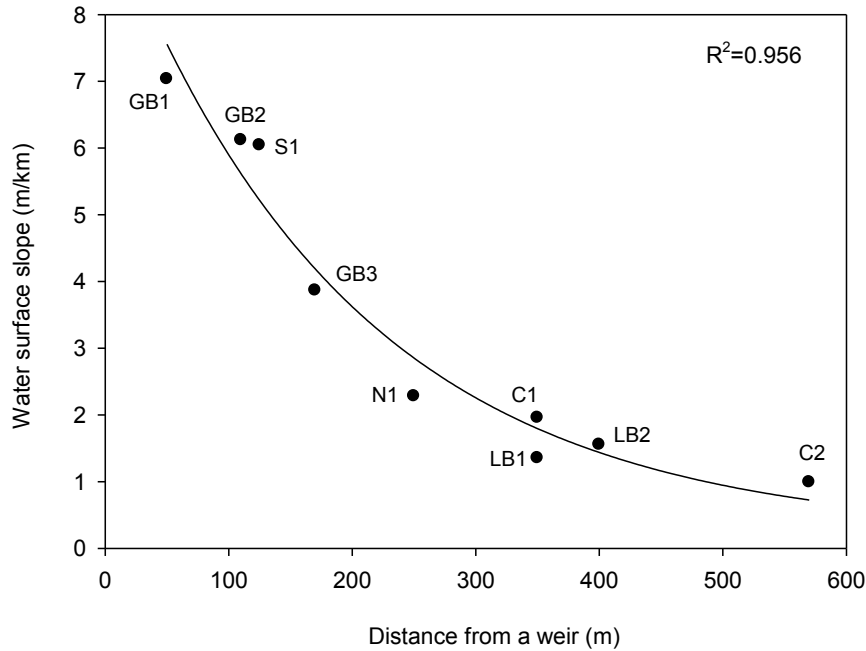


Fig. 3.2.1 Water surface slope relationship with increasing distance from the nearest upstream weir, based on nine field sites. The regression curve is a hyperbolic decay and the function is $f(y) = -7.91 + (2582.85 * 0.27) / (0.27 + x)$. (Probability of curve fitting is 95%).

Alongside the slopes and distances, meander geometry will also influence the bank stability and river erosion forces. Geometric attributes of a meander such as radius, amplitude and sinuosity were measured for each site as shown on the Fig. 3.2.2.

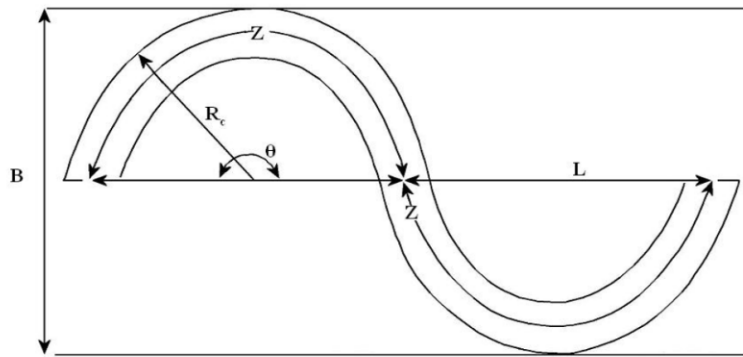


Fig. 3.2.2 Meander geometry variables where R_c is the meander radius, θ is the meander arc angle, B is the meander width/amplitude $\times 2$, L is the wavelength and Z riffle spacing. Therefore sinuosity: Z/L (Thorne et al. 1997).

In addition, the bankfull channel width was measured at the peak of the meander's amplitude. Also the channel's angles of high flow approach were obtained as the angle of thalweg to the tangent line of the outside meander curve using measurement tools in Google Earth (Google Inc. 2009). Site sinuosity was the ratio of the length of channel between riffle spacing to the meander wavelength (Table 3.2.3).

Table 3.2.3 Meander geometry, channel and bank properties at the field sites.

Field site code	Meander radius (m)	Meander amplitude (m)	Site sinuosity	Bankfull channel width (m)	Bankfull channel depth (m)	High flow angle of approach (degrees)
GB1	5.8	200.0	1.92	5.6	2.0	28
GB2	40.0	45.0	1.02	5.7	1.9	<25
GB3	17.5	67.3	1.07	10.7	2.1	<25
LB1	31.0	81.8	1.04	9.9	1.7	<25
LB2	44.0	115.0	1.15	3.5	1.5	<25
C1	30.5	196.1	1.77	9.6	1.8	35
C2	17.0	237.3	2.38	15.6	3.0	70
S1	29.3	127.3	1.15	25.3	1.9	25
N1	52.0	208.2	1.71	22.0	2.3	27

The most sinuous sites C2 and N1 also had the largest meander radius. The maximum sinuosity was 2.38 whilst the minimum was 1.02 with the mean \pm SD sinuosity 1.47 ± 0.49 . As a comparison, the mean sinuosity over the length of the studied river was 1.12 ± 0.11 . The highest flow impact angle was 70 degrees at site C2. It can be estimated that the banks located on the outer bends of the most sinuous reaches would have the highest shear stresses; however on the other hand, these would have the lowest slope. More sinuous banks may therefore not necessarily be associated with the highest shear stresses. (The test of water surface slope and sinuosity against erosion rates is performed in Chapter 3.5).

Although shear stress is dependent on slope and depth, in naturally meandering channels determining the boundary, shear stress on the outer bank is complicated due to the secondary flows that operate in a channel cross section. The outer bank shear stress is proportional to the velocity gradient (Section 2.3.2), but it is difficult to theoretically predict these without measuring in the field. Access and safety make it difficult to take these measurements during bankfull flows. According to a model described by Hey (1986), during medium flow, the peak in the boundary shear stress is on the outer bank.

3.2.3. SOIL ASSOCIATIONS

In terms of soil strength and cohesion, there are two types of material that comprised the observed banks: cohesive and non-cohesive. Downstream, the cohesive soils were naturally wet, loamy and clay floodplain soils with high ground water while in the

upstream reaches the banks were created in freely draining and slightly acid loamy soils (Table 3.2.4).

To describe the soils of a studied bank in more detail, firstly site-specific soil information was obtained from the National Soil Research Institute (NSRI). This included four characteristics: (1) soil association: groups of soil types which are typically found together and are associated with the landscape, (2) soil hydrology that describes the dominant pathways of water movement through the soil considering the underlying substrate, (3) soil parent material or the underlying geology and (4) soil texture (NSRI 2010a-e).

Table 3.2.4 *Soil associations, hydrology types, parent materials and texture characteristics for the floodplain soil at research field sites. Sourced from regional reports by National Soil Research Institute (NSRI, 2010a-e).*

Field site code	Soil association	Hydrology of soil type	Soil parent material	Soil texture
GB1	Ludford			
GB2	<i>Deep well drained fine loamy, coarse loamy and sandy soils locally flinty and in places over gravel</i>	<i>Free draining permeable soils in unconsolidated sands or gravels with relatively high permeability and high storage capacity</i>		
GB3			<i>Glaciofluvial drift</i>	
LB1				
LB2	Thames			
C1	<i>Stoneless mainly calcareous soils affected by groundwater</i>			<i>Loamy</i>
C2				
S1		<i>Seasonally waterlogged soils by fluctuating groundwater and with relatively slow lateral saturated conductivity</i>	<i>River alluvium</i>	
	Fladbury 1			
N1	<i>Stoneless clay soils, in places calcareous variably affected by groundwater</i>			

The Thames Association consists of dark greyish brown to grey stoneless calcareous clay of moderate coarse prismatic structure. The Ludford Association is more varied and represented by medium and light loamy and sandy drift with siliceous stones and over non-calcareous gravel. The Ludford component of this Association is represented by brown and yellowish brown sandy silt loam or clay loam trough, slightly stony clay loam or sandy clay loam, with moderate medium angular blocky structure to slightly or moderately stony clay loam, with a moderate medium angular blocky or prismatic structure. Fladbury consists predominantly of Fladbury, Thames and Wyre clayey river alluvium soil series. The profile of Fladbury component is represented by dark greyish

brown, slightly mottled, stoneless calcareous clay to clay with strong coarse prismatic structure and grey, mottled, stoneless clay with moderate angular blocky or massive structure (NSRI 2010a-e).



Fig. 3.2.3 Example samples from field sites in Clare (C1), left and Great Bradley (GB1), right illustrating the variability in texture and colour between the Thames and Ludford Associations. The samples are arranged into rows based on the section of the bank profile: bank top (A), middle (B) and bank foot section (C).

3.2.4. SOIL TEXTURES

The fabric of soil is crucial in defining its engineering properties because it determines the physical properties of the soil such as shear strength, compressibility, porosity and permeability (Craig 2004). For example, the different erosion patterns between cohesive and non-cohesive material that were outlined in Chapter 2.2. Sand consists of rock particles that have been formed by physical weathering or are the resistant components of rocks broken down by chemical weathering (Atkinson & Springman 2000). The individual grains have relatively small specific surface area ($0.1 \text{ m}^2/\text{g}$) and the resistance of a mass of such material to any movement is largely frictional. On the other hand, clay particles are the product of chemical weathering and the particles have 'plate-like' forms (Craig 2004). The thickness to length ratio can reach 1:1000 (in the case of smectites), therefore clay particles have a high specific surface area (e.g. $10-1,000 \text{ m}^2/\text{g}$). These surfaces carry small electrical charges that will attract water molecules and cations. This additional force is proportional to the specific surface and it is known as cohesion. In some clay soils such as smectites (e.g. montmorillonite), considerable amounts of water may be held as adsorbed

water within a clay mass. Table 3.2.4 shows British Soil Classification System soils categorised into soil types according to particle size.

Table 3.2.5 *British Soils Classification of soils based on particle size (in mm), BS 5930 (British Standards Institution 1999).*

Very coarse soils	Boulders		> 200
	Cobbles		60 – 200
	Gravel	Coarse	20 – 60
		Medium	6 – 20
		Fine	2 – 6
Coarse soils	Sand	Coarse	0.6 – 2
		Medium	0.2 – 0.6
		Fine	0.6 – 0.2
Fine soils	Silt	Coarse	0.02 – 0.6
		Medium	0.006 – 0.02
		Fine	0.002 – 0.006
	Clay		< 0.002

Soils can be classified as sandy if the percentage of silt and twice the percentage of clay is less than 30%. Clay soils are soils with more than 18% of clay size particles. All other soils of intermediate composition can be regarded as loamy. These can be further subdivided into coarse loamy soils (with more than 20% of sand and less than 18% of clay); fine loamy soils (with over 20% of sand and over 18% of clay) and silty loamy soils (with less than 20% of sand and less than 18% of clay), (NSRI 2007). Typically a soil texture triangle (Fig. 3.2.4) is used for identification of the main soil texture types based on the proportion of sand, silt and clay particles.

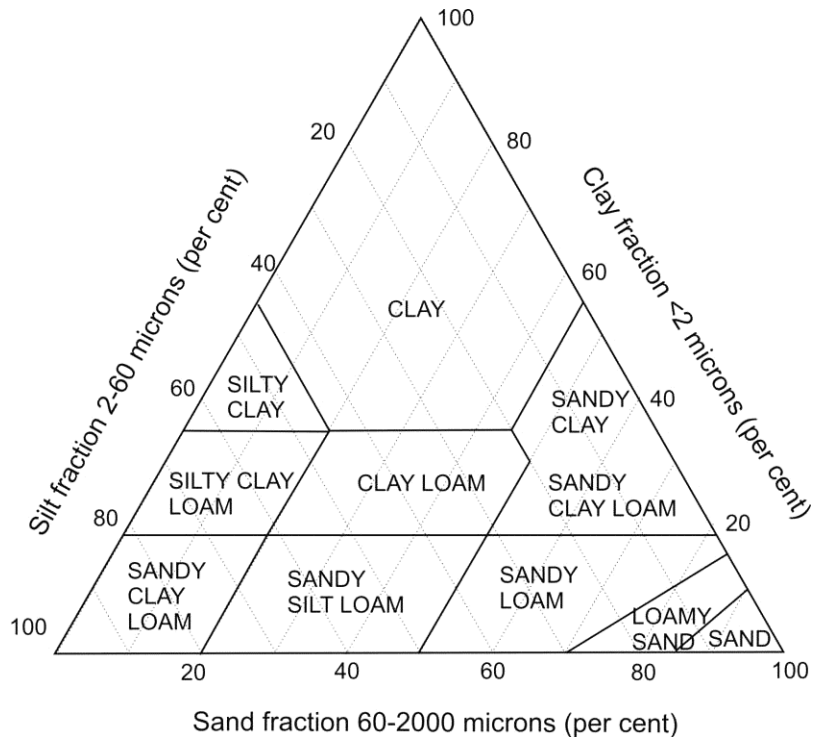


Fig. 3.2.4 Soil texture triangle (Burton 2006).

3.2.4(A) SAMPLING STRATEGY AND PARTICLE SIZE DISTRIBUTION PROCEDURE

Three profiles were sampled from 8 sites with soil taken from the upper, middle and lower sections of the bank surface to correspond with the approximate locations of the erosion pins (Section 3.4). Samples (about 10 g fresh weight) were collected from the bank surface so there was no disturbance to the pins. In total, 71 samples were collected from 24 profiles. Site N1 was not sampled because it differed from the other sites by being composed of non-cohesive gravels. This material was unsuitable for the installation of erosion pins (Chapter 3.4) and was therefore excluded from the particle size analysis.

Laser diffraction was used for samples with particle sizes below 2.0 mm. Prior to analysis, samples were dispersed in water and 1 ml 10% calgon (sodium hexametaphosphate) and passed through 1.7 mm diametre standard sieve (BS 410). Samples were further dispersed in ultrasonic and magnetic stirrers before being added to a particle sizer. A Malvern Mastersizer 2000 with the Hydro 2000G dispersion unit was used for the analysis. Each sample was run three times to obtain an average result for percentage volumetric distribution in each individual size class.

Laser diffraction is a very accurate method to determine the particle size distribution of fine soil fractions between 2 mm to 20 nm. The volumetric proportion of the three main size soil fractions can be easily determined. The method is based on the principle that

large particles scatter light at low angles while smaller particles scatter light at high angles. The instrument measures the scattered light energy over a range of angles and this can then be resolved into a particle size distribution using a scattering model and the optical properties of the material (Malvern 2000).

The resulting soil texture is the volume-based ratio of clay, silt and sand (Fig. 3.2.5). In addition to this, some further attributes were obtained from the analysis and these are given in Table 3.2.5 and in Appendix (3.2.A). The volume weighted mean D (3,4) returns the volume mean of the particles in the sample, the $d(0.5)$, $d(0.1)$ and $d(0.9)$ are standard percentile readings from the analysis. For example, $d(0.1)$ is the size of particle below which 10% of the sample lies. As an assumption from the laser diffraction, the specific surface area was also given. This is defined as the area of particles per unit mass of particles.

3.2.4(B) RESULTS OF PARTICLE SIZE DISTRIBUTION

All soils from the river banks were found to be generally low in clay content (up to maximum of 16.3%), with a mean \pm SD of $1.70 \pm 2.78\%$. Silt and sand particles ranged greatly between the samples with a mean for silt particles being $50.52 \pm 19.25\%$ and a mean for sand particles of $47.78 \pm 20.23\%$. The soil texture was therefore largely dependent on the ratio of sand to silt. This composition was expected for soils in the upper reach (GB and LB sites) because it is typical of the Ludford association. Based on the soil triangle (Figs. 3.2.4 and 3.2.5), the resulting texture types were identified as silt loam, sandy loam, sandy silt loam and loamy sand. Higher clay content was expected for the Thames and Fladbury soil associations (the C, S and N sites). The coarser composition of riverbanks was likely a result of river incision and dredging. A good example of this is the Nayland site that is possibly a historic channel bar. On the other hand, local lenses of clay did occur at some bank toes and higher clay content is reflected at sampling locations GB2-1C, GB2-3C and LB1-1C. Chalk bedrock was also visible in the profile at GB1, GB2 but also at S1.

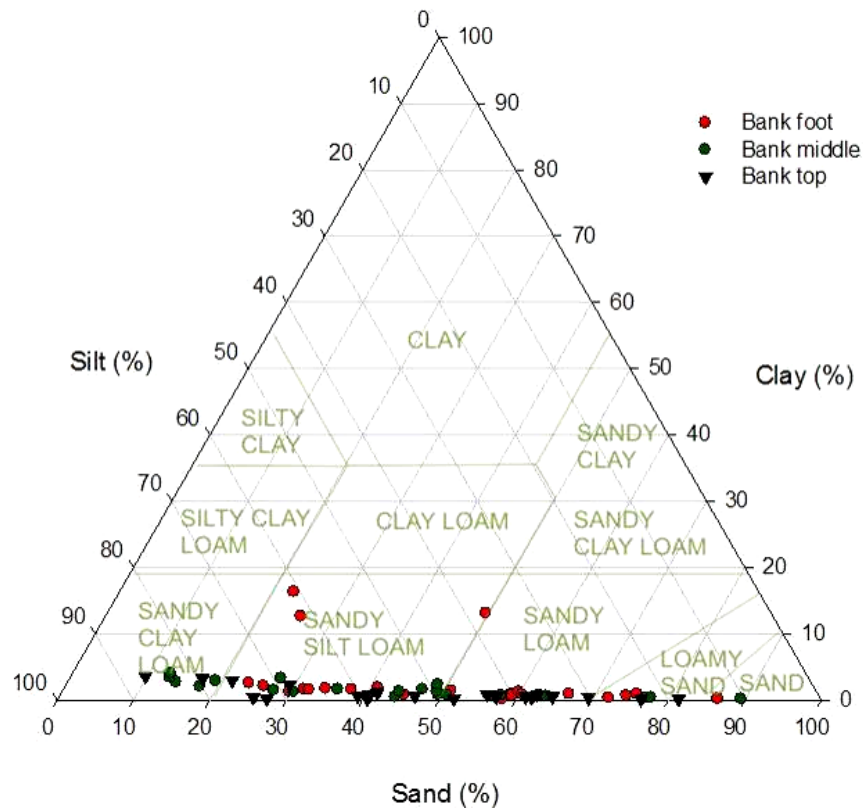


Fig. 3.2.5 Soil triangle for each of the soil samples taken from the bank top, middle and bank foot sections based on volumetric percentage of soil, silt and sand particles in the sample.

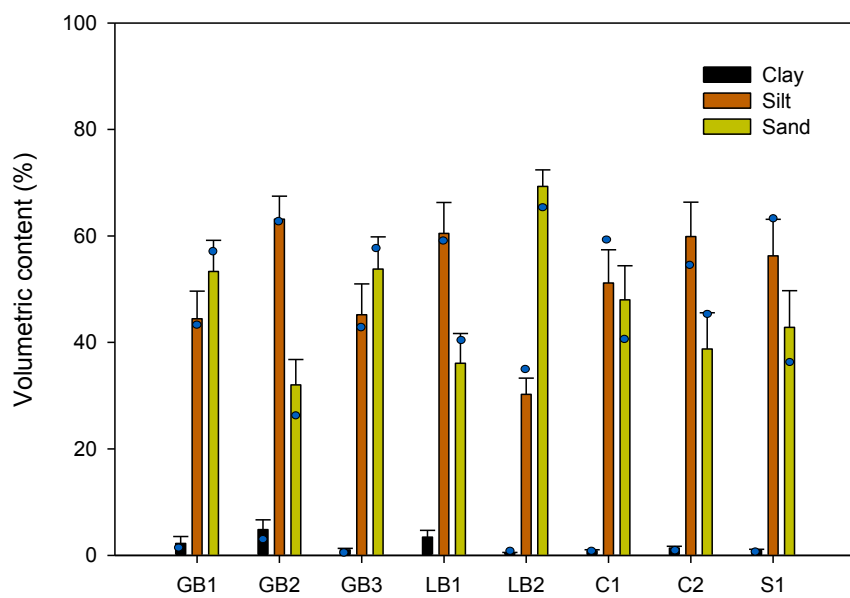


Fig. 3.2.6 Volumetric content of clay, silt and sand across the field sites. The blue circles indicate median values.

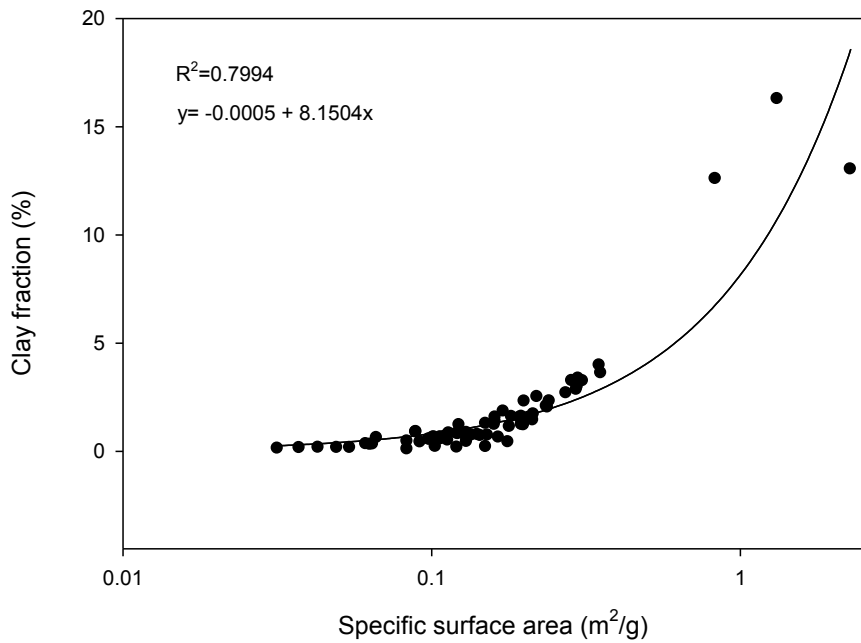
Overall, most soil samples could be classified as sandy silt loam (48%) and sandy loam (28%). Less samples had the texture of loamy sand (11%), silt loam (8%) and sand was represented only in three cases (4%). Texture categorisation for each of the sampling points is shown in Table 3.2.A in the Appendix. Because of local variability in soil fractions, the distributions were not normal at most sites. The values of median, alongside the mean sand, silt and clay contents are shown in Fig. 3.2.6 which demonstrates the variability.

Numerical results for clay, sand and silt content along with the volume weighted mean, uniformity, surface specific area, $d(0.1)$, $d(0.5)$ and $d(0.9)$ values are presented. Table 3.2.5 shows the mean results for the three sections of each bank separately (top, middle and toe). Results from an analysis for each sample are shown in Table 3.2.A in the Appendix.

Table 3.2.6 *Soil texture parameter means for each bank section across eight sampled sites (n=24): Volume weighted mean (μm), specific surface area (m^2/g), percentile readings (μm) and percentage of clay, silt and sand particles. The confidence interval of the mean is the standard deviation.*

Bank section	D [4, 3] Volume weight. mean	Unifor- mity	Specific surface area	d (0.1)	d (0.5)	d (0.9)	Clay (%)	Silt (%)	Sand (%)
Banktop	142.08	1.98	0.15	7.10	83.91	362.04	0.95	51.12	47.92
	± 70.63	± 1.16	± 0.08	± 4.52	± 62.72	± 169.83	± 1.02	± 18.77	± 19.48
Mid	137.76	2.19	0.17	7.55	82.74	343.15	1.47	54.26	44.28
	± 86.68	± 1.39	± 0.08	± 10.53	± 89.68	± 181.34	± 1.11	± 20.81	± 21.74
Bank foot	158.08	2.38	0.30	7.87	101.60	397.16	2.61	46.52	50.87
	± 87.37	± 2.43	± 0.50	± 8.07	± 94.35	± 167.65	± 4.36	± 18.16	± 19.77

The volume weighted mean based on the spherical diameter of the particles in samples averaged to $146.31 \pm 82.18 \mu\text{m}$. The highest volume weighted mean of $412.2 \mu\text{m}$ occurred at GB1-3C reflecting a high proportion of larger size particles. The specific surface area had a mean of $0.21 \pm 0.309 \text{ m}^2/\text{g}$ and reached its maximum at $2.28 \text{ m}^2/\text{g}$. This is still relatively low in comparison to clay soils (typically $10\text{-}1,000 \text{ g/m}^2$). The samples with the highest specific surface areas in relation to the other samples were GB2-1C, GB2-3C and LB1-1C, and corresponded with those mentioned earlier with the highest clay content. The relationship of surface specific area and clay content is shown in Fig. 3.2.7.



Figs. 3.2.8 to 3.2.11 represent the volumetric fractions as percentage with size classes positioned on a logarithmic scale. The variability between the different sections within each site is presented for the individual bank sections – top, middle and bottom. Some bank sections appear to be nearly identical or very similar, for example bank sections GB3-B, C1-C, C2-B and S1-A, while others show greater variability. The variability occurs within the silt and sand fractions, the clay content is mostly low, the exception is GB2-1C, GB2-3C, LB1-1C. Greater variability in the mud content (clay and silt) within the observed bank sections suggests different soil cohesion and erodibility. This attribute of bank soils is examined in 3.5.

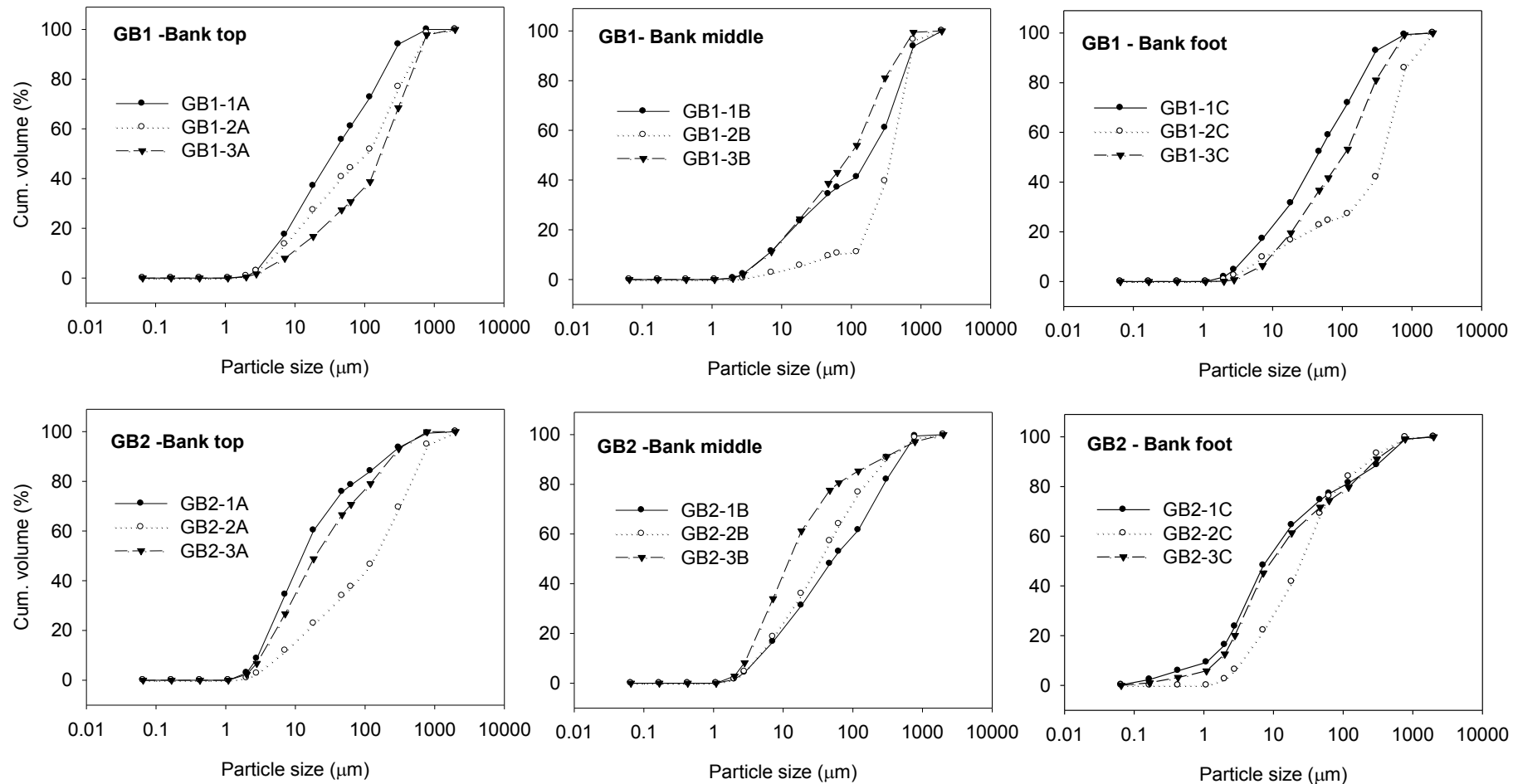


Fig. 3.2.8 Cumulative volumetric percentage of particle size fractions for two sites GB1 and GB2 for particles of size below 2 mm. The x axis is logarithmic expression of particle size in μm . Each site is represented by the three charts – for top (A), middle (B) and lower section of the bank(C).

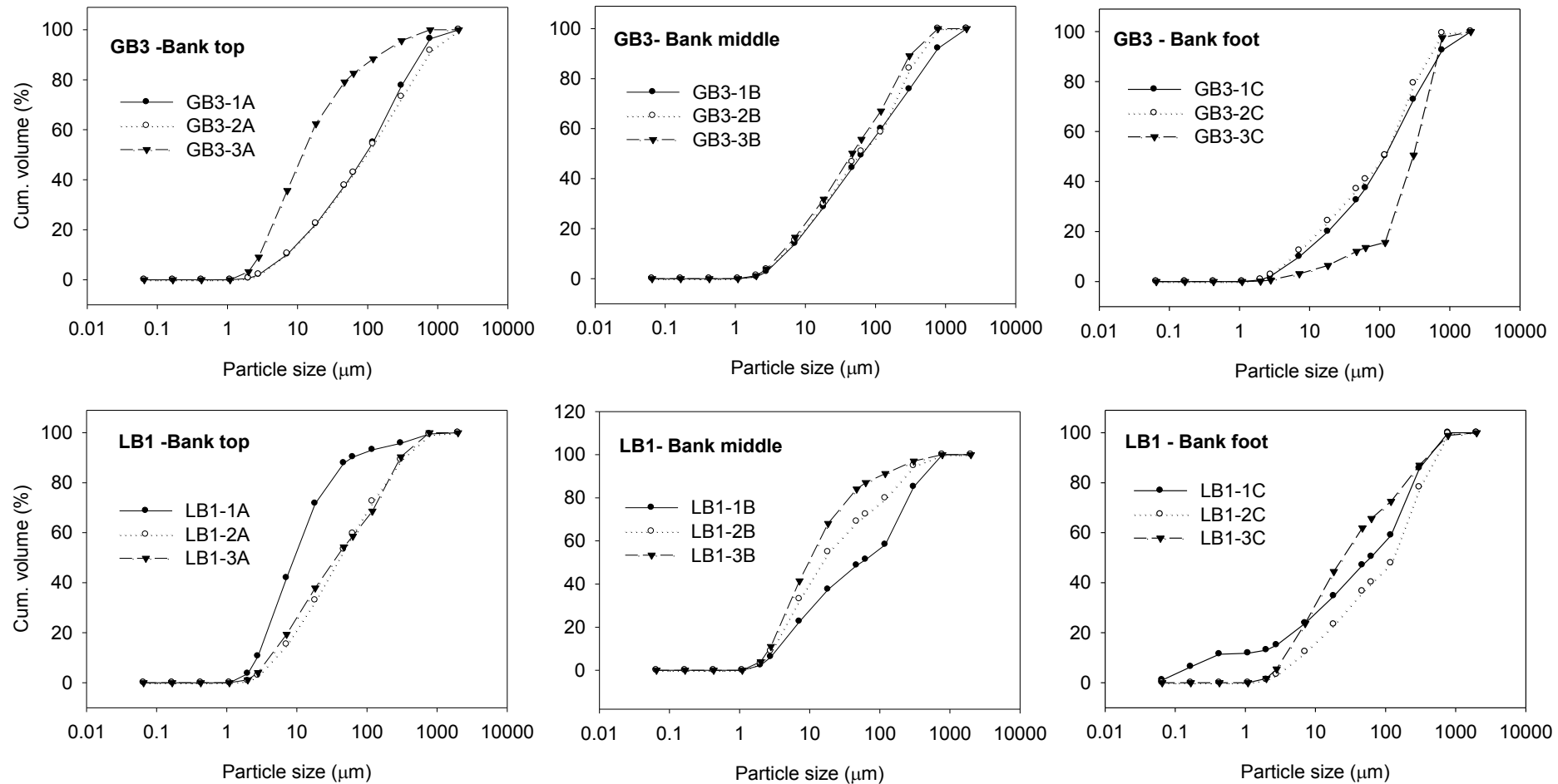


Fig. 3.2.9 Cumulative volumetric percentage of particle size fractions for three sections of banks at sites GB3 and LB1 for particles of size below 2 mm. The x axis is logarithmic expression of particle size in μm . Each site is represented by the three charts - for top (A), middle (B) and lower section of the bank(C).

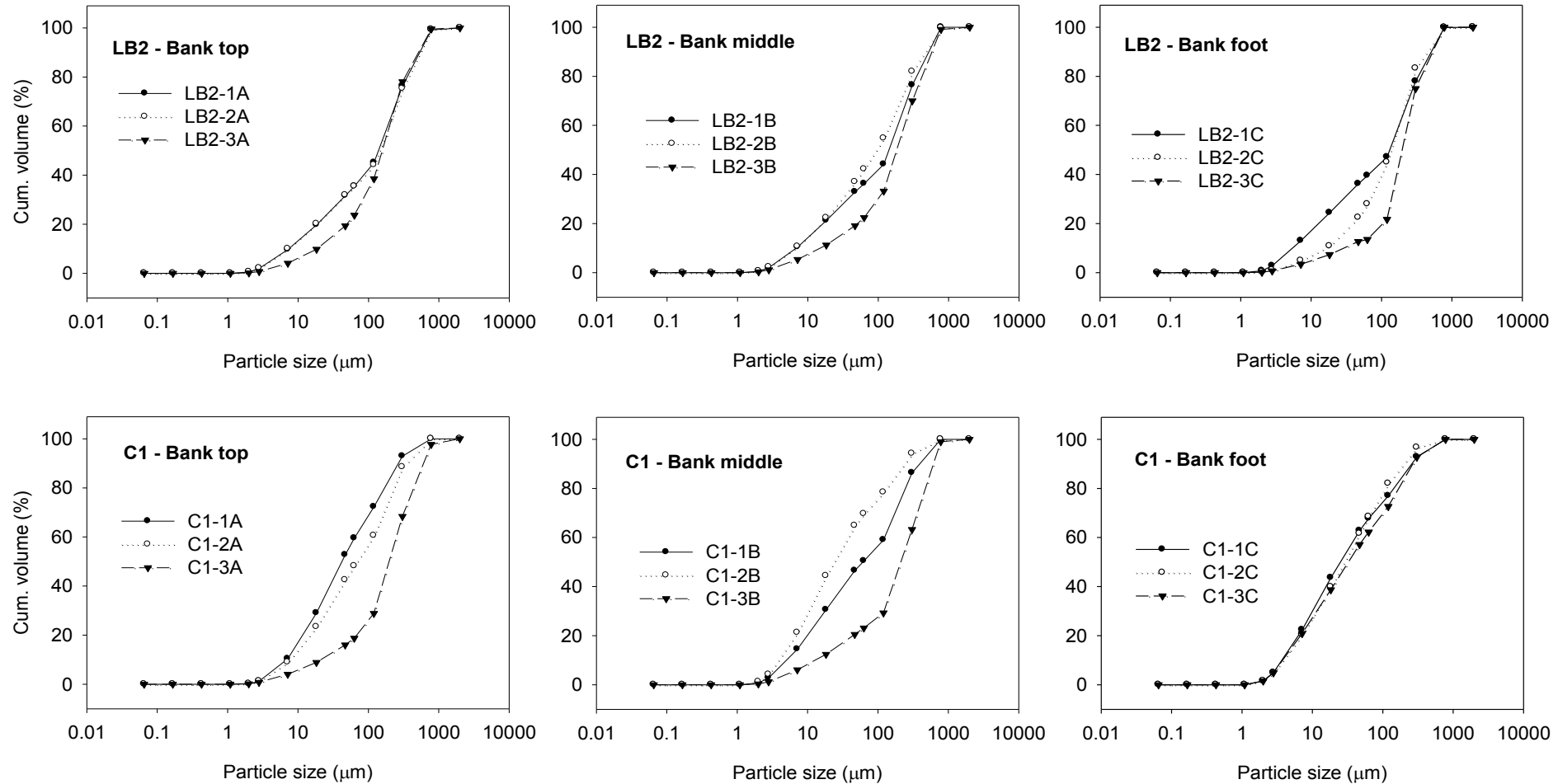


Fig. 3.2.10 Cumulative volumetric percentage of particle size fractions for three sections of banks at sites LB2 and C1 for particles of size below 2 mm. The x axis is logarithmic expression of particle size in μm . Each site is represented by the three charts – for top (A), middle (B) and lower section of the bank (C).

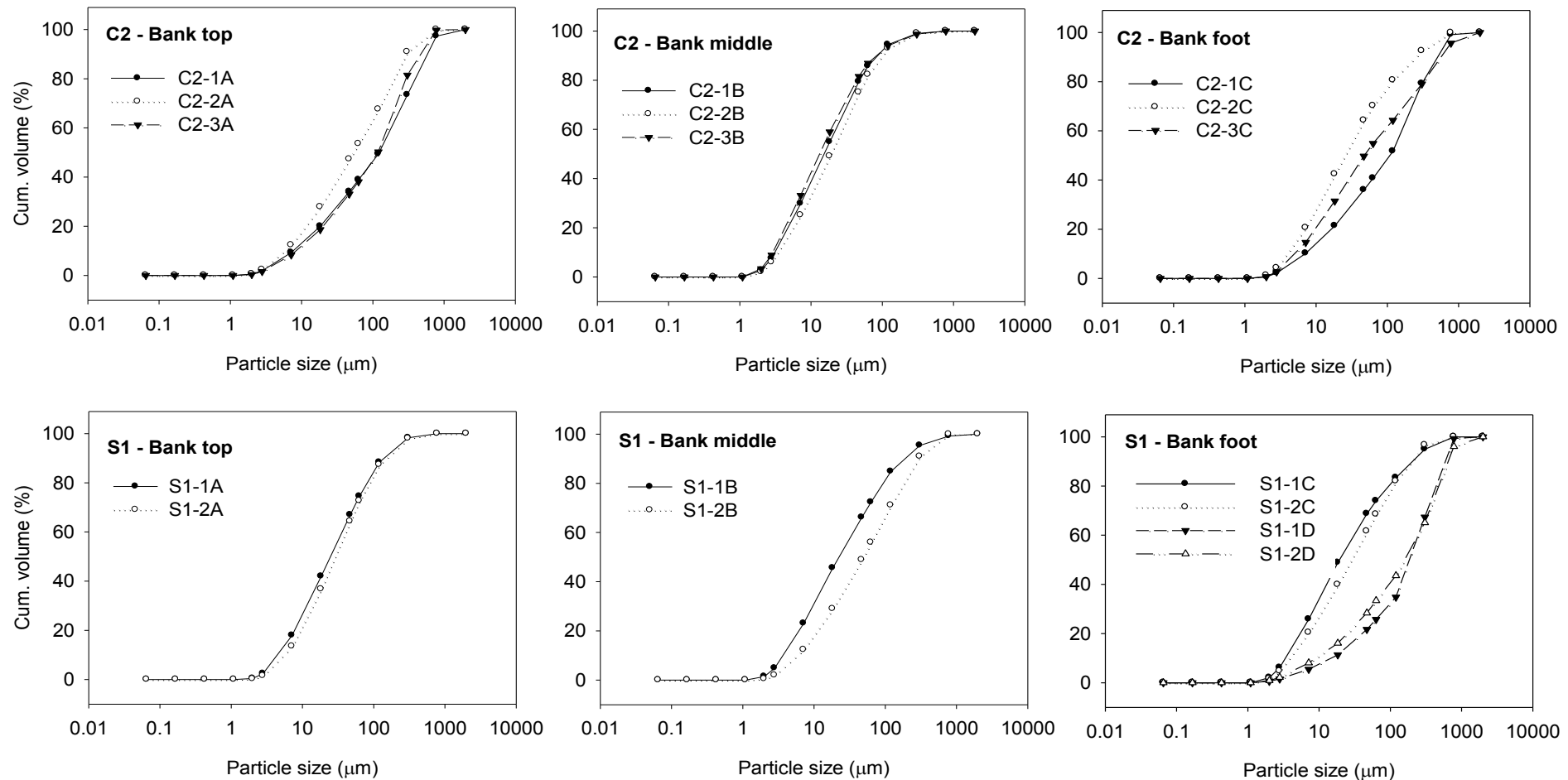


Fig. 3.2.11 Cumulative volumetric percentage of particle size fractions for three sections of banks at sites C2 and S1 for particles of size below 2 mm. The x axis is logarithmic expression of particle size in μm . Each site is represented by the three charts – for top (A), middle (B) and lower section of the bank (C).

3.2.5. SHEAR STRENGTH OF SOILS AND VARIABILITY WITH MOISTURE CONTENT

The erodibility of soils can be explained in terms of their inherent shear strength (Tengbeh 1989). As pointed out in Chapter 2, shear strength is reliant on cohesion, normal stress and the angle of internal friction. For cohesive soils, under saturated conditions, the angle of internal friction is considered to be zero and therefore the shear strength force is equal to the effective cohesion force. Conversely, for non-cohesive soils where a cohesion force can be expected to be zero, the shear strength is dependent on the angle of internal friction and normal stress force (Craig 2004).

There is a decreasing trend in soil shear strength with increasing soil moisture content in cohesive soils (Tengbeh 1989). This is because at high moisture content, large amounts of water molecules are absorbed on the surface of soil particles (diffuse double layer). These create positive pore water pressures which are large enough to push the soil particles apart and so reduce cohesion and weaken the cementation effects of the organic matter and the cations that may be present which decreases the soil shear strength to the minimum. On the other hand, at low moisture contents the thickness of the moisture films between particles decreases. This leads to increases in shear strength due to increased suction causing negative pore pressures and an apparent increasing cohesion (Baver *et al.* 1972).

The shear strength and moisture content relationship is exponential and the increases in shear strength with decreasing moisture content are not uniform throughout the range of moisture contents (Baver *et al.* 1972; Tengbeh 1989). In much geotechnical literature, these relationships are transformed into logarithmic plots as the relationship then plots as a line (Schofield & Wroth 1968; Wood 1990). At high moisture contents, the shear strength increases are small for a small decrease in moisture content but at low moisture content, the shear strength increases rapidly with small decrease in moisture (Tengbeh 1989).

Spoor *et al.* (1982) attributed this behaviour to the shrinkage characteristics of the soil: (1) At high moisture content, structural soil shrinkage occurs and a large amount of water flows through. Drying leads to only a small shrinkage and thus to a small increase in shear strength. (2) At intermediate moisture contents (between Atterberg's Liquid and Plastic Limits), when normal shrinkage occurs, the volume of shrinkage is proportional to the volume of water loss. This results in a higher increase in shear strength. (3) At moisture contents below the shrinkage limit which is usually slightly less than the Plastic Limit, no further shrinkage takes place on further drying (Young 1975).

Atterberg's Liquid Limit defines the minimum water content at which the soil behaves like liquid. It can be found through a cone penetration test. The Plastic Limit is the minimum water content needed for soil to exhibit plastic behaviour (BSI 1975). It can be found from the water content at which a 3 mm thick soil thread starts cracking if further rolled (Lee & Seed 1967; Das 2006).

3.2.5(A) SHEAR STRENGTH TESTING

Several field and laboratory methods exist to estimate the shear strength of soils, the most common methods being the triaxial test, torsional box and shear vane. Triaxial test and translation box require the use of core soil samples, the strengths of which may not reflect the true field shear strengths (Tengbeh 1989). The torsional shear box was developed to give *in situ* shear strength at various normal stresses (Payne & Fountaine 1952), but the method was shown to be suitable only during saturated conditions (Tengbeh 1989).



Fig. 3.2.12 *In situ* soil shear strength testing using the Field Vane at the S1 site (Fig. 3.1.1). Sedimentary layers with material of different texture are distinctive in the bank, mainly the grey lens of clay below more sandy and silty material.

The Field Vane designed by Cadling and Odenstad (1950) allowed for direct *in situ* determination of the undrained cohesion of soft soils, avoiding the disturbance to the samples which can occur during the sampling process and manipulation of core samples for laboratory tests (Bouassida & Boussetta 1999). The values obtained by Vane field tests were shown to be more consistent (Serota & Jangle 1972) and represented actual soil failures at least as equal to laboratory compression tests, however the main problem with

the shear vane is that the shear strength parameters, cohesion and friction, cannot be separated (Tengbeh 1989).

Shear strength measurements were taken *in situ* using a Pilcon DR 1240 shear vane tester with 19 mm and 33 mm blades and with a range of 120 kPa (Fig. 3.2.12). The vane was inserted into soil at a depth of approximately 15 cm and a clockwise rotation at a constant rate was applied to the vane. This loading induced the reaction of the soil which was transmitted from the rod to the metre by spring. The value of the torque was determined on the scale. Readings of the maximum deflection of the spring in kPa and the residual (remoulded) strength were taken from the bank surface at depths of approximately 10 cm in the top (below plant roots), middle and lower sections of the bank. However, sometimes the upper section of bank was too stiff for the vane blades to penetrate and in this case the torque was greater than the 120 kPa range.

3.2.5(B) SOIL MOISTURE AND SPECIFIC GRAVITY

Samples were taken horizontally from the bank profile during low flows using 10 cm long metal sampling tubes of 2 cm inner diameter. Three samples were taken from each bank profile on a single occasion from top (A), middle (B) and bottom (C/D) sections of the bank. The bottom section at the water level was saturated. The samples of approximately 25 g for finer (< 0.5 mm) and 50 g for coarser samples (< 2 mm) were oven dried at 110° C to a constant weight and weighed on a Fischer brand DB - 401 scale to the nearest 0.1 g. Gravimetric water content μ was used to express the water content in every sample:

$$\mu = \frac{m_w}{m_s} \cdot 100$$

Where m_w is the mass of water and m_s is the mass of dry solids. Other definitions of moisture content exist, such as by volume, but this approach is that of geotechnical literature.

Dry soil samples were put in a 100 ml graduated cylinder, topped up with water, mixed thoroughly to remove any captivated air and the suspension was weighted. The specific gravity of soil G_s was then estimated from the equation:

$$G_s = \frac{m_s}{m_s + m_{cw} - m_{cws}}$$

Where m_s is the mass of dry soil, m_{cw} is the mass of cylinder with 100 ml of water and m_{cws} is the mass of cylinder with soil and topped up with water.

3.2.5(C) SATURATED AND UNSATURATED SHEAR STRENGTH PARAMETERS AT SOME CHOSEN PROFILES

In situ measurements of undrained shear strength were undertaken at the C1, C2, S1 and N1 sites during unsaturated and saturated conditions immediately after high flows. During the unsaturated state, torque readings were taken in the eroding bank both at the cohesive (S1) and the non-cohesive (N1) site. The values were plotted against the distance going downstream (Fig 3.2.13).

Although shear vane testing is designed for cohesive soils, it was also used at the N1 site to get readings from profiles composed of sand and fine gravel. As illustrated in Fig. 3.2.13, these values fall within a small interval of low shear strengths. The mean undrained shear strength \pm SD for this non-cohesive site was 3.55 ± 0.52 kPa, while the shear strength at the cohesive site was 32.47 ± 4.38 kPa.

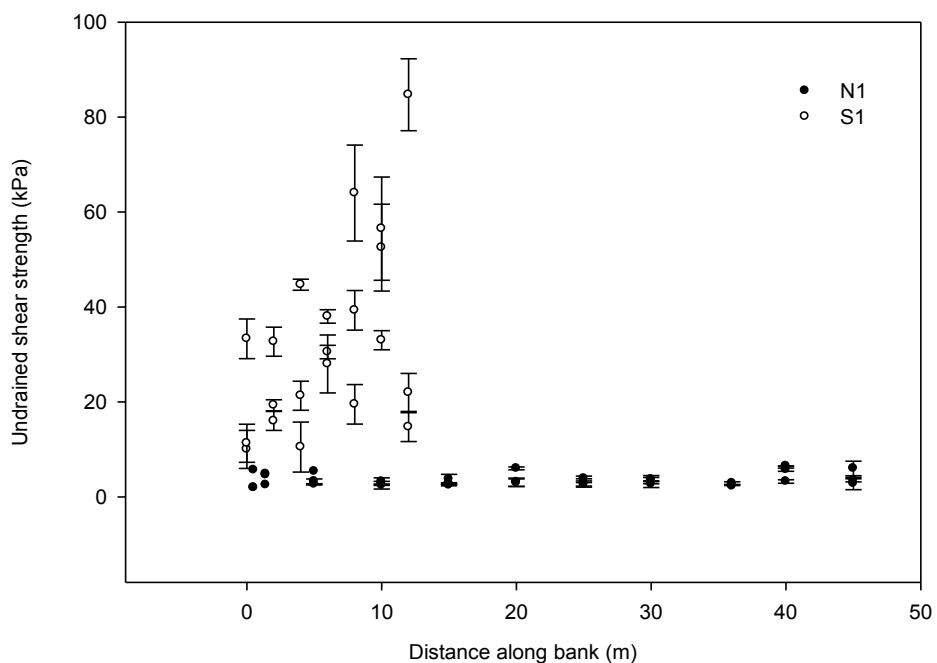


Fig. 3.2.13 Comparison of the mean undrained shear strength measured at the S1 site on 24.6.2008 and at N1 site on 25.1.2008 under unsaturated conditions using Pilcom Field Tester (in kPa). Error bars represent the standard deviation (square root of variance, representing the spread of values around the mean). Measurements were taken in three bank sections: top, middle and lower.

The specific gravity of soils did not vary much between the sites ($p>0.05$) and the values fell within the range 2.68 to 2.04. The mean specific gravity was 2.35 ± 0.16 and the lowest values occurred at N1 (Table 3.2.6). Specific gravity is independent of moisture content and should be typical for the particular sampling point.

Table 3.2.7 *Wet (m_{ws}) and dry sample masses (m_s) in g; gravimetric water content (u) in% and the specific gravity (G_s) for sample locations taken on the following dates: S1 on 31.5.2009, N1 on 14.6.2009 and C1 on 6.6.2009*.*

Sampling code	Wet sample mass (g)	Dry sample mass (g)	Gravimetric water content (%)	Mass of topped up cylinder with sample (g)	Specific gravity
S1-1A	24.3	15.3	37.04	148.2	2.04
S1-1B	32.3	24.0	25.70	152.3	2.35
S1-1C	48.3	31.5	34.78	148.7	2.28
S1-2A	40.3	33.8	16.13	160.2	2.41
S1-2B	26.5	23.3	12.08	155.0	2.68
S1-2C	56.4	46.6	17.38	168.7	2.55
N1-1A	17.4	16.8	3.45	150.1	2.37
N1-1B	22.2	21.3	4.05	152.4	2.29
N1-1C	39.3	29.8	24.17	157.4	2.33
N1-2A	21.9	19.7	10.05	150.6	2.07
N1-2B	18.1	17.9	1.11	150.5	2.29
N1-2C	48.1	41.2	14.35	164.9	2.47
C1-5A	59.1	51.6	12.69	170.1	2.36
C1-5B	43.6	35.5	18.58	161.7	2.50
C1-5C	41.9	28.0	33.17	155.7	2.21
C1-6A	57.0	48.5	14.91	168.4	2.37
C1-6B	40.3	32.6	19.11	159.6	2.43
C1-6C	39.8	26.5	33.42	155.1	2.25

*The mass of cylinder with 100 ml water was 140.4 g and the weight of an empty cylinder was 41.4 g. The mass of cylinder with sample topped up with water (m_{cw}) is also shown. At each site, the codes 1A, 1B, 1C etc. relate to the bank section as top (A), middle (B) and lower (C/D) where 1, 2, 3 etc. are the numbers of vertical sections.

The undrained shear strengths of the individual points are presented under unsaturated (Table 3.2.7) and saturated (Table 3.2.8) conditions. Some testing points have corresponding gravimetric moisture content. Under the unsaturated conditions, shear strength at each sampling location varied between 5.8 kPa (N1-1B) and 80 kPa (S1-2A). The mean shear strength across the C1, C2 and S1 sites during unsaturated conditions was 42.5 ± 8.4 kPa. When the soil was saturated after a bankfull event, this was reduced to 29.3 ± 4.8 kPa.

Table 3.2.8 Mean shear strength taken under unsaturated conditions at the sampled profiles (kPa). Where available, gravimetric water content is also shown as u (%). At each site, the codes 1A, 1B, 1C etc. relate to the bank section as top (A), middle (B) and lower (C/D), where 1, 2, 3 etc. are the numbers of vertical sections.

Sampling code	Date	Soil texture	Shear strength ± SD (kPa)	u (%)
S1-1A	23.5.2009	sandy silt loam	37.5 ± 3.9	37.04
S1-1B		sandy silt loam	33.9 ± 3.4	25.70
S1-1C		sandy silt loam	29.8 ± 1.3	34.78
S1-2A		sandy silt loam	82.0 ± 14.0	16.13
S1-2B		sandy silt loam	34.8 ± 3.7	12.08
S1-2C		loamy sand	32.4 ± 5.4	17.38
S1-1A	30.7.2009	sandy silt loam	57.5 ± 12.9	-
S1-1B		sandy silt loam	41.7 ± 0.6	-
S1-1C		sandy silt loam	33.0 ± 6.2	-
S1-2A		sandy silt loam	57.7 ± 4.7	-
S1-2B		sandy silt loam	56.8 ± 4.7	-
S1-2C		loamy sand	35.0 ± 4.1	-
S1-1A	9.8.2009	sandy silt loam	52.6 ± 18.8	27.52
S1-1B		sandy silt loam	60.4 ± 10.2	32.70
S1-1C		sandy silt loam	42.3 ± 7.0	34.68
S1-2A	9.8.2009	sandy silt loam	45.3 ± 13.8	29.47
S1-2B		sandy silt loam	45.5 ± 5.2	29.67
S1-2C		loamy sand	28.3 ± 3.8	24.07
C1-5A	6.6.2009	loamy sand	50.5 ± 6.4	12.69
C1-5B		loamy sand	75.3 ± 13.7	18.58
C1-5C		sandy silt loam	34.5 ± 11.3	33.17
C1-6A		loamy sand	31.0 ± 17.2	14.91
C1-6B		loamy sand	74.5 ± 13.3	19.11
C1-6C		sandy silt loam	43.2 ± 8.6	33.42
C1-5A	1.8.2009	loamy sand	38.5 ± 14.6	10.61
C1-5B		loamy sand	81.3 ± 9.3	16.62
C1-6A		loamy sand	37.0 ± 11.5	10.31
C1-6B		loamy sand	74.0 ± 16.4	17.74
C2-3A	12.12.2006	sandy loam	14.2 ± 7.2	-
C2-3B		silt loam	21.6 ± 6.5	-
C2-3C		sandy silt loam	43.0 ± 7.0	-
N1-1A	14.6.2009	gravel	8.6 ± 11.4	3.45
N1-1B		gravel	5.9 ± 4.0	4.05
N1-1C		gravel	7.4 ± 4.9	24.17

Table 3.2.9 Mean shear strength (kPa) during saturated conditions. At each site, the codes 1A, 1B, 1C etc. relate to the bank section as top (A), middle (B) and lower (C/D), where 1, 2, 3 etc. are the numbers of vertical sections.

Sampling code	Date	Soil texture	Shear strength \pm SD (kPa)	
S1-1D	23.5.2009	loamy sand	20.0	\pm 3.0
		loamy sand	20.8	\pm 5.3
S1-1D	30.7.2009	loamy sand	14.8	\pm 2.8
		loamy sand	18.8	\pm 1.9
S1-1A	19.1.2010	sandy silt loam	24.7	\pm 5.9
		sandy silt loam	41.5	\pm 15.1
		sandy silt loam	33.7	\pm 2.3
		loamy sand	38.7	\pm 3.1
		sandy silt loam	33.3	\pm 4.6
		sandy silt loam	44.0	\pm 4.0
		loamy sand	42.3	\pm 7.5
		loamy sand	31.7	\pm 1.5
S1-2A	26.1.2010	sandy silt loam	39.0	\pm 9.0
		sandy silt loam	33.0	\pm 4.2
C1-5C	1.8.2009	sandy silt loam	26.7	\pm 4.7
		sandy silt loam	25.5	\pm 3.3
C2-3C	12.12.2006	sandy silt loam	9.80	\pm 3.4

To test whether or not there is a characteristic shear strength for a given soil texture typical for the particular banks, the soils were grouped into the five texture types that were represented within the samples: gravel, loamy sand, sandy loam, sandy silt loam, and silt loam. Three of these that had more than one sampling point were plotted against the moisture content of the sample. This was to observe the relationship with water content and illustrate the breath of typical values for shear strength (Fig. 3.2.14). A weak correlation was observed in the plotted dataset for sandy silt which indicated an inverse relationship between shear strength and soil moisture ($R^2=0.208$). The sandy silt loam data on the top of the chart are close to saturation. If more data was available, it should be possible to show that the nature of this relationship, as given by the soil cohesion and the decrease in shear strength with increasing moisture content, will be more prominent in soils with lesser proportions of sand and gravel.

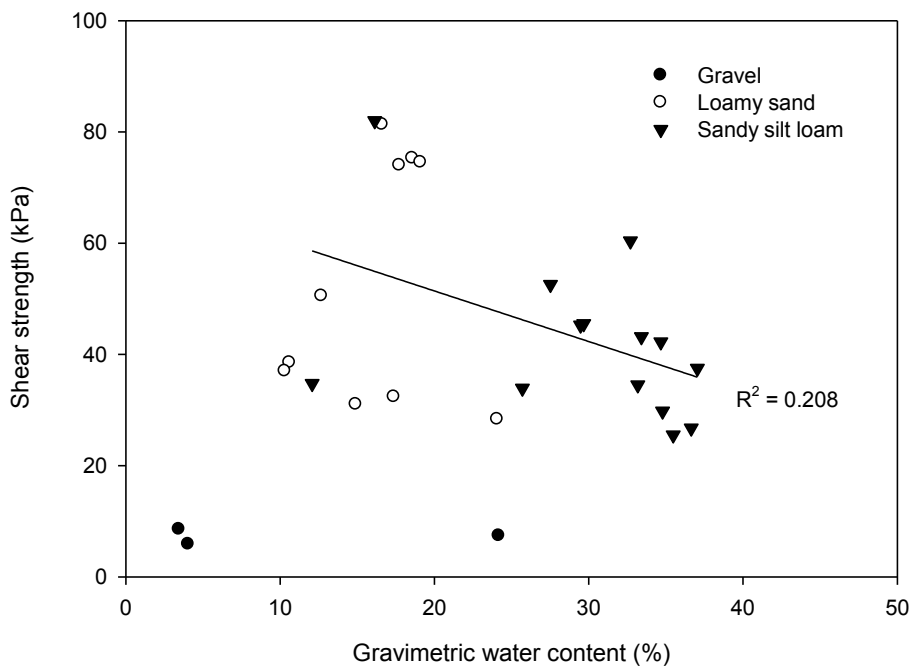


Fig. 3.2.14 Sample shear strength with given water content for some chosen gravel, loamy sand and sandy silt loam samples under undrained conditions. Linear regression applies to sandy silt loam samples.

The main limitation of this analysis is that the mean values were compared with a single soil moisture value. Ideally, soil taken out after each Vane test should have been collected from the vane and analysed. So even though a large number of Vane readings were undertaken, these were of limited value because the corresponding moisture content data were not available. Under saturated conditions, these measures are indicative of soil erodibility as the strength of cohesive samples would, under fully saturated state, correspond with the soil cohesion (Chapter 2.3). Therefore, under saturated conditions, the shear strength would be dependent on the particle size. For example, the mean shear strength of less cohesive, loamy sand \pm SD was 42.42 ± 7.81 kPa and that of more cohesive, sandy silt was 52.28 ± 11.15 kPa. The correlation between the shear strength under saturated conditions and the erosion rate is presented in Chapter 3.5.

3.3. HISTORICAL EROSION RATES

Maps and old photographs are a valuable data source in fluvial geomorphology, especially when investigating lateral channel migration. River bank erosion is regarded as one of the most rapid geomorphic processes (Hooke 1979) and therefore it can be well observed and quantified from historical maps. An analysis of old maps and aerial photography has been used for timescales between 10 and 150 years (Hooke 1979). However, with increasing frequency of updating and accuracy in cartographic mapping and the advanced technology used in aerial photo resolution, together with rapidly developing software applications, this timescale is being reduced. Historical map sources appear to be, by far, the most popular method of observing lateral channel migration. Lawler (1993a) found that 51% of all research papers on bank erosion measurement techniques published between 1863 and 1988 used historical map resources. Intensive field studies are typically carried out over a period of a couple of years, making it difficult to establish whether the observed rates and types of erosion that are recorded are typical of long-term changes. Therefore, data derived from historical sources is invaluable in placing detailed field studies into the context of larger-scale and longer-term channel evolution (Thorne 1981). In this section, changes to the channel planform at nine field sites over 150 years are presented. The data is compared with the short-term field erosion rates, as proposed in the Objective 2 at the beginning of this study (Section 3.4.3).

3.3.1. METHODOLOGY OF HISTORICAL ANALYSIS

3.3.1(A) ORDNANCE SURVEY MAPS

For this thesis a number of historical maps and photographs were consulted (Table 3.3.1). Historical maps went back about 150 years, aerial photographs 56 years. Maps of 1:2,500 scale in digital form were used for analysis, downloaded from Edina Digimap service. At this larger scale, the map sheets were richer in detail and higher in precision. The width of the bank line on the map, for example, corresponded to the actual dimensions of $\pm 0.5\text{--}1\text{ m}$, whilst on the 1:10,000 maps this came to a far less precise $\pm 2.5\text{--}3.0\text{ m}$. For GIS analysis, maps from three historical editions were chosen and these were aligned with a recent Mastermap in the British National Grid coordinate system projection OSGB 1936. This was done using the widely deployed GIS software package ESRI ArcGIS, version 9.3. The list of maps used for this is shown in Table 3.3.2 and snapshots of the field sites are in the Appendix (Fig. 3.3.A).

Table 3.3.1 Historical maps and aerial photographs available for the research area. Time intervals indicate period of survey for the particular edition.

Date	Source	Scale/resolution
1854-1901	Ordnance Survey County Series: 1st Edition	1:2,500
1893-1915	Ordnance Survey County Series: 1st Revision	1:2,500
1906-1939	Ordnance Survey County Series: 2nd Revision	1:2,500
1924-1949	Ordnance Survey County Series: 3rd Revision	1:2,500
1945	Aerial photographs, The Geoinformation Group	1:10,000
1943-1995	National Grid, National Survey	1:2,500
1995-recent	National Grid, Latest Editions	1:10,000
1945	RAF aerial photographs	1:10,000
2000	Aerial photograph, Infoterra (Google Earth)	25 cm
2004/2005	Aerial photograph (Microsoft Live Earth)	12.5 cm
2006	Aerial photograph, Infoterra (Google Earth)	25 cm
2007	Aerial photograph, Infoterra (Google Earth)	25 cm

Firstly, a point Shapefile was created in ArcCatalog (part of the ArcGIS package), to accommodate the x,y reference points. In ArcMap, the raster file of the ordnance survey map and the shapefile were uploaded. Reference points, typically about 10, were created in critical places: in the corners and spread across the map sheet on objects that were clearly identifiable across all the maps and were unlikely to have changed over time (e.g. corners of church buildings, historical hedge junctions). These points were used to construct a polynomial transformation that shifted the raster dataset from its original to the spatially correct location (ESRI 2009). A number of links were created between the original raster map and the Mastermap, Edina Digimap 2008, in order to achieve the smallest Root Mean Square (RMS) error possible. RMS describes how consistent the transformation is between the different links (ESRI 2009). The map editions and map tiles used alongside the RMS value for each of the field sites are shown in Table 3.3.2. RMS ranged from 0.88 to 3.51m. The mean RMS \pm SD was 1.63 \pm 0.59 m.

Table 3.3.2 *Historical maps used for bank retreat measurement in GIS for each of the field sites. RMS is the final Root Mean Square Error (m).*

	Map	Edition	Year	Tiles	RMS
GB1	County Series	1st edition	1886	04049151	1.30
	County Series	1st revision	1903	04049152	1.35
	National Grid	1st edition	1981	TL6653a5	1.22
GB2	County series	1st edition	1886	04049151	1.30
	County series	1st revision	1904	04049152	1.35
	National Grid	1st edition	1981	TL6753a5	1.25
GB3	County series	1st edition	1886	04049151	1.30
	County series	1st revision	1904	04049152	1.35
	National Grid	1st edition	1981	TL6753a5	1.25
LB1	County series	1st edition	1886	33061031	2.38
	County series	1st revision	1904	33061032	1.54
	National Grid	1st edition	1981	TL6752a5	1.67
LB2	County series	1st edition	1886	33061071	1.50
	County series	1st revision	1904	33061072	1.75
	National Grid	1st edition west	1981	TL6751a5	-
	National Grid	1st edition east	1982	TL6851a5	-
C1	County series	1st edition	1886	33071071	1.93
	County series	1st revision	1904	33071072	2.34
	National Grid	1st revision north	1968	TL7745b6	1.32
	National Grid	1st revision south	1968	TL7744b6	0.88
S1	County series	1st edition	1886	33072151	1.38
	County series	1st revision	1904	33072152	1.50
	National Grid	1st revision	1966	TL8641b6	-
N1	County series	1st edition	1886	33086031	3.51
	County series	1st revision	1904	33086032	2.55
	National Grid	1st edition	1962	TL9733a5	-

Secondly, a section of channel containing the field site was digitised from the maps for two historical and one recent date so that the channel variability could be compared visually. Measurements of the bank retreat were also taken as the total eroded area in m^2/m and as the maximum retreat that occurred within the field site stretch in m. The rate of migration was calculated as a total loss of land in m^2 per m of bank length per year.

3.3.1(B) VERTICAL AERIAL PHOTOGRAPHS

Aerial photographs also represent a valuable resource in fluvial geomorphology. They have been used effectively for a rapid assessment of recent changes in channel morphology. With the availability of high resolution imagery online, these resources can

be accessed instantly and freely. Some vertical photographs from 1945 were also available for the upper part of the studied area (example on Fig. 3.3.1).

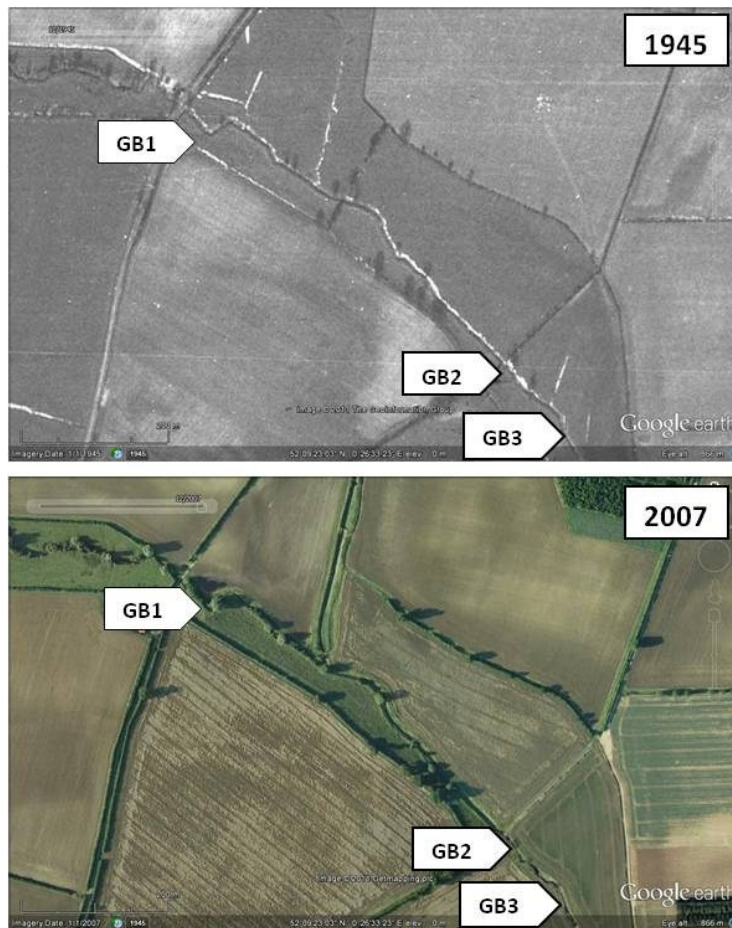


Fig. 3.3.1 Identical reach near Great Bradley in 1945 (obtained from Geoinformation Group, 2011) and 2007 (Getmapping plc. 2010). White arrows show the location of the field sites near Great Bradley.

Aerial photographs covering a number of years between 2000 and 2007 were downloaded from Google Earth 6.1. The photographs were compared visually for three field sites that had a clearly identifiable bank line (as opposed to the other field sites where vegetation cover shaded the bank line). As shown in Table 3.3.1., the resolution of these photographs varied between 25 to 12.5 cm, which is greater detail than the 1:2,500 scale maps, but the lack of reference points close to the field sites made it difficult to georeference the images from Google maps in the GIS programme. The imagery from satellites was also explored as a possible resource, but resolution was found to be too coarse for the purpose.

3.3.2. RESULTS OF HISTORICAL CHANGES

3.3.2(A) CHANGES TO THE RIVER CHANNEL AS IDENTIFIED FROM ORDNANCE SURVEY MAPS SINCE 1886

Over a 150-year timescale, one might have expected greater changes within the study channels but the meanders generally retained their recognisable shapes and sizes. As a common observation, the channels on recent maps appear to be 'smoother'. By observing the sequences shown in the Appendix, some broad deductions can be made. Starting upstream, at Great Bradley (GB1 site), the river preserved its engineered pattern throughout the whole period. Changes do not appear to be large and this would be expected for a small clay stream with chalk bedrock. A noticeable change in channel planform occurred at the outer river bank of the engineered channel, copying field boundaries at the site GB1 and along the downstream end of the reach (Fig. 3.3.2).

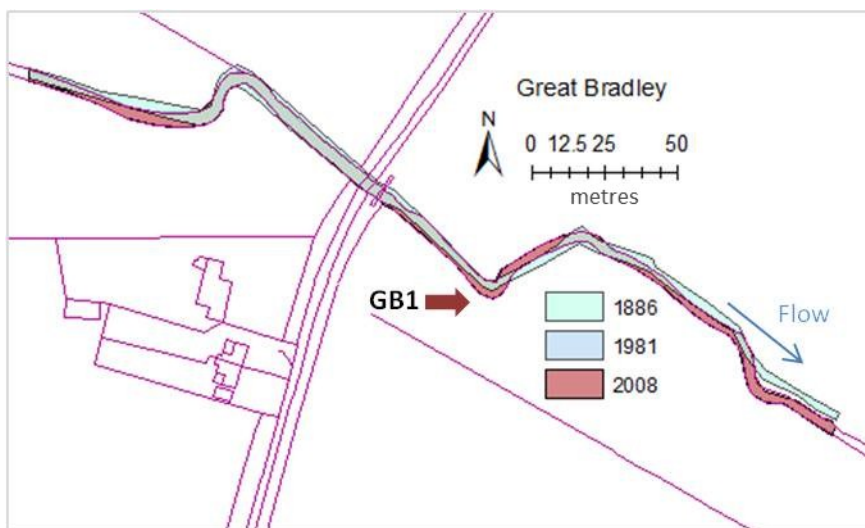


Fig. 3.3.2 The engineered channel planform of the River Stour with the GB1 site in 1886, 1981 and 2008. (Base map is 2008 Mastermap © Crown Copyright/database right 2008. An Ordnance Survey/EDINA supplied service).

Further downstream, the river reaches sites GB2 and GB3. The channel platform did not change visibly and keeps its straight course throughout the sequence. The level of migration was limited, because a considerable length of bank was supported by hard engineering. Some channel movement could possibly be a response to the introduction of transferred flows and dredging works related to the water transfer scheme (Fig. 3.3.3).

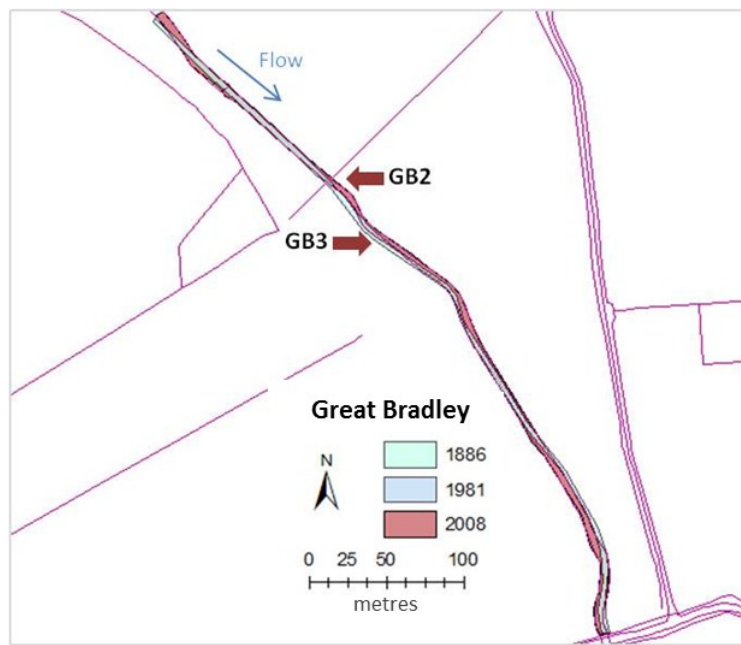


Fig. 3.3.3 The channel of the River Stour showing GB2 and GB3 sites in 1886, 1981 and 2008 (Base map is 2008 Mastermap © Crown Copyright/database right 2008. An Ordnance Survey/EDINA supplied service).

Above Little Bradley, more significant changes in the meander pattern between 1886 and 1981 can be seen in the channel form in the reach upstream from the bridge. Three weirs were built here to improve water quality from the transfer scheme and as part of flood protection. This in combination with high, steep and silty river banks was the most likely cause of the increased channel migration, leading to the development of a sinuous river course (Fig. 3.3.4).

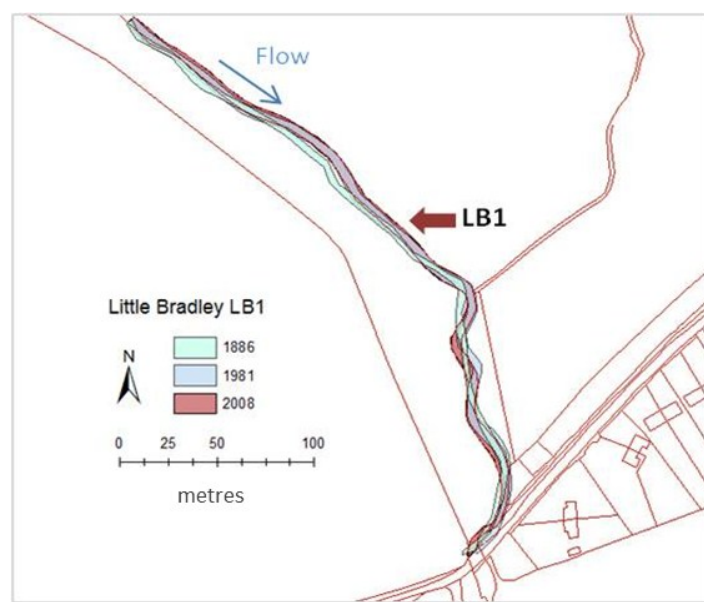


Fig. 3.3.4 The channel of the River Stour with the LB1 site in 1886, 1981 and 2008. (Base map is 2008 Mastermap © Crown Copyright/database right 2008. An Ordnance Survey/EDINA supplied service).

The river channel has also been altered near the LB2 site and the planform appears to be artificial. A number of gabion basket structures were put in place upstream of the site and some straightening and dredging occurred in conjunction with the water transfer scheme. In this case especially, the width of the channel in 2008 appeared to be more uniform than the channel in 1886 (Fig. 3.3.5).

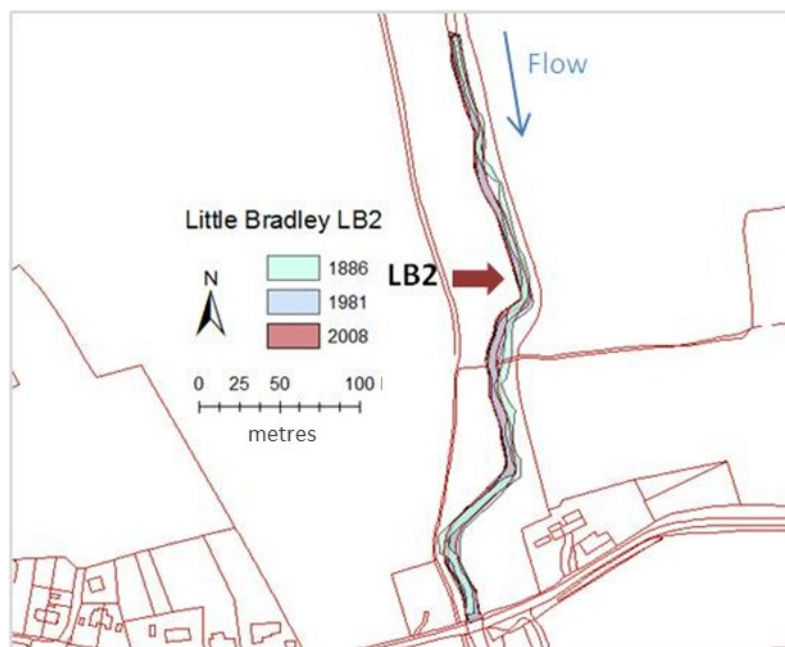


Fig. 3.3.5 The channel of the River Stour with the LB2 site in 1886, 1981 and 2008. (Base map is 2008 Mastermap © Crown Copyright/database right 2008. An Ordnance Survey/EDINA supplied service).

In Clare (Fig. 3.3.6), the channel in 1886 appears less smooth with varied widths, but the general platform remains similar throughout the sequence. The 1886 map also reveals banks lined with trees. Since then, these have been removed and riparian land turned into agricultural field right up to the bank edge. Conservation efforts over the past 15 years have aimed to restore the riparian vegetation with an emphasis to increase the stability of the river banks, but most of the trees failed to establish because the water table was either too low or the young trees eroded with the bank. Although the river's connection with the floodplain has been lost through dredging, the new landowner left the loop between C1 and C2 sites and a 10 m strip along the channel as a buffer and wildlife zone. At C1, minimal erosion occurred, or even a bank accretion. This was, once again, most likely caused by engineering alterations rather than natural processes. Substantial erosion occurred at the C2 site, where the tight meander migrated downstream.

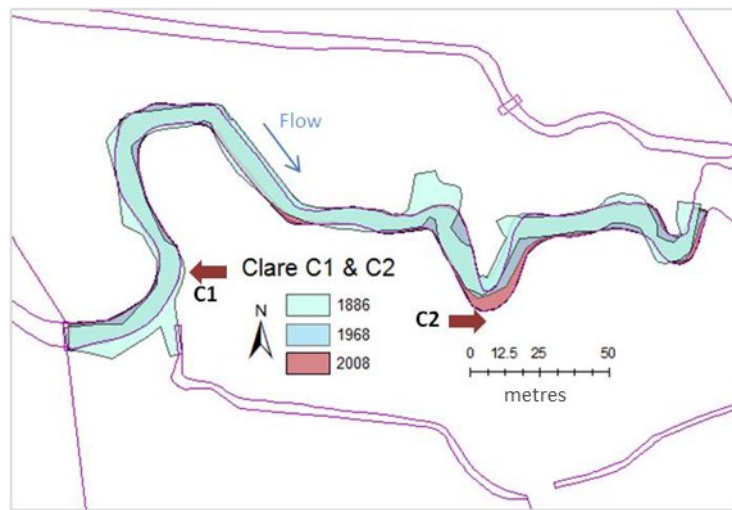


Fig. 3.3.6 The channel of the River Stour showing C1 and C2 sites in 1886, 1968 and 2008. (Base map is 2008 Mastermap © Crown Copyright/database right 2008. An Ordnance Survey/EDINA supplied service).

In Sudbury, the channel flowing through the meadows has been historically altered to take the water to the mill. The reach shown in Fig. 3.3.7 is the original river channel, while the channel diagonally across the northeast corner is the new channel cut for the Sudbury Mill in 1960s. A new weir installed in the 1960s, in combination with channel straightening, had a significant effect on the channel form as seen on the digitized outline from 1966. With the new weir, the channel started its adjustment process of bed and bank scouring, and the effects are noticeable on the outline from 2008.

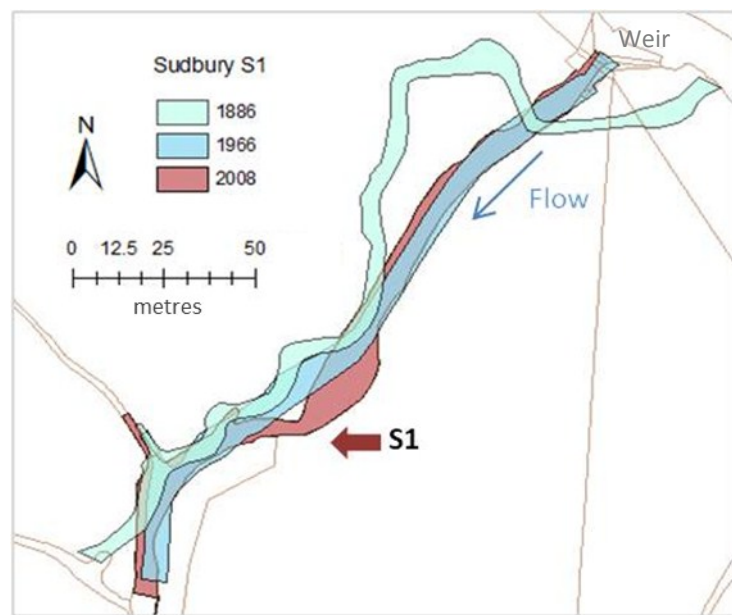


Fig. 3.3.7 Position of the channel of the River Stour showing the S1 site in 1886, 1966 and 2008. (Base map is 2008 Mastermap © Crown Copyright/database right 2008. An Ordnance Survey/EDINA supplied service).

Further downstream, at Nayland, meanders have migrated downstream significantly (18.7 m in 122 years), Fig. 3.3.8. Here, the channel edge in 1962 appears to have shifted in the opposite direction, by 6.5 m. This is likely to reflect engineering intervention as part of the Nayland flood protection scheme. The new flood relief channel that was connected to the main river increased the water surface slope and deflected the river flow to the opposite bank, causing bank instability. This problem was treated by gabion deflectors, which have protected the bank, but increased the water surface slope and initiated erosion at the second bend further downstream, the project site N1.

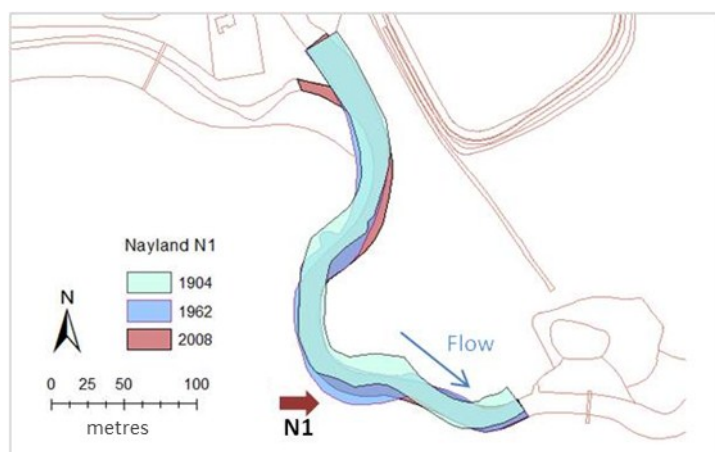


Fig. 3.3.8 River channel with the N1 site in 1904, 1962 and 2008. (Base map is 2008 Mastermap © Crown Copyright/database right 2008. An Ordnance Survey/EDINA supplied service)

To quantify the historical changes, bank erosion was summarized as maximum retreat at the site, total retreat along the stretch of bank for the given period and as annual erosion rate (Table 3.3.3). Between 1886 and 1904 banks eroded by up to 1.7 m in Nayland. The average maximum retreat \pm SD across all sites was 0.93 ± 0.67 m. The maximum annual retreat was $0.06 \text{ m}^2/\text{m/year}$ and occurred at S1 in Sudbury and $0.054 \text{ m}^2/\text{m/year}$ at LB1 in Little Bradley. The mean overall retreat for this period (from 1886 until 1903/4, Table 3.3.3) was $0.02 \pm 0.03 \text{ m}^2/\text{m/year}$. In the second period (from 1904 until 1960s or 80s, see Table 3.3.3), a record retreat of 13.5 m occurred at N1 in Nayland. The mean across all sites was 5.23 ± 3.98 m. Mean annual bank retreat was also highest at N1: $0.141 \text{ m}^2/\text{m/year}$ while the mean annual erosion for all sites was $0.04 \pm 0.04 \text{ m}^2/\text{m/year}$. In the third period (since 1960s or 80s until 2008; see Table 3.3.3), the bank receded most in Sudbury, by up to 9.5 m. On the other hand, the bank in Nayland accreted by up to -6.5 m (Fig. 3.3.8). The maximum annual retreat was in Sudbury: $0.126 \text{ m}^2/\text{m/year}$ and the mean annual retreat across all field sites was $0.028 \pm 0.06 \text{ m}^2/\text{m/year}$.

Table 3.3.3 Bank retreat at each field site as maximum retreat within the stretch (m), average retreat as eroded area over the length of the stretch (m^2/m) and mean annual retreat ($m^2/m/year$) alongside the time periods used. Negative value means bank accretion, positive is bank retreat.

	I.	Max. retreat (m)			Total retreat m^2/m			II.	Max. retreat (m)			Total retreat m^2/m			III.	Max. retreat (m)			Total retreat m^2/m			Mean annual retreat ($m^2/m/year$)	
		Max. retreat (m)	Total retreat m^2/m	Mean annual retreat ($m^2/m/year$)	Max. retreat (m)	Total retreat m^2/m	Mean annual retreat ($m^2/m/year$)		Max. retreat (m)	Total retreat m^2/m	Mean annual retreat ($m^2/m/year$)	Max. retreat (m)	Total retreat m^2/m	Mean annual retreat ($m^2/m/year$)		Max. retreat (m)	Total retreat m^2/m	Mean annual retreat ($m^2/m/year$)	Max. retreat (m)	Total retreat m^2/m	Mean annual retreat ($m^2/m/year$)		
GB1	1886-1903	0.6	0.17	0.009	1903-1981	1.6	0.95	0.012	1981-2008	1.0	0.51	0.019											
GB2	1886-1904	0.0	-0.07	-0.004	1904-1981	4.7	1.86	0.024	1981-2008	1.5	0.85	0.032											
GB3	1886-1904	0.0	-0.06	-0.003	1904-1981	2.4	1.03	0.013	1981-2008	1.8	1.20	0.044											
LB1	1886-1904	1.5	0.98	0.054	1904-1981	2.2	1.53	0.019	1981-2008	2.0	0.07	0.003											
LB2	1886-1904	1.5	0.64	0.036	1904-1981	4.0	0.10	0.001	1981-2008	1.5	1.55	0.057											
C1	1886-1904	1.5	0.20	0.011	1904-1968	2.7	1.17	0.018	1968-2008	0.8	0.08	0.002											
C2	1886-1904	0.5	0.10	0.006	1904-1968	6.5	2.60	0.041	1968-2008	4.5	2.70	0.068											
S1	1886-1904	1.1	1.10	0.060	1904-1966	9.5	5.40	0.087	1966-2008	9.5	5.30	0.126											
N1	1886-1904	1.7	0.80	0.040	1904-1962	13.5	8.20	0.141	1962-2008	-6.5	-4.71	-0.102											

These results show several extremes that have been mentioned above, but overall (1904-2008), the mean annual erosion varies only between 0.02 and 0.04 $m^2/m/year$. There is no significant difference between the datasets for each of the three periods ($p>0.05$).

To find out what tendency there was for channel sinuosity in the reach to evolve, calculations have been made for each period (Table 3.3.4). Sinuosity was calculated as the ratio of channel to valley length for the reach (Chapter 3.2). Considering all the reaches pictured in Figs 3.3.2-8, sinuosity increased at 56% of sites and decreased at the remaining 44%. The highest increase was recorded in the reach around the LB1 site (by 1.6%) and the highest decrease was at the S1 site (by 16.1%). Between 1886 and 1981, sinuosity dropped by -0.0552 ± 0.098 on average and by 2008 the mean sinuosity increased by 0.0103 ± 0.0206 . However, statistically there was no significant difference between the two

periods ($p>0.05$). Over the entire time period, the sinuosity decreased across all sites by -0.045 ± 0.081 m/m, which can be attributed to engineering measures.

Table 3.3.4 Evolution of channel sinuosity of the digitized reaches measured as the length of the channel at midpoint/direct length. Delta is the change in sinuosity between 1886 and 2008.

	I.	Site sinuosity (m/m)	II.	Site sinuosity (m/m)	III.	Site sinuosity (m/m)	Delta (m/m) (III.-I.)
GB1	1886	1.139	1981	1.145	2008	1.149	0,0094
GB2	1886	1.038	1981	1.038	2008	1.048	0,0099
GB3	1886	1.038	1981	1.038	2008	1.048	0,0099
LB1	1886	1.141	1981	1.171	2008	1.159	0,0179
LB2	1886	1.133	1981	1.114	2008	1.092	-0,0406
C1	1886	1.738	1968	1.606	2008	1.629	-0,1087
C2	1886	1.738	1968	1.606	2008	1.629	-0,1087
S1	1886	1.313	1966	1.051	2008	1.101	-0,2122
N1	1886	1.371	1962	1.383	2008	1.389	0,0181

3.3.2(B) CHANGES OBSERVED FROM VERTICAL AERIAL PHOTOGRAPHS SINCE 2000

Similar to historical maps, visual observations can be helpful when making initial assessments. To demonstrate this, the sequences below show recent aerial photographs for three field sites: C2, S1 and N1, taken during different seasons since 2000.

At the C2 site in Clare, the bank line is only clearly visible at the meander apex on photographs from 2006 and 2007 (taken during winter months). The low resolution of images in conjunction with the short time interval is not suitable for measuring the erosion rate although it is useful to point out larger failures or changes in longer reaches. The photographs show that land management changed some time before 2006 and there is now a 10 m wide (approximately) buffer zone on the south bank (Fig. 3.3.9).



Fig. 3.3.9 Aerial imagery sequence for the C2 field site in Clare (© Infoterra Ltd. & Bluesky, Google Earth, 2011).

The situation is also complicated at the S1 site in Sudbury, because the bank line can be clearly identified only in the image taken in winter 2007. In 2000, more vegetation appears to be located at the bank foot. The fence is of a different shape than seen in 2006, which may indicate that it had been damaged by erosion (this was also mentioned by the landowner), (Fig. 3.3.10).



Fig. 3.3.10 Aerial imagery sequence for the S1 field site in Sudbury (© Infoterra Ltd. & Bluesky, Google Earth, 2011).

In Nayland, the N1 site shows some important changes through the sequence of pictures. The 2000 image illustrates a tree growing in the middle of the site that is missing on further images. The ownership of the land has changed since then so no information is available on whether the tree had been cut or its loss was caused by erosion. Possibly, since deflectors were installed upstream of the site, increased erosive force has undermined the tree which was sitting on loose gravel sediments. Vegetation appeared to be covering the bank face in 2000, which is now mostly bare. The 2005, 2006 and 2007 images show fast progressing erosion that is 'eating' the bank edge, and is progressing both upstream and downstream (Fig. 3.3.11).



Fig. 3.3.11 Aerial imagery sequence for the N1 field site (© Infoterra Ltd. & Bluesky, Google Earth, 2011).

3.3.3. CHALLENGES IN ANALYSING HISTORICAL RESOURCES

In a review, Lawler (1993a) lists a number of problems connected with the use of historical resources, for example the assumption of continuity and linearity in channel change over time, survey and plotting errors, map distortion or variations in river channel definition.

3.3.3(A) ASSUMPTION OF CONTINUITY AND LINEARITY OF CHANGE

From historical resources, one can too easily make the hypothesis that bank retreat has been simple, continuous and regular between any set two dates. Peak rates of erosion and more complex processes would have then been underestimated. Hooke (1979) found that the erosion rate measured in the field was much higher than the rate calculated from old maps. It appeared to her that the longer the period over which the data is taken, the lower the resulting erosion rate. The data for longer periods are regarded as 'smoothed' and are largely unaffected by short-term, high magnitude events. This is further examined in Chapter 3.4.

3.3.3(B) ACCURACY OF MAPS AND AERIAL PHOTOGRAPHS

The process of creating a map can include errors at various stages, from the initial surveying, through the plotting stage, to the deterioration of the map in storage. Older maps tend to have a higher level of distortion as the accuracy increases with advances in surveying, processing technology and digital storing. As an example, Tithe parish maps from the mid 19th century are unsuitable for this study due to large discrepancies in accuracy, as described by Lewin and Hughes (1976).

In the case of historic aerial photographs, errors are caused mostly by tilt in the plane of the film at the moment of exposure and also by displacement of the object position due to ground relief (Schofield & Breach 2007). Therefore, no aerial photograph is truly vertical. However, the tilt distortion can be compensated for by creating a stereo pair or by orthophoto rectification in GIS. In Google maps, georegistration problems have been identified, i.e. large errors in aligning linear features such as roads or coastlines (Potere 2008). In Europe, the RMS (root mean square) error was 25.7m. In terms of this study, the accuracy interval was greater than the level of change in the bank line. Comparison was

only possible for photographs taken during winter months with a clearly identifiable bank lines.

3.3.3(C) CHANGE IN CHANNEL DEFINITION OVER TIME

Yet another source of error is also introduced by the confusion over map revision and a change in the definition of the channel's edge. Ordnance Survey understands the bank line to be the normal winter water level, whilst other surveyors have taken the width at the time of surveying or the bank top (Lawler 1993a). The accurate identification of the bank top alone can be a challenge if there is no clear transition between the channel edge and floodplain.

3.3.3(D) DIGITIZING ERRORS

In this type of study, further to errors associated with the map source, one has to consider inaccuracies that come into account during georeferencing and digitizing the raster maps or images.

Downward *et al.* (1994), during digitizing a test reach of the River Towy, found that the error margin for maps in the scales 1:10,000 or 1:10,560 was approximately ± 2.02 and ± 2.12 m respectively. Furthermore, they recommended that, due to combined errors, spatial displacements in excess of 5 m are required before a section of genuine channel movement can be confidently inferred. This threshold varies to some extent with the age and nature of the historical maps (Downward *et al.* 1994).

3.3.3(E) GEOREFERENCING CHALLENGES

Root mean square (RMS) error indicates the extent of the quality of georeferencing map raster data. Some of the most significant challenges of decreasing root mean square error in this study were the lack of control points in rural areas, especially in close proximity to the field site, and possibly the accuracy of raster maps alone. To maximise the accuracy of coordinate transformation in georeferencing, it is recommended that one places enough link points to achieve RTM equal to the raster resolution (ESRI 2009). The general assumption that the more georeferenced points then the more accurate the result, did not appear to be correct from the results in this research study. The best procedure to achieve

the least possible RMS error is to place a reference point in each corner in the map and some points spread throughout the map.

Depending on the source of error, the combined uncertainty can be large and the viability of historical analysis can be therefore questioned on a site-specific scale. Although visual observations or comparisons of longer reaches are valuable, data obtained from lateral channel changes have to be of considerable magnitude in order to have a reasonably high level of confidence in the apparent trend in channel change.

3.3.3(F) LEVEL OF INTERVENTION

One of the major difficulties in interpreting the results was the lack of information on engineering interventions to the river channel. Most of the data and schemes for the River Stour were lost during the transition from the National Rivers Authority to the Environment Agency in the 1990s. It is, therefore, difficult to establish whether the changes presented are a consequence of channel migration caused by flow or the change occurred simply because the channel has been altered by humans, and to separate the magnitude of influence of each of these factors.

3.4. FIELD EROSION RATES

When considering riverbank erosion, two parameters are of interest (Hooke 1979): (1) the rate at which the erosive processes are operating and (2) the proportion of bank under attack (i.e. the percentage of erosion pins that recorded a change). The study of river bank erosion has been very popular. In a review, Lawler (1993a) lists 168 papers that have utilised bank erosion measurement techniques since 1863. More recent studies document that traditional methods such as erosion pins or cross-profiling are still popular in bank erosion research (Wynn & Utley 2011; Veihe *et al.* 2011).

In this chapter, the findings from field measurements that were undertaken between January 2006 and March 2010 are presented to supplement historical analysis from old maps and aerial photographs (Chapter 3.3). This directly addresses the Objective 1 of this study and the data is a fundamental part of an analysis of the first research hypothesis. Three conventional monitoring methods were employed in a complementary way to balance some of the limitations that the individual methods have. These methods use (1) erosion pins, (2) repeated cross-sectional and bank profile surveys and (3) bank edge surveys. Photo-Electronic Erosion Pins (PEEPs) were also tested at one of the field sites. This mixture of field monitoring techniques was employed in order to capture the bigger picture about the changes to the river bank sites. However, it was not possible to implement all methods at each site and observations on the limitations of these methods are discussed.

3.4.1. FIELD METHODS FOR QUANTIFYING THE RATE OF EROSION

3.4.1(A) EROSION PINS

The first use of pins to measure erosion on river banks was by Wolman (1959). Since then, the method has been widely used in studies that observe slope changes to river banks in short timescales of up to a year (*e.g.* Thorne & Lewin 1979; Hooke 1980; Veihe *et al.* 2011). Pins are a precise and economical method, suitable mainly for measuring bank retreat caused by fluvial and subaerial processes, but their application has to be planned carefully. The effectiveness and drawbacks of this method are summarised in Section 3.4.3.

In this project, 102 erosion pins were installed at eight out of the nine field sites (Table 3.4.1, Fig. 3.4.2). The pins were made of 50 cm long steel rods with a 0.5 cm diameter and

were horizontally inserted into the bank (Fig. 3.4.1) protruding by 5 cm. This starting value was the zero initial value against which all future readings were referred. If necessary, pins were adjusted back to 5 cm. This strategy limited the need for paint marks which would have been inaccurate and also limited the chance of losing the pin.



Fig. 3.4.1 Detail of erosion pins on field site LB1 in Little Bradley (see location map on Fig. 3.1.1). The flat piece of bank is possibly indicating the level of a prolonged water transfer. Erosion pins show retreat that occurred between June 2007 and May 2009 (see also Fig. 3.5.1).

Up to six pins were installed in each vertical bank section. At least one pin was located in the top, one in the middle and one in the bottom bank section (Table 3.4.1). Up to six profiles was sampled at each site. This depended on the suitability and also the accessibility of the bank for the installation and pin readings.

Erosion pins were not installed at the non-cohesive gravel site N1. According to Thorne & Tovey (1981), the shear strength of gravel material is determined by the frictional forces that are directly related to the packed density, and degree of imbrication of the particles. Inserting a pin in the gravel bank at site N1 would disturb the packing and imbrication of the gravel. Consequently, this would weaken the material at the point of insertion and lead to accelerated erosion.

Table 3.4.1 Number of pins installed at each field site.

Field site name	Erosion pins
GB1	9 pins (3 sets)
GB2	12 pins (3 sets)
GB3	9 pins (3 sets)
LB1	15 pins (6 sets)
LB2	6 pins (2 sets)
C1	29 pins (6 sets)
C2	14 pins (6 sets)
S1	8 pins (2 sets)

The readings were taken along the top edge of the pins for consistency and any scours on the sides of pins were not considered for the analysis (although they have been recorded). Readings were undertaken during low flows. Both positive (bank retreat) and negative (material accumulation) values were recorded. The frequency of pin monitoring was dependent on flow and other conditions (Section 3.4.3) and is shown in Fig. 3.4.2. The measurements were taken using callipers and the accuracy was ± 0.1 cm.

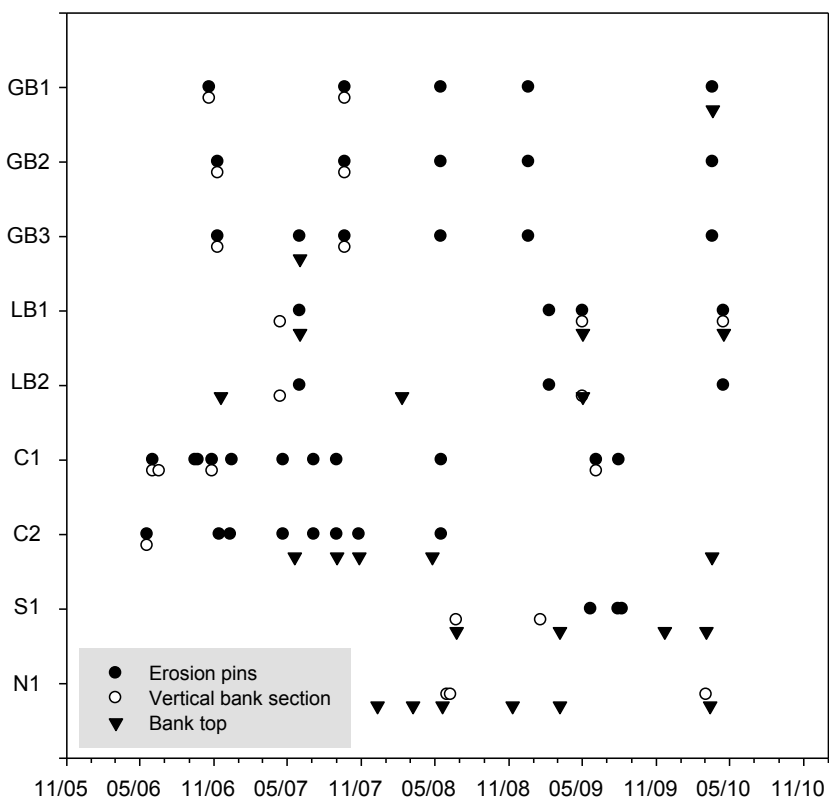


Fig. 3.4.2 Frequency and timing of field readings of erosion pins, vertical bank sections and bank edge surveys. The data presented are for each of the field sites and for the period between May 2006 and March 2010.

3.4.1(B) REPEATED VERTICAL BANK PROFILING

Repeated vertical bank profiles of the eroding bank are important in order to understand and quantify the processes in operation. Although the data obtained from surveys of bank profile are of lower accuracy than erosion pins, they are more descriptive. Apart from calculating the magnitude of erosion, data on bank geometry can be obtained from these and modes of any failure can be established. Furthermore, the Factor of Safety can be calculated using the geometry data for that given mode and also the critical conditions of failure can be predicted (Chapter 2.3). Leopold and Wolman (1957) were the first researchers to use monumented cross sections to record channel change and their efforts led into an astonishing 20-year record of annual profiles. Since then, this technique has been at least as popular as erosion pins, as documented through a number of studies (Knighton 1973; Thorne & Lewin 1979; Goodson 2002).

In this study, vertical bank profiles were measured using an automatic level (Nikon AX-2S) and a total station (Nikon DTM 330) and a set of rulers with balance for overhangs (Fig. 3.4.3). Bank profiles were measured for approximately each 10 cm of vertical height. The elevation (m AOD) was obtained by measuring the difference in vertical height between the survey station and a reference point against a given elevation on the map.



Fig. 3.4.3 Channel cross section surveying using Nikon automatic level at GB2 site in Great Bradley.

Computer software (VistaMetrix 1.35.0), (SkillCrest 2008) was used to measure the area of retreat and the maximum level of retreat. This tool was also used to establish bank angles and bank heights. The software works on the principle of transparent tool overlay and allows one to accurately adjust the scales of any underlying image.

3.4.1(C) REPEATED BANK TOP SURVEYS

Planimetric bank top surveys are one of the oldest methods for observing lateral channel change. Lawler (1993a) writes that Dryer and Davis were the first researchers who used this method when observing channel migration in 1911. In the UK, surveys of bank line have been employed, for example by Lewin (1976) and Thorne (1978) in Wales and by Hooke (1980) in Devon.

In this research, repeated bank top surveys were undertaken at the LB1, C1 and N1 field sites where the bank had a clearly identifiable edge, making the use of laser distance measurement easy and accurate. The observations from using this method are further discussed in Section 3.4.4.



Fig. 3.4.4 Total station positioned in the centre of the meander with the surveyed bank line in the background at C2 site in Clare.

A total station (Nikon DTM 330) with a 50 mm target was used to measure the distance and angle of densely placed points along the bank edge (Fig.3.4.4). The target was placed exactly on the bank edge where soil under the vegetation prevented the target from slipping through.

Data were collected either as xyz coordinates or as vertical (VA) and horizontal angles (HA) and slope distance between the total station and the target (SDx). From this, the horizontal distance (HD) was calculated as:

$$HD = \cos(VA) \cdot SDx$$

All angles in the trigonometric equations must be in radians. The raw angles in degrees as measured on the total station were converted appropriately.

In standard surveying practice, it is common to measure horizontal angles to a point of interest by referring to the angle to a reference point. The measured horizontal angles thus had to be converted to relevant angles by difference. The new HA were calculated for the rotated datasets. Following this, the x (easting) and y (northing) coordinates were obtained as follows:

$$x = HD \cdot \sin(HA)$$

$$y = HD \cdot \cos(HA)$$

When x and y coordinates had to be rotated, the following transformation was applied:

$$x_{\text{trans}} = x \cdot \cos - y \cdot \sin \alpha$$

$$y_{\text{trans}} = x \cdot \sin \alpha + y \cdot \cos \alpha$$

where α is angle of rotation in radians.

The standard error from the surveying was established from repeating the reading at reference points three times. For the horizontal angle (HA) it was 0.0233 degrees (1.4 minutes); vertical angle (VA) was 0.0100 degrees (0.6 minutes) and the direct distance error (SDx) was 0.0333 m. When overlaying, coordinate sets for the reference points were compared and the standard error for xy coordinate displacement was 0.086 m.

The results from the bank line surveys were analysed using MatLab R2011a (MathWorks Inc. 2011). Each programme was run for three datasets of xy coordinates of the bank edge corresponding to different dates of observation. First of all, the interpolation range and interval was set for the maximum and minimum range of the entire dataset. In the example below, this was (0.2938 m, 1.847 m). The interval to define the new data points xx was set to 0.1m. Corresponding yy values were calculated using an interpolation function *interp1* (1-dimensional interpolation) that allocates interpolated values to the xx dataset. The programme syntax for up to this step is shown below and the interpolated points as well as the original data points are shown in Fig. 3.4.5.

```

load data1                                Identifies dataset
xx=0.2938:0.1:11.847;                    Interpolates x values in the given interval,
                                         spaced by 0.1 m
yy1=interp1(data1(:,1),data1(:,2),xx);    Calculates corresponding interpolated y
                                         coordinates
plot(xx,yy1,'*b');                      Plots the graph of interpolated data
hold
plot(data1(:,1),data1(:,2),'*r');        Plots the graph of original data

load data2                                Identifies second dataset
yy2=interp1(data2(:,1),data2(:,2),xx);    For the same interpolated x coordinates
                                         calculates y
plot(xx,yy2,'*b');
plot(data2(:,1),data2(:,2),'*r');

load data3                                Same as above for third dataset
yy3=interp1(data3(:,1),data3(:,2),xx);
plot(xx,yy3,'*b');
plot(data3(:,1),data3(:,2),'*r');

```

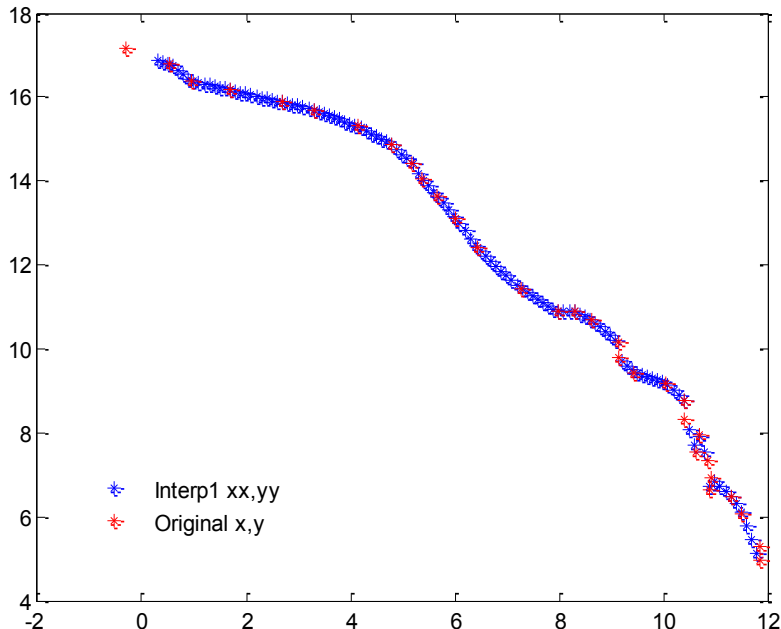


Fig. 3.4.5 Example data interpolation of bank line survey in MatLab (LB1 site). The original dataset is shown in red and the blue are the interpolated values for each 0.1 of x. The top left point is out of the range set for interpolation, hence the gap in the interpolated data. The xy axes are the planimetric coordinates in m.

For each generated xx value, yy was obtained for all three datasets (data1, data2 and data3 which were the bank lines taken at three different dates). The values were then subtracted to plot the difference between the yy coordinates (Fig. 3.4.6).

```

diff1=yy3-yy1;                                Subtracts the third and first dataset
diff2=yy2-yy1;                                Subtracts the second and first dataset

plot(xx,diff1, '-*r')                          Plots the overall difference
hold
plot(xx,diff2, '-*g')                          Plots the intermediate difference
YLIMIT([0 1.5])

```

Lastly, the area between obtained curves was calculated using the *trapz* function. This quantified the overall (data3 – data1) and intermediate (data2 - data1) eroded area.

```

intint_diff1=trapz(xx, diff1)                  Calculates overall eroded area under the red curve
intint_diff2=trapz(xx, diff2)                  Calculates the intermediate eroded area under the green curve

```

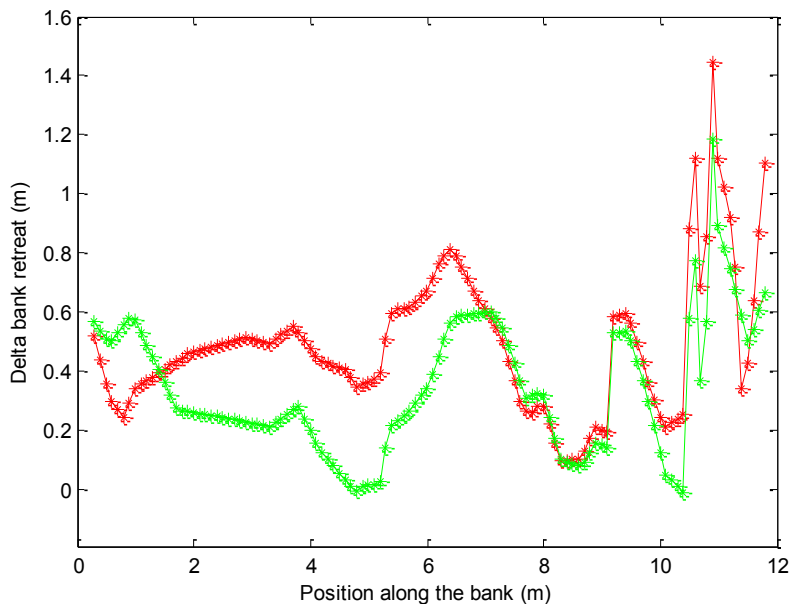


Fig. 3.4.6 Subtracted bank lines, $diff1$ ($yy3-yy1$) is the overall change in red and $diff2$ ($yy3-yy1$) is the intermediate change in green, shown as retreat in m along the bank. The curves were calculated as the differences between three datasets obtained from bank line surveying in 2007, 2009 and 2010. Both erosion and accretion is shown.

This analysis determined where along the bank any change occurred and what was the magnitude of the change. The subtraction of interpolated yy coordinates was performed once the bank line was rotated in the direction parallel to the x axis. This was to avoid any problems with deep indentations when more than one y value could otherwise occur for the same value of x.

3.4.1(D) PHOTO-ELECTRONIC EROSION PINS (PEEPS)

Photo-Electronic Erosion Pins (PEEPs) are competent to record the scale, frequency and timing of erosion or deposition events. Since the data from PEEPs can be continuously captured electronically, they are believed to be one of the most detailed riverbank erosion investigation methods (Lawler *et al.* 2001; Mitchell *et al.* 1999; Veihe *et al.* 2011).

Developed and first used by Lawler (1992a), the sensors generate an analogue voltage output that is related to the total length of the tube exposed to light and also to the brightness of that light. The PEEP sensor consists of a row of 10 photo-voltaic cells connected in series (Fig. 3.4.7), enclosed within a waterproof, transparent, acrylic tube (10 I.D. and 16 mm O.D.), about 60 cm long. The system is designed in such a way, that 1 mV of output from the array of cells corresponds to the exposure of 1 mm of tube in length. Therefore any surface erosion will have, during the daylight hours, an immediate effect on the voltage output stored on a logger. The scanning frequency can be set up on the data logger.

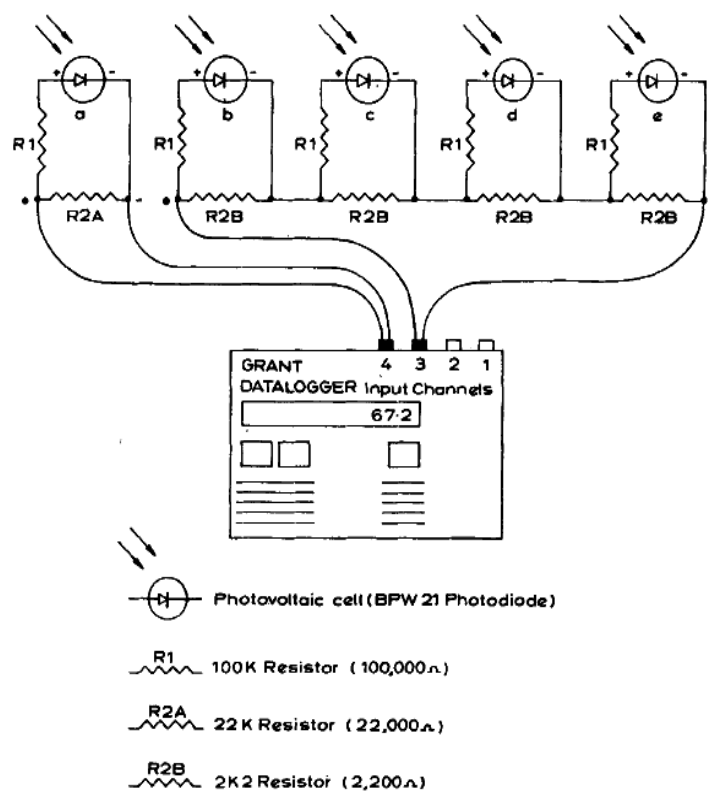


Fig. 3.4.7 Circuit design for the PEEP system. Cell A is an independent reference cell connected separately, B-E cells are connected in series (Lawler 1992a).

Two photo-electronic pins were constructed based on the design developed by Lawler (1992a) but using flat rectangular Si PIN photodiodes S8385/S8729 series from Hamamatsu in Japan. These were housed in a small clear package and the resulting pin was highly sensitive with a quick response rate. They work in the visible to infrared spectrum ($\lambda = 320-1100$ nm) with an active area of 2x2 mm. The pins were tested using a black sleeve to check that the design corresponded to 1 mV/1 mm. The two pins were installed at the C2 site on an eroding lower part of the bank. A Grant's Squirrel 1200 data logger was connected to the system for three periods between November 2009 and March 2010. The scanning frequency was 1 minute and data were recorded on four channels: Channel 11 = reference cell on top pin, Channel 12 = top pin array, Channel 9 = reference cell on the bottom pin and Channel 10 = array of the bottom pin. A scheme of the system installation by Lawler (2005a) is shown on Fig. 3.4.8.

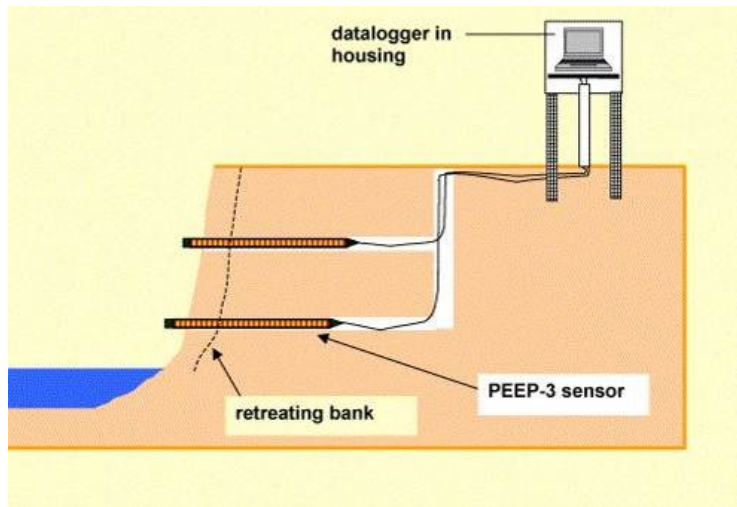


Fig. 3.4.8 Schematic installation of PEEPs sensors in river bank by Lawler (2005a).

3.4.2. RESULTS

3.4.2(A) EROSION PIN READINGS

Rates of erosion observed on pins ranged from negative values to 30 cm per year. Negative values were caused by material accumulation, usually from upper parts of the bank. Out of 102 monitored pins, 7 were lost or covered with material and were not replaced. Cumulative erosion in the case of 11 pins was negative; two pins recorded no change and a further 8 pins recorded erosion of less than 1 cm. The cumulative erosion to number of days ratio was at its maximum at 0.83 mm/day and minimum at -0.09 mm/day occurring on a single pin. The mean retreat \pm SD across all pins was 0.18 ± 0.18 mm/day. Similarly, annual data were calculated based on the number of years that the measurements were taken. These ranged from 30.42 cm per year to -3.43 cm per year, the negative meaning material accretion. The mean retreat per year across all pins was 6.56 ± 6.61 cm. The variability of the individual readings based on peak discharges and the summer and winter aspects are presented in Chapter 3.6. Full results are included in Table 3.4(A) in the Appendix, of the measurement period in days, total cumulative erosion and ratios of cumulative erosion/number of days and cumulative erosion/years are presented. A, B and C are the sections of the bank where A is the top of the bank face, B is the mid part and C is the lower part/bank foot. Negative readings indicate sedimentation or an accumulation of material from above. Full results are in Tab 3.4(A) in Appendix.

Table 3.4.2 Summary pin readings at the eight research sites expressed as the mean annual erosion based on all pins and the mean erosion divided by channel width, maximum recorded erosion per year and these values expressed also as the ratio to channel width/ 10^2 .

	Mean erosion/ year (cm)	Mean annual erosion/ channel width/ 10^2	Max. erosion/ year (cm)	Max. annual erosion/ channel width/ 10^2
GB1	9.33	± 9.00	1.67	± 1.61
GB2	5.97	± 3.57	1.05	± 0.63
GB3	5.44	± 7.46	0.51	± 0.70
LB1	7.74	± 4.57	0.78	± 0.46
LB2	3.40	± 3.63	0.97	± 1.04
C1	4.58	± 2.08	0.48	± 0.22
C2	10.24	± 11.53	0.66	± 0.74
S1	6.57	± 10.84	0.26	± 0.43

Two tests have been performed to check for significant differences in the dataset: firstly, between the sites and secondly, to compare the top, middle and lower bank sections. The mean values are plotted on Fig. 3.4.9. From the figure, it is likely that the C2 and GB1 sites eroded the most, while LB2 eroded the least. When comparing sections of the bank, the

top section has eroded the least and lower bank foot eroded the most. As the mean values were associated with large standard deviations and statistical tests confirmed the null hypothesis ($p>>0.05$), there was no significant difference in erosion rates between the eight individual sites or between the three vertical bank sections.

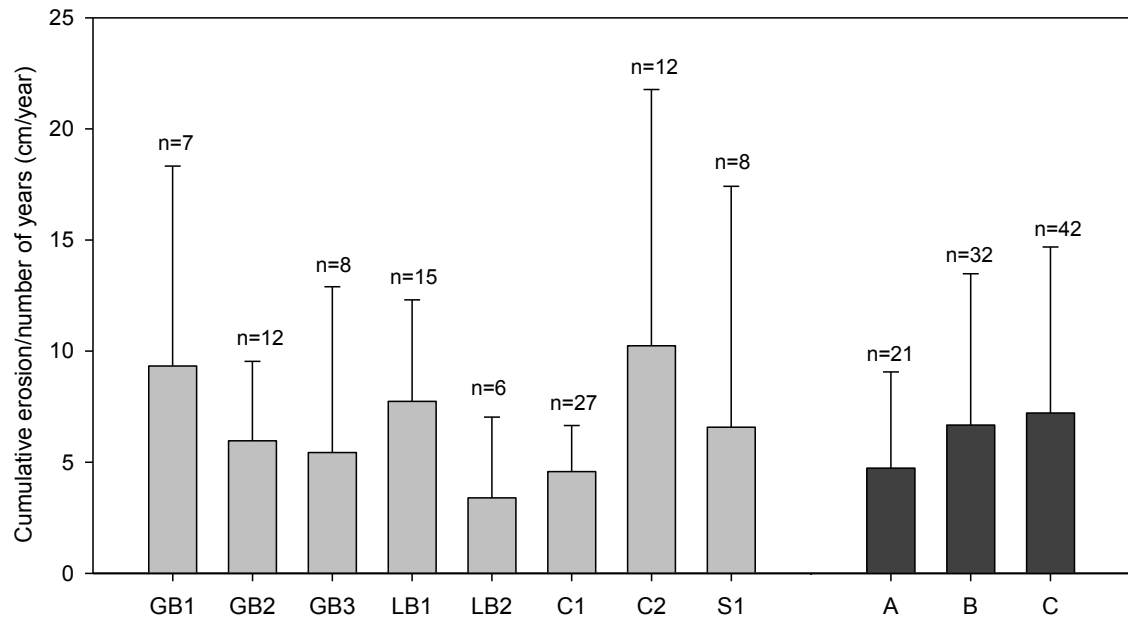


Fig 3.4.9 Site-specific and bank section-specific summaries based on field readings of 95 erosion pins; and based on the cumulative erosion/number of years ratio in cm/yr. Error of the mean is the standard deviation, n is the number of active pins with data and A, B and C are the bank sections where A is the top of the bank face, B is the middle part and C is the lower part/bank foot.

When comparing the rates of bank erosion recorded on pins, the channel scale was also taken into account. Mean and maximum annual erosion rates were expressed non-dimensionally as the ratio to channel width (Table 3.4.2). There was no statistically significant difference, but the trend was different. Site GB1 had the highest annual erosion rate/channel width (0.0167), followed by sites GB2 and LB2. The lowest value was calculated for C1 and S1 sites, a different result from the values that did not consider the channel width (Fig. 3.4.9).

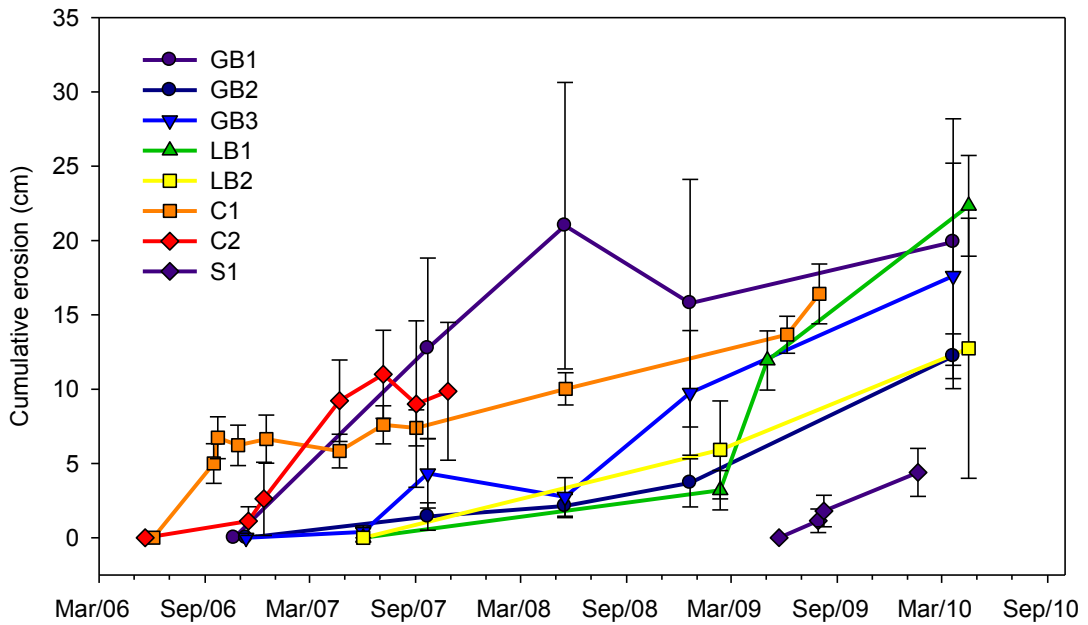


Fig. 3.4.10 Timeline showing the mean cumulative erosion in mm at each of the field sites. Vertical bars are the standard error.

The values of mean cumulative erosion at the individual monitoring points at each field site are shown in Fig. 3.4.10. Standard errors were used in this case as the standard deviations were simply too large to be of a graphical value. Some of the 'big jumps' can be seen on the graphs during winter 2006/07 and also during winter and spring 2008/09. However, summer periods at some sites such as LB1 or C1 show a notable increase in bank retreat. The possible impact of summer and winter flows on erosion rates, as well as the proportion of the time the pins were subjected to bankfull flow, are explored in Chapter 3.5.

3.4.2(B) CHANGES IN CROSS-SECTIONAL PROFILES

Vertical bank profiles were resurveyed on two or three occasions and sketches from 17 profiles at 6 field sites are presented. The following Figs. 3.4.11-3.4.15 show the position of bank profiles together with the position of erosion pins and descriptions of the changes for each profile.

At GB1 site, repeated profiles of Sections 2 and 3 are shown. The Fig. 3.4.11 reveals a failure in the lower part of the bank between October 2006 and September 2007. There was a further retreat towards creating an overhang around the top pin and a hypothetical retreat based on pin readings from March 2010 is shown by a dotted line. On the other hand, there was little change within Section 3 at the same site. This section is downstream

along the meander, but was being surveyed from the same station point as Section 2. The influence of bankfull flow is visible at GB1 Section 3 by a slight overhang, where the bank angle changes to almost vertical and the erosion (of up to 5 cm) was concentrated in this place.

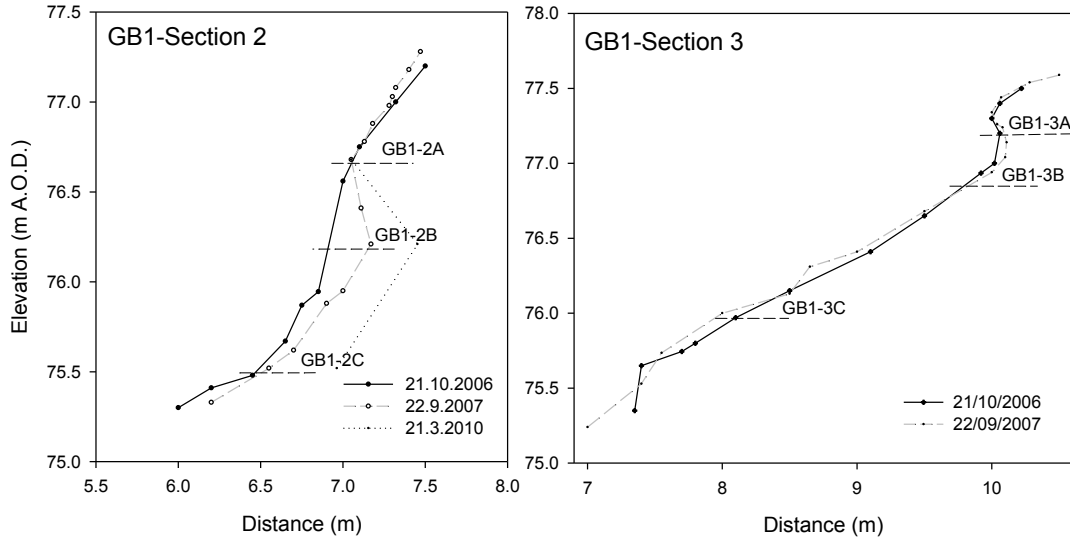


Fig. 3.4.11 Bank profiles at GB1. The dotted line in Section 2 is the magnitude or retreat recorded on pins. Dashed horizontal lines show the position of erosion pins.

Further downstream, at the GB2 site, Section 2, the riverbank has retreated along most of its face. Again, there appears to be an overhang supported by grass roots at the top of the bank. A small slice from the upper section fell and retreat of up to 20 cm occurred in the bank foot as shown in Fig. 3.4.12. At GB3, Section 2 appears to have two flow impact points, but the uneven surface in the middle is in fact a sliding overhang that has stopped mid-way down the bank. One impact point is located at the bankfull elevation, and one lower around the possible elevation of a long-term water transfer flow (Fig. 3.4.12 – right).

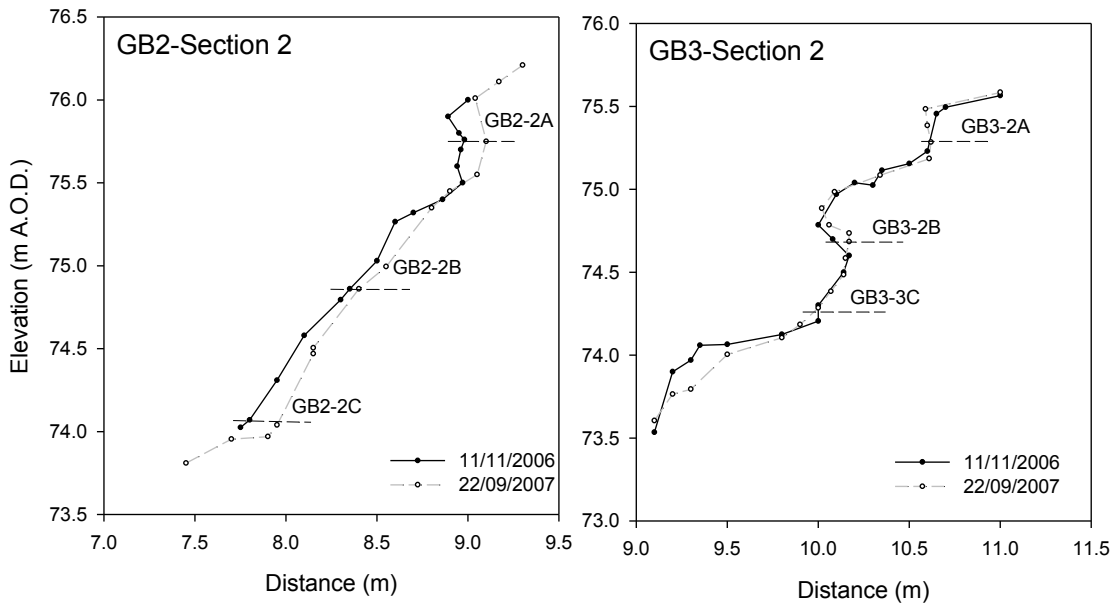


Fig. 3.4.12 Bank profiles at the GB2 and GB3 sites, Sections 2. The horizontal lines are erosion pins with their coding.

At the Little Bradley, LB1 site, the bank profile has been re-taken at Section 1. Sections 2-5 were profiled only once towards the end of the project and the dotted lines show the position of the bank back in 2006 when it was recorded using pins. At Section 1, erosion occurred within the upper half of the bank of up to 12 cm and accretion up to 8 cm occurred at the bank foot (Fig. 3.4.13).

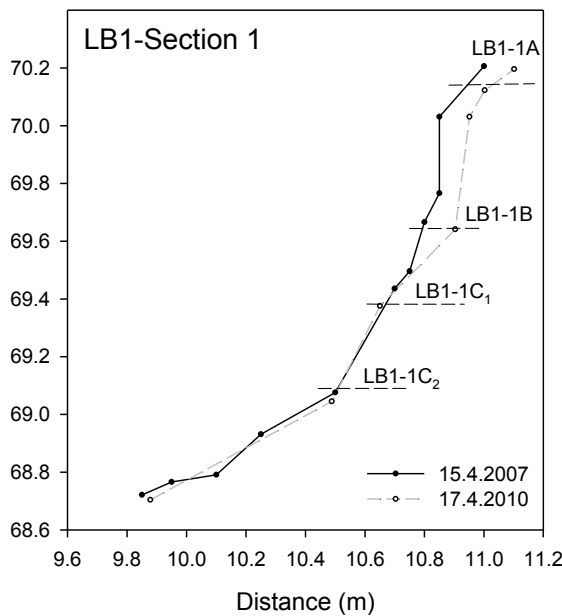


Fig. 3.4.13 Bank profiles at the LB1 site, Section 1. The horizontal lines are erosion pins with their coding.

The following sketches show schematic profiles of Sections LB2-5, located upstream of the section LB1 (Fig. 3.4.14). These demonstrate steep bank profiles and the approximate position of the bank face based on pin readings in June 2007 and surveying in April 2010. As these cross profiles are not complete and were surveyed from the top of the bank due to limited access, the area of retreat was not measured.

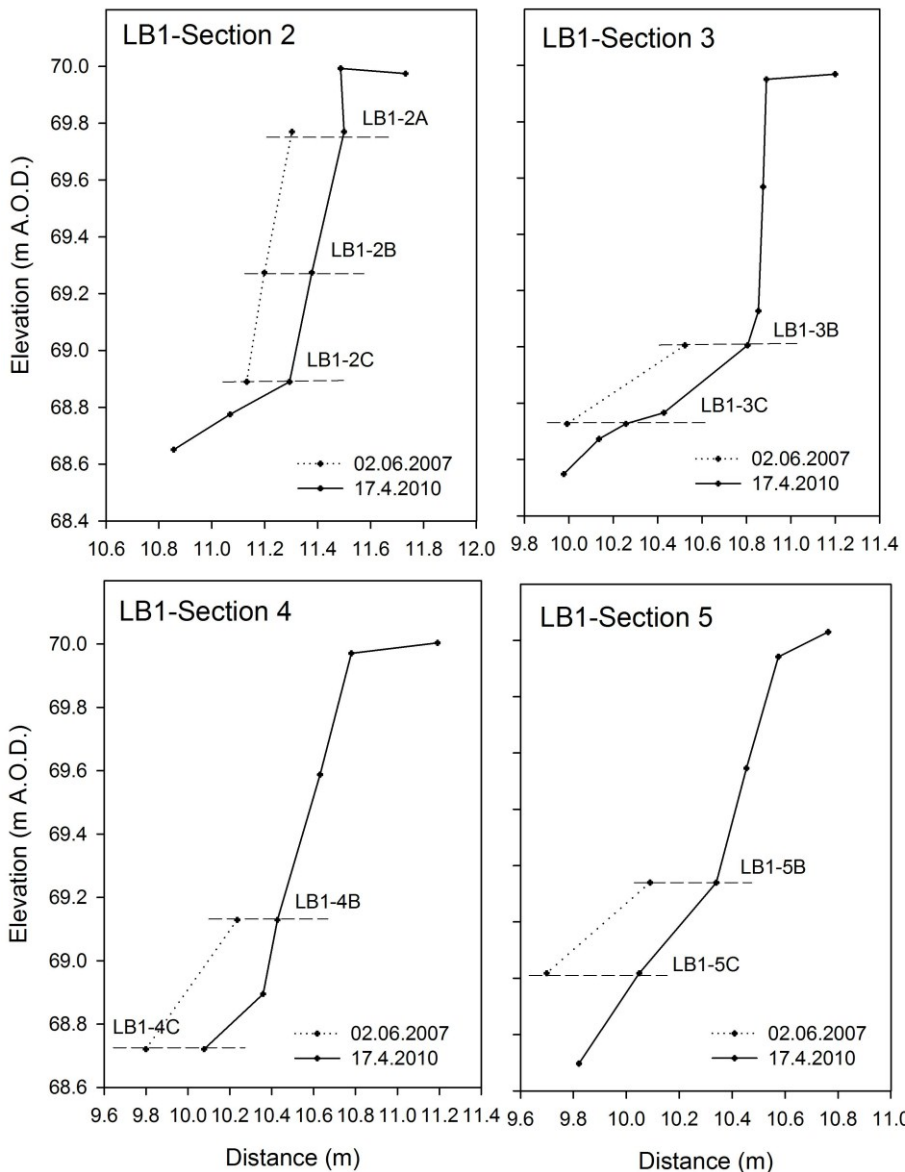


Fig. 3.4.14 Bank profiles at the LB1 sites, Sections 2-5. The horizontal lines are erosion pins with their coding.

At LB2 site, Section 1 appears to have retreated more than Section 2. The profile at Section 1 was estimated from pin readings taken in April 2010. A retreat of up to 23 cm occurred at Section 1 where most material was eroded from the top of the bank and from the bank foot. On the other hand the erosion at Section 2 was much less, only 11 cm of soil was eroded and mainly from the bank foot (Fig. 3.4.15).

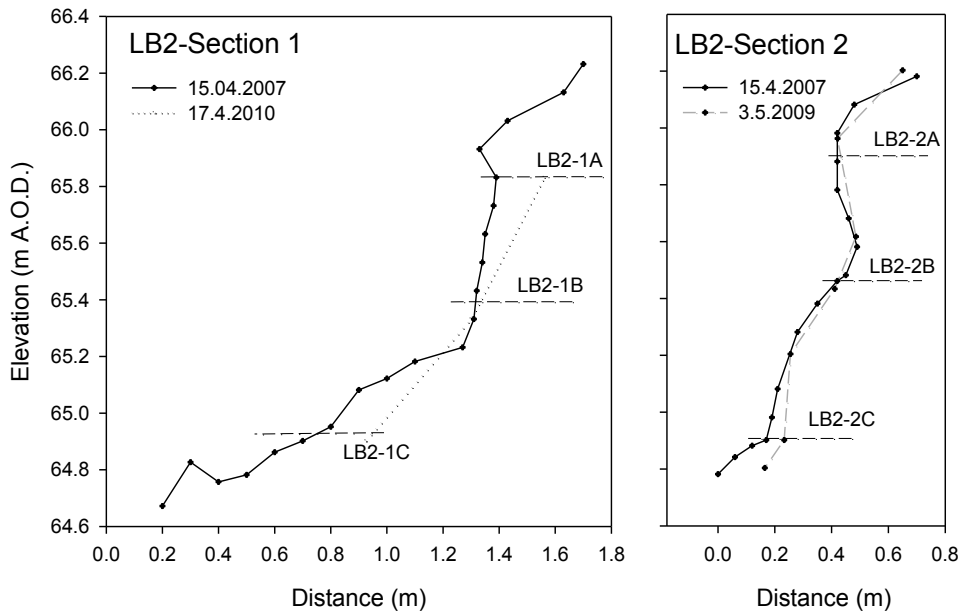


Fig. 3.4.15 Bank profiles at the LB2 sites, Sections 1-2. The horizontal lines are erosion pins with their coding.

At the Clare C1 site, the steep sections of the bank were profiled in October 2006 and then re-plotted in June 2009. While signs of mass failures were not present, the bank still retreated by up to 44 cm during the period (Fig. 3.4.16). Section 4 eroded the most, by 0.276 m^2 , which represents the total loss in the cross-sectional profile. Section 3 eroded the least, by 0.105 m^2 . The mean retreat $\pm \text{SD}$ over the six profiles was $0.170 \pm 0.066 \text{ m}^2$.

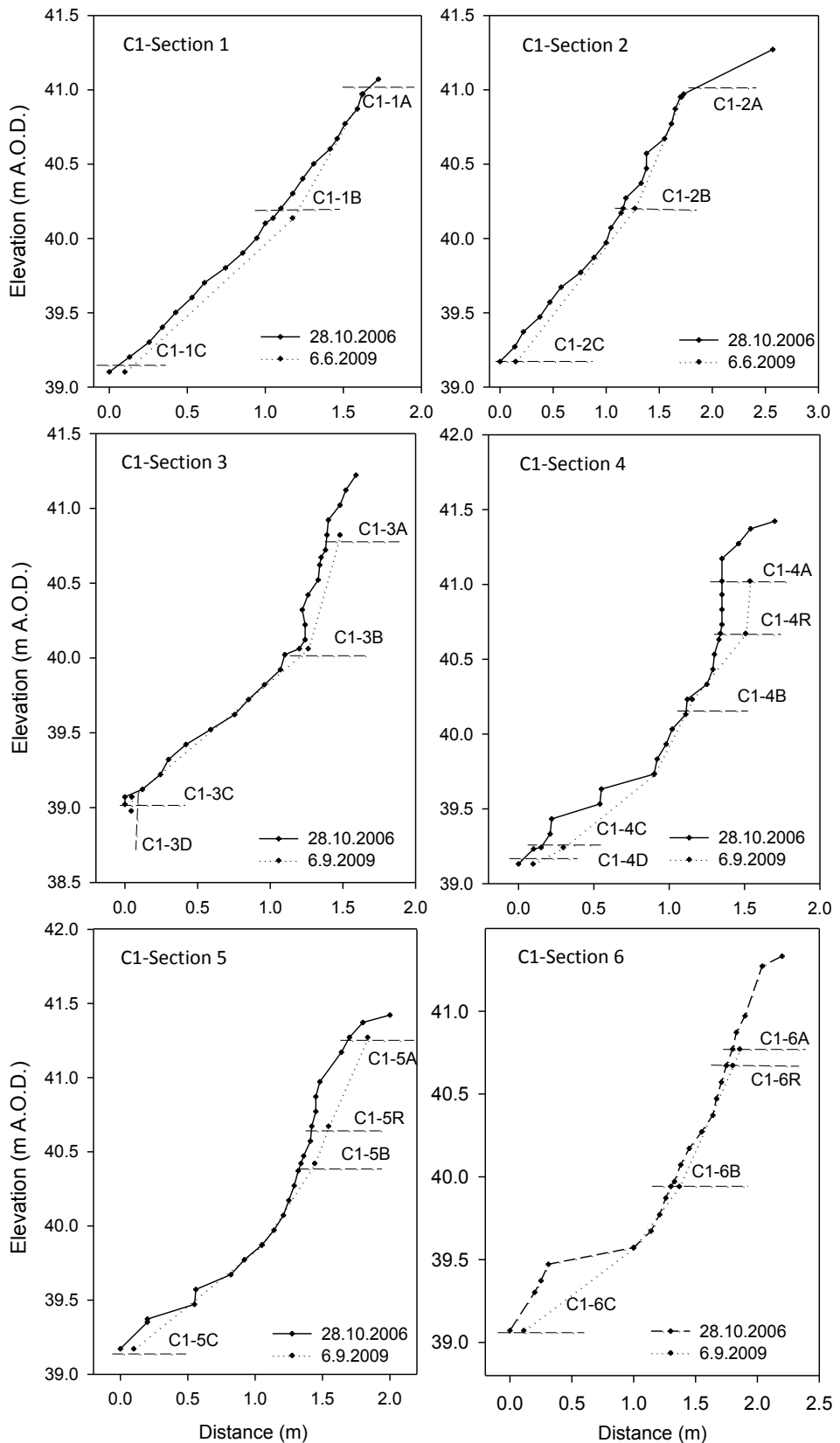


Fig. 3.4.16 Bank profiles at site C1 in Clare. The dotted lines show the hypothetical erosion based on pin readings. Dashed horizontal lines show the position of erosion pins with their coding.

Within the sections chosen for this analysis, the total retreat from the bank was expressed as the change in the cross-sectional area. The data on the erosion gained from the cross sections, data on maximum retreat that occurred within the given profile and the lengths of the periods of observation are shown in Table 3.4.3. The retreat is expressed as change in cross-sectional area in m^2 . Furthermore, in order to compare the sites with the varying bank height and over a varying timescale, the cross-sectional area that eroded has been divided by bank height (in m) and by time factor (in years).

Table 3.4.3 *Erosion data delivered from repeated cross-profiling. Time factor is the number of years calculated as the number of days/365 ratio. H is the bank height in m, total retreat is the change in the cross-sectional area in m^2 , retreat per m is the ratio of total retreat in m^2 to bank height in m and the maximum retreat is the maximum erosion measured at one point between the two profiles divided by the time factor, in m.*

Section	Time factor (years)	Bank height (m)	Total retreat as change in profile area (m^2)	Retreat per m as total retreat/m of bank height/year in m/year	Maximum retreat/year (m/year)	Maximum annual retreat/ch- annel width
GB1-2	0.92	1.92	0.157	0.089	0.316	0.056
GB1-3	0.92	2.15	-0.065	-0.033	0.072	0.013
GB2-2	0.86	1.82	0.169	0.108	0.190	0.033
GB3-2	0.86	1.92	0.117	0.071	0.326	0.030
LB1-1	0.86	1.57	0.052	0.038	0.139	0.014
LB2-1	3.01	1.49	0.087	0.019	0.076	0.022
LB2-2	2.05	1.42	0.054	0.019	0.054	0.015
C1-1	2.61	1.89	0.118	0.024	0.069	0.007
C1-2	2.61	1.71	0.136	0.030	0.066	0.007
C1-3	2.61	2.15	0.105	0.019	0.067	0.007
C1-4	2.61	2.25	0.276	0.047	0.118	0.012
C1-5	2.61	2.22	0.209	0.036	0.079	0.008
C1-6	2.61	2.27	0.174	0.029	0.168	0.018

To summarise the results, the mean bank retreat expressed as the difference in cross sectional area divided by bank height and number of years, was 0.038 (± 0.035) m/year. The profile that recorded the most significant change per metre of bank height was GB2-2. Material accumulation prevailed over erosion at the GB1-3 Section (-0.033 m/year). The highest maximum retreat occurred at the GB3-2 Section and was 0.326 m/year closely followed by GB1-2 Section with 0.316 m/year. Considering the channel width, the ratio of maximum annual retreat per channel width was highest at GB1-2 profile (0.056) and lowest at the three sections at site C1 (0.007).

3.4.2(C) BANK TOP RETREAT

Fluvial erosion (recorded on pins), the clean out at the basal end point in the bank foot and weathering on the exposed bank face all combine to cause bank retreat. The continued rate of bank retreat is explained by the state of basal endpoint control first introduced by Carson and Kirkby (1972) and this concept is further discussed in Chapter 3.5. The last stage of the bank erosion cycle, mass failure, can be identified by changes in the position of the bank line and is referred to as bank top retreat.

Repeated bank top surveys at three sites are presented here. LB1, C2 and N1 sites were chosen since the bank top was clearly identifiable in the field. The analysis of changes in lateral channel movement represents an accurate and a continuous representation on the location and magnitude of failure events within the top section of the bank. The following figures (Figs. 3.4.17-22) represent the position of bank lines in time of surveys and the MatLab analysis of eroded areas for each of the three sites.

At LB1 site, up to 0.58 m of bank retreat occurred between June 2006 and April 2010. The mean retreat for the same period \pm SD was 0.12 ± 0.16 m. The total area of lost bank was 5.65 m^2 which, divided by downstream length in metres, comes to $0.11 \text{ m}^2/\text{m}$. Erosion occurred at both ends, although more area was lost in the upstream section of the bank.

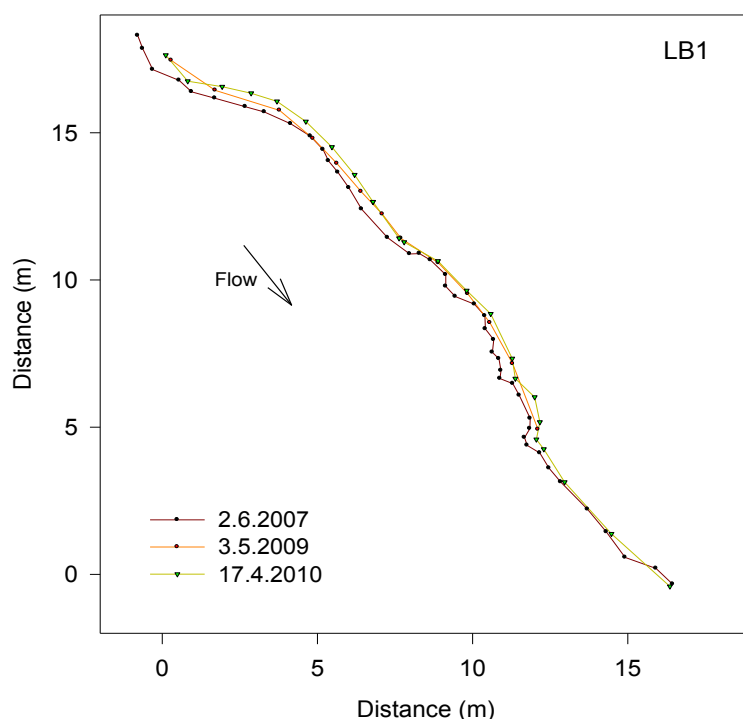


Fig. 3.4.17 Plan of bank top line at the LB1 site surveyed in 2007, 2009 and 2010. The coordinates are in m and the x axis is in the direction of downstream (indicated by the arrow).

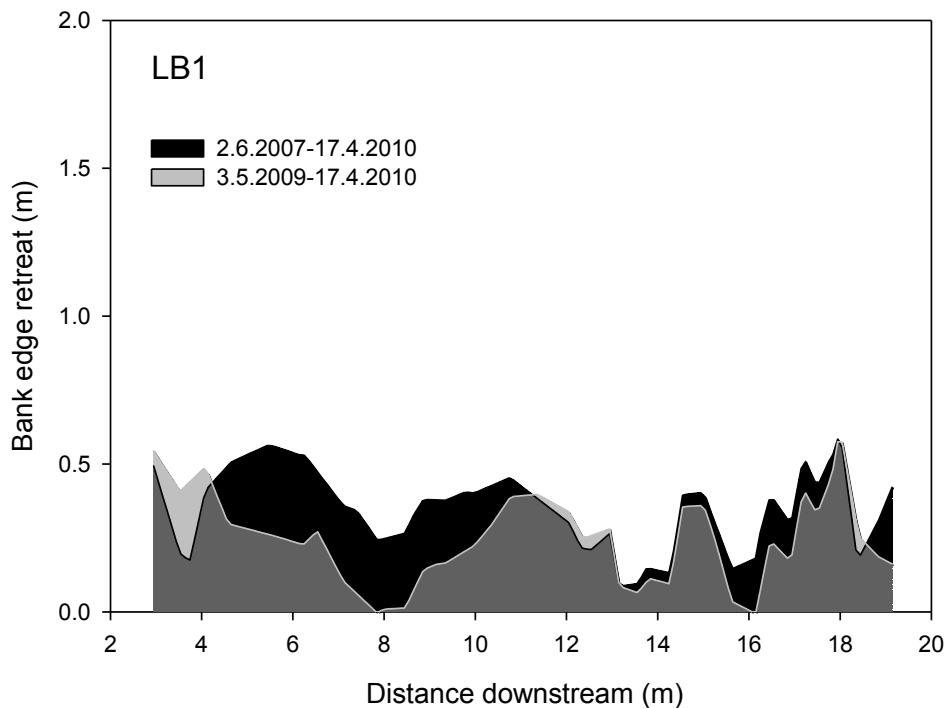


Fig. 3.4.18 Bank edge retreat at LB1 site expressed as the overall difference (in black) between June 2007 and April 2010 and the intermediate difference (in grey) between June 2007 and May 2009. X axis is the distance along the bank going downstream and y is the eroded amount in m.

At site C2, the retreat between May 2007 and May 2008 was generally low, with the total area of land lost from the surveyed bank being 0.91 m^2 , but more erosion occurred before March 2010 and the total area lost for the whole period came to 5.94 m^2 . Divided by the length of the bank, this gives $0.07 \text{ m}^2/\text{m}/\text{year}$. The maximum retreat for the entire period was 0.413 m , and the mean was $0.10 \pm 0.30 \text{ m}$. Most retreat occurred within the upstream and downstream sections and interestingly, a minimal retreat occurred in the middle of the section.

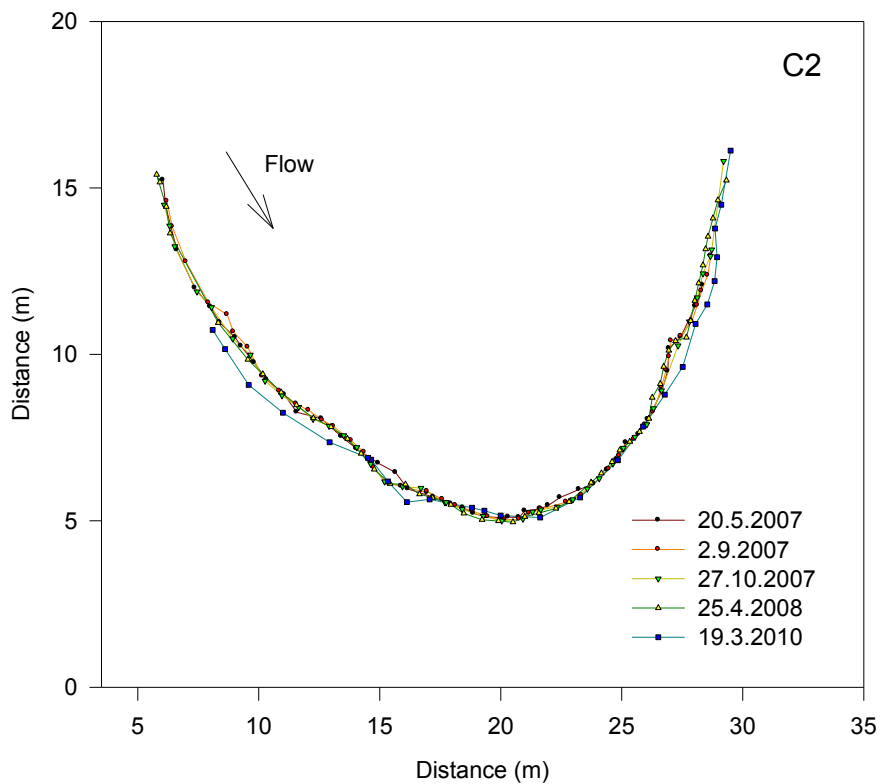


Fig. 3.4.19 The position of the bank top at the C2 site surveyed on five occasions in 2007, 2008 and 2010. The coordinates are in m and the x axis is in the direction of downstream (shown by the arrow).

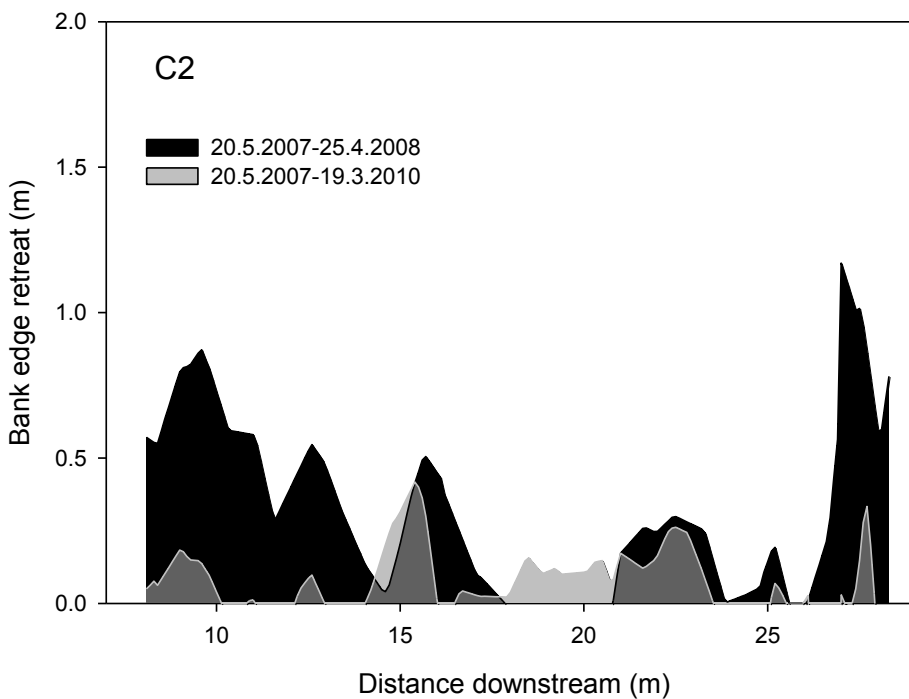


Fig. 3.4.20 Bank edge retreat at C2 site expressed as the overall difference (in black) between May 2007 and March 2010 and the intermediate difference (in grey) between May 2007 and April 2008. X axis is the distance along the bank going downstream and y is the eroded amount in m.

At N1 site, a total retreat of 10.09 m^2 occurred between December 2007 and March 2009. This stretch was nearly 55 m long and the average erosion thus can be expressed as an average rate of $0.15 \text{ m}^2/\text{m/year}$, a similar rate to the average figure at C2 site. However, the bank retreated by up to 1.33 m over the period. The mean erosion was $0.21 (\pm 0.36) \text{ m}$. The peak erosion occurred within the first 10 m of the upstream section.

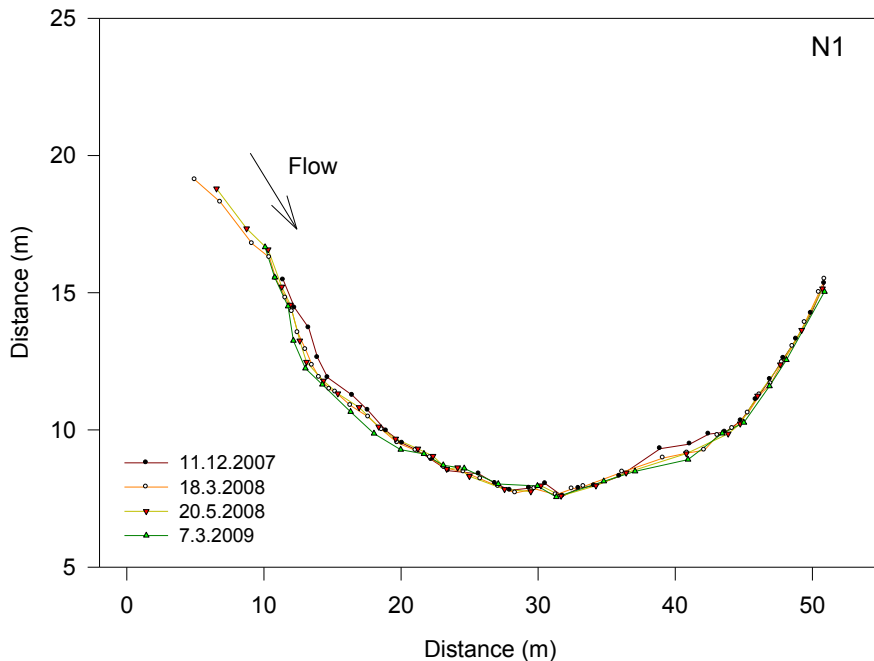


Fig. 3.4.21 The position of bank top at the N1 site surveyed in 2007, 2008 and 2009. The coordinates are in m and the x axis is in the direction of downstream (shown by the arrow).

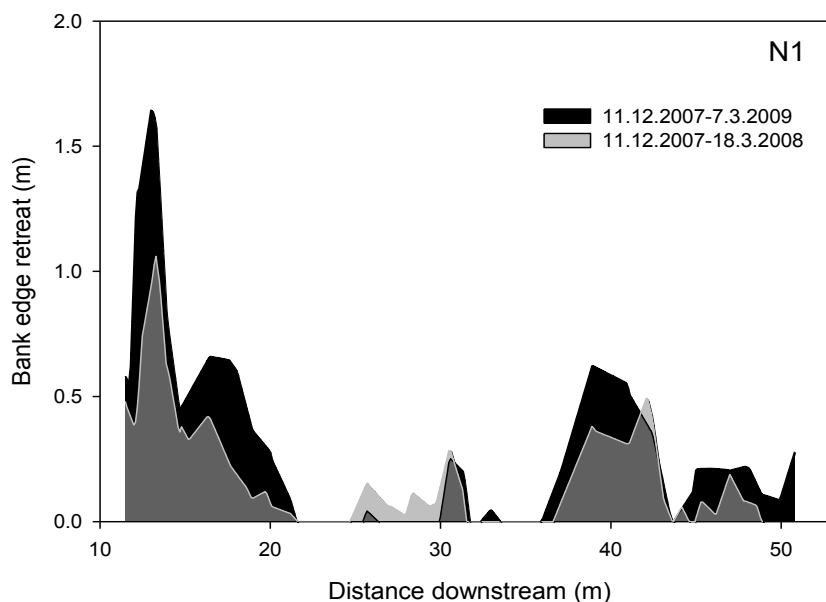


Fig. 3.4.22 Bank edge retreat at the N1 site expressed as a difference between the interpolated (yy) coordinates between 2.6.2007 and the two dates shown. X axis is the distance along the bank going downstream, where xx are interpolated coordinates in 0.1 m intervals.

Table 3.4.4 presents summary data in relation to the time factor so the magnitude of erosion can be compared between the sites. Two time periods have been chosen to demonstrate the mid-way and the overall land loss at the surveyed banks as these data were available for each of the sites. The results have been divided by time factor in order to compare the three sites. Minimal mean bank edge retreat (in m/year) occurred at the site C2, while the highest bank edge retreat occurred at site N1, where about 0.15 m² of floodplain (per m of bank per year) was been lost between the surveys while at the site C2 this was only half of this amount. Maximum retreat per year occurred, by far, at site N1 (1.328 m/year). Considering channel size, the maximum annual erosion to channel width ratios were highest at the site N1, but were more closely spaced (Table 3.4.4).

Table 3.4.4 Summary bank edge retreat data for sites LB1, C2 and N1 as mean retreat, maximum retreat, maximum retreat/channel width, total area of the overall land loss and the eroded area per m of bank per year. White rows are partial, mid-way values, grey rows is the final retreat.

	Time period (years)	L (m)	Mean retreat (m/year)	Max. retreat (m/year)	Max. annual retreat/channel width	Total eroded area (m ²)	Eroded area (m ² /m/year)	
LB1	1.92	18.20	0.126	±0.139	0.299	0.030	3.963	0.11338
	2.88	18.20	0.121	±0.165	0.203	0.021	5.6518	0.10795
C2	0.93	31.70	0.046	±0.159	0.446	0.047	0.9066	0.03061
	2.83	31.70	0.104	±0.304	0.413	0.043	5.9442	0.06619
N1	0.44	54.50	0.336	±0.224	2.401	0.109	5.823	0.24222
	1.24	54.50	0.208	±0.358	1.328	0.060	10.091	0.14952

3.4.2(D) CONTINUOUS EROSION MONITORING USING PEEPS

Two Photo-Electronic Erosion Pins were installed in 2009/10 at the bank foot at an unstable section of the downstream end at C2 site in Clare. This section was suitable for the installation and burying of the waterproof data logger casing in the spoil bank at the top because it was not accessible to public and it was free from any land management work that could damage the wiring. Data were collected during three periods: 28.11-5.12.2009; 25.1-22.2.2010; 22.2-19.3.2010. These were chosen at random as a test, but it would have been interesting to have longer-term continuous data. Alongside the output of potential in mV, the length of protruding pins was recorded manually as a control on three occasions. Eroded lengths are shown in Table 3.4.5 below. The allocation to the channels on the data logger is also shown as these relate to the values later. Each pin is associated with two channels; the first being the control photovoltaic cell, the second is the actual array.

Table 3.4.5 *Length of the Photoelectric Erosions Pins (PEEPs) protruding at the C1 site between May 2009 and March 2010, in cm. The allocation of channels on the data logger is also shown. The start date for the manual control check was 24.5.2009.*

Pin	Channels	24.5.2009 (cm)	6.6.2009 (cm)	13.6.2009	19.03.2010
top	11,12	2.30	2.30	under water	4.20
bottom	9,10	1.80	1.80	under water	5.30

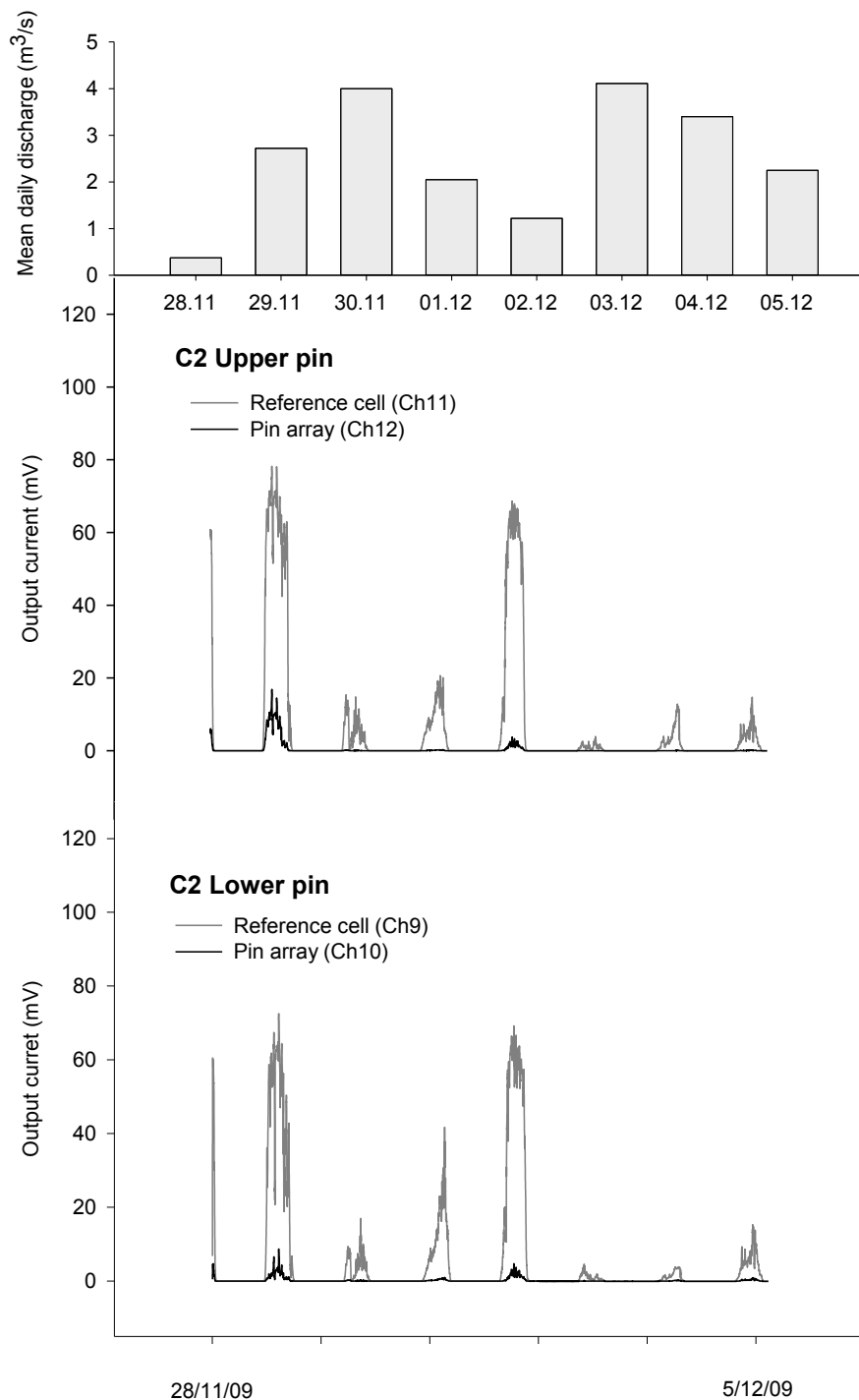


Fig. 3.4.23 Mean daily discharge as m^3 per second as gauged at Westmill (based on data from the Environment Agency) and the output current from upper and lower PEEPs between 28 November and 5 December 2009. Taken at 10-minute intervals. The daylight hours are shown by the peaks in output currents axis.

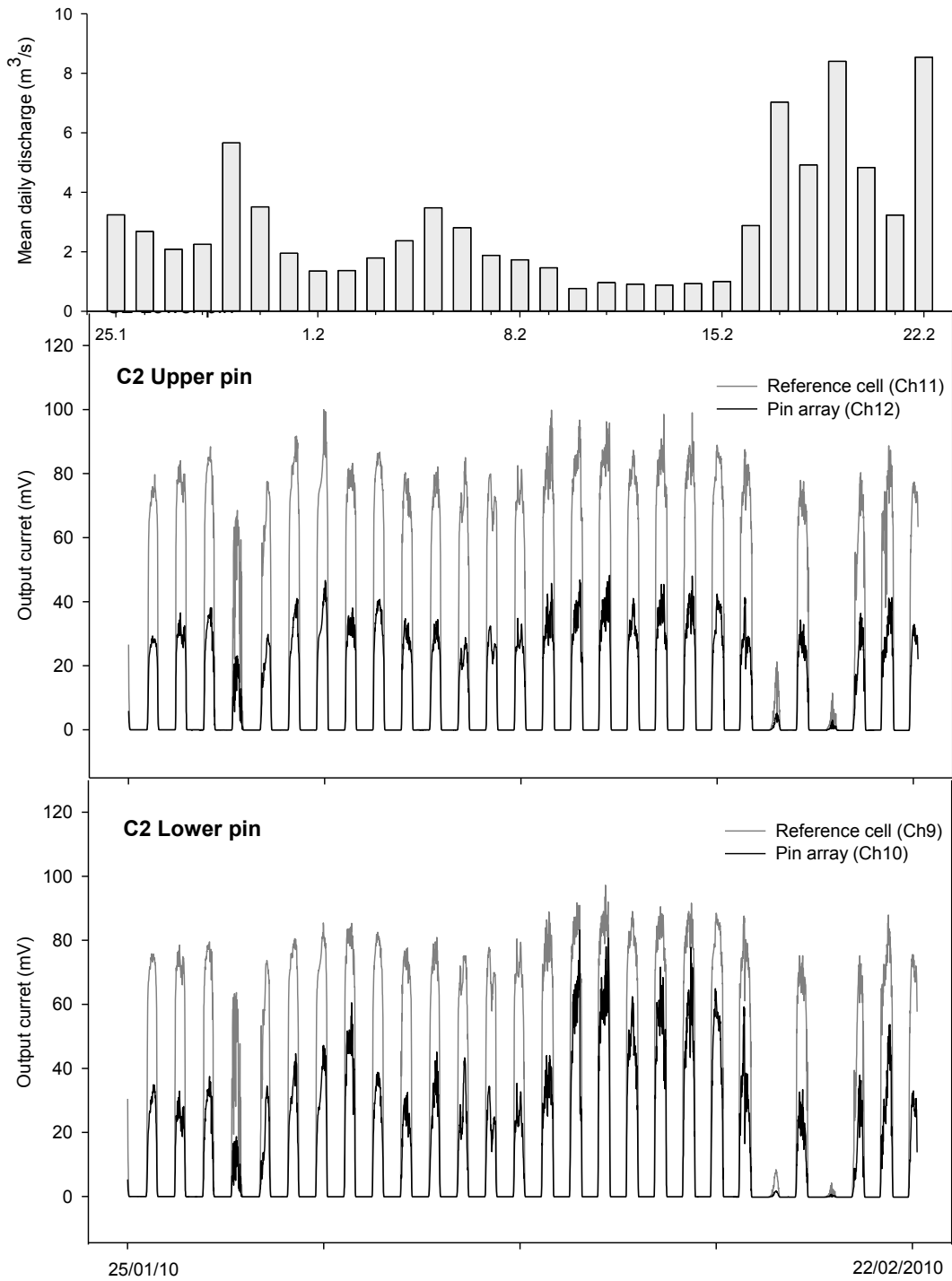


Fig. 3.4.24 Mean daily discharge as m^3 per second as gauged at Westmill (based on data from the Environment Agency) and the output current from upper and lower PEEPs between 25 January and 22 February 2010. Readings of potential were taken at 10-minute intervals. The daylight hours are shown by the peaks in output currents axis. The daylight hours are shown by the peaks in output currents axis.

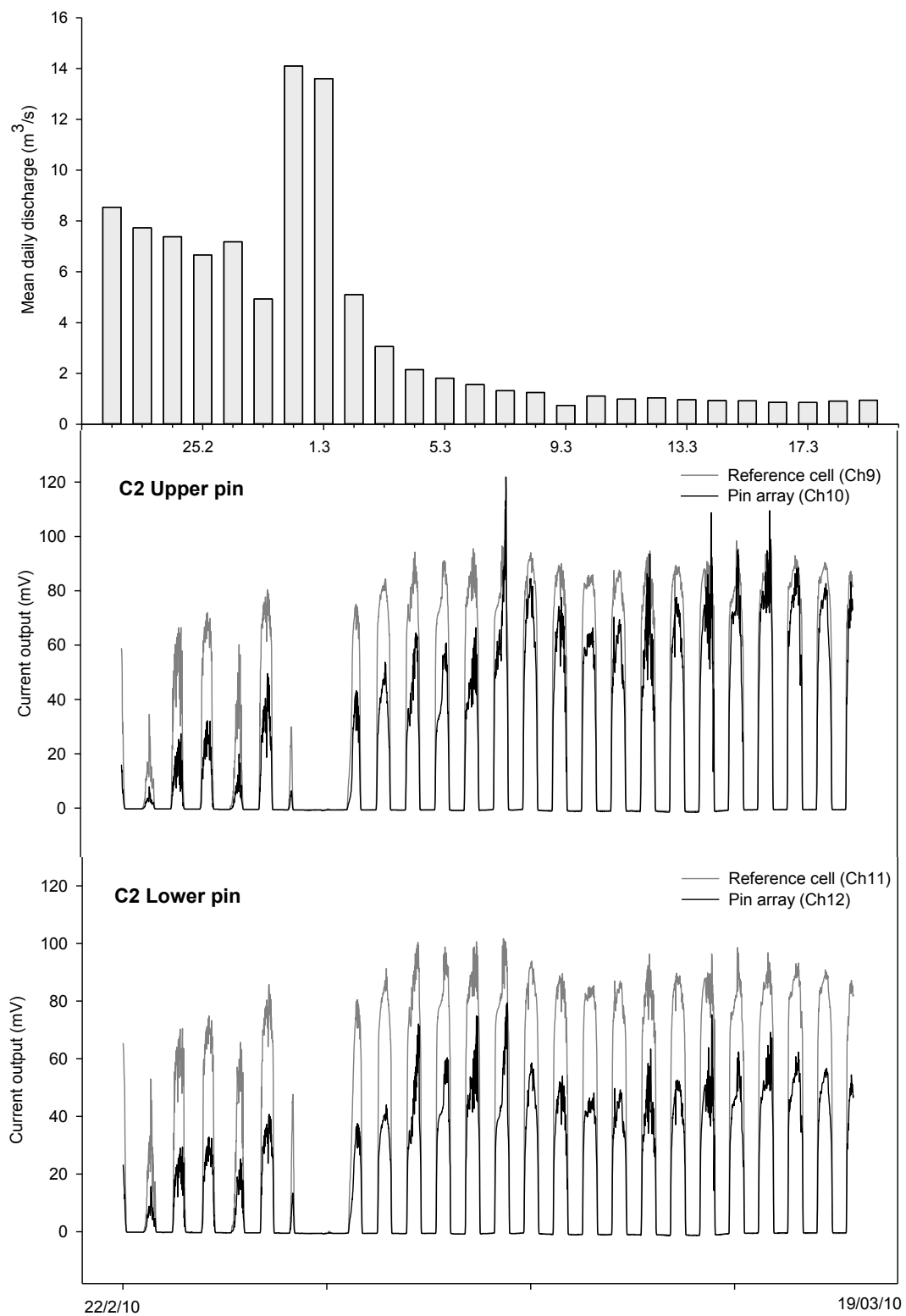


Fig. 3.4.25 Mean daily discharge as m^3 per second as gauged at Westmill (based on data from the Environment Agency) and the output current from upper and lower PEEPs between 22 February 2011 and 19 March 2010. Taken at 10-minute intervals. The daylight hours are shown by the peaks in output currents axis.

According to the field checks (Table 3.4.5), between May 2009 and March 2010, the upper pin eroded by 1.90 cm while the lower eroded by 3.00 cm. On the other hand, Fig. 3.4.23 shows the outputs from the first recorded period (28 November to 5 December 2009). The readings on the reference cells reached up to 78 mV during bright days, while the readings on the arrays were up to 17mV but mostly close to zero. Higher readings occurred on the top pin. The mean daily discharge is reflected by low pin readings because these would be the days when one or both pins were submerged under water (reduction in light). These data are also summarised in Table 3.4.6.

During the second period, between 25 January and 22 February 2010, the readings on the reference cells reached 100 mV. The readings on the upper array were up to 48.20 mV while on the lower array were 83.20 mV. A day with high flow of around 6 m³/s (mean daily discharge gauged at Westmill) occurred on 29 January and following this, the readings on the lower pin appeared to have increased. Other high flow events occurred on 17, 19 and 22 February with flows up to 8 m³/s. Subsequently, the pin readings increased once more. Soon after that, an extreme event with a discharge of 14.1 m³/s occurred around 1 March and thus certainly facilitated a failure of some material around the pins. The input from the pins increased with a delay. On the lower pin, increased readings occurred around 7 March (up to 121.90 mV) and on the upper pin this was sometime around 4 March and the changes were less severe (up to 79.40 mV).

Table 3.4.6 Statistical summary of PEEPs outputs with maximum, mean and standard error for each sample dataset, in mV. Channels 9 and 10 are the reference cell and an array of the lower pin, Channels 11 and 12 are the reference cell and an array of the upper pin. N is the number of readings in that particular dataset.

		Ch9 (ref. lower pin)	Ch10 (lower pin array)	Ch11 (ref. upper pin)	Ch12 (upper pin array)
28.11-5.12.09 n=10,225	Maximum	72.5	8.70	78.20	16.80
	Mean	5.484	0.15	6.05	0.35
	Standard error	0.145	0.01	0.16	0.02
25.1.-22.2.10 n=4,024	Maximum	97.2	83.20	100.00	48.20
	Mean	24.96	11.17	26.16	9.99
	Standard error	0.539	0.28	0.56	0.22
22.2-19.3.10 n=3,583	Maximum	98.6	121.90	101.70	79.40
	Mean	29.7	19.40	30.90	15.50
	Standard error	0.63	0.48	0.64	0.35

3.4.3. A DISCUSSION ON THE MAGNITUDE OF RIVER BANK RETREAT AND SOME OBSERVATIONS ON THE MEASUREMENT METHODS USED

3.4.3(A) THE VARIABILITY OF EROSION PIN READINGS

A variety of erosion rates recorded by the pins was expected given the nature of the sites. Research bank profiles were similar in being both steep and high, with a mean angle $\pm SD$ of 51.07 ± 6.87 degrees and mean height of 1.91 ± 0.29 m. The geotechnical properties of the sites are described in Chapter 3.2.

In general, there was a large standard deviation in mean erosion data collected at each site. Despite this, some deductions of causes could be made. For example, GB1 and LB1 sites appeared to retreat the most. The data at GB1 site were vastly influenced by a bank slump that occurred sometime during floods in spring 2007, while the retreat at LB1 site was driven by the weathering of the bare bank. The lowest retreat occurred at the LB2 site which was possibly due to a number of factors such as the low bank height or that the bank face was more sheltered from weathering. These factors are considered further in Chapter 3.5. Generally, the top sections eroded a little less than middle sections and the lower sections eroded the most overall. This is explored further in Chapter 3.5 and could highlight the potential correlation between the number of days the pins were submerged (or exposed to high flow) and the magnitude of erosion.

Both positive (bank retreat) and negative (bank accretion) figures were recorded. Negative pin readings were equally important as the accretion is an integral stage in the cycle of bank erosion (Chapter 2.1). Material that most likely failed from the top of the bank or was deposited by flow from upstream, remained at the bank foot until it was completely eroded by the flow, hence the negative readings on lower pins at times (Fig. 3.4.26).

Pin readings ranged from 30.42 cm erosion per year to -3.43 cm accretion per year and the mean retreat $\pm SD$ was 6.56 ± 6.61 cm, see Section 3.4.2(A). These rates are similar to those found on cohesive banks on comparable size lowland rivers in other parts of the UK (Section 3.4.3(G)).



Fig. 3.4.26 Slumped piece of the right bank at GB1 site (Fig. 3.1.1) with the uprooted tall herbal vegetation, June 2007. Failed material is covering the lower pin.

Round, slim steel erosion pins, that were 50 cm long offcuts from a local manufacturing company, seemed suitable for the purpose of measuring erosion. They were inserted into the bank with ease causing relatively little disturbance. The ease of pin insertion is a function of soil moisture content. Cohesive soils tend to swell when absorbing moisture and this fact should be taken into account if the clay content of bank material is high. Clay swelling can, in theory, cause negative pin readings, but because the clay content was low at the research sites, this was not considered (Chapter 3.2).

Erosion pins serve as effective, detailed gauges in measuring the bank retreat of particles or lumps that are localised around them. On the other hand, they can be counter-productive by either accelerating erosion or aiding bank stability. This has been also observed by Thorne (1978, 1981). He found that erosion pins in composite river banks reinforced the top cohesive layer. He noticed that where 100 cm pins were used, cantilevers of up to 80 cm in width developed. As natural cantilevers rarely exceed 50 cm in width, he recommended the use of shorter pins than the typical width of cantilever (around 30-50 cm). Although 50 cm pins were used in this study, they were observed to aid riverbank stability in the upper section of the bank (i.e. GB3 site), where they contributed to the tensile strength of the bank and may have prevented some tension cracks forming. Observations such as failures adjacent to the profile but not on the profile with pins, suggest this can be a significant drawback and thus other methods, such as bank top surveys and bank edge profiling, were also employed. In further research, it would be interesting to set up a number of 'control' profiles that would be surveyed alongside profiles with installed pins. Alternatively, a large number of pins could be inserted along

the top section of the bank and intensive observation on the evolution and dimensions of tension cracks could be undertaken.

Furthermore, the author observed that pins accelerated the retreat. As documented by Lawler (1993a), pins facilitate moisture seepage or heat loss that weakens the surrounding material. Protruding pins also generate extra local turbulence when submerged, or capture material moving down the slope from above (Lawler 1993a). A number of such cases was observed (example on Fig. 3.4.27). Normally, a ruler was placed across the hollow and bank retreat readings were taken from the ruler to the end of the pin as if the hollow was not there. However, this method can be questioned as it was not clear what measurement along the pin was not affected by turbulence from the protruding pin. It would be also interesting to explore what the presence and dimensions of these cavities mean in terms of the flow characteristics or bank material properties. The cavities were observed at some, but not at all sites.



Fig. 3.4.27 A large cavity formed around the pin LB1-3B. Left bank at LB1 site near Little Bradley, January 2008 (Fig. 3.1.1).

3.4.3(B) OBSERVATIONS FROM REPEATED VERTICAL PROFILES

Repeated cross sections of the river bank provide an interesting insight into the type, stage and magnitude of erosion. For example, the development of overhangs can be seen on GB1-3 (Fig. 3.4.11) or GB2-2 (Fig. 3.4.12) sites, while there are no signs of overhangs on C1 but on that site erosion occurs in the bank foot (Fig. 3.4.16).

Similar to pin readings, the magnitude of bank retreat varied within the vertical profiles. Sections GB1-2, GB2-2 and GB3-2 eroded the most or had the maximum retreat out of the

13 observed sections. The maximum linear retreat varied between 0.054 and 0.326 m/year.

The magnitude of erosion recorded on the pins and the retreat calculated from the changes in the vertical bank profiles correlate (Fig. 3.4.28). Exceptions will occur, for example when significant erosion takes place below or above the nearest pin, as illustrated by the toe scour at Section GB3-2 (Fig. 3.4.12 in Section 3.4.2B), but generally the results from both methods correspond.

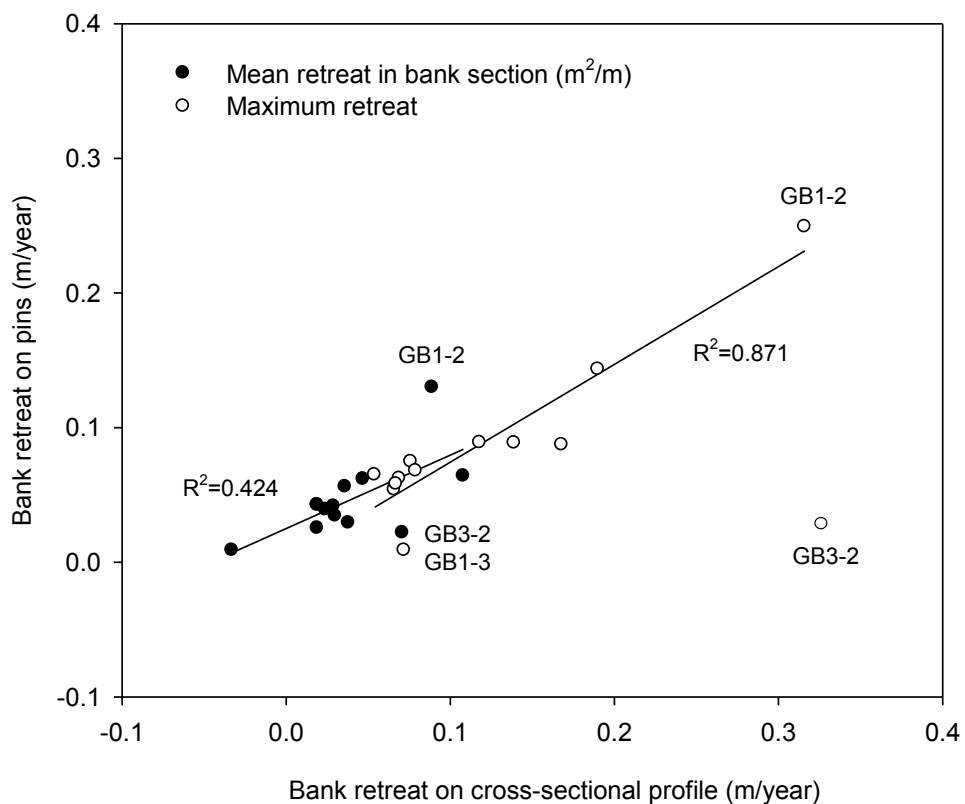


Fig. 3.4.28 Relationship between the retreat calculated from the vertical bank profiles and retreat recorded on erosion pins, for all sections listed in Table 3.4.3. The mean retreat in the bank section is expressed as $\text{m}^2/\text{m}/\text{year}$ while all other units are in m/year . All data are relative to the time factor (as years).

For mean bank retreat, the coefficient of determination (R^2) was 0.424 and the relationship $y = 0.03 + 0.55x$. For the maximum bank retreat, the coefficient was 0.286 initially, but after the vertical bank section GB3-2 was excluded from the correlation, it increased to 0.871. The relationship for the maximum retreat was $y = 1.64 + 0.73x$. With the exception of site GB3-2, the two methods do appear very consistent.

3.4.3(C) OBSERVATIONS FROM REPEATED BANK TOP SURVEYS

Repeated surveys of the river bank edge provide a similar type of information to that obtained from historical analysis of maps and satellite images. Surveys highlight changes in the lateral position of the bank top albeit with greater accuracy and more detail than one can obtain from old maps. On the other hand, an accurate establishment of the bank line may be a challenge in the field. Some authors suggest that the bank edge is located at the maximum break of the slope or the minimum width/depth ratio (Wolman 1955; Schumm 1961); or the exact position is based on signs of vegetation or flow. However, there are limitations: such assumptions greatly reduce the accuracy of this method (Lawler 1993a).

To limit the variation, sites with an easily identifiable bank top were chosen for the surveys: LB1, C1 and N1. The results that were obtained were of a high accuracy and the establishment of a network of field reference points allowed for accurate data overlay. A common feature found at all three sites was that the mean retreat was above 40 cm per year and also that the banks retreated more at the upstream end of the sites. Despite this there was no clear decrease in retreat going downstream and the changes in the erosion pattern with distance require further investigation. By far, the maximum retreat occurred at the N1 site (up to 1.3 m/year). This was probably caused by the non-cohesive texture of the bank material at this site. Unfortunately, data on the erosion/sedimentation of the river bed adjacent to the surveyed banks were not recorded at the time as they would have provided very useful information about processes such as toe scour and undercutting. Fig. 3.4.29 and 3.4.30 show some examples of mass failures that occurred at LB1 and C2 sites and that were captured by bank top surveys.



Fig. 3.4.29 Two instances of slumped bank at the upstream end of the surveyed bank at LB1 site (see Fig. 3.1.1 for a location map). Photographs were taken from the top of the bank in January 2009. The grey colour of material on the left indicates high clay content.



Fig. 3.4.30 Two instances of slumped bank at the downstream section of C2 site (Fig. 3.1.1) in November 2006 (left) and October 2007 (right).

Lawler (2005b) summarised some of the major drawbacks of all three manual erosion measurement methods:

- (1) surveys or pin readings only reveal changes since the last field measurement;
- (2) the response of the channel to a specific geomorphologic event cannot therefore be defined with any certainty;
- (3) due to the unknown timing of the erosion event, it is not possible to precisely measure its magnitude, frequency and duration; and
- (4) that any change measured is always just the net change between two set dates and may ignore intermediate processes of fill and scour. These problems were overcome by the invention of Photo Electric Erosion Pins (PEEPs).

Despite Lawler's comment in (4) above, there are significant drawbacks also in the use of PEEP pins as discussed below.

3.4.3(D) NOTES ON EXPERIENCE OF USING PHOTO-ELECTRONIC EROSION PINS

Quantifying the magnitude of erosion is only part of the problem. Relating the magnitude to the timeline and flow provides more comprehensive geomorphologic data. Installing Photo-Electronic Erosion Pins (PEEPs) was a fascinating test despite being implemented on a small scale in this research. The author's observations are similar to Lawler's (1992a; 2005a). The results presented in Fig. 3.4.23-25 document a relationship between the pin readings and river flow. The voltage output from pins increased, although with a delay, after each high flow event. Flows of around 6 m³/s (at the Westmill gauging station downstream) were enough to initiate particle entrainment near the pins. Flows in March 2010 were of 14 m³/s and they clearly eroded some soil around the pins. This was a pilot test and data collected over a longer period of time would help to test these observations.

The downside, however, was that the data did not reflect the true bank retreat as a scour of around 12 cm was observed around each pin. The scour has evidently influenced the length of array that received light and thus increased the voltage outputs from the pins. Furthermore, dirt, debris or vegetation can often get trapped around the pin, reducing the length of tube that receives light. Thus, although it is a fully automated system, it still requires frequent field visits to check the pins and take control readings.

3.4.3(E) SUMMARY CHARACTERISTICS OF EROSION MONITORING METHODS

Each of the methods used can capture only a certain part of the bank erosion cycle as they each have a different level of accuracy and different level of spatial extend. Bank erosion pins, although an old method from the 1950s, are still popular (Veihe *et al.* 2011) and can be very precise in monitoring and reporting on fluvial or subaerial erosion especially in the lower wetted part of the bank profile. The vertical bank profiles and cross-sectional resurveys tell us, less accurately, what is happening in the bank sections, for example about bank toe scouring, and thus they can examine what critical bank angle has to be reached before it collapses. These profiles are localised on a specific narrow bank section only and it is not clear what is happening to the right or left to the section. Planform resurveys reflect the situation over the whole site but do not provide data on what is happening in the basal zone, which is important for controlling the river bank stability. They only give details of the final failure once it happens. All of these are limited also by the time extend, and the data collected are averaged over the period between the two field checks and this problem was tackled by the Photo-Electronic Erosion Pins. Many of the

advantages, drawbacks and recommendations for all four methods used in the research are presented in Table 3.4.7.

Table 3.4.7 Summary characteristics of applied methods: advantages, drawbacks and recommendations.

	Advantages	Drawbacks	Recommendations
Erosion pins	Suitable for short to mid timescales Time effective Readily available Low cost	Only concentrates on the area immediately around the pin Disturbance to bank during the installation Can increase bank stability Flow cavity around the pin Not suitable for non-cohesive or composite banks Not suitable for mass failures Can be difficult to find, thus gaps in data due to lost or invisible pins	Pins should be inserted on banks only during saturation to limit disturbance Clay swelling should be taken into account Metal detector can be used to locate invisible pins Pins should be reset to starting value Establish a range of control profiles next to the pins
Cross sectional bank surveys	Suitable for mid to longer time- scale Detects mass failures Looks at the whole cross section	Only looks at small vertical proportion of the bank Requires permanent benchmarks Requires access to the whole river cross- section At least two people needed Time consuming Errors from re-surveying	Establish more cross-sections through the site and take these alongside repeated cross-profiles Extend the survey to both banks
Banktop surveys	Suitable for mid to longer timescale Able to record the whole top of the bank Does not require access into the river channel Low disturbance to the bank	Only records the changes to the horizontal bank line Requires more than two permanent benchmarks Difficulty in defining bank line At least two people required	Set starting benchmark and reset the total station angle to this one to eliminate the need for coordinate transformation Any cracks and undercutting should be recorded
Photo-Electronic Erosion Pins (PEEPs)	Suitable for very short timescales Automated No power supply needed as powered by PV cells Not expensive if made from basic components	Requires calibration Disturbance to the bank on insertion Tricky installation of the system No records when the visibility is low Scouring around the pin Manual checks required	Frequent control field visits Cable lead out front-end to avoid drilling into the bank, or better still a wireless device More pins inserted in one section so they can also act as a water gauge Thermistor to allow for accurate timing of erosion events Camera to check if anything was not trapped on the pin

3.4.3(F) THE RELATIONSHIP BETWEEN LONG-TERM HISTORICAL AND SHORT-TERM FIELD EROSION RATES

An analysis of maximum retreat and land loss through bank erosion at the research field sites was presented in Chapter 3.3. The discussion outlined a number of challenges, including the assumption of continuity of change when analysing historical resources. To examine the magnitude of retreat, a comparison has been undertaken between the information obtained from historical maps against the field results presented in this chapter, resulting in the maximum annual retreat (m/year) at each field site. The historic period between 1886 and 2008 was considered in three stages (Table 3.4.8).

Table 3.4.8 Maximum retreat (m/year) derived from historic map sources during the three examined periods, as defined by the mapping intervals, and the maximum retreat (m/year) as recorded in the field between 2006-2010.

	I. Interval Max. retreat m/year	II. Interval Max. retreat m/year	III. Interval Max. retreat m/year	Field max. retreat m/year				
GB1	1886-1903	0.035	1903-81	0.021	1981-08	0.037	2006-10	0.249
GB2	1886-1904	0.000	1904-81	0.059	1981-08	0.056	2006-10	0.143
GB3	1886-1904	0.000	1904-81	0.030	1981-08	0.067	2006-10	0.214
LB1	1886-1904	0.083	1904-81	0.028	1981-08	0.074	2007-10	0.203
LB2	1886-1904	0.083	1904-81	0.051	1981-08	0.056	2006-10	0.075
C1	1886-1904	0.083	1904-68	0.042	1968-08	0.020	2006-09	0.089
C2	1886-1904	0.028	1904-68	0.102	1968-08	0.113	2007-10	0.413
S1	1886-1904	0.061	1904-66	0.153	1966-08	0.226	2008-10	0.304
N1	1886-1904	0.094	1904-62	0.233	1962-08	-0.141	2007-09	1.328

In seven out of nine field sites, the field work revealed considerably higher annual retreat than was obtained through analysis of old maps. Exceptions were LB2 and C1 sites, where the field erosion rates were similar to the values obtained over the period 1886-1904. Both the historic maximum and field recorded maximum rates at these sites were relatively small. The remaining sites, at least two of which were altered by engineering (S1 and N1, Chapter 3.2), displayed results consistent with the observations by Hooke (1979). According to her findings, the erosion rates measured in the field were much higher than the ones that were found from old maps (Section 3.3.4.A).

Indeed, Hooke further suggested that the longer the period, the lower the erosion rate. This is because the historical analysis tends to 'smooth' the erosion extremes equally over a period of time. The values from Table 3.4.8 were correlated against the length of period of observation and the resulting relationship appears to agree with this theory. There is a decreasing trend with increasing length of time period (Fig. 3.4.32).

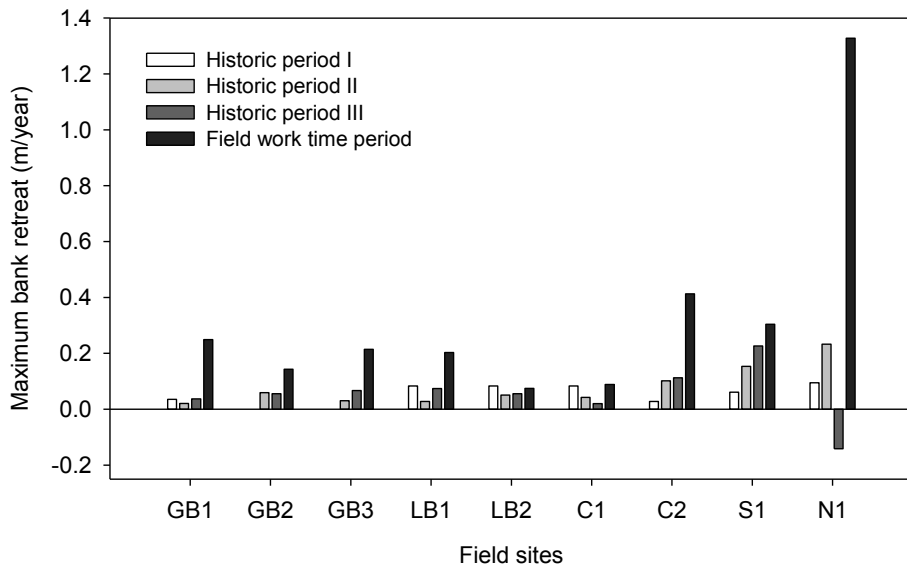


Fig. 3.4.31 Maximum retreat per year during the three historic intervals and maximum readings recorded in the field, both as m/year. The years attributable to each time interval for each site are in Table 3.4.7.

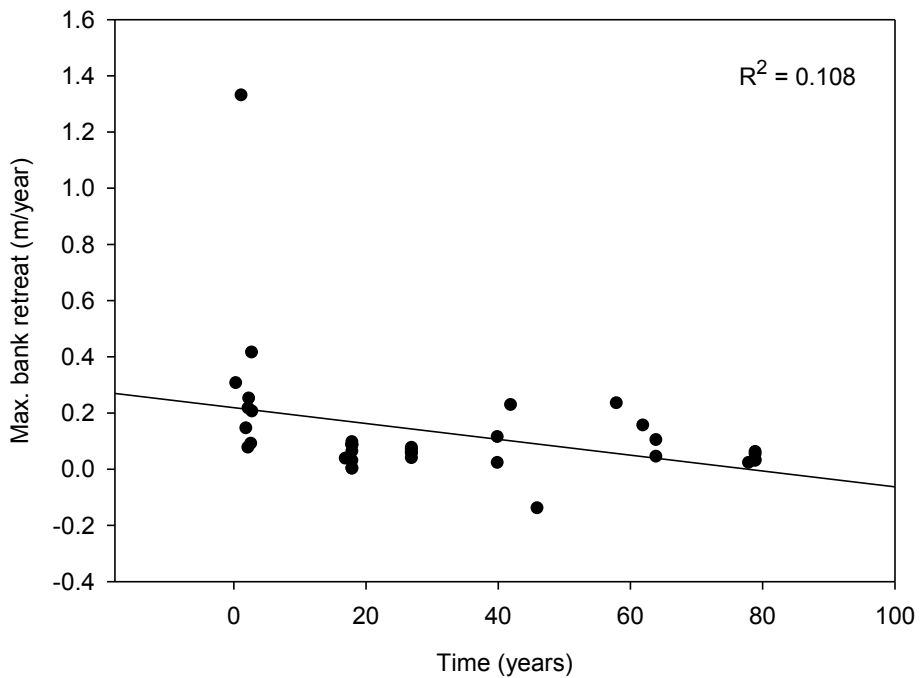


Fig. 3.4.32 Maximum retreat (m/year) versus time interval over which this retreat was measured.

Thus, historic resources can be useful in finding out about the channel form but they should be referred to as averaged data. They may have omitted bank accretion and are poor in explaining whether the final bank retreat is a result of a single extreme event or whether the process was spread more evenly over a period of time. Field data are necessary in establishing a current erosion magnitude, especially on short stretches of a small river as studied in this work. This conclusion answers the Objective 2 set out in the beginning.

3.4.3(G) FIELD EROSION RATES IN THE CONTEXT OF OTHER BRITISH AND WORLD RIVER BANK EROSION STUDIES

The maximum erosion rate assessed in the field by pins was 0.30 m/year, by cross-profiling 0.33/year and by channel planform resurveys 1.32 m/year (2.40 m/year based on three extreme months at the N1 site). The differences between the sites or within a single site given by the standard deviations of mean were large (Section 3.4.2). The assumption at the beginning of the research was that the field rates of bank retreat found on the River Stour would be significantly higher than on a comparable lowland stream of similar size and climate in the UK. Despite the fact that the field sites in this research were not necessarily representative of river conditions in general and could be regarded as extreme in their nature, research indicates that the bank retreat rates on the River Stour correspond to those reported by other authors elsewhere in Britain.

Knighton (1973) using erosion pins found that bank erosion rates ranged from 6 to 33 cm/year on the River Bollin in Cheshire. A study by Hooke (1980) on rivers in Devon over a 25 year period reported retreat rates ranging from 0.08 to 2.58 metres per year. Hooke localised a retreat of 7 m on the River Exe at one site over a 2.5 year period, which is higher than the maximum rate found at N1 site on the River Stour (Section 3.4.2.(C)). Hooke (1980) noted a situation, similar to that found on the River Stour sites, of a 'considerable variation even between sections close to one another on the same river', but observed that there was some relationship of erosion rates with the catchment size. The data from the River Stour sites appear to fit this trend (Fig. 3.4.33). On the Swale-Ouse river system Lawler *et al.* (1999) identified erosion rates of 0.08 m/year to 1.76 m recorded at one mobile reach over 4 months. Most field bank erosion studies in the UK were concentrated on Welsh streams and the rates varied from a few centimetres to over a metre of bank retreat per year. For example, an erosion rate of up to 1.25 m/year was measured in the valley of Pennard Pill (Lawler & Bull 1977), between 0.038-0.31 m/year on the River Ilston (Lawler 1986), between 0.35-0.6 m/year on the River Severn (Thorne 1978; Thorne & Lewin 1979) and from 0.03-0.96 m/year in the River Trannon (Leeks *et al.* 1988).

Much greater rates (>5m/year) have been observed on river banks of large rivers such as the Mississippi (Kesel *et al.* 1974) and Ohio (Hagerty *et al.* 1981) in USA or on the Jamuna River in Bangladesh (Haque 1988), where the river channel shifted by hundreds of metres per year. A comparison of the world, British and the River Stour bank erosion data against catchment size is shown on Fig 3.4.33.

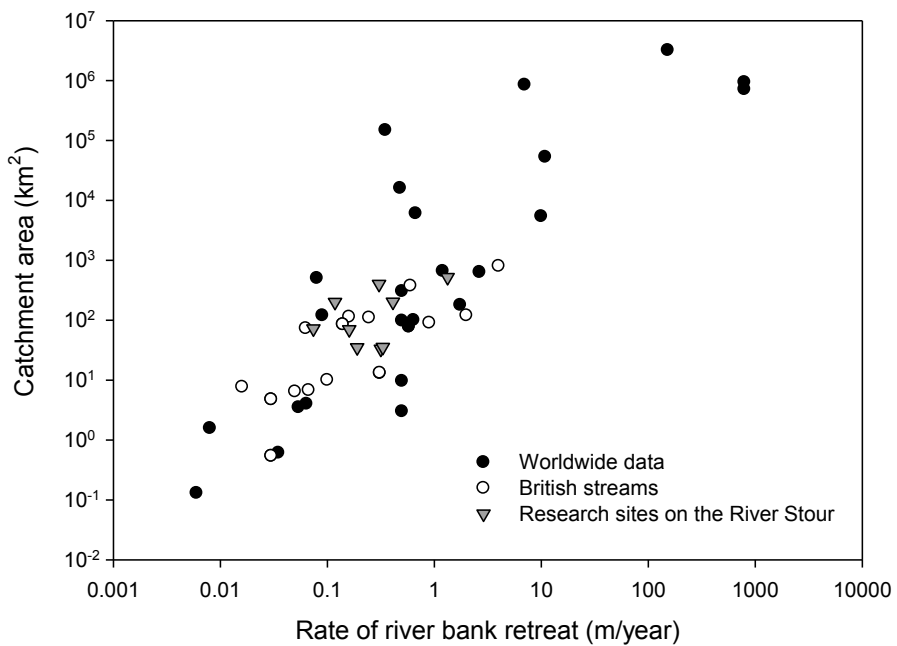


Fig. 3.4.33 Relationship between the maximum erosion rates and the catchment area on a logarithmic scale from worldwide and British rivers (data from reviews by Hooke 1980 and Lawler 1993), and from this research on the River Stour (Section 3.4.2).

Based on the review of some studies published on erosion rates on the rivers in the UK, the field data on maximum erosion/retreat rates from the River Stour do not appear to be substantially higher than on other lowland UK rivers ($P=0.66$). The maximum erosion rate within the research field sites occurred at the N1 site which was furthest downstream and therefore the water transfer or engineering works related to the transfer had, probably, the least effect on erosive forces (Chapter 2.1). The sites chosen were not representative of the river conditions in general and eroding sites were chosen as a priority, but these data were comparable with the maximum retreat rates in the studies cited. Based on this data, the first part of the first research hypothesis that argues that the erosion rates on the River Stour are substantially higher than on other similar lowland UK streams was not found to be the case.

3.5. EROSION RATES AND SITE PROPERTIES CORRELATIONS

In a natural environment, a large number of factors interact with each other and these interactions create complex relationships (Goodson 2002). To examine the composite relationships between all the factors that have an impact on the riverbank is beyond the scope of this study. A simplification is made to outline some of the key hydrological conditions and bank properties, to determine whether any of these were important contributors to the bank erosion rates and bank top retreat, although it would have been appealing to deal with this in more detail had more time and resources been available. As mentioned in the introductory Chapter 2, understanding the bank erosion processes is a key for its effective management. The establishment of the most likely reasons behind river bank erosion is at least as valuable as identifying the extent and nature of the erosion processes that have been occurring. The scope of this research was set to examine the effect of additional flows and engineering interventions to the river channel on retreat and erosion rates. The difficulty encountered was how to separate the joint combination of the fluvial processes and bank properties that result in river bank erosion or material accumulation.

The effects of bank geometry, bank material properties and river flows on bank erosion rates have been researched (Hooke 1979; Thorne & Tovey 1981; Couper 2003; Rinaldi *et al.* 2004). This part aims to test some of the properties presented in Chapter 3.2 with an aim to uncover the most significant factor, if such exists, whilst specifically reflecting on the research aim – the need to establish what impact, if any, the transferred flows could have had on the river geomorphology. This chapter raises a series of questions and indicates areas where further investigation would be useful. It speculates on: (1) the influence of soil texture on erosion rates; (2) the influence of the bank and channel geometry and (3) the influence of flows, both natural and transferred, on erosion readings. This chapter is therefore the key one addressing the second part of the first research hypothesis that argued that the erosion rates on the river were mainly caused by engineering interventions to the river channel or transferred river flows.

3.5.1. THE INFLUENCE OF BANK MATERIAL PROPERTIES ON EROSION RATES

3.5.1(A) AN EXAMINATION OF SOIL TEXTURE

Higher proportions of cohesive silt and clay are believed to increase the strength of riverbanks in an event of fluvial erosion or mass wasting (Wolman 1959; Thorne & Tovey 1981; Osman & Thorne 1988). This analysis follows on from the work by Couper (2003) who demonstrated the impact of silt and clay content on bank erosion processes, with an emphasis on subaerial processes. Couper's vertical dominance process zones divide the banks into upper and lower zones. According to this model, in the upper bank zone subaerial erosion dominates and a higher silt-clay content will lead to higher erosion rates. However, the lower bank is dominated by fluvial erosion and a higher silt-clay content will result in a reduced erosion rate. In addition to this theory, when considering mass wasting, the basal endpoint control will correspond with the rates of bank retreat and thus a higher silt-clay content will conversely result in reduced bank retreat due to mass failure.

In the research sites, three typical vertical process dominance zones have been identified: (A) top zone, where overhangs tend to develop due to the added soil strength from roots; (B) middle zone, where subaerial processes dominate and there is no added strength from roots; and (C) toe zone, which is the zone most subjected to fluvial erosion (Fig. 3.5.1). The prominence of this division can be seen on the cross-sectional profiles in Chapter 3.4. Erosion pins recorded the rate of subaerial and fluvial erosion, while vertical sections informed about the state of basal endpoint control and, together with bank top resurveys, reported on the bank retreat: the change in the position of the bank line.

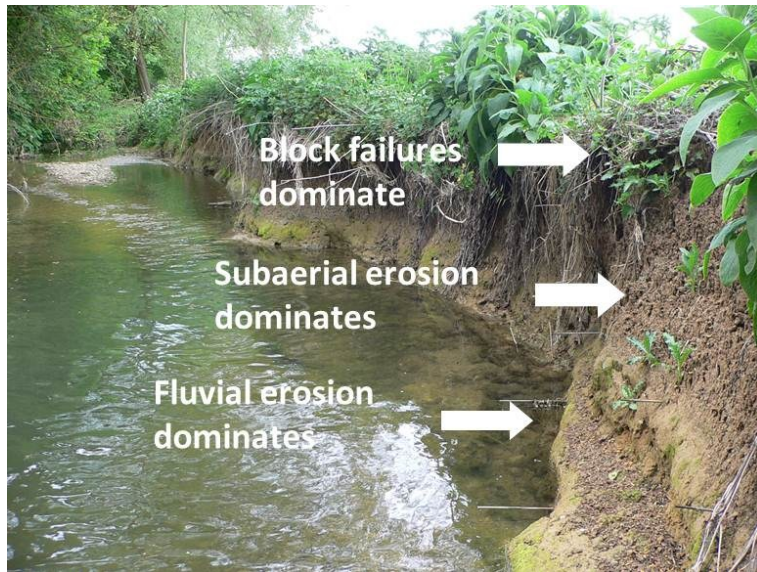


Fig. 3.5.1 Vertical process dominance zones applied to the study sites with the formation of a 'step' on the boundary between where fluvial processes and subaerial processes dominate (see also Fig. 3.4.1).

The sampling strategy for pin recordings and soil texture analyses followed the process of vertical dominance zonation (A, B and C zone) so it was possible to examine data for the upper, lower and middle zones separately (Fig. 3.5.2). The relationship between the clay and silt-clay contents (Chapter 3.2) were related to the mean annual erosion rates recorded on pins (Chapter 3.4).

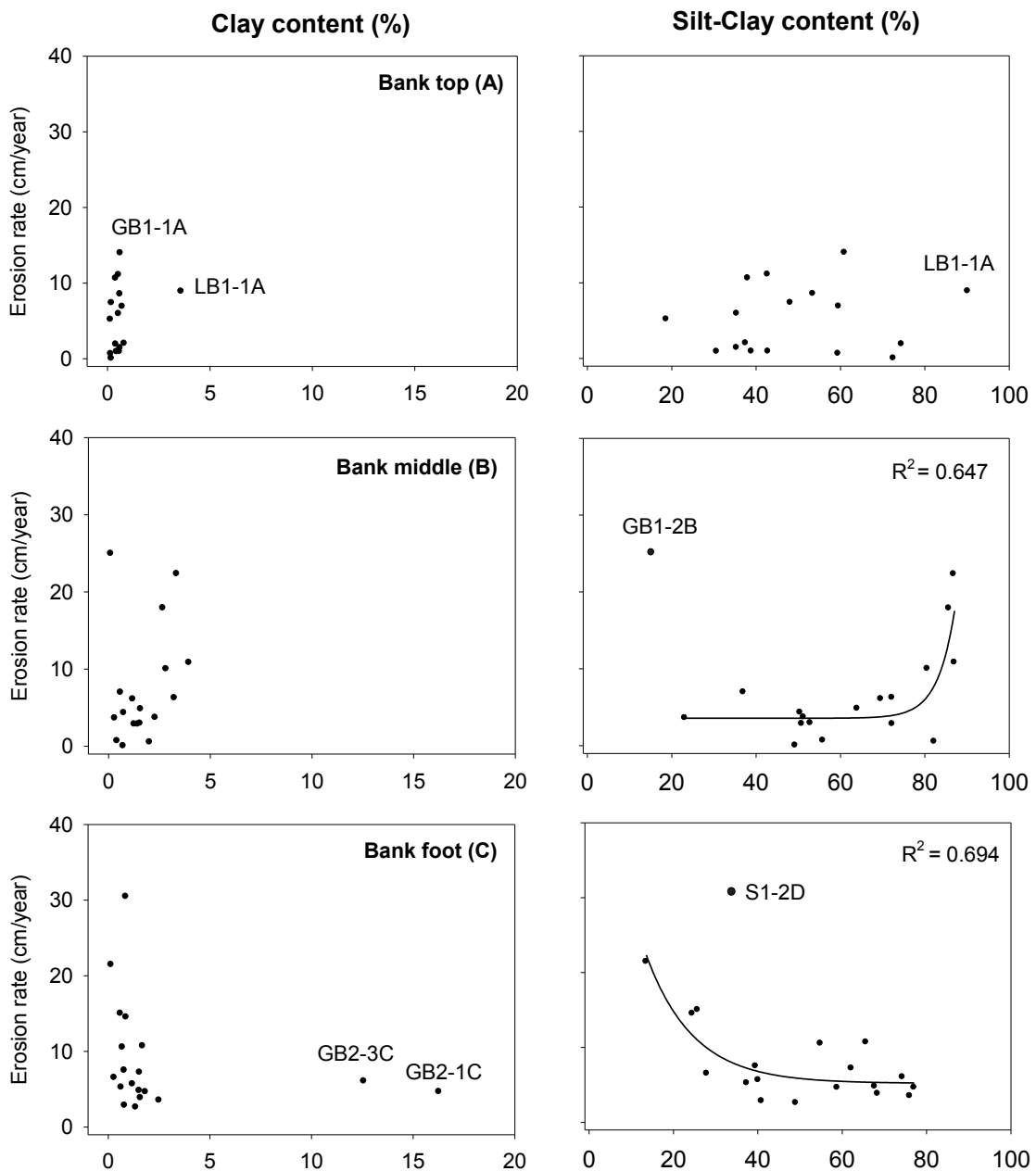


Fig. 3.5.2 Clay content and silt-clay content (as volumetric %) versus annual erosion rate recorded on pins (cm of retreat/year) for three vertical bank zones: top (A), middle (B) and bank foot (C). Accretion is excluded from the analysis.

The clay content was low and for all bank sections, the values fell within 5% of the sample volume, with the exception of GB2-1C and GB2-3C samples. Such small variability in clay content within the samples did not have a notable effect on the erosion rate. GB2-1C and GB2-3C samples were higher in clay content (6.2 and 4.8-times more than the mean for all samples) and the erosion rate was lower than the mean (by 31% and 47% respectively), suggesting the clay content in the lower bank zone may increase the resistance of the bank to fluvial scour. (Accretion rates were not considered in the analysis).

Considering summed silt-clay content, at the bank top (zone A) the plot did not show any correlation between the soil textures and pin erosion readings. The volumetric silt-clay content in this zone varied greatly, between 18.7 to 90.2%, and erosion rates were up to 13.94 cm. In the middle section (zone B), the data showed a correlation and a 2-factor exponential function was fitted in the data ($R^2=0.647$). GB1-2B point was an exception and was removed from this correlation analysis. The relation became steeper towards higher silt-clay content and thus such pins were more susceptible to erosion. In the fluvial erosion dominated bank toe (zone C), there was an exponential decay in erosion rates with increasing clay-silt content ($R^2=0.694$). The point S1-2D was exceptional and was not considered in the curve fitting. Accretion readings were removed from all datasets. These trends are in agreement with the theory suggested by Couper (2003).

There is a notable step in the boundary between the fluvial dominance and the subaerial dominance zones in the cross-sectional profile on Fig. 3.5.1 (detail in Fig. 3.4.1). This was most distinct on the LB1 and C1 sites. The difference in bank stratigraphy, higher clay and silt content in the bank foot, could be the justification for this, however there was not a notable difference between the middle and lower bank zones within the researched profiles. The profiles where the step boundary occurred (LB1-2B, 2C, 3B, 3C and C1-2B, 2C, 3B and 3C) all had a low clay content (between 3.96 and 0.32%) and were all composed of sandy silt loam, only the 3B profile was loamy sand (Table 3.2(A)). Because the bank stratigraphy did not play a role at these sections, the presence of the flat area is the morphological evidence of the EOETS transfer scheme. The result of prolonged flows of constant and controlled discharge produced by the water transfer have influenced the channel form. Such a form, although it was less prominent, occurred also at LB2 and C2 sites. Unlike some sites (e.g. S1, Fig. 3.2.12) where distinct sedimentary layers were observed in the bank, no change in bank slope associated with these observed layers was found.

3.5.1(B) SHEAR STRENGTH EFFECT

Shear strength is believed to be a critical factor for bank erosion rates (Chapter 2.3). The saturated shear strength of cohesive material is an indicator of the material's ability to resist fluvial shear forces (Chapter 2.3). The undrained (unsaturated and saturated) shear strength of bank material has been measured *in situ* at some research bank profiles (Chapter 3.2). The results suggest that samples with a higher content of cohesive component (silt-clay) had, on average, higher shear strengths. Thus in theory, it would be

possible to apply the Couper's erosion dominance zone model also to the saturated shear strength readings at the research sites.

Linear regression relationships between shear strength and erosion pin readings were examined for loamy sand and sandy silt loam under saturated and unsaturated conditions (Fig. 3.5.3). In all four cases, however, for a 95% probability and the given degrees of freedom, the determination coefficient was low to be statistically significant ($R^2 = 0.431$ for saturated loamy sand, 0.032 for saturated sandy silt loam, 0.019 for unsaturated loamy sand and 0.002 for unsaturated sandy silt loam). If trend lines were drawn for loamy sand, the erosion rate would decrease gently with increasing shear strength, more during saturated and less during unsaturated conditions. Saturated conditions were present for most of the time in the bank foot (C zone). The upper sections (A and B) were rarely saturated.

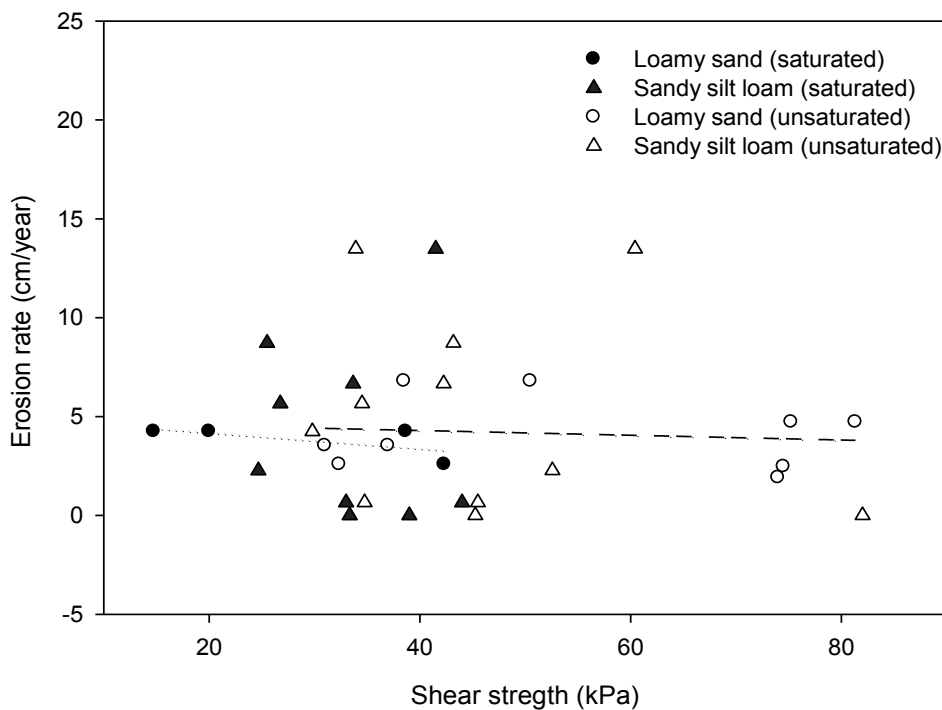


Fig. 3.5.3 Shear strength (kPa) versus erosion rate (cm/year) for loamy sand and sandy silt loam during unsaturated and saturated conditions. The lines represent an estimation of trends for loamy sand values during saturated (dotted line) and unsaturated (dashed line) conditions.

In total, 11 sampling locations had data available on mean saturated shear strengths and erosion rates. The erosion rates varied between 0 and 30.4 cm/year and shear strength was in the interval of 0.5 to 2.3 kPa (Fig. 3.5.4). When examined, the linear regression between erosion rates and shear strength gave too small determination coefficient ($R^2 =$

0.249). The erosion rates were highest where the shear strength was reduced, such as at S1-2D and C2-3C.

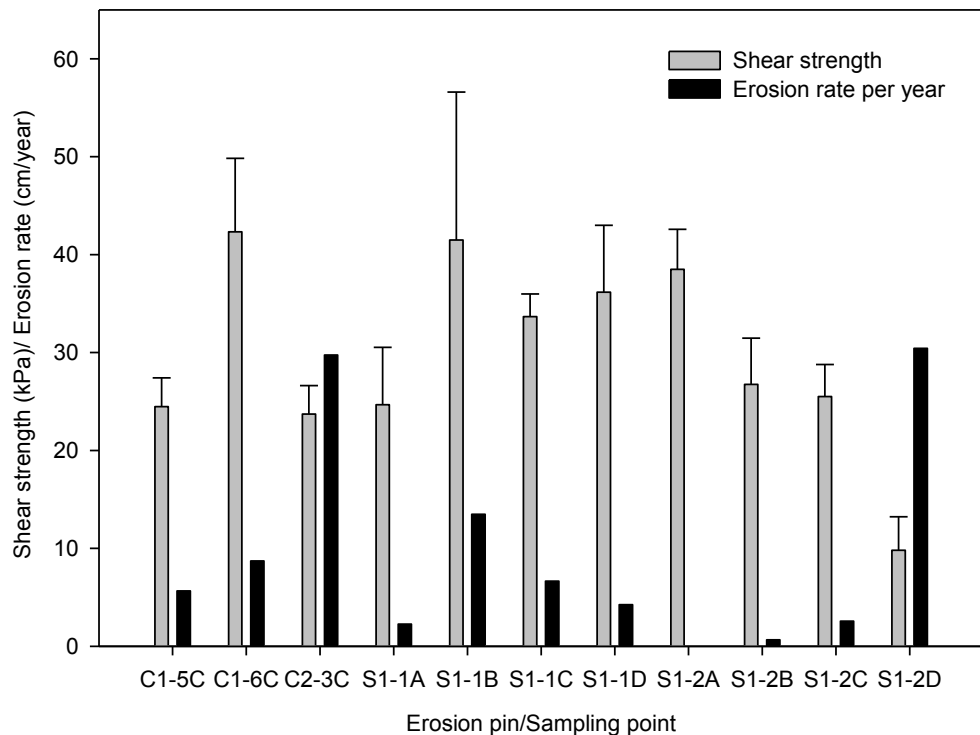


Fig. 3.5.4 Mean shear strength (\pm standard deviation) of saturated soil (kPa) and corresponding erosion rates, as recorded on the individual pins and expressed as cm retreat per year.

3.5.2. THE INFLUENCE OF BANK AND CHANNEL GEOMETRY

A stable river is more easily achieved if the bankfull dimensions are in regime and bank heights are appropriate. One of the problems where bank failures are occurring is that the banks may be too high and/or too steep. Banks that are higher than the natural bankfull elevation will be more prone to failure (R. Hey, personal communication 2006), for example incised channels in the UK. This is typically the case on the incised channel also at the research sites. Alongside bank geometry, other factors that are important for bank stability such as meander dimensions and water surface slopes were measured for the research sites (Chapter 3.2).

3.5.2(A) BANK HEIGHT AND SLOPE

It has been discussed that pin readings are not a good indicator of mass failures by reinforcing the bank through the failure plane (Chapter 3.4). As reviewed by the slope stability theory (Chapter 2.3), bank heights and angles (which depend on bank material properties), are critical in various mass wasting modes of failure. To study a relationship between the retreat rate and bank properties, results of repeated bank top surveys were examined (Chapter 3.4).

The relationship between the retreat rate and bank height/bank angle was studied using data from the bank top surveys at LB1 and N1 sites. At LB1, the results showed no well-defined correlation of the bank geometry to the retreat rates between June 2007 and April 2010. Bank height varies only by an interval of 25 cm, between 1.21 and 1.46 m, whereas bank angles are more diverse, ranging from 36.6 – 77.7 degrees. The bank angle is at its maximum at around 7 m in the downstream direction and then has a decreasing trend going further downstream. Steeper banks could be the reason why the first 7.4 m of bank line at LB1 site retreated more, by 2.9 m^2 , as opposed to the 2.14 m^2 of floodplain that eroded in the downstream half (Fig 3.5.5).

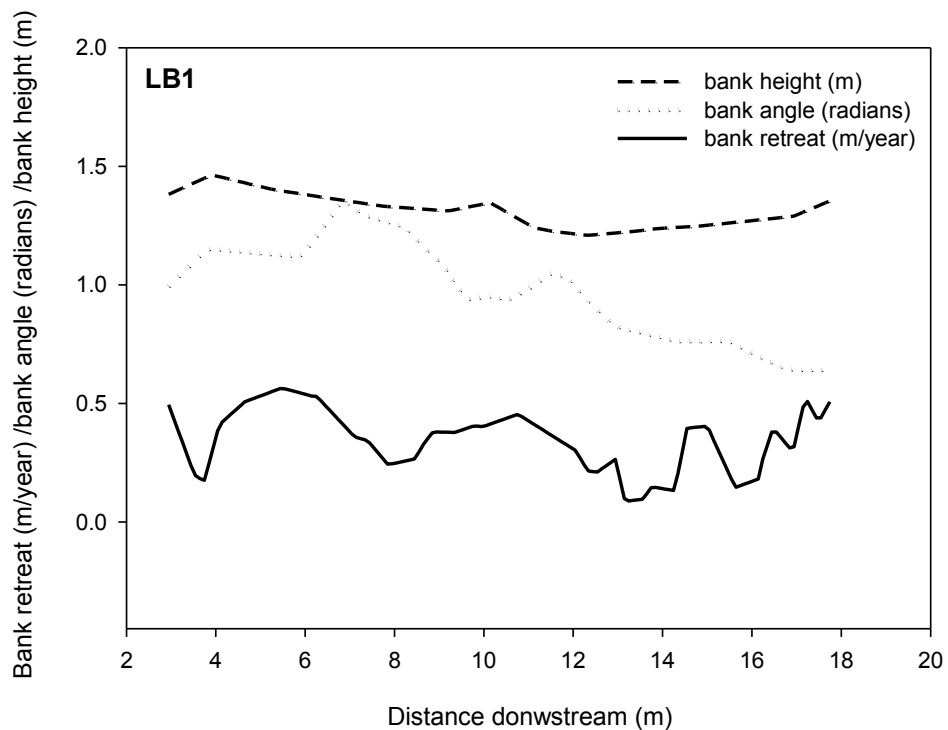


Fig. 3.5.5 Bank heights (in m) and angles (in radians) with the corresponding retreat rates (m/year) recorded between June 2007 and April 2010 at site LB1. These charts are based on extrapolated data (for each 10 cm of downstream length, section 3.4.1(C)) and are shown in relation to the distance downstream (m).

At N1, the influence of bank height and angle appears to be apparent at the upstream end. Overall, the banks were higher than at the LB1 site, ranging from 1.67 to 2.12 m. On the other hand, while the angles were less steep than at the LB1 site, they still varied greatly, between 20.3 and 63.4 degrees. In a similar trend to the LB1 site, the bank angle is decreasing in the downstream direction. The bank was at its steepest angle in the first 5 m of studied length and it was here that highest rate of bank top retreat occurred. In this area the bank retreated by up to 1.64 m per year. This suggests that the bank top retreat might depend on the bank angle in the upstream half (Fig. 3.5.6). Overall for the studied period, 5.96 m² of land was eroded in the upstream half, while 4.1 m² was eroded in the downstream half of the researched reach.

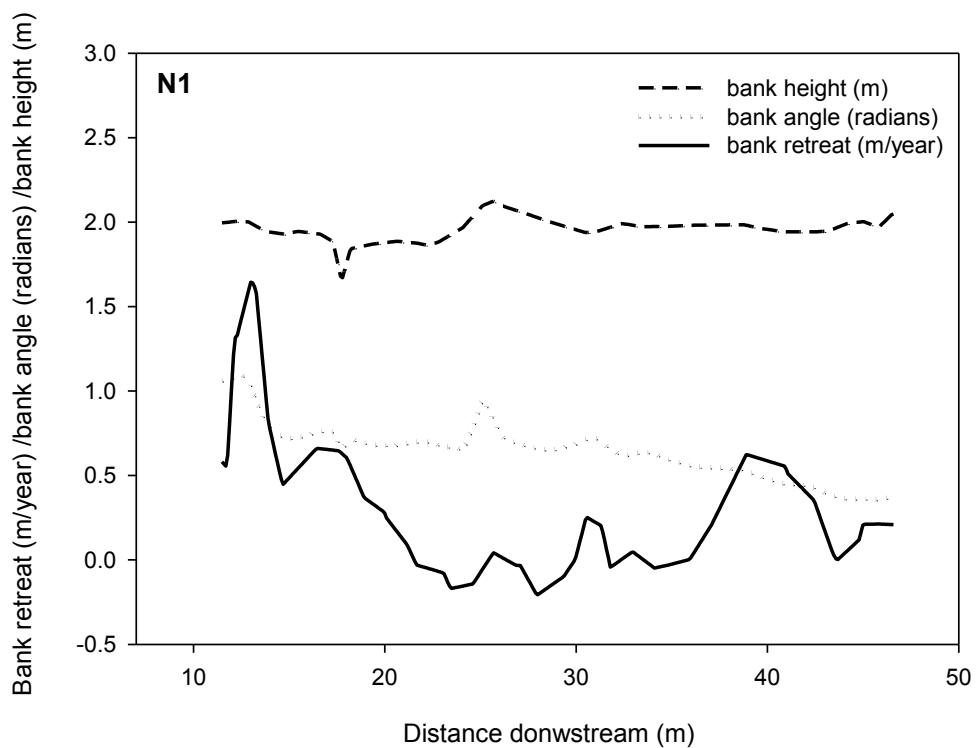


Fig. 3.5.6 Bank heights (in m) and angles (in radians) with the corresponding retreat rates (m/year) recorded between December 2007 and March 2009 at site N1. These charts are based on extrapolated data (for each 10 cm of downstream length, section 3.4.1(C)) and are shown in relation to the distance downstream (m).

The results reflect the fact that the bank at N1 responds to high flows quicker and with greater retreat than the bank at LB1 site. The reason lies in the bank material and the different way the erosion cycle operates at each site. It has been observed by the author that it is shorter and less complex on a non-cohesive (such as N1) as opposed to a cohesive bank.

These results also suggest that bank heights and angles can be useful indicators of bank top retreat if the erosion rate is significant and the bank is composed of non-cohesive material. As discussed, the drawback of bank top surveys is that they record only the mass failure stage of the erosion cycle, not the subaerial or fluvial stages (Chapter 3.4). These cycles operate in a sequence (undercutting, mass failure, restabilising) over a period of several years in cohesive banks (Chapter 2.2). The stage the bank varies within a single stretch and thus the actual retreat of the bank may not occur during a given study period. Hence, bank retreat and bank properties data over a longer period than presented in this study (>5 years) may demonstrate a correlation which is better defined.

3.5.2(B) WATER SURFACE SLOPE AND CHANNEL PLANFORM

The boundary shear stress in a uniform straight channel depends on the water surface slope and the water depth (Chapter 2.3). Faster flowing water will expose the bank to higher shear forces at greater depths that would in turn be responsible for the entrainment of boundary material. Pin readings were used in this instance to explore the relationship between the erosion rate, water slope and channel planform on eight of the research sites.

At more sinuous sites, the water slope is reduced because the length of the river channel is significantly more than the length of the river valley. It was demonstrated that sinuosity decayed exponentially with an increasing water surface slope ($R^2=0.491$). Water slopes were related to the distance from weirs (Chapter 3.2), with increasing distance dropped ($R^2=0.952$). Both increasing water slope and increasing sinuosity would increase the boundary shear stresses operating on the river bed and banks (Section 2.3.2).

Plots of site sinuosity or site water slope versus maximum annual erosion rates recorded on the site did not show satisfactory correlations (Fig. 3.5.7). This was because the channel form and sinuosity are inversely related, such as in the case of the C2 site. Significant erosion was recorded there and the site had the lowest site water surface slope but the highest site sinuosity. On the other end of the data scale is LB2, the site where the maximum recorded erosion was lowest, and slope and sinuosity were also low.

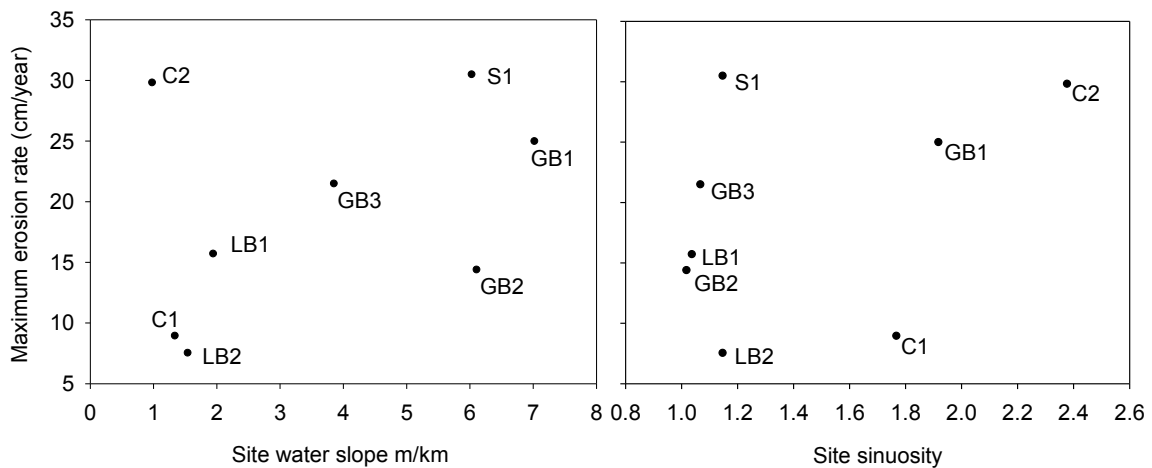


Fig. 3.5.7 Maximum erosion rate recorded on pins (cm/year) versus site water slope (left) and site sinuosity (right) at the research sites shown.

At some sites it could be the slope, at others the sinuosity that is more critical to bank stability. At most sites it is the relationship between both. For a site with a peak combination of slope and sinuosity, the boundary shear stresses will be high (such as S1) and the probability of maximum bank erosion is most likely. As the channel constantly changes over time, the sinuosity changes and consequently does the site water surface slope. If left unmanaged, sinuosity will continue to increase at all sites, up to the point of meander cut-off on mature meanders such as the one at the C2 site. Sinuosity is helping the channel planforms to recover from straightening in the past (Chapter 3.3), such as at the GB2, GB3, LB1, LB2 and S1 sites. GB1 site is recovering from being modified to a channel with angles that copy land boundaries.

Separating the individual bank or channel processes and relating them to erosion rates only gives an indication of the cause of erosion, if any, because all the processes interact and their combined effect is what matters in terms of bank stability. Such analysis is therefore restricted on what it can prove (and has limitations in addressing Objective 3 of this study). Planform geometry is an integral part of this problem. It was not considered at the individual sites in any other way than sinuosity, but the differences between the channel planform at the sites could be important evidence in explaining the variability in river bank erosion and retreat rates (C. Thorne, personal communication 2012). Channel planform changes in the context of meander development were studied by Hickin and Nanson (1975) who found that the rate of lateral channel migration reached a maximum where the ratio of meander radius to stream width approximated 3.0. Above or below this value channel migration rapidly declined, although some authors found a different ratio due to non-homogenous bank material (*i.e.* Hudson & Kesel 2000). Channel migration rates were found to be a function of stream power, concave bank height and a coefficient

of resistance to lateral migration, which depends on the texture of the outer bank materials (Hickin & Nanson 1984). This approach, similar to the stream power approach (Simons *et al.* 1965; Ferguson 1981), combines a number of key parameters, some of them analysed in this chapter, and if it was applied initially, it could have helped to explain the differences in erosion and retreat rates more fully. A maximum meander radius to channel width ratio could be established for the river and predictions of migration rates could have possibly been made.

3.5.3. THE EFFECTS OF NATURAL AND TRANSFERRED FLOWS

As introduced earlier, higher discharges generate higher velocities that impose higher shear forces on the channel boundary. The wetting of the bank also reduces the shear strength and minimises the effect of negative pore water pressure (Chapter 2.2). The concept of boundary material entrainment by river flow and critical (dimensionless) shear stress was developed by Shields *et al.* (1936). While shear strength was easily tested *in situ* using the Field Vane, the establishment of near bank shear stress would be very difficult in the field because of the nature of turbulent river flows.

Maximum flow velocities used for engineering design are usually associated with Q_{10} , discharge that is equalled or exceeded only 10% of the time (USGS 2008). For the two gauging stations close to the research field sites with pins (all except N1), Q_{10} values were used as 2.317 m³/s for Keddington and 2.725 m³/s for Westmill (Chapter 3.1).

The number of days the discharge was over the threshold Q_{10} flow were counted using the following two Excel functions:

$$\begin{aligned}
 &=IF(AND(Date_n>Date_{start}, Date_n<Date_{finish}, Q>Q_{10}), 1, 0) \\
 &=COUNTIF(Q:Q, "=1")
 \end{aligned}$$

In the first row, the two arguments of the IF function are linked by AND. It is set to mark rows from the data column holding dates that are greater than the given start date but smaller than the given finish date AND at the same time, in the discharge data column the values are over the Q_{10} threshold. If the result is true, then it assigns 1 as a value. The COUNTIF function then just simply counts the number of instances the discharge was above the threshold during the particular erosion pin reading period.

With regards to the transfer scheme, a study by Essex and Suffolk Water (ESW 2007) suggests that river discharges in excess of 0.58 m³/s at Great Bradley and Little Bradley,

and $2.31 \text{ m}^3/\text{s}$ at Westmill (Q_{Eff}) will produce velocities of at least 1m/s that are thought to be necessary for particle entrainment on the channel boundary (Chapter 3.1). Discharges in the field were measured on a number of occasions and the Q_{Eff} discharge effective for particle entrainment at Clare was estimated to be approximately 1.336 times smaller than the effective discharge at Westmill, $1.73 \text{ m}^3/\text{s}$. In Sudbury, the effective discharge is approximately 1.157 times higher than the discharge at Westmill, at $2.672 \text{ m}^3/\text{s}$. Similar steps in Excel were taken to count the number of days the individual erosion pins or the entire sites were exposed to these effective flows.

Between June 2006 and April 2010, a number of high flow events occurred (Fig. 3.5.8). At the upstream section, the Q_{10} flows occurred, depending on the site, between 31 to 63 days (or between 4-5% of all flows). The highest discharge was captured at Keddington on 10 February 2009 and it was $11.60 \text{ m}^3/\text{s}$ (5 times higher than Q_{10} for this profile). The transfer flows did reach the Q_{10} threshold in 2006, but this was before the pin reading period began at GB and LB sites. The effective discharge for entrainment (Q_{Eff}), for which velocity was approaching 1m/s , occurred, depending on the site, between 255-397 days at this section and formed between 30 and 38% of all flows. Out of this, the water transfer flows produced between 32 to 44% of the effective flows at GB2, GB3, LB1 and LB2 sites. GB1 was not affected by the water transfer. The number of days for both threshold flows and percentage of total flows are listed in Table 3.5(A) in Appendix.

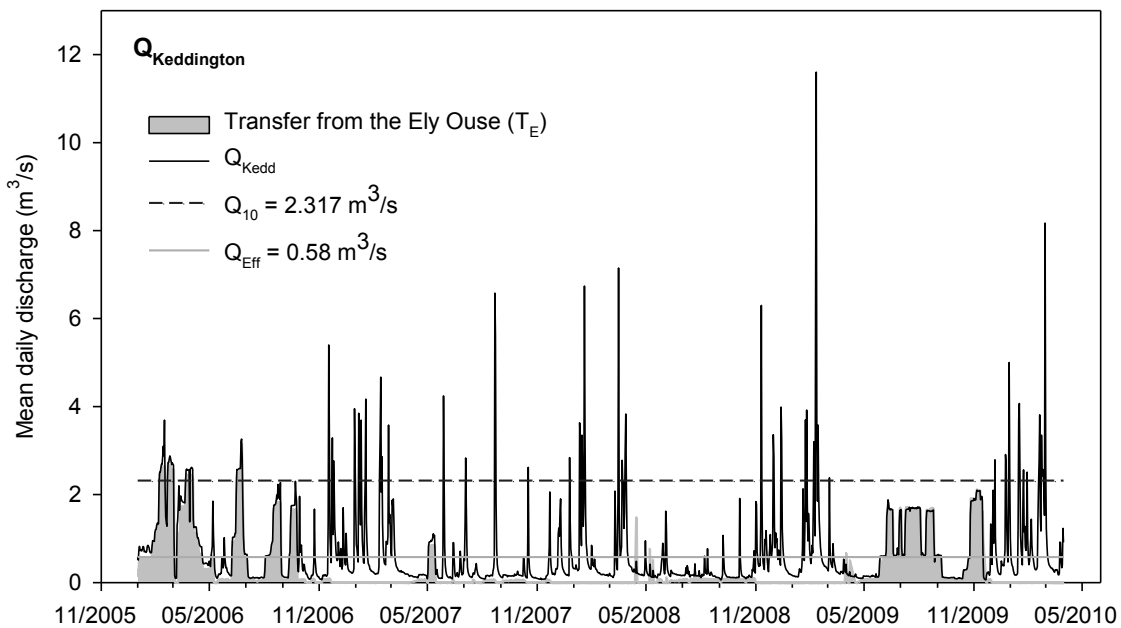


Fig. 3.5.8 Hydrograph for the study period (2006 until 2010) based on mean daily flows as gauged at Keddington station (Q_{Kedd}), overlaid with transferred discharges (in grey). The two horizontal lines are the values for the 10% flow exceedance (Q_{10}) and Q_{Eff} is the minimal effective flow necessary for generating velocities 1m/s .

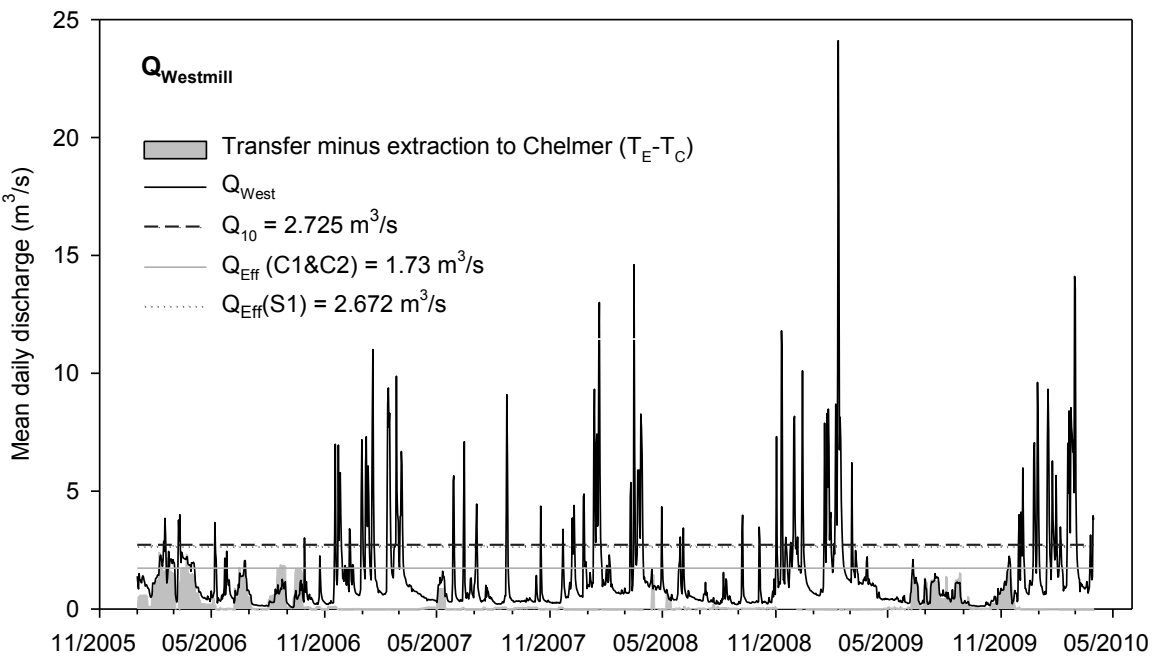


Fig. 3.5.9 Hydrograph for the study period (2006 until 2010) based on mean daily flows as gauged at Westmill station (Q_{West}), overlaid with transferred discharges from the Ely Ouse minus the amounts taken out to Chelmer (in grey). The two horizontal lines are the values for the 10% flow exceedance (Q_{10}) and Q_{Eff} is the minimal effective flow necessary for generating velocities from 1m/s.

Downstream of Wixoe (where part of the water was extracted to Chelmer), Q_{10} flows occurred between 16 (S1 site) and 213 days (C sites) in total (6.2-18% of all flows), which is a big range. Maximum discharge at Westmill gauging station was 24.10 m³/s, also on 10 February 2009 (8.8-times higher than Q_{10}). Transfer flows reached the Q_{10} threshold only during 11 days in 2006. The effective discharge (Q_{Eff}) occurred at around 200 days at C1 and C2 sites but only during 16 days at S1. In contrast to the upstream section (GB, LB and C sites), the transfer flows here represented only 5% of the effective flow occurrences.

For each pin, the number of days exposed to the Q_{10} flows was related to the erosion rate. Specific monitoring periods were considered that varied between and within the field sites (all sites apart from N1). The relationships were plotted for pins at each of the three bank zones (Fig. 3.5.10). While the erosion pins in the top bank zone (A) may not have been always submerged; the pins in the middle and lower zones (B and C) were submerged during these flows. The correlation analysis did not show any relationship in any of the zones. Although high flows are thought to play a significant role in erosion, the number of Q_{10} events did not appear to influence the erosion rates recorded on pins.

Although the trend is not identifiable, Fig. 3.5.10 shows some marked differences in the data pattern between the top, middle and lower bank pin readings versus the frequency of

Q_{10} flows. The data appears to be based on the Q_{10} flows frequency, clustered into two groups. The first group of data is concentrated between the 4-6% of Q_{10} , while the other group is concentrated between 11 and 15%. The upper bank sees the erosion data more spread in the lower frequencies of Q_{10} while the lower bank section has data with lower readings more concentrated in lower frequencies of Q_{10} flows (in an interval of approximately 10 cm of erosion) and in higher frequencies of occurrence these data are spread over a larger interval (over 30 cm). These patterns indicate that in the upper bank the direct impact of river flows (the fluvial entrainment) matters less and subaerial erosion or mass failure dominate. In the lower bank, the lower frequencies of Q_{10} flows are most likely responsible for less erosion. Higher frequencies produce a data spread over a wide interval and other factors discussed earlier would dominate.

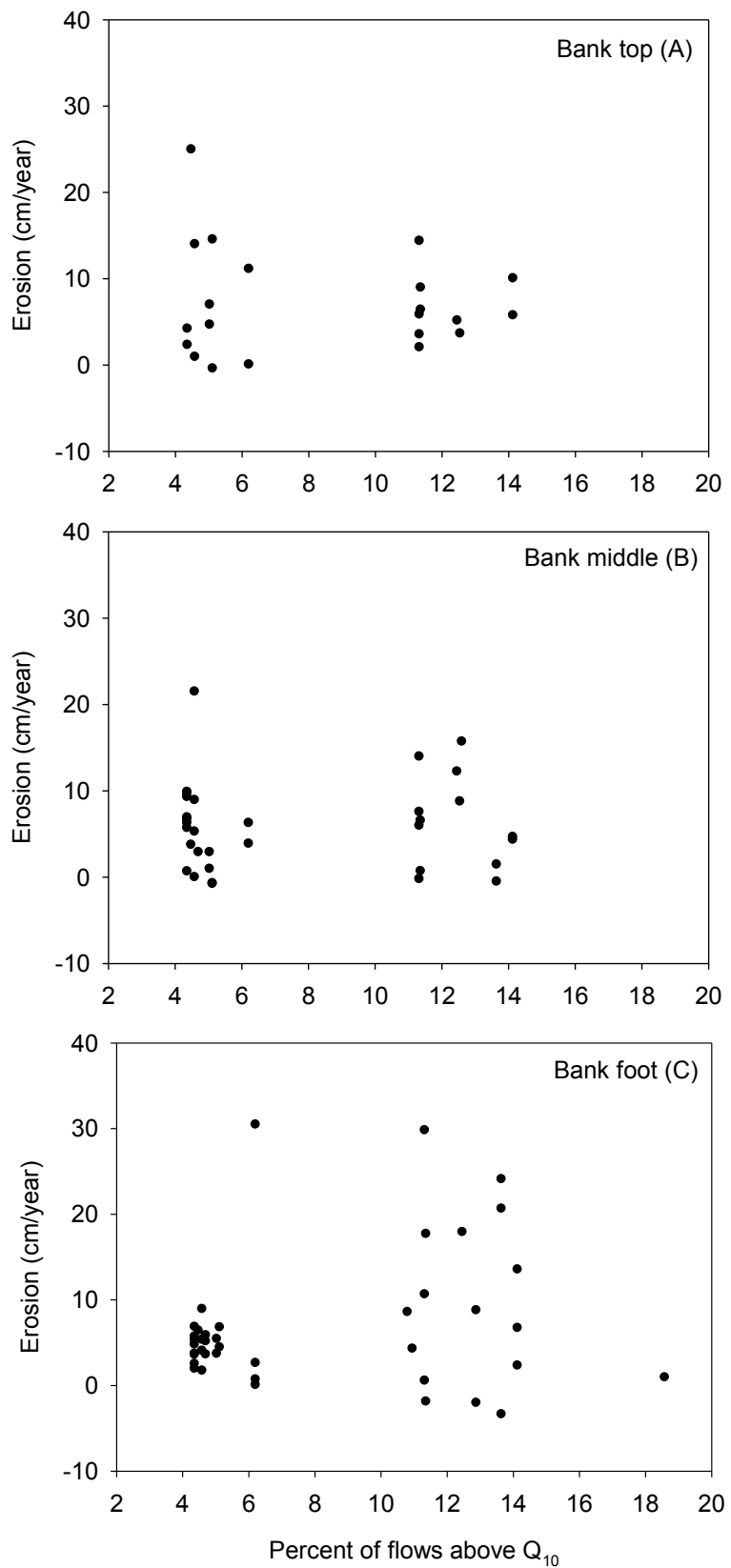


Fig. 3.5.10 Proportion of days with flows above Q_{10} to the specific pin reading period against the mean annual erosion rate (cm/year) for the pins at the bank top (A), bank middle (B) and bank foot zone (C).

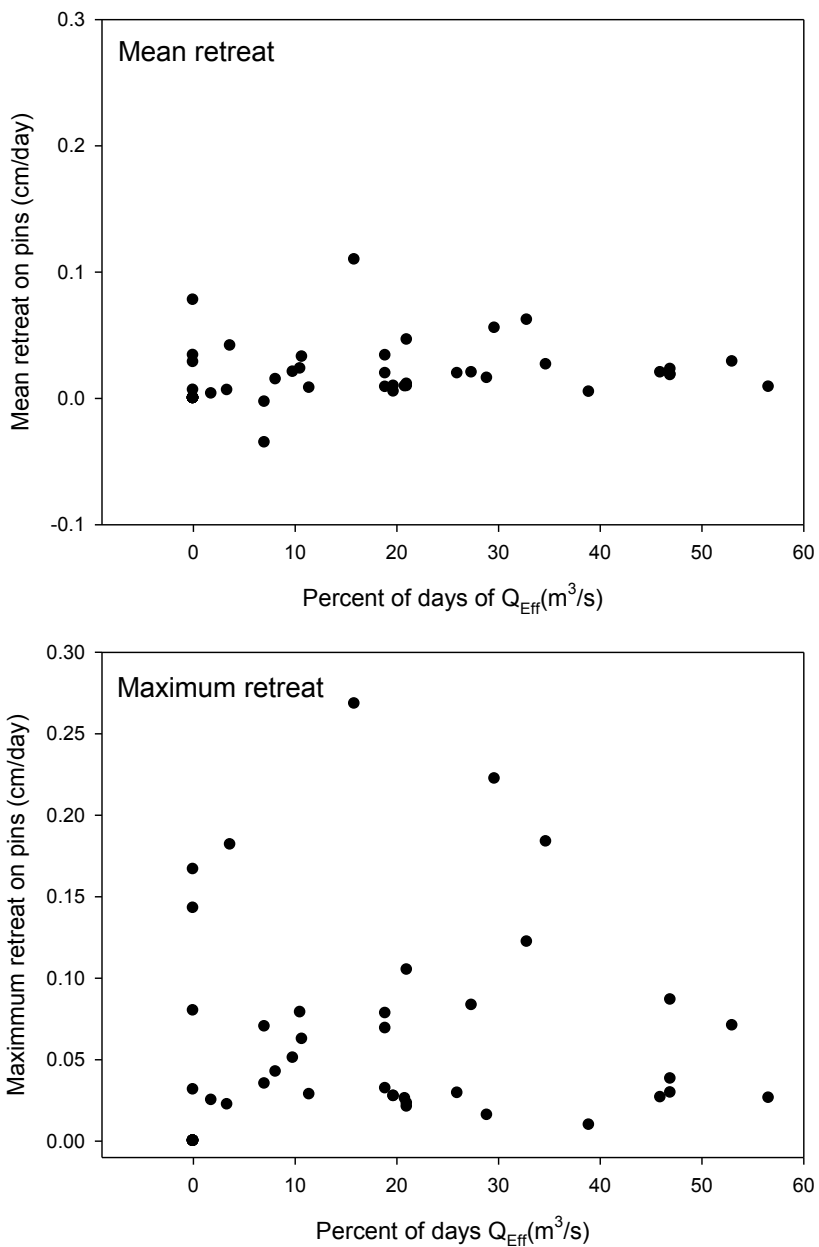


Fig. 3.5.11 Proportion of days with flows above effective discharge (Q_{Eff}) between the individual pin readings against erosion rate, expressed as the site mean and the site maximum on a single pin (cm/day).

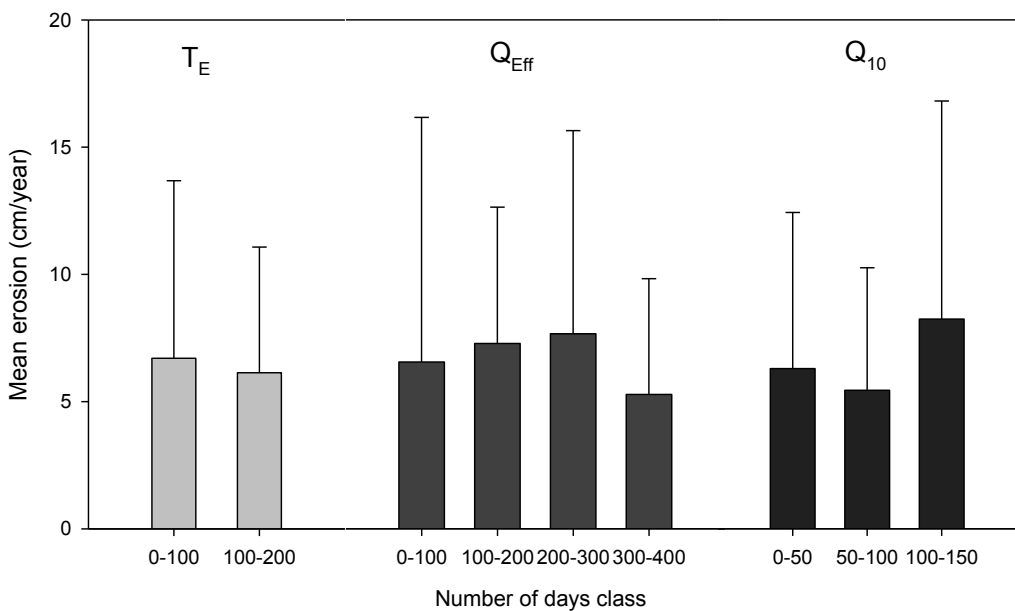


Fig. 3.5.12 Flow-specific summaries of the erosion rates: T_E is the number of days class when the water transfer was greater than 0.58 m^3 , which is the effective discharge for entrainment at GB and LB sites, Q_{Eff} is the number of days when the river flow was above the effective discharge at all sites and Q_{10} is the number of days class when the flow was above the 10% exceedance of time.

As a different approach, the number of days with effective flows during a partial period (between single pin readings) were correlated against the corresponding mean daily and maximum erosion rates. Similarly, this analysis did not show any clear relationship (Fig. 3.5.11). It has been found that high flows and prolonged wet periods (Knighton 1988), such as those caused by the water transfer, would contribute to increased erosion. The manual pin readings were not taken frequently enough to capture the bank response to a flow event, but the two Photo-Electronic Erosion Pins (PEEPS) demonstrated some response (Chapter 3.4). Figures in Section 3.4.2 (D) illustrate the responsiveness of the pins to a high flow event, although quantification of this relationship is problematic due to the bank retreat occurring with a varying time delay.

Fig 3.5.12 shows the summary of mean annual erosion rates versus the number of days when the pins were exposed to three types of flow: water transfer flows above effective discharge at the upstream GB and LB sites, all flows above the effective discharge typical at each site, and flows higher than Q_{10} discharge that is exceeded only 10% of the time. Based on the size classes presented, there is no significant difference between any of the groups ($P>0.5$). This is caused by a large overlap in standard deviations. Based on these findings, the critical river flows do not appear to correlate with erosion rates.

Because the transferred flows were not observed in isolation during intensive pin monitoring, other properties and processes have 'shaded over' the effect of the flows on bank erosion. The morphological information shown on Figs. 3.4.1 & 3.5.1 and further vertical profiles in Section 3.4.2(B) are evidence that the water transfer does produce flows that have an effect on channel morphology and this fact provides a partial answer to the Objective 4 and second part of the first research hypothesis. The water transfer produced nearly 40% of all the effective river flows in the upstream sites (GB and LB). The impact of water transfer was decreasing downstream with further tributaries and increasing catchment size. The transfer produced only around 5% of the effective flows at the downstream sites S1, N1.

3.5.4. RELATING STABILITY INDEXES TO BANK EROSION RATES

To further establish the effect that the principle factors impose on river bank erosion, bank stability analysis could be used (Chapter 2.3), if sufficient data targeting this from the beginning of the research had been collected. In addition to determining which sites have the most critical properties in combination, this analysis would define threshold properties such as the maximum bank angles or bank heights at failure. These will be important in terms of predicting future stability for further river management at the research sites or along longer river stretches. There are a number of ways to approach this, for example: (1) by establishing the new bankfull discharge and new bank height/bankfull height ratios, (2) by calculating the Factor of Safety for varying modes of failure or (3) by calculating bank stability indexes.

Establishing the new bankfull discharge is important to determine the stable bank height. A stable river is more easily achieved if bankfull dimensions are correct and bank heights are appropriate. One of the reasons bank failures were occurring at the research sites was that the banks were too high. A key issue therefore would be to establish the new bankfull discharge and bankfull depth for the various reaches of the river. Banks with heights greater than the critical height for mass instability would be more prone to failure (R. Hey, personal communication 2006).

On most active, natural rivers, the bankfull height can be established from hydraulic geometry equations. According to Wolman (1959), bankfull stage usually corresponds with the lowest value of the width to depth ratio. Furthermore, bankfull elevation can be identified from signs such as new bar and floodplain deposits. In reaches where these are absent, the bankfull stage is understood to correspond with the elevation of the lowest

prominent surface along the river which produced a regular longitudinal profile sub-parallel to the bed profile (Hey *et al.* 1997). However, channels with both banks engineered and regularly maintained may lack any of these signs. In such cases, the channel-forming or dominant discharge can be used (this is different from the effective Q_{Eff} discharge referred to in Section 3.5.3).

The dominant discharge is defined as the discharge that has the most impact on the channel form (Wolman & Miller 1960; Pickup & Warner 1976; Ashmore & Day 1988, Copeland *et al.* 2005). While the flood discharges will be highest in magnitude, the frequency of flood events may be not sufficient to have a cumulative effect on the channel form (Knighton 1988). Hence, intermediary flows of higher frequency (once or twice a year) have been established to transport most sediment, but this would depend on the river flow regime and the climatic region. The concept of dominant discharge is regarded by Soar & Thorne (2001) as a geomorphological concept and not a measurable parameter in itself, although three identifiable discharges are used to represent the dominant flow: (1) the bankfull discharge; (2) the flow that occurs over certain specified interval (i.e. flood peaks) and (3) the effective discharge. Flow duration and sediment rating curves are used to identify each of these (Soar & Thorne 2001, Copeland *et al.* 2005).

Some methodologies exist that combine a mixture of critical factors such as river flows and channel geometry into stability indexes. The most widely used is the Factor of Safety concept (Chapter 2.3). In addition, the Channel Instability Index (I_i) has been developed by Simon and Downs (1995) to 'score' the river channels in order of their instability. The index estimates that the channels with the highest score will have the most potential for rapid geomorphological change, including bank erosion (Thorne *et al.* 1996b). The index I_i uses a scoring system against a list of variables such as the stage of channel evolution (Chapter 2.1), bed material, bank erosion, bed and bank protection etc.

Furthermore, a Bank Erosion Hazard Index (BEHI) was developed by Rosgen (2001) as a method for the quantitative prediction of streambank erosion rates. This index, in combination with boundary shear stresses, is utilised in the Rosgen's (2001) erosion prediction model. Streambank characteristics used for the index include measurements of bank heights, angles, materials, presence of layers, rooting depth, rooting density and percentage of bank protection. Measured data are then converted to a normalisation index for application on a wide range of channel types (Rosgen 2001). Utilising this model and exploring the relationship between its outcomes and field erosion rates would be an important model assessment and if it would prove effective, it would allow for useful bank

stability predictions to be made. Stretches of river banks, assigned to the BEHI values, could be classified based on the erosion risk. Some of the data collected could be used for the model and carrying out this assessment would be useful in the context of the wider application of this research.

4. WILLOW SPILING IN THE UK

4.1. REVIEW OF THE METHOD

4.1.1. HISTORY AND RECENT RESEARCH

Willow spiling, sometimes also referred to as a wattle fence, willow hurdle, willow weave, willow plait, fisher's fence or willow wall, is currently the most widely used willow-based system in river engineering in the UK (D. Holland, personal communication 2008).

Live willow as building materials have been used for centuries for the protection of river and stream banks (Schiechtl & Stern 1997). There is evidence that willow bundles were used as an erosion control measure as far back as 28 BC along the Yellow River in China (Hoag & Fripp 2005). Romans also used willow fascines to build structures to control water erosion (Evette *et al.* 2009). During the Middle Ages when neither machinery nor modern building materials were used, riverbanks in Europe were stabilised successfully using plants and plant materials. In the 16th century, Leonardo da Vinci recommended planting willows along river banks to prevent erosion (Schlüter 1984). Remains of old willow spiling found near the river Seine in Paris and in the Jura Mountains in Switzerland date back to the 7th century (Evette *et al.* 2009). Willow spiling is one of the methods used for sediment control in torrential catchments in the Alps (Rey 2009) since the 18th century. In Germany and Austria, willow based soil bioengineering methods have a strong tradition in civil engineering and forestry sectors (Simon & Steinemann 2000).

As introduced in Chapter 1, the engineering properties of vegetation are usually more complex than those of hard materials (*e.g.* Thorne *et al.* 1998; Abernethy & Rutherford 2001; Pollen 2007) and these properties change over time. Many engineers believe that the type and amount of information available on soil bioengineering methods is inadequate for the promotion of their wider use (Thorne *et al.* 1998; Li & Eddleman 2002). For example, there is a good understanding of the root system development of mature vegetation and its role in slope stability (Coppin & Richards 1990; Abernethy & Rutherford 2001) but less is known about the development phase of live cuttings soon after installation and their response to different environments. The early stages of vegetation establishment are the most important in terms of surface protection and slope stability and the structure must withstand erosion until root systems develop (Jarvis & Richards 2008). The success of soft engineering projects generally depends on how well the structure is built whilst in case of hard engineering, this will depend more on the initial design rather than on the actual control of the construction (Coppin & Richards 1990).

Several studies have examined specifically the genus *Salix* and its potential and limitations for environmental projects (e.g. Eliasson & Brunes 1980; Jackson & Attwood 1996; Elowson 1999; Pezeshki *et al.* 1998; Karrenberg *et al.* 2002; Schaff *et al.* 2002; Kuzovkina & Quigley 2005). The performance of willow cuttings on stream banks has been researched in Shanghai, China by Li *et al.* (2006), and in northern and central-east Mississippi by Pezeshki *et al.* (1998, 2007) and Watson *et al.* (1997). Li *et al.* (2005) also examined the potential for willow dormancy extension in warmer regions and Conroy & Svejcar (1991) examined the impact of cattle grazing on willow survival in north-east California, sheep grazing and other limiting factors on willows were reported by Goodson (2002). Inundation tolerances of riparian willows have been studied by Amlin & Rood (2001) and the tolerances of Central European riparian species have been reviewed by Glenz *et al.* (2006). A comprehensive critical study discussing the use of willows in bank stabilisation projects has been published by Thorne *et al.* (1998)

These research publications and practical guidelines create a wide-ranging theoretical resource that is reviewed, in association with Objective 5, in this chapter. In addition, information from nearly 140 willow spiling projects in the UK is examined for causes of project failure (where this occurred), and solutions to some of the problems are highlighted.

4.1.2. PRINCIPLES OF WILLOW SPILING

Willow spiling is made of long live willow canes interwoven tightly between live willow stakes (Fig. 4.1.1). There is no exact definition of this method and individual willow projects can vary considerably in the type of material used and ways of installing it. The most preferred option is to build a structure made of local live material that will take root and grow.



Fig. 4.1.1 Installation of willow spiling at N1 site in Nayland, March 2009 and the completed willow spiling wall with the initial growth, May 2000 (see location map on Fig. 3.1.1).

Willow revetment benefits the river ecosystem by:

- (1) moderating extremes of the temperature and moisture content of air close to the soil surface, thereby creating stable conditions for growth of riparian vegetation;
- (2) improving soil–water relationships by drainage of waterlogged soils and water storage in plant tissues, and by reducing surface runoff;
- (3) increasing soil and humus formation;
- (4) providing habitat for flora and fauna, and shading riverbanks and spawning areas;
- (5) retaining pollutants in root zones; and
- (6) protecting against wind action (Schiechtl & Stern 1997).

Willow spiling may also absorb carbon dioxide from the atmosphere at a rate of approximately 17 kg/m² per year (Jarvis & Richards 2008). Willow is probably the second best supporter of biodiversity in created shrub/tree habitats, after oak (Jarvis & Richards 2008). Over 250 invertebrate species have been associated with willows (Morgan *et al.* 1999) and a number of endangered bird and mammal species benefit from willow cover. Willow spiling has been a preferred solution in water vole conservation sites (Strachan 2004) and in stretches of river with otters or brown trout.

Thus far, willow spiling has been used to control bank erosion, to increase slope stability, to colonise bare ground, to assist with river narrowing, and to trap sediment or in combination with artificial otter holts (McCulloch 2000). Its potential lies also in combination with other entirely vegetation-based, geotechnical or structural engineering methods. In situations where previous erosion control measures have failed, instead of their costly removal, willow spiling can assist with securing these failed or unstable stretches, thus limiting greater habitat disturbance.

4.1.3. PROJECT PLANNING CONSIDERATIONS

The aim of every project practitioner is a successful outcome. To further this, projects should be designed to take into account the landscape context and the project's impact on river hydromorphology, ecology and the local community. Comprehensive lists of factors to be considered have been published by Hemphill & Bramley (1989) and Schiechtl & Stern (1997). From these lists factors which are specifically important for willow spiling projects have been selected: (1) hydrological character of the stream, (2) species selection, (3) site conditions, (4) dimensions, (5) timing, (6) cost, (7) maintenance and (8) monitoring.

4.1.3(A) HYDROLOGICAL CHARACTER OF THE STREAM

Erosive forces vary between individual streams and stretches. Two approaches are usually used to express the tolerance of a revetment to erosive force: permissible (or critical) velocity and permissible shear stress (Hoag & Fripp 2005). Permissible velocity is the maximum channel velocity that will not cause erosion of a channel boundary. Shear stress results in a force that acts on a channel boundary in the direction of flow and that is proportional to the square of near-bank velocity (Chapter 2.3). A critical shear stress and consequential force is reached when the latter equals the resistive forces acting on the channel boundary (Fischenich 2001). The stream velocity and the shear stress of the river

flow must not be higher than the threshold for the individual bank stabilisation method (Sotir & Fischenich 2001), although several years after installation the threshold values for vegetation-based methods can be much higher (Gray & Sotir 1996; Schiechtl & Stern 1996). For example, the maximum permissible velocity that willow stakes (in conjunction with erosion control fabrics) can sustain is between 0.32 and 0.82 m s⁻¹ before establishment and 0.91 to 3.05 m s⁻¹ 1–3 years after establishment. In a study by Sotir and Fischenich (2007), the critical shear stress of live revetment was initially 21.5 N/m² and increased to between 100.6 N/m² and 148.3 N/m². Threshold values for some of the most common bank stabilisation methods are listed in Table 4.1.1. Published values describing willow spiling alone appear to be lacking.

Table 4.1.1 *Tolerance thresholds for flow velocity and shear stress for different stream banks stabilization methods (modified from Fischenich 2001; Sotir & Fischenich 2007).*

Method	Permissible velocity (m.s ⁻¹)	Permissible shear stress (N.m ⁻²)
Wattles	0.91	9.6-47.9
Live willow stakes	0.98-3.05	100.6-148.3
Live brush mattress	3.66	186.7-392.6
Gabion baskets	4.26-5.79	478.8
Concrete	>5.49	598.5

4.1.3(B) SPECIES SELECTION

Their vegetative propagation and natural proximity to rivers make willows attractive woody species for soil bioengineering. Willow is a pioneer that roots from a small fragment of live material and tolerates a range of environmental conditions such as contaminated ground, infertile substrata and areas of frequent disturbance (Newsholme 1992). Vigorous growth withstands severe damage and willows rejuvenate easily. The root system develops quickly within the first growing season (Jarvis & Richards 2008) producing adventitious roots from latent root primordia which are specialist cells located throughout the plant. For example, primordia develop rapidly in roots when stem pieces of *Salix fragilis* L. are removed from the parent tree and placed in water (Carlson 1950). The resulting fine fibrous root mats are very effective in reducing bank erosion (Wilkinson 1999). The total lifespan of willows is about 40 years under natural conditions, but in the absence of competition from other woody plants and if bushes are pruned on a regular basis, lifespan may exceed 100 years (Schiechtl & Stern 1997).

For the most cost effective and environmentally sensitive solution, species that grow naturally within the project area should be chosen (Schiechtl & Stern 1997). If material is not freely available, it may be obtained from UK growers (Jarvis & Richards 2008).

Three willow species are commonly used for willow spiling in the UK: crack willow (*Salix fragilis* L.), white willow (*Salix alba* L.) and common osier (*Salix viminalis* L.). Crack willow and white willow are usually used to make stakes (Brooks & Agate 1981; Agate & Brooks 2001). Common osier is preferred for weaving because of its long (up to 4 m), pliable and slender canes (RRC 2002). Grey sallow (*Salix cinerea* L.) and goat willow (*Salix caprea* L.) may also be used and both tolerate infertile and contaminated soil conditions (Newsholme 1992). Other species are less suited for weaving so the local availability of riverbank willow for spiling may be limited (RRC 2002). A combination of several willow species within a single site is desirable because this is likely to increase the richness of invertebrates and will also increase genetic diversity and limit the risk of plant disease (Jarvis & Richards 2008). A serious disease affecting *Salicaceae* is the Watermark disease caused by the bacterium *Brenneria salicis* which is spread by asymptomatic cuttings (Hauben *et al.* 1998).

4.1.3(C) SITE CONDITIONS

Willows have ranges of ecological tolerance that can limit their use at particular sites:

- (1) they are not very tolerant of shade (Schiechtl & Stern 1997; Laing 2003; Jarvis & Richards 2008);
- (2) their root systems are wide-spreading, but will penetrate to a great depth only in permeable loose soil;
- (3) willows do not tolerate dense grass cover;
- (4) they have a high moisture demand during April and May when above average rainfall and short flooding are beneficial (Schiechtl & Stern 1997);
- (5) although willows tolerate flooding and hypoxic conditions (Jackson & Attwood 1996; Kuzovkina & Quigley 2005; Glenz *et al.* 2006), the period of total submergence in floodwater should not persist for more than eight days. However, partial flooding may last for several weeks without substantial damage to the bushes (Schiechtl & Stern 1997). Schiechtl (1992) observed that within the European *Salix* spp., *S. alba* and *S. fragilis* showed the highest flooding resilience and *S. caprea* showed the least.

The tolerance of riparian willows to flooding is enhanced by special metabolic and morphological adaptations such as hypertrophied lenticels (exaggerated pores on stems for direct gas exchange), aerenchyma (tissue with large air-filled intercellular spaces where gas exchange occurs) and adventitious roots (generally negatively geotropic thicker roots with large intercellular spaces that grow on original root systems or from submerged parts of stems (Amlin & Rood 2001; Glenz *et al.* 2006)).

Willow spiling is particularly suitable for steep riverbanks that need both support and erosion protection (Morgan *et al.* 1999; RRC 2002). However, it is recommended that the maximum height of willow spiling walls should be one metre and if the banks to be protected are higher than this, the revetment should be built in several tiers (Fig. 4.1.2) or with considerably longer, robust stakes. The ends of the willow structure must be placed carefully to avoid areas where active bank erosion is occurring (Polster 2002). The natural riverbed must be stable (Allen & Leech 1997) because willow cannot prevent bed scour or erosion at the toe of the bank; this constraint applies also to structural engineering methods. Willow plantings should not be placed below the mean summer flow level (Schiechtl & Stern 1997) so additional toe protection or stabilisation where the riverbed is scouring may be necessary (Morgan *et al.* 1999). Additionally, the structure may need to be protected against animal grazing.

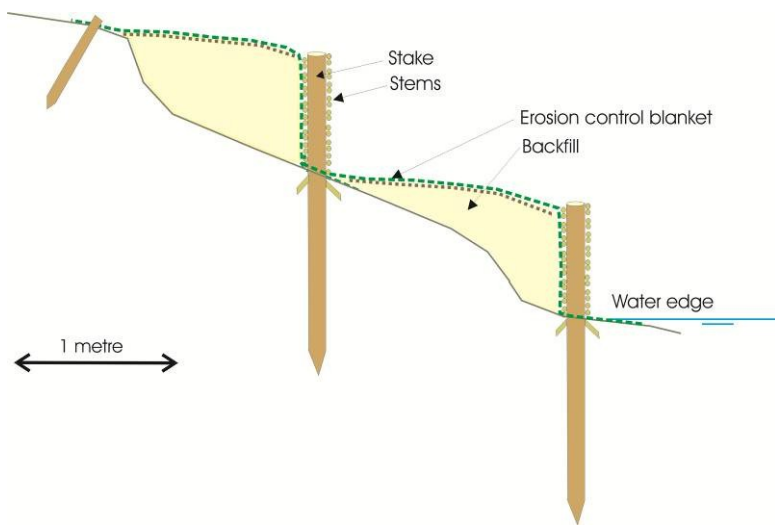


Fig. 4.1.2 Cross-sectional view of a two-staged willow spiling revetment with incorporated erosion control blanket made of coir (natural fibre extracted from the husk of coconut, (Based on Schiechtl & Stern 1996).

4.1.3(D) DIMENSIONS

Willow stakes should be at least 6 cm to 10 cm in diameter and 200 cm long and they should be hammered in the ground roughly 50 cm apart. At least two thirds of the stake's length should be embedded firmly in soil (Schiechtl & Stern 1996). Stakes should also be inserted deep enough to reach the water table during dry periods; cuttings that are planted in soil that dries out below the developing roots have poor survival rates (Crowder & Pullman 1995). Pre-augered holes help to avoid damage to the stakes. Canes should be long enough to weave along five spaced stakes, typically about 2.5 m (Brooks & Agate 1981). About 20–30 canes of 2.5 m length are needed for a square metre of spiling and 6 m or 7 m long canes can be used to produce very strong structures (Polster 2002). The start of the canes should ideally be staggered to enhance the longitudinal stability of the spiling. The diametre of canes could be important since research by Hoag & Short (1993) shows that larger diametre cuttings survive better than smaller ones.

Most practitioners recommend using only freshly cut material (Murphy & Vivash 1998; Morgan *et al.*, 1999; Laing, 2003) while some authors (Schaff *et al.* 2002; Tilley & Hoag 2008) have found that soaking willow cuttings in water for up to two weeks can stimulate root and shoot growth and may increase project success.

After weaving, the structure should be backfilled with soil to ensure successful rooting. Exposed cuttings may dry out and die (Schiechtl & Stern 1996). The soil from spoil banks can be used for backfilling although the material should not carry any rhizomes or seeds of plant species that would eventually compete with the establishing willow. Ideally, the material should be easily permeable. If the available material is very clayey, ponding may occur and an elevated water table might result in increased pore water pressures on front of the bank. To avoid this, some non-cohesive material such as sand and fine gravel can be added to minimise this effect.

4.1.3(E) TIMING

Timing is important for two reasons: to limit the disturbance to wildlife and secondly to maximise the structure's survival rate without damaging the donor willow plant. The best time to work with willows – including coppicing, weaving and planting – is between November and March (Gray & Sotir 1996; Allen & Leech 1997; Schiechtl & Stern 1997; Morgan *et al.* 1999). The use of dormant cuttings also provides more time to produce roots before energy is diverted into leaf production (Crowder & Pullman 1995). Coppin &

Richards (1990) identified the start of the growing season in the UK as being when the accumulated daily temperature reaches 5.6 °C. The willow's dormant period over winter is becoming shorter due to climate change (Menzel 2000). Frequent extreme weather conditions and high flows limit the time available for installation. A solution may be the cold storage of the material. Li *et al.* (2005) found that willows stored at 4 °C in dark and moist conditions can be successfully planted months after the growing season starts.

4.1.3(F) COST

Constructing a willow spiling is cost-effective compared with other methods of riverbank protection (McCulloch 2000). In working hours per linear metre, it is one of the cheapest methods requiring only 0.8 h to 1.5 h of work per person per metre (Schiechl & Stern 1997). The cost can be as low as £4.00 to £5.00 per metre (2009 prices) if a work force of volunteers is employed (Morgan *et al.* 1999). The relative costs of installation by a professional engineering contractor can be approximately 50% of the costs of using hard engineering techniques (Jarvis & Richards 2008). In addition to construction expenses, the cost of project planning, transport, equipment, maintenance and monitoring should be factored into restoration budgets.

4.1.3(G) MAINTENANCE

Regular pruning increases root development (Schiechl & Stern 1997) and encourages growth of pliable young shoots that bend with river flow. Pruning can also significantly increase the lifespan of the revetment (Morgan *et al.* 1999). After parent plants are harvested for the first time, subsequent growth produces more cuttings of better quality (Crowder & Pullman 1995).

Maintenance of the project depends upon project objectives, but it is always beneficial to coppice the revetment at least once every three years. Some stems can be left to mature into trees. The cut stems can be used as new material (McCulloch 2000) for repairs or extensions, making the project self-sustaining. The maintenance needs can be limited by choosing the correct species. For example, a small stream would not benefit from a vigorously growing variety of willow which would need frequent cutting back (Jarvis & Richards 2008). Any maintenance on regular basis requires labour which can be deterrent in some places as opposed to hard engineering; however it is not time intensive and serves as a regular inspection which is beneficial to every project.

4.1.3(H) MONITORING

Project monitoring is especially important immediately after project completion to ensure willow survival and development (Allen & Leech 1997). Most of the cuttings that survive the first year should also survive the next season (Pezeshki *et al.* 2007), depending on soil moisture content. An established revetment after its first two seasons provides long-term protection which is capable of self-regeneration. If the vegetation dies however, the protection lasts only for two to five years. Early roots and shoots are supported by energy reserves in the willow cuttings that allow plants to survive the initial period (Jarvis & Richards 2008). The first shoots do not therefore confirm success.

Failure of some plantings is expected in all bioengineering applications. A survival rate of 75% to 80% after 1–2 years is considered good and a rate of 40% to 70% is regarded as satisfactory (Gray & Sotir 1996). There should be five stems on average and a minimum of two shoots per linear metre of spiling to ensure project success (Schiechl & Stern 1997). In cases of failure, replanting should be undertaken as soon as possible (Simon & Steinemann 2000).

4.2. PROJECT EXPERIENCE

Information about willow spiling projects in the UK was collected by contacting public and private sector organisations, conservation charities and volunteer groups. The author helped to build a willow revetment in Bedford and monitored other ongoing projects. Three projects in Bedfordshire have been visited to record the growth rates of willows. The outcome of the analysis of this collated information is summarised below.

4.2.1. INVENTORY OF WILLOW SPILING PROJECTS IN THE UK

The inventory includes 139 projects that represent only a proportion of all projects carried out in Britain over the last 20 years. Project documentation older than 20 years has generally proved untraceable, except streambank stabilisation schemes in the UK carried out between 1978 and 1985 that have been documented by CIRIA, the Construction Industry Research and Information Association (Hemphill & Bramley 1989).

At least 47 km of riverbank in the UK has been protected by willow spiling during the last 20 years, mostly on lowland clay or chalk streams (86% of projects). The largest single project (6500 metres) was carried out on the River Ancholme in Lincolnshire. Willow spiling has been used in a wide range of environments from heavily engineered rivers in London, tidal rivers in north Norfolk to gravel-bed rivers in Scotland and Wales. The use of spiling in uplands and in coastal areas has not been extensive. Most projects have been carried out in England with a large concentration in the Thames basin. Fig. 4.1.3 shows the distribution of the willow spiling projects in Great Britain included in my inventory.

Most of the 139 projects reviewed aimed to increase channel stability where bank erosion was in conflict with land use. Most common was protection and repair of public footpaths, private gardens, arable or grazing land and roads. Willow spiling was also used to protect bridge abutments, gas pipe lines, residential areas, parks, footbridges, cricket grounds and a golf course. Other aims alongside erosion control were to improve marginal and instream habitat for wildlife, to improve visual appearance, to narrow over-wide channels and limit siltation, to achieve better water quality, and to improve safe access to the riverbank. Previous bank protection methods such as sheet piling, concrete blocks, brickwork, sand bags and toe boarding were removed in six cases and replaced by willow spiling. Willow spiling has also been used in two projects to control invasive plant species such as Japanese Knotweed (*Fallopia japonica* (Houtt.) Ronse Decraene) and Floating Pennywort (*Hydrocotyle ranunculoides* L. fil.).

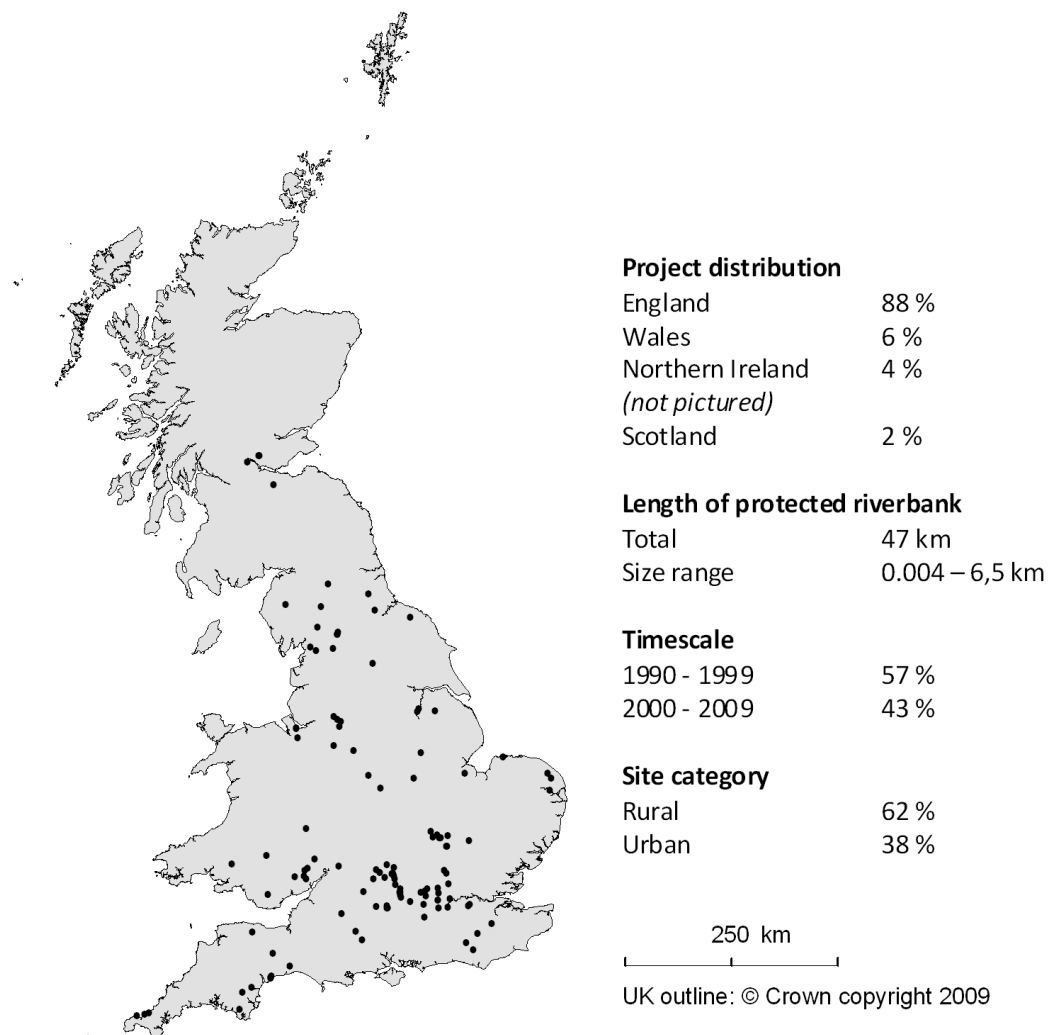


Fig. 4.1.3 Distribution of inventoried willow spiling projects in Great Britain carried out since 1989.

Where several species of willow were used, the most successful species was *S. fragilis* and the least successful *S. caprea*. Locally harvested material was most commonly used, although some project contractors used their own grown willow material.

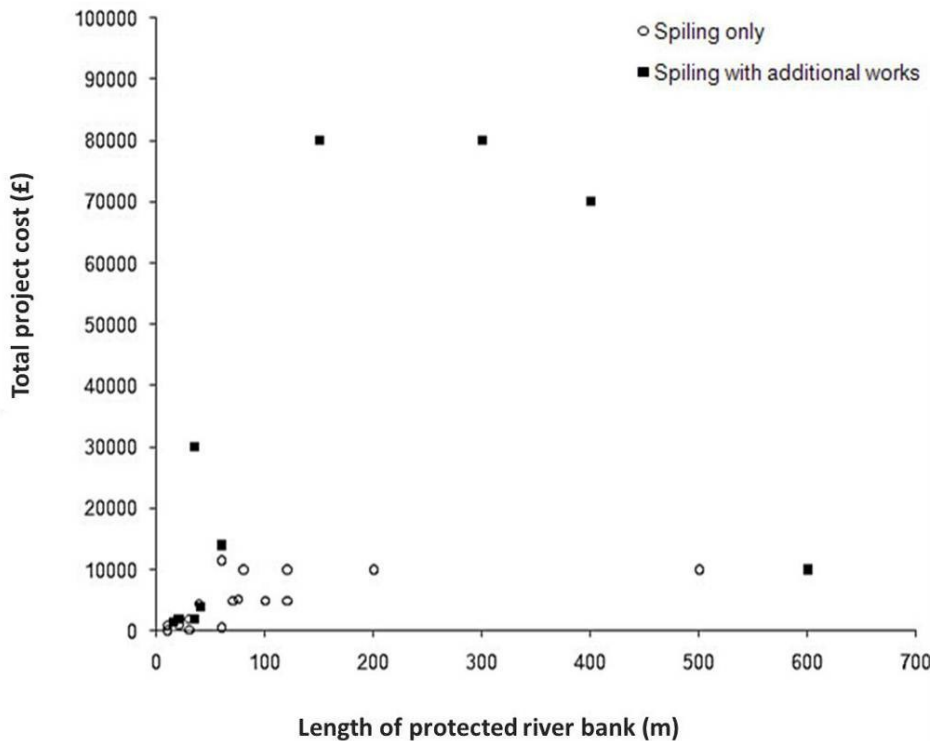


Fig. 4.1.4 Project cost in relation to project length, based on 26 projects.

Costs varied considerably between individual projects (from as little as £7 to £857 per linear metre of spiling). Examples of project expenses in relation to length of protected riverbank are shown in Fig. 4.1.4. Project costs were reduced when material was sourced locally, site access was easy and if an estate workforce or conservation volunteers were involved. For example, on a 60 m long project on the River Thames installed by volunteers, the cost was £10 per metre of river bank (Laing 2003). Occasionally, further tree planting and fencing was carried out, as in a 600 m long project on the River Cennen in Wales (£17 per metre). Where previous bank protection had collapsed and needed to be removed prior to spiling, the project cost was greater – £50 per metre when concrete had to be removed and £88 when sheet piling was removed. For project sites with riverbanks that required re-profiling and where additional materials such as timber, rock or reed rolls were used to ensure success, the costs were much higher. For example, a project incorporating rock toe and toe board on the River Skerne in Darlington cost £115 per metre and one involving stone toe on the River Medway in Kent cost £533 per metre. Higher banks that required more tiers and additional toe protection were also more expensive, for example a project with four tiers on River Trothi in Wales (£857 per metre).

4.2.2. UK PROJECT PERFORMANCE AND CASE STUDIES

Although the willow spiling projects on the inventory were installed successfully, evidence is largely lacking about whether they have been effective in fulfilling their long-term purpose. Only 37 of the documented projects included post-project information: 22 of these projects were successful, 11 involved partial failures (e.g. damage to the structure or erosion of backfill that could be repaired) and in four cases the willow spiling had failed completely and no longer fulfilled its long-term objectives. Examples of successful, partly failed and failed projects are described below.



Fig. 4.1.5 Disintegrating spiling structure two years after installation on the River Great Ouse, Bedford, East Anglia.

A demonstration project involving four soil bioengineering designs was carried out during 1995–96 on the River Skerne in Darlington (County Durham) by the River Restoration Centre (and other UK partner organisations). Two willow spiling structures with a total length of 75 m were monitored during two growing seasons after installation. One revetment established in November grew vigorously but the growth was limited to vertical poles only. Initial sprouting on half of the revetment had died. The second revetment installed the following May was much more successful and established quickly. The net vertical growth of new canes reported over the period July 1996 to October 1997 was 1.5 m to 3.0 m with upright poles growing the most. The willow material (*Salix viminalis* L.) used in November had been stored for six weeks while the material used in May was freshly harvested (Murphy & Vivash 1998).

On the River Great Ouse in Bedford (Bedfordshire), a one-tiered revetment was installed in 2007. Poor growth was recorded and loose weave with erosion signs indicated a potential failure (Fig. 4.1.5). Growth along this 91 m revetment came from the bottom

canes but was patchy and occurred only along 10.5 m. The net vertical growth was 1.0 m to 2.5 m from March 2007 to October 2008.

Another one-tiered, 2-m tall revetment was installed on a turbulent stretch of the River Ives in Bedfordshire, 100 m downstream of a mill weir. It was put in place in the mid 1990s and so far has been very successful. Along this 15 m spiling, ten willows have grown into mature trees of 20 cm diameter and over 10 m high. Many thicker stems and shoots have appeared along the whole length of the revetment (Fig. 4.1.6.).



Fig. 4.1.6 Successful willow spiling approximately 15 years old on the River Ives in Bedfordshire.

In a project installed on a lake by the Great Ouse in 2008, growth has occurred along an 11 m structure, although shade from a nearby willow tree inhibited growth along the first 3 m of the structure. The rest of the revetment had dense shoots with net vertical growth of 1.5 m to 2.0 m (from March to October 2008). Fig. 4.1.7 shows sprouting on one of the stakes.

Two projects on the River Dove in Derbyshire were monitored for erosion rates by Goodson (2002) and she reported a range of pressures to which the spiling was subjected, ranging from drought and grazing pressures during the summer months to extreme floods in 2000 which damaged the lower tiers at both sites and eroded backfill. Three projects on the River Thames documented by Laing (2003) have also shown signs of partial failure that have required repair due to incorrect installation or undercutting. In one case, failure was serious.

The most common signs of failure were limited growth, drying and decomposing of willow material; eroded backfilled material; and gaps in the revetment or its collapse.



Fig. 4.1.7 Shoots growing on a willow stake installed one year ago, Bedford, East Anglia.

When parts of a single revetment were compared, the spiling exposed to higher shear stress showed signs of failure while spiling exposed to lower flow velocities functioned effectively. Where two tiers of spiling were built, the lower tier grew better than the top. Exposed points of revetments or the part joining two revetments failed more quickly than the rest of the revetment. Shaded areas of willow spiling grew poorly, but after some pruning, growth re-appeared. The causes of poor performance and failure are summarized in Table 4.1.2.

Table 4.1.2 Frequency of various causes of failure in willow spiling projects in the UK carried out between 1989 and 2009, based on documentation from four failed and 11 partially failed projects.

Cause of failure	Occurrence	Cause of failure	Occurrence
Erosion at the bank toe	5	Incorrect installation	2
Poor quality material	4	Animals grazing	1
Shade	4	Leaf invertebrates	1
Damage by floods	4	Dense substrate	1
Erosion of backfill	3	Lifting due to growth	1
Drought during establishment	2	Invasive species colonisation	1

Post project surveys reported noticeable improvement in stream structure and habitats a few months after project establishment. Numbers of fish and other wildlife increased, for example sea trout on the River Cennen in Wales, brown trout, kingfishers and sand martins on the River Bollin in Cheshire, and signs of otters on the River Lugg in Wales. However, willow spiling has also been observed to have a limiting impact on water voles on the River Ancholme in Lincolnshire. Growing willow shoots from spiling can shade marginal areas, suppressing emergent plants and grasses on the water's edge used by water voles as food and shelter, although during winter when other food is scarce, willow becomes useful. Willow spiling should not be installed on a bank used as burrowing habitat by water voles: the restricted access to voles might be improved by installing pipes or gaps through the spiling, but the water vole population could still be further compromised by the shading effect of the growing spiling. Coir rolls have been observed to be a more suitable alternative for erosion control in water vole populated areas (P. Smith, personal communication 2008).

4.2.3. WILLOW SPILING OUTSIDE UK

A considerable amount of experience in practising willow spiling is found outside the UK. The method is integrated with modern river engineering and management and is practised by statutory bodies and private owners as well as community organisations. In The Netherlands, for example, techniques similar to willow spiling are used to protect river banks of large rivers, to form small dams and also to create islands. The dams provide a zone of shallow still water along banks, attractive for aquatic plants and macro-invertebrates (U. Menke, personal communication 2008). Streambank erosion problems and sediment pollution is tackled in California by using willow spiling as deflectors that direct flow away from eroding banks, narrow the channel and allow fine sediment to accumulate. Instead of soil backfill, additional live willow is sometimes packed behind the spiling and weighted down by rock, a practice not so common in the UK. Instead of weaving with willows, a flexible board can be installed behind live stakes. Willow spiling is not used extensively in the USA or Canada, however, as it is regarded as more labour intensive than other soil bioengineering methods (R. Sotir, personal communication 2008). In more arid parts of the world, live willow spiling may not be the most suitable option because irrigation would be required for successful establishment and growth. Other species with similar geotechnical qualities to willows that naturally occur along the river bank could potentially be used.

4.2.4. PROPOSALS TO IMPROVE SUCCESS RATES BASED ON THE REVIEW

Although some confounding factors cannot be managed, their impact can be limited by referring to the project planning considerations discussed earlier. Projects should not end after installation because regular visits during the establishment period and prompt repair of minor damage are important for limiting the vulnerability of the structure (Goodson 2002).

In situations where revetments could be subject to high flow erosive forces and bank toe undercutting (e.g. on steep sections of the channel), a stronger design using an extra row of deeply driven stakes or a combination with another soil bioengineering method could be more successful. Thin jute or coir geotextile is frequently applied behind spiling and on top of backfill to prevent wash out of fine material. Live fascines, reed rolls, large logs, boards, stone or rock have been used also to further stabilise the bank toe. Willow spiling incorporating rock toe and toe boards has been carried out on the River Skerne (RRC, 2002). On a project in California, deflectors upstream from the structure helped to direct the highest velocities away from the structure. Hybrid solutions that combine soil bioengineering and conventional technologies have proved feasible and effective in some situations (Allen & Leech 1997; Watson *et al.* 1997; Li & Eddleman 2002). An example of a successful large-scale streambank stabilisation and restoration project that integrates soil bioengineering (live staking, live fascines, brush layers) with the biotechnical methods (vegetated geo-grids and geo-gabions) has been carried out at Airport Town in Shanghai (see Li *et al.* 2006).

Willow survival is the key factor in ensuring a long lifespan for a spiling project. Using dead hazel or willow hurdles often results in failure within two to three years (as in the example shown in Fig. 4.1.5). This type of material is best used for temporary protection before repairs with live material can be carried out. Similarly, willow material stored out of water results in poor growth emphasising the importance of using only healthy, freshly cut or properly stored material. Poor growth of upper tiers of spiling is a result of water deficiency, suggesting that replacing willows with species that naturally occur at higher elevations on the riverbank could be an effective solution.

Occasionally, pests (moths, willow beetles and weevils) caused damage to foliage. Willows normally respond to defoliation by regrowth and repeated attacks rarely cause permanent damage (Newsholme 1992). Chemical control is best avoided because of possible impacts on the aquatic environment.

5. TWO APPLICATIONS OF WILLOW SPILING ON THE RIVER STOUR, EAST ANGLIA

5.1. INTRODUCTION AND JUSTIFICATION

Two research field sites, S1 (in Sudbury) and N1 (in Nayland), were selected out of the nine monitored field sites on the River Stour for implementing the soil bioengineering approach of willow spiling (Fig. 5.1.1). The magnitude of erosion was significant at both sites and willow spiling was chosen to demonstrate its geotechnical function and its other advantages over hard engineering approaches. Both sites are located in the Areas of Outstanding Natural Beauty (AONB), the river banks are grazed by livestock and used as public footpaths, and the river stretches are used for recreation by fishermen and canoeists. The proposed willow spiling presented an aesthetically and ecologically sustainable option to address local erosion. Whether it was also an effective approach at these two sites is addressed in the following section, presenting the results related to Objectives 6 and 7 of this study (Chapter 1.2).

The riverbank at the Nayland site (N1) consists of non-cohesive sands and gravels that are easily entrained by flow, while the bank at the Sudbury site (S1) is composed of cohesive clays and silts where the interparticle forces make the banks more resistant to erosion (see Section 3.2.4). The river bank at both field sites was subjected to significant erosion between 2006 and 2010; the bank at the cohesive site had previously eroded at the rate of up to 0.3 m per year and at the non-cohesive gravel site at the rate of up to 1.3 m per year (see Chapters 3.3 and 3.4). From historical and field analysis it appeared that this instability was triggered by human intervention (installation of a weir upstream of the S1 site and gabion deflectors upstream of the N1 site).

Both sites are positioned on the outside of meander bends (concave banks). The water surface slope at the S1 site, located 125 m downstream from a weir, was 0.0060 (calculated as drop in elevation in m/horizontal distance in m), is comparable to some UK upland rivers (see Ferguson 1981), although the average water surface slope for this reach over several kilometres is considerably lower, 0.0009. The N1 site, located 250 m downstream of a major confluence, has a water surface slope 0.0023, while the average water surface slope for the reach was much lower, only 0.0005 (see Table 3.2.2 in Section 3.2.2).

The gross stream power, which is a channel characteristic dependent on the water surface slope and the bankfull discharge (Simons *et al.* 1965), was 2.01 kW/m for the cohesive S1 site (where bankfull discharge was 34.10 m³/s) and 0.88 kW/m at the non-cohesive N1 site (with bankfull discharge 38.77 m³/s). The specific stream power expressed as the ratio of gross stream power to the channel width was found for the clay site to be 0.08 kW/m² and for the gravel site 0.04 kW/m², values comparable with some upland streams in the UK (see Ferguson 1981).

The site sinuosity was 1.15 at the S1 site and 1.71 at the N1 site. At both sites, the bank angles (35 degrees at the cohesive site and 27 at the gravel site) and heights (1.8 m at both sites) were similar. Width/depth ratio at the cohesive site was 13.68 and at the gravel site 9.57 (see data in Table 3.2.3, Section 3.2.2).



Fig. 5.1.1 Aerial maps of the project sites on The River Stour (yellow circles). Blue arrows indicate the direction of river flow (© 2012 Nokia, Getmapping Plc., Microsoft Corporation).

5.2. DESIGN AND IMPLEMENTATION

The two willow spiling projects differed in the length of spiling and the amount of material installed but they were similar in the species of willow used and in their basic design. Both structures were made using local and recycled resources and designed to fit within the natural environment. The main parametres of the two projects are summarized in Table 5.2.1.

Table 5.2.1 Technical comparisons between willow spiling projects: cohesive (S1) and non-cohesive (N1) site.

	S1 (Sudbury, cohesive site)	N1 (Nayland, non-cohesive site)
Length of revetment	6 m (upper tier), 7 m (lower tier)	45.5 (upper), 13.5 m (lower tier)
Number of tiers	2	2
Number of stakes	22	141
Salix species	<i>Salix alba</i> L.	<i>Salix alba</i> L.
Average stake diametre	6.3 cm (\pm 0.92 cm)	6.5 cm (\pm 2.3 cm)
Way of planting stakes	upside down	upside down
Age of most withies	3-4 years	3-4 years
Soaking of material	1 week before installation	freshly coppiced material
Date of installation	10 March 2009	12 March, 14 March, 18 March (upper tier), 25 March, 31 March 2009 (lower tier)
Person-hours*	33 person-hours (2.75 per linear m)	108 person-hours (1.66 per linear m)
Timing of backfill	1 week after installation	1 week after installation (for top tier); one day after installation (bottom tier)
Amount of soil used for backfill	0.5 tonnes	3 tonnes
Additional materials	None	Recovered jute geo-textile, grass seed (lower tier)

*as total person-hours for the project and person-hours per linear m of spiling

Two-tiered spiling was installed at each site: (1) a lower tier (LT) was placed at the mean summer water level as recommended by Schiechl and Stern (1997) and (2) an upper tier (UT) was installed one metre above the LT to account for the maximum retaining height of a willow revetment (Polster 2002), see Chapter 4.

Willow stakes, about 2.0-2.5 m long, were vertically inserted into the riverbank roughly 0.5 m apart and then tightly interwoven horizontally with long pliable willow withies. A key design criterion was to have at least two thirds of the stake's length embedded in the ground. After weaving, the structures were backfilled with soil. The spiling revetments were installed in March, which is the optimum planting time for the river bank in the East Anglian region. It is after the winter high flow season and before the vegetation growth season starts.

At S1 (cohesive site), willows were coppiced one week before installation and stored in a lake 200 m from the site. The upper and lower tiers were installed in one day on 10 March 2009 by seven volunteers in 3 hours (that is 1.31 hours effort per linear m). Accounting for the time needed for material coppicing and backfilling, the total time needed was 2.75 hours per linear metre. At N1 (non-cohesive site), coppicing and installation ran simultaneously over several days during March 2009.

The landowner's team of six people plus four volunteers were involved in the coppicing, installation and backfilling of the revetment. The installation of all stakes in the top tier was completed on 18 March and installation of the lower tier on 31 March. The backfill originated from local land within one mile of the sites. Due to wet conditions, backfilling was delayed on both sites by one week. Other than bringing backfill, no machinery was used and all work including coppicing was done using hand tools.

The coppiced willow material came from within a few hundred metres of the site and was a product of regular pollarding and coppicing. If not used for spiling, the material would have been redundant. Withies for weaving were 3-4 years old and although most were over 3 m long, they were less pliable than the younger withies normally used in this approach. They provided additional strength but extra care was exercised to prevent them from breaking. Both sites before, during and after the project work are on Fig. 5.2.1 (S1 site) and Fig. 5.2.2 (N1 site).

After installation, both projects were studied for their biological and geomorphological function during the first year. The weather conditions in the first weeks after installation were extremely dry and the following winter saw a number of high flow events. While the mean long-term summer rainfall (April to September) is 282 mm for the area and in winter (October to March) is 292 mm, during the study period from April 2009 to March 2010, the summer rainfall was 221 mm and winter 329 mm. (The effects of weather and other external factors on the success of the willow spiling are discussed in Chapter 5.5). The protruding willow stems demonstrated how effective they are at reducing the river

flow in this research, and this was tested by an experiment before and after coppicing (Section 5.5.1(A)).



Fig. 5.2.1 Photographs from the project diary at the cohesive site in Sudbury S1: (A) site before stabilisation works, looking downstream; (B) Sudbury Common Lands volunteers weaving the lower tier; (C) finishing the weaving on both tiers; (D) completed spiling before backfill – all March 2009; (E) finished backfilled spiling with first shoots appearing – May 2009; (F) summer growth on the spiling, viewed from the right bank – August 2009.



A



B



C



D



E



F

Fig. 5.2.2 Photographs from the project diary at the non-cohesive site N1 at Nayland: (A) project site before the works, downstream view - December 2008; (B) and (C) volunteers and landowner's staff weaving in the eroding gravel bank - March 2009; completed works: (D) view downstream and (E) upstream - April 2009; (F) spiling with first growth - May 2009.

5.3. BIOLOGICAL PERFORMANCE

5.3.1. INTRODUCTION TO POST-CONSTRUCTION EVALUATION

A drawback of soil bioengineering as an effective approach for streambank stabilisation is the lack of available quantitative post-construction evaluation (Chapter 1). Although some studies have monitored biotechnical projects after one growing season (Akridge *et al.* 1999; Shields *et al.* 1995; Simon & Steinemann 2000) for the most part, quantitative post-construction evaluation has not been widely undertaken. Despite the wide application of willow spiling, with the exception of some unpublished reports and personal observations (Goodson, 2002; Laing 2003; Murphy & Vivash 1998), quantitative information about the biological and geomorphological performance of willow spiling has not yet been published.

The success of willow spiling is dependent on many factors and the ones regarded as the most important have been discussed in Chapter 4. The successful survival and growth of willow stakes and stems is essential for the revetment's successful performance. In this chapter, the biological performance of the two willow spiling projects at the cohesive (S1) and non-cohesive (N1) sites for both the upper (UT) and lower tiers (LT) are presented (which partly fulfils Objective 6 of this study).

5.3.2. METHODS OF SAMPLING AND DATA ANALYSIS

Biological performance was measured in three different ways: (1) stake survival rate; (2) shoot extension size and (3) increase in the number of shoots. The sampling was undertaken six times at monthly intervals between May and October 2009.

For measuring trends in stake survival, the whole population of stakes was sampled by checking for the presence of living buds and shoots. A stake with at least one living bud or shoot was considered alive.

Shoot extension was sampled on randomly chosen stakes ($n=12$ at the cohesive site and $n=31$ at the non-cohesive site). All visible shoots on sampled stakes were measured for their length with an accuracy ± 0.1 cm for shoots up to 1 cm long and with ± 0.5 cm for shoots longer than 1 cm.

Initially, the whole population of stakes was sampled and both the population mean μ and sample mean \bar{x} were calculated. The error of sampling E_s was obtained as:

$$E_s = \mu - \bar{x}$$

The standard population and sample errors $\sigma_{\bar{x}}$ were calculated using approximation from the sample standard deviation S where:

$$\sigma_{\bar{x}} = \frac{\sigma}{\sqrt{N}} \approx \frac{S}{\sqrt{N}}$$

Values obtained for both calculations in all cohorts are shown in Table 5.3.1. Population and sample values are presented for each of the four cohorts. The highest difference between sample and population mean and therefore also the error of sampling was at the N1-UT cohort. The error of sampling fell just below 1.00 cm and this interval was then used as the sampling error for the other cohorts.

Table 5.3.1 Values for mean shoot length: Size of population (N) and sample (n), population mean (μ) and sample mean (\bar{x}), standard deviation (σ) of population and sample (S), standard error ($\sigma_{\bar{x}}$) and error of sampling (E_s). All values are in cm.

Cohort	Type	N/n	μ/\bar{x}	σ/S	$\sigma_{\bar{x}}$	E_s
S1-UT	Population	11	1.50	1.18	0.35	-0.346
S1-UT	Sample	6	1.84	1.46	0.59	
S1-LT	Population	11	4.18	2.90	0.88	0.579
S1-LT	Sample	6	4.32	3.40	1.39	
N1-UT	Population	111	5.30	2.58	0.56	0.220
N1-UT	Sample	22	5.08	3.31	0.99	
N1-LT	Population	30	3.48	1.27	0.34	0.921
N1-LT	Sample	9	3.76	1.63	0.73	

The sample size was derived from comparing the population (or true) mean with the cumulative sample mean (Fig. 5.3.1). The minimal sample size was determined as the point where the cumulative mean started to approximate to the true mean and the values fell within an accuracy interval of the true mean of ± 1.00 cm, based on the maximum error of sampling (Table 5.3.1). The sampling for the increase in the number of shoots measurement was obtained from the same sample stakes as the shoot extension measurement.

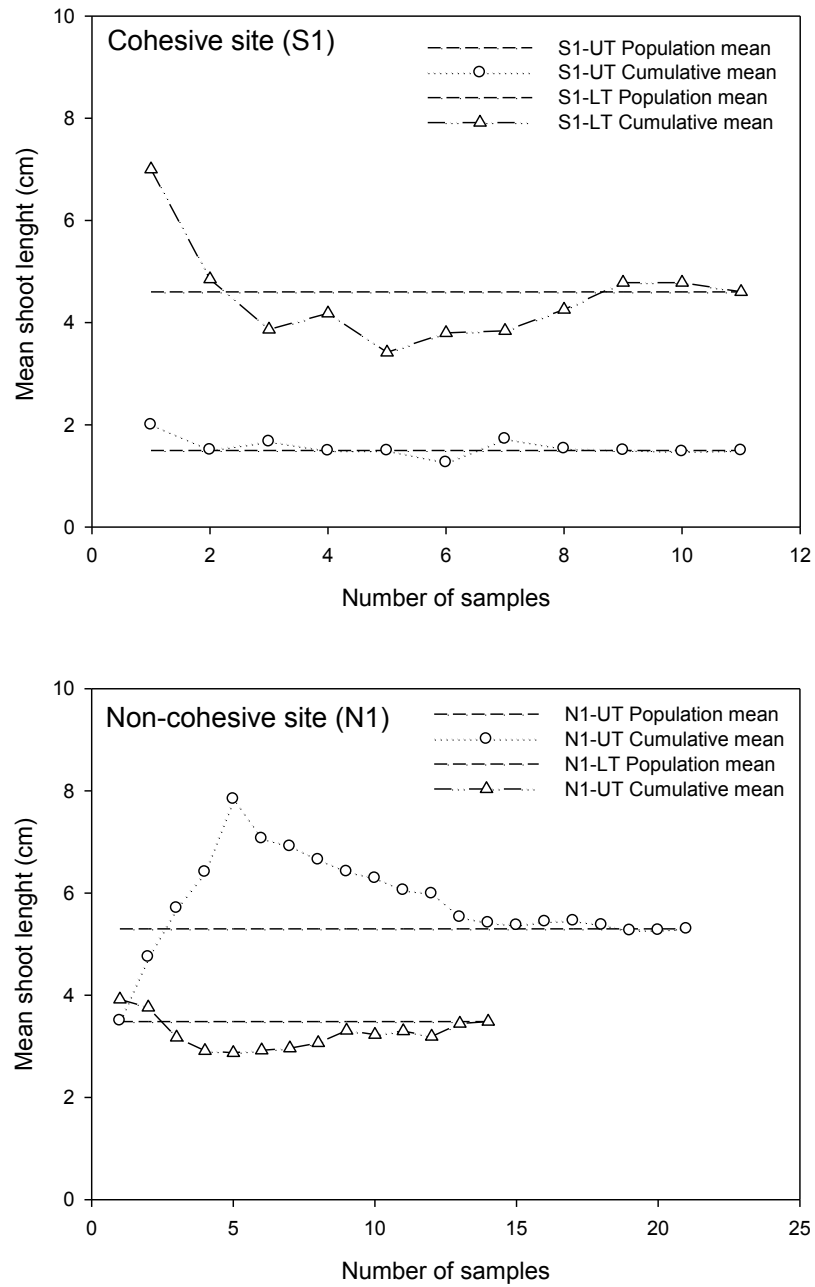


Fig. 5.3.1 Number of samples versus the cumulative mean (cm) at the cohesive (S1) and non-cohesive site (N1) for both upper (UT) and lower tiers (LT). The true means are shown by the dashed lines parallel to x axis.

5.3.3. RESULTS

5.3.3(A) STAKE SURVIVAL

Four to eight weeks after installation, most stakes had sprouted. Four weeks later, all stakes were considered alive. June, July and August 2009 (and in the case of the cohesive site S1, also September and October 2009) were very successful growth months. The first noticeable decline in stake survival occurred at the non-cohesive N1 site in September. Here, the end of season field visit revealed a significant decline in stake survival. Only about 17% of stakes were detected as alive (Table 5.3.2). Most of the dead stakes were located in the upper tier (UT): only 11 were identified as alive out of 111. In the lower tier (LT), the number of living stakes was 13 out of 30. In contrast at the cohesive site, only two stakes in the lower tier had no shoots.

Table 5.3.2 *Percentage of stakes with at least one living shoot between May and October 2009. At S1, n=22 and at N1, n=141.*

	May	June	July	August	September	October
Cohesive site (S1)	96.5	100.0	100.0	100.0	100.0	90.91
Non-cohesive site (N1)	97.8	100.0	100.0	98.58	82.27	17.02

In addition to the number of living stakes, roots were also observed. Although the primary roots of a willow stake are generally invisible, some secondary roots were found growing from four lower stakes at the cohesive site S1-LT (Fig. 5.3.2).



Fig. 5.3.2 *Adventitious roots growing from submerged parts of stems in the lower tier at the cohesive site S1.*

5.3.3(B) SHOOT EXTENSION

The first shoots appeared four weeks after installation, in mid-April 2009 (and at the beginning of May in the case of N1-LT). Table 5.3.3 shows a summary of shoot lengths at time of field visit as mean and median values.

Table 5.3.3 Mean (μ) and median (\tilde{x}) shoot lengths at individual sampling dates (with standard deviation and minimum/maximum values respectively) based on mean values on sampled stakes at cohesive (S1) and non-cohesive site (N1) in the upper (UT) and lower tiers (LT) between May and October 2009. All values are in cm.

		May	June	July	August	September	October
S1-UT	μ	1.8	7.9	22.0	35.2	41.7	49.8
		± 1.5	± 3.9	± 8.2	± 19.2	± 24.6	± 31.8
S1-LT	μ	1.6	7.2	21.8	34.5	39.2	44.5
		(0.1 - 4.5)	(3.2 - 15)	(13 - 35.3)	(11.6 - 64)	(10.6 - 82)	(14.5 - 107.3)
N1-UT	μ	4.3	9.6	30.8	26.5	23.5	36.1
		± 3.4	± 2.1	± 7.6	± 15.7	± 23.9	± 29.9
N1-LT	μ	3.9	8.9	30.5	22.8	15	32.2
		(0 - 9)	(7.4 - 12.7)	(22.7 - 43)	(8.3 - 53.7)	(0 - 67.9)	(0 - 85)
N1-UT	μ	5.4	21.2	12.5	13	13.4	6.8
		± 3.6	± 7.6	± 5.2	± 5.9	± 6.5	± 2.2
N1-LT	μ	4.3	22.9	11.6	13.7	12.6	0
		(0 - 6)	(5.1 - 33.5)	(3 - 24.4)	(0.8 - 20.9)	(0 - 31)	(0 - 8.1)
N1-UT	μ	3.3	47.7	33.3	35.7	30.3	64.1
		± 1.5	± 7.7	± 16.4	± 18.1	± 13.8	± 17.4
N1-LT	μ	3.2	43.2	31.7	27.3	23.3	0
		(2.5 - 6.5)	(37 - 60.7)	(15.3 - 70.3)	(13.7 - 70.6)	(18 - 59.3)	(0 - 80)

At the cohesive site, LT initially showed a slightly higher shoot extension rate than UT, but interestingly the situation changed in August 2009 when the UT had a higher mean growth rate than the LT (Fig. 5.3.3). A slight decline in mean shoot length occurred on the LT in early August, but a noticeable, almost 35% increase was recorded in October 2009. In general, the differences between the shoot extensions on both tiers at the cohesive site were not as obvious as at the non-cohesive site. The initial visit to the non-cohesive site showed better first growth of the UT which was installed earlier than the LT. However, the situation changed rapidly in early June and the LT was progressing twice as fast as the UT.

There was a considerable decline in mean shoot length on both tiers in July, which continued in the UT until the end of the growing season. This was due to grazing which started in July and continued until the end of the season (Chapter 5.5.3). In October, the mean shoot length in the LT was 9.5-times of the mean shoot length in the UT, with shoots of up to 98 cm long.

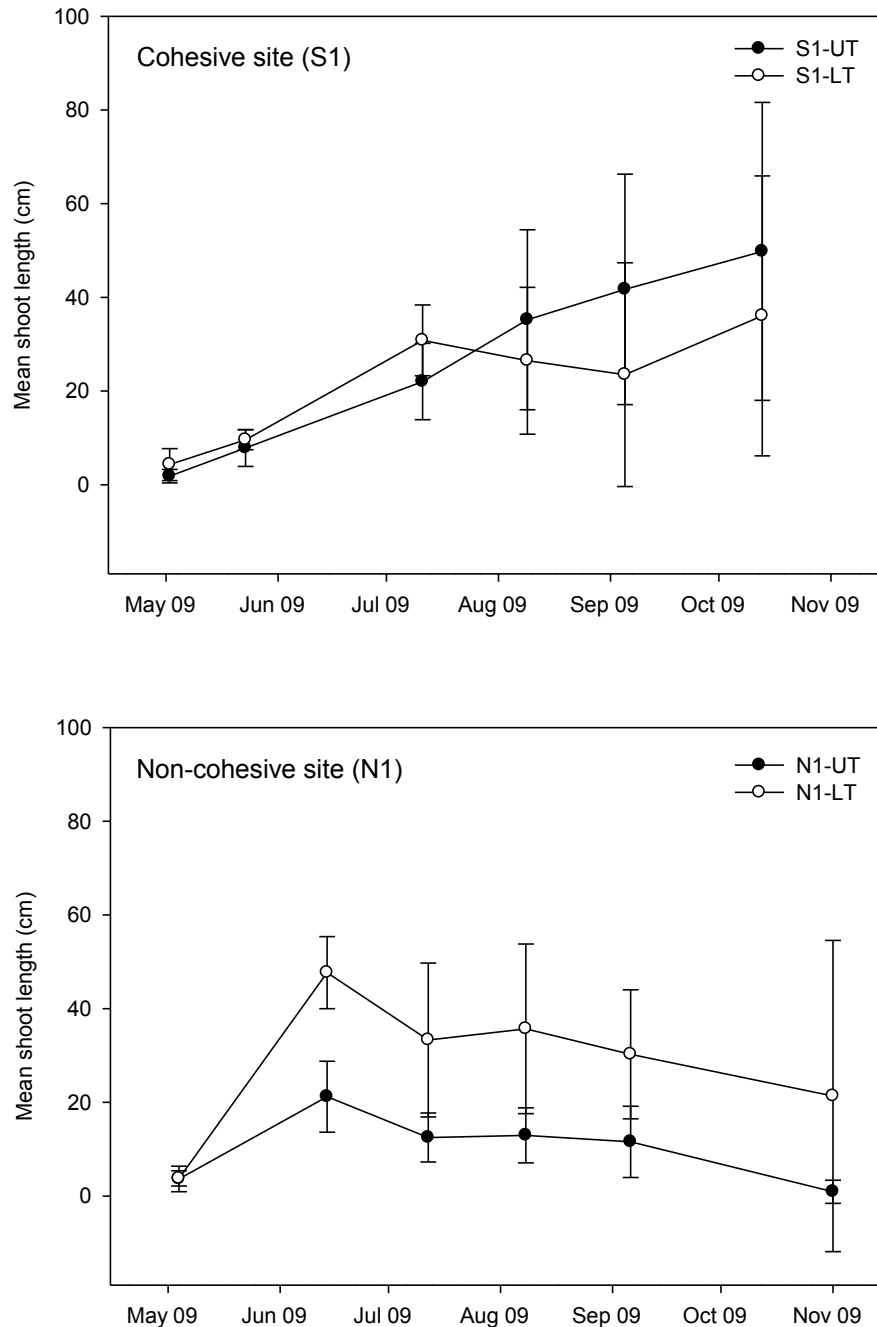


Fig. 5.3.3 Mean shoot length based on stake means (cm). The error bars are the standard deviation of the stake means. The data shown are the values for each sampling date between May and November 2009.

At the cohesive site, the mean shoot length in the UT increased regularly on all stakes with the exception of a moribund stake at 1.12 m (upstream end) that had a mean monthly shoot extension \pm SD of only 2.65 ± 3.62 cm. In contrast, the shoots extending the most were on a stake at 3.85 m (downstream end) with a monthly extension of 21.1 ± 6.2 cm. Growth on the LT was less predictable with monthly decreases in shoot extension of up to 32.1 cm. Here, the stake at the downstream distance 1.15 m had a monthly shoot extension of 20.5 ± 16.2 cm. Mean monthly shoot extension on all sampled stakes at the cohesive site was 9.6 ± 2.9 cm for the UT and $10.4 \text{ cm} \pm 5.4$ cm for LT (Fig. 5.3.4).

At the non-cohesive site, mean shoot lengths and mean monthly shoot extension values were much lower than those recorded at the cohesive site (Fig. 5.3.5). Decreases in shoot length were common. The largest decrease in shoot extension of 38.8 cm was recorded on the LT in July 2009. In this month almost all of the sampled stakes (93.6%) decreased in shoot length. The best performing stakes overall were at the downstream distance 1.5 m and 3.7 m (upstream end of the LT), with a mean monthly increase in shoot length of $6.3 \text{ cm} \pm 14.6$ cm and 6.0 ± 17.3 cm respectively. The mean monthly shoot extension on all sampled stakes at the non-cohesive site was -5.1 ± 2.0 cm in the UT and -6.6 ± 3.6 cm in the LT.

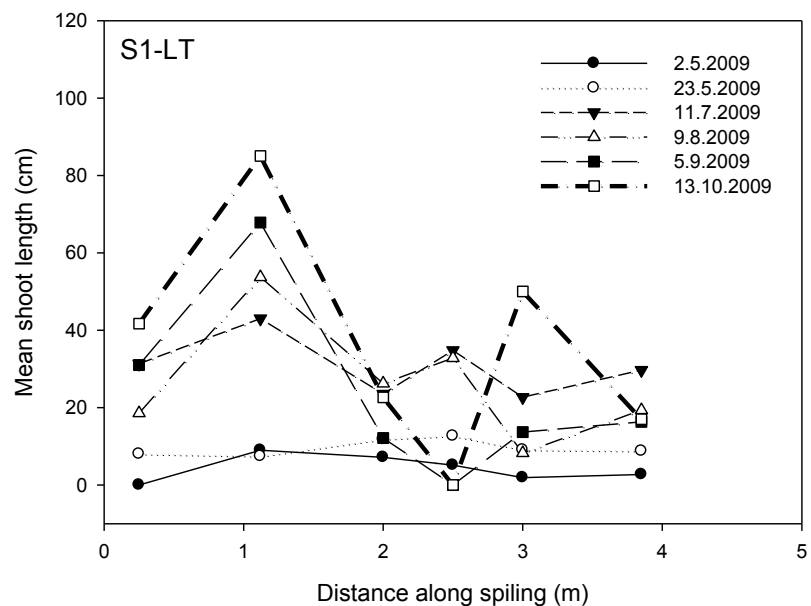
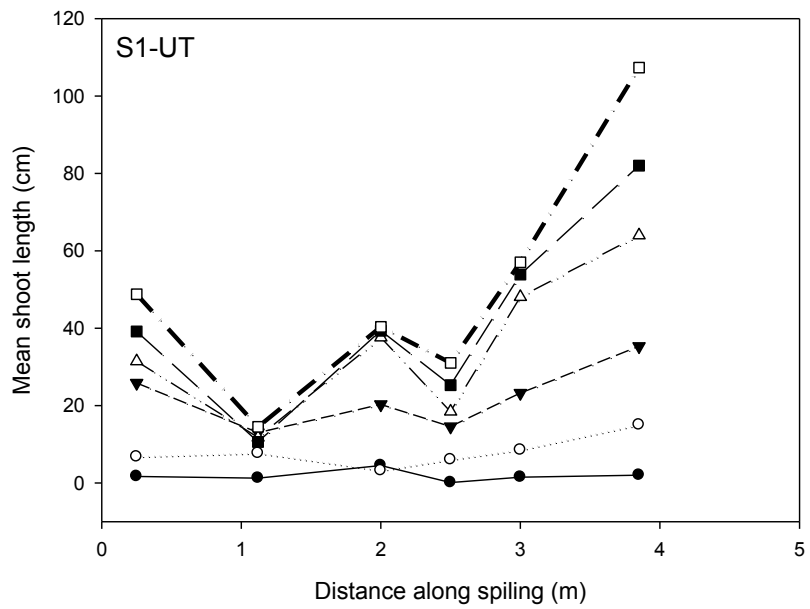


Fig. 5.3.4 Mean shoot lengths at the cohesive site on the upper tier (S1-UT) and lower tier (S1-LT) in cm. Each line represents a different sampling date between May and October 2009. The final date is highlighted. Values on the x axis are the exact positions of sampled stakes, going downstream.

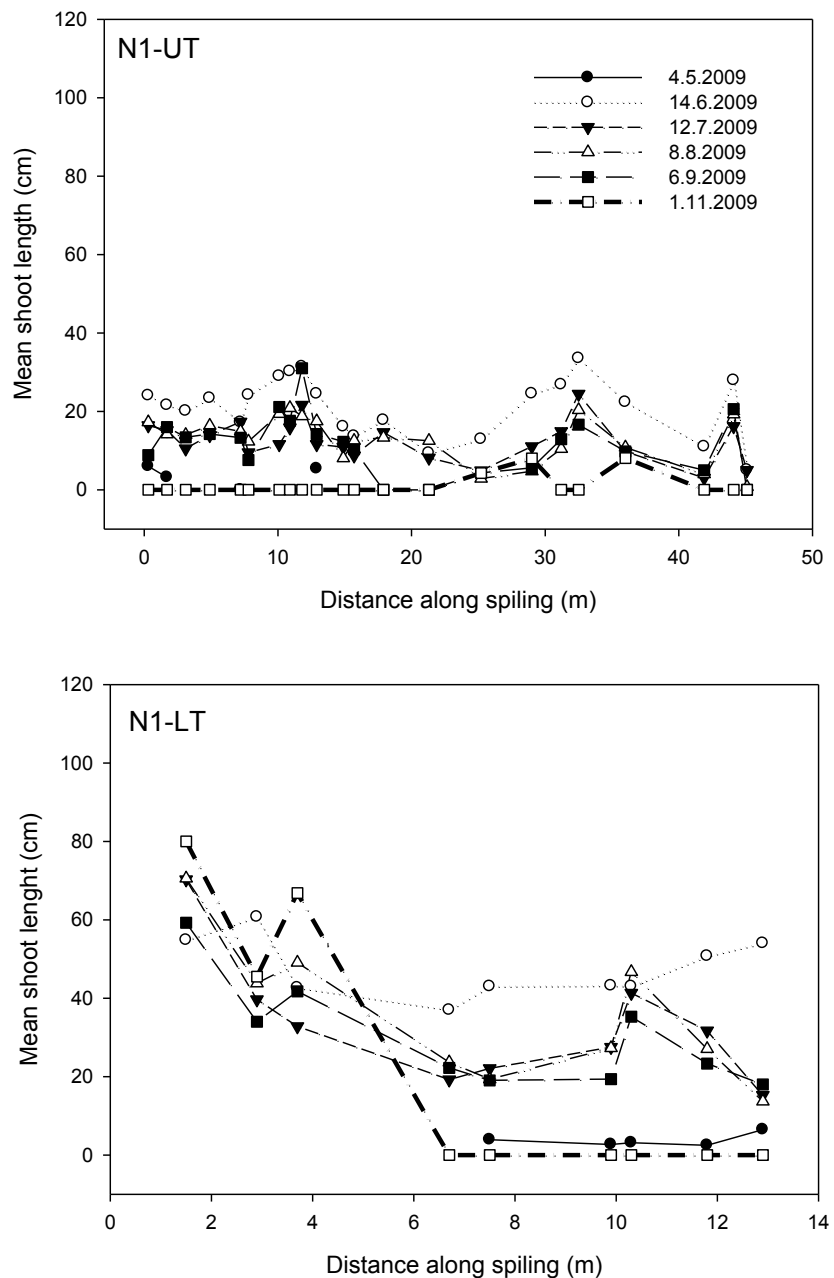


Fig. 5.3.5 Mean shoot lengths at the non-cohesive site on the upper tier (N1-UT) and lower tier (N1-LT) in cm. Each line represents a different sampling date between May and October 2009. The final date is highlighted. Values on the x axis are the exact positions of sampled stakes, moving downstream.

5.3.3(C) NUMBER OF LIVE SHOOTS

Initial sprouting on most sampled stakes was vigorous with abundant new shoots. Later in the season, the number of live shoots on the majority of stakes had decreased. Shoots located around the top of the stakes were affected the most (Fig. 5.3.6).



Fig. 5.3.6 Appearance of new shoots from a willow stake at N1-UT in May 2009 (left) and dead shoots on a stake at S1-LT in August 2009 (right).

At the beginning of the monitoring period, sampled stakes had anything between 0 and 12 shoots. At the cohesive site, the highest monthly increase in the number of shoots occurred during May 2009, with the total number of shoots being 112 and the mean number of shoots \pm SD being 7.0 ± 7.1 per stake in the UT and 11.7 ± 6.7 in the LT (Fig. 5.3.7). UT stake at 0.25 m (upstream end) and two LT stakes at 1.5 m and 3.9 m (middle and downstream end) had the highest number of shoots during the entire monitoring period: 20, 21 and 18, respectively. The July survey revealed the highest decrease in the number of live shoots on all stakes (down by 43.75% to 63 shoots). At the LT, all stakes apart from one were subject to a decline. Conversely, at the UT only shoots at two upstream stakes decreased. There was some recovery and further decreases towards the end of the season but these were of a lesser significance (Fig. 5.3.8).

At the non-cohesive site the fluctuations were more intensive, with the highest increase of live shoots during May and June 2009, totalling 388 shoots. The mean number of shoots was then 12.1 ± 7 per stake in the UT and 13.6 ± 5.7 per stake in the LT. Stakes with a high number of shoots (15+) were located at the upstream end of the UT, at 12.9 m and the downstream end, at around 32 m. In the LT, the most active sprouting stakes were located in the middle part, between 3.7 and 10.3 m.

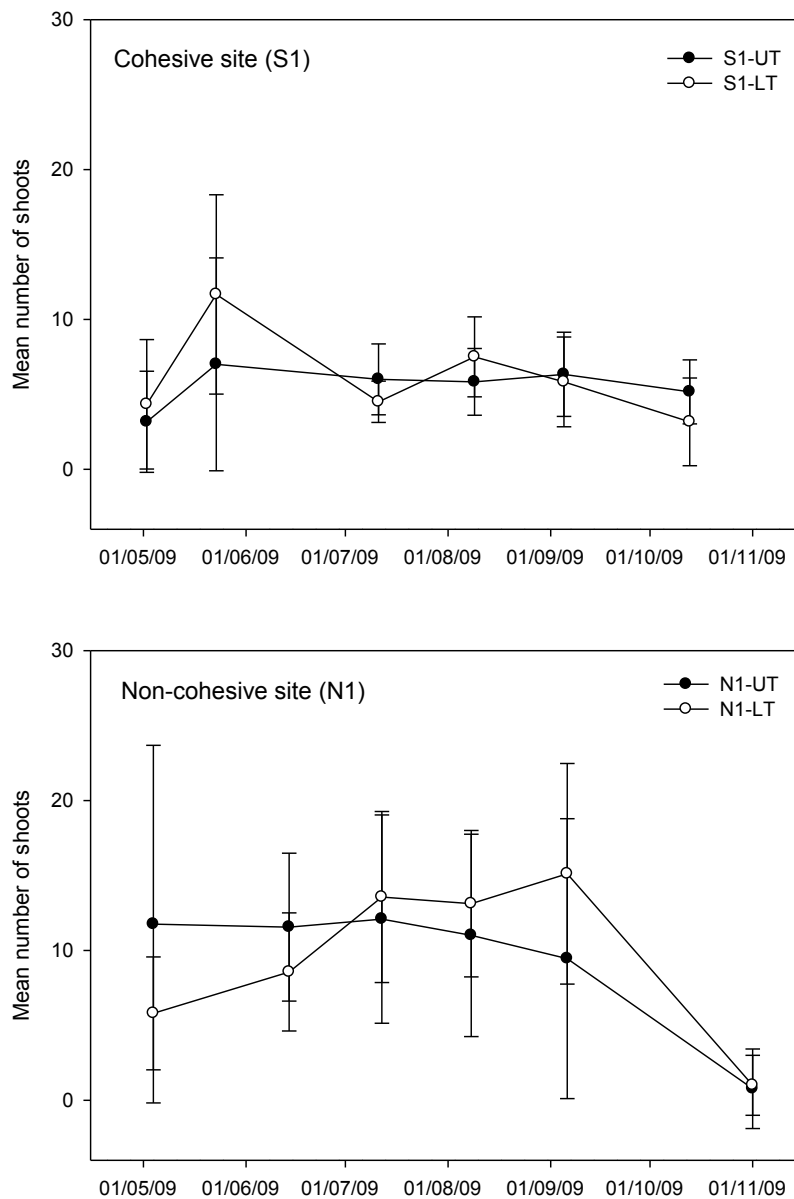


Fig 5.3.7 Mean number of shoots per stake at individual sampling dates at cohesive and non-cohesive sites between May and October 2009. The error bar is the standard deviation.

The following field visits recorded a slight decrease in July (down to 360 shoots) and in August (down to 344 shoots), but some new shoots appeared at the end of summer, including the first upstream stake in the UT which sprouted with 39 shoots. However, a radical decline was recorded at the end of monitoring period, when the number of all live shoots fell by 92.44% to 26 only (Fig. 5.3.9).

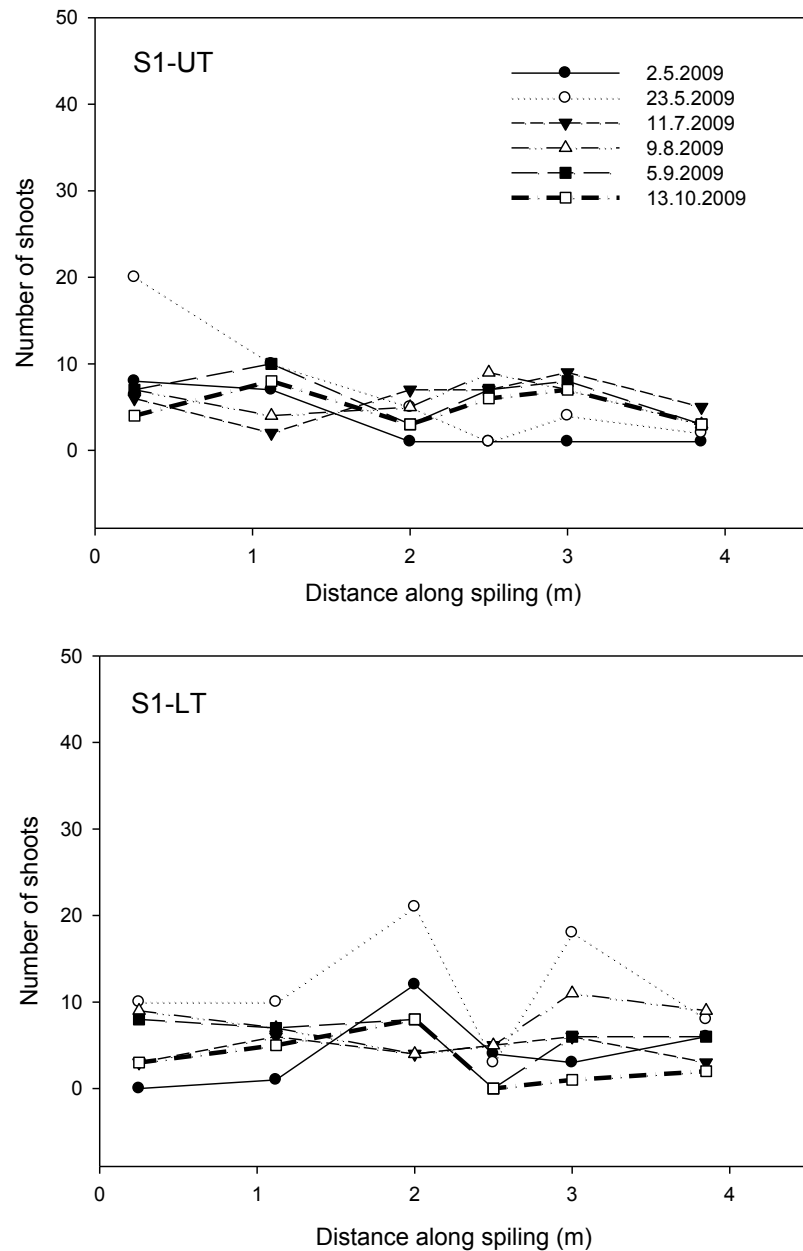


Fig.5.3.8 Number of live shoots on sampled stakes in upper (S1-UT) and lower tier (S1-LT) at the cohesive site. Each line represents a sampling date. The final date is highlighted. X axis represents the position of stakes in spiling, going downstream, in m.

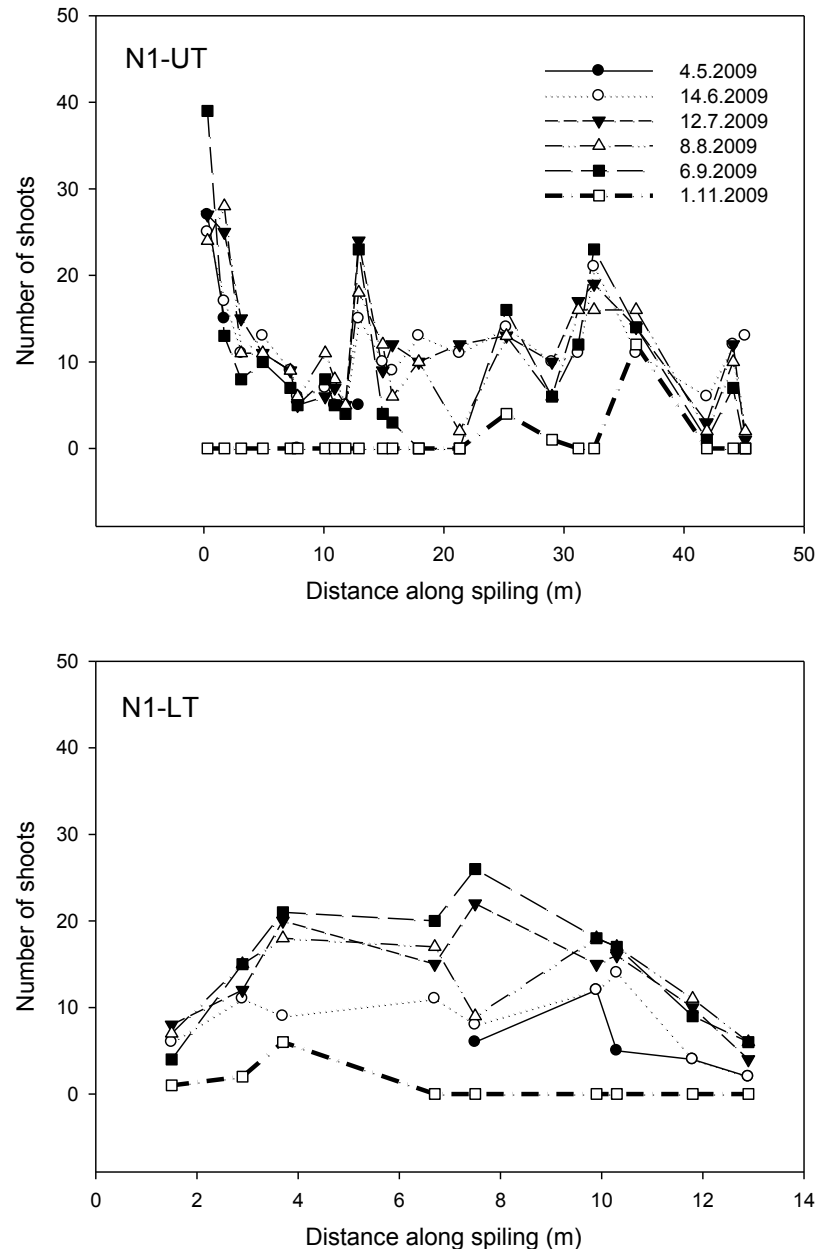


Fig. 5.3.9 Number of live shoots on sampled stakes in upper (N1-UT) and lower tier (N1-LT) at non-cohesive site. Each line represents a sampling date. The final date is highlighted. X axis represents the position of stakes in spiling, going downstream, in m.

5.3.3(D) FREQUENCY SIZE DISTRIBUTION

Frequency distribution charts analyse both the shoot length and the number of shoots at the same time. They visually illustrate the distribution of shoot lengths throughout the monitoring period and thus enable one to follow spiling growth processes in detail.

All shoots have been divided into size classes with intervals of 1 cm and the number of shoots for the given size class were counted during each field visit (Figs 5.3.10-13). At the cohesive site, plots are skewed left towards low size classes with the majority of shoots up to 2 cm long. Later, this trend changed towards a more normal distribution, with the sample mean closer to the sample median (Table 5.3.3, Section 5.3.3(B)). Further into the monitoring season, distribution became wider with shoots across size classes up to 150 cm. At the non-cohesive site, the situation was similar at the beginning of the season and distribution was skewed to the low size classes. Similarly, there was a tendency towards more normal distribution in June 2009. However, in July the distribution became again strongly skewed to the left and this situation remained until nearly the end of season. An exception was the final month when the distribution had significantly less shoots.

The distribution was influenced by shoot mortality due to grazing when the goats shortened or removed the stems and the stakes then started to produce new young shoots. Competition from other stems or from herbal vegetation resulted in the survival of less but longer stems, especially in the lower tiers. A lack of soil moisture increased shoot mortality. Evaporation from the stake tops caused shoots sprouting from the top of the stake to die, shade made the shoots growing around the base thin and weak and thus more likely to die. The conditions and causes of the shoot population dynamics are discussed in Chapter 5.5.

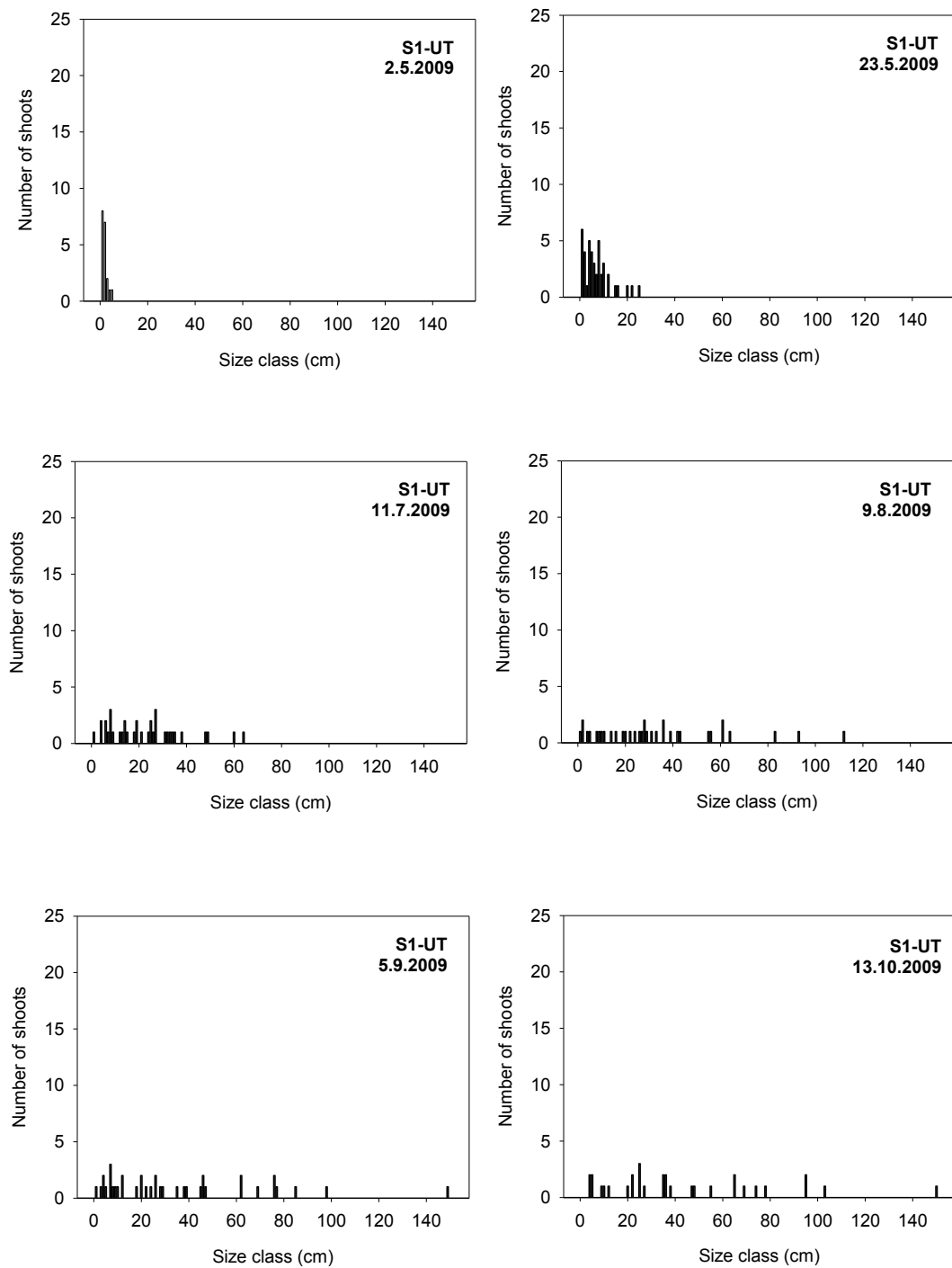


Fig. 5.3.10 Frequency distributions for the cohesive site – upper tier (S1-UT) showing shoot length size classes (cm) against number of shoots. The size class interval was 1 cm.

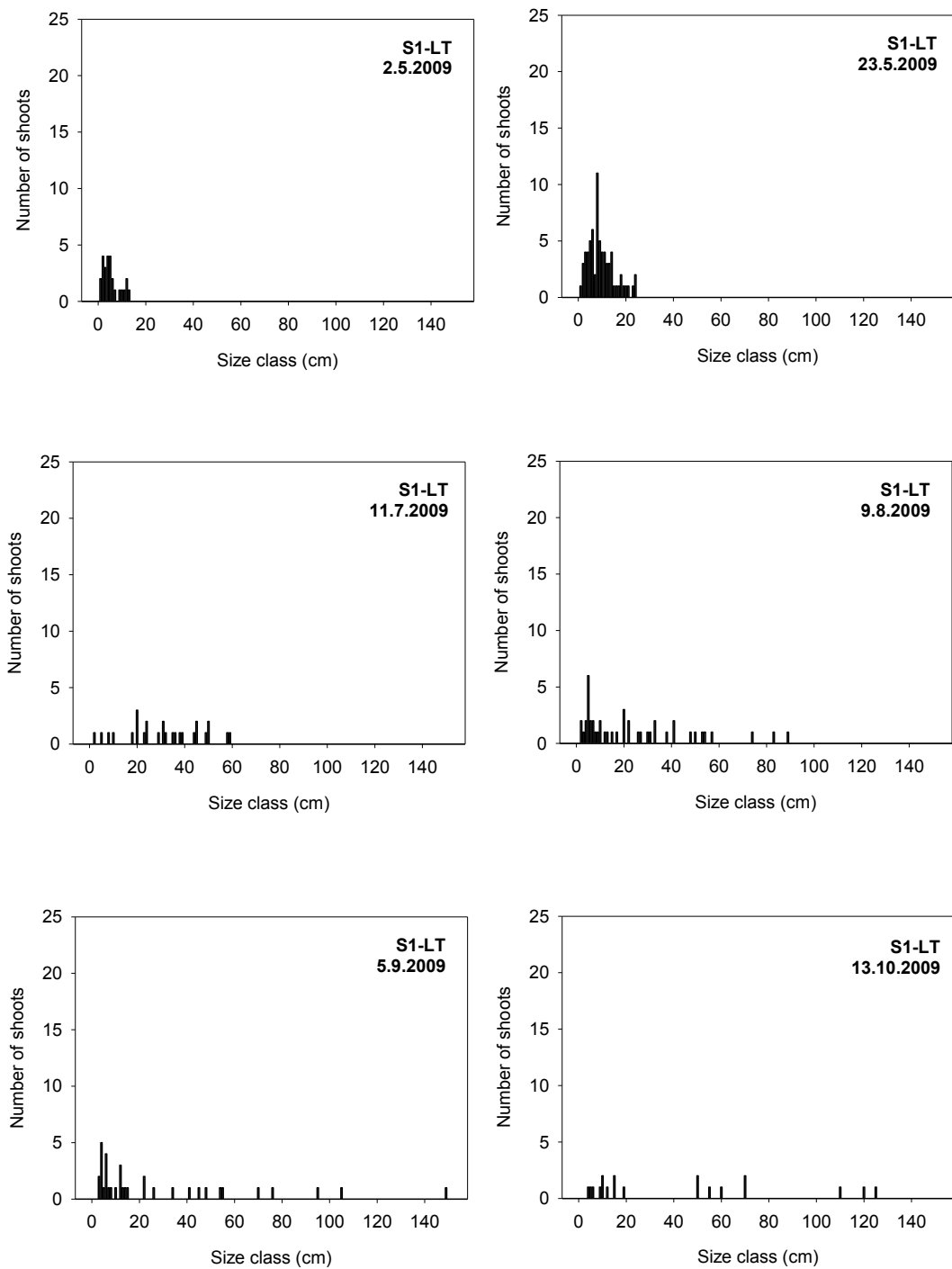


Fig. 5.3.11 Frequency distributions for the cohesive site - lower tier (S1-LT) showing shoot length size classes (cm) against number of shoots. The size class interval was 1 cm.

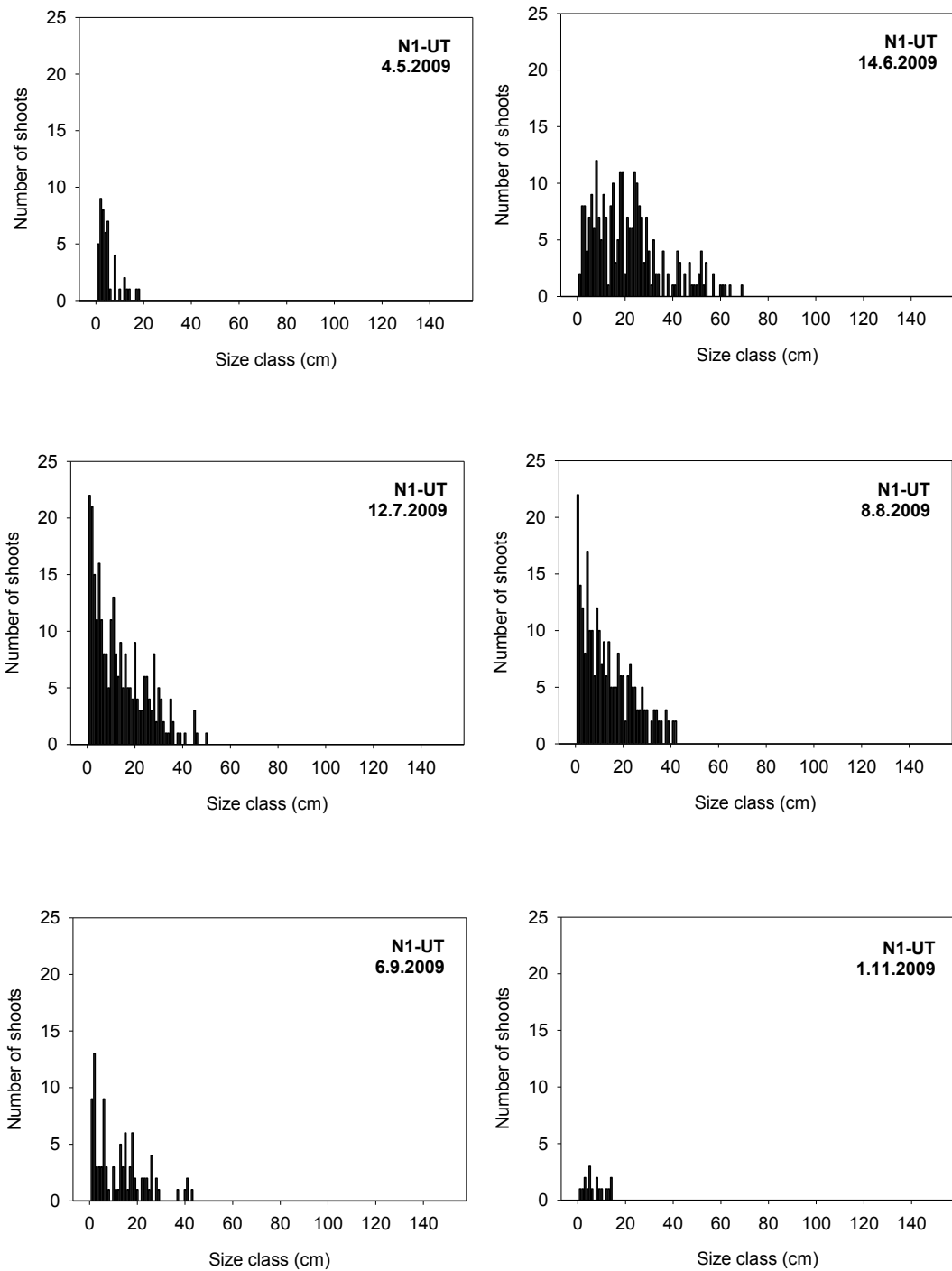


Fig. 5.3.12 Frequency distributions for the non-cohesive site – upper tier (N1-UT) showing shoot length size classes (cm) against number of shoots. The size class interval was 1 cm.

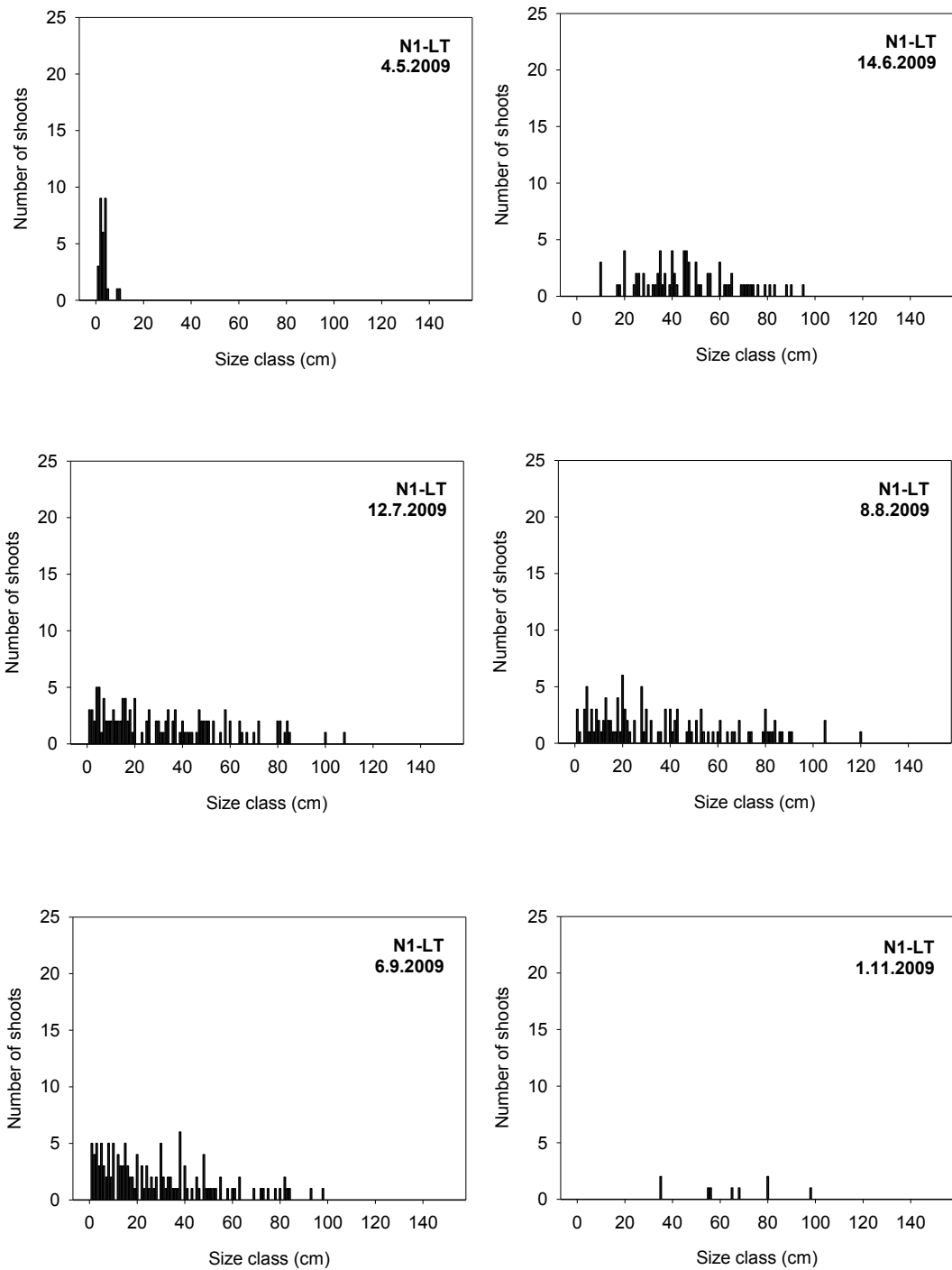


Fig.5 3.13 Frequency distributions for the non-cohesive site - lower tier (N1-LT) showing shoot length size classes (cm) against number of shoots. The size class interval was 1 cm.

5.3.4. DISCUSSION ON BIOLOGICAL PERFORMANCE

5.3.4(A) STAKE SURVIVAL

Live stakes are a key component of willow spiling, acting in a similar way than the piles in sheet piling. Even if the woven part of the spiling fails, living stakes can provide enough initial support to stabilize the bank. Being embedded in the riverbank by at least two thirds of their length, they have good contact with the soil to develop substantial root systems to prevent fluvial erosion and undercutting. However, if they do not survive, their supportive function can last as little as two years (Chapter 4). Factors that could have influenced stake survival at the two projects are discussed in Chapter 5.5.

The stake survival trend showed that a high growth rate in initial shooting does not secure long term survival as the energy stored within the stake tissues is depleted. Without an effective root system the individual stakes were not able to survive independently from their parent tree. The evidence of functional root systems from each stake would have been a good indicator of the potential for their survival and therefore the success of the revetment. Unfortunately, an observation of roots was not possible without disturbing the spiling structure, which would have been undesirable. However, smaller roots were observed after some backfilled soil was removed from behind the stakes. These were a result of latent root primordia (Chapter 4), specialized stem cells that became active in contact with moist soil.

Dense root systems were observed on some stand-alone stakes just upstream of the spiling at the non-cohesive site N1. These were partially inserted willow stakes positioned at the mean summer water level, 2 m above and only 0.5 m below the ground. They were left with the intention to extend the structure upstream but as the growing season had already started, it was too late to do so. Although erosion occurred around the stakes, the one year old root systems were strong enough to hold the stakes in place. It can be assumed that similar root systems might have developed on other stakes within the spiling.

Root systems are important, but they do not develop to a great depth in waterlogged soils. If the erosion of the river bed adjacent to a spiling is significant, the willow root system from stakes may simply not be strong enough to uphold the revetment. Although willows develop secondary aerial roots that help the plants to survive anoxic conditions during flooding (Section 5.3.3, Fig. 5.3.2), they have no stabilizing function. However, they provide biological refuge and reduce near bank velocities.

5.3.4(B) SHOOT EXTENSION AND NUMBER OF LIVE SHOOTS

Measuring the mean shoot extension and the number of live shoots helps to identify stagnation, inhibition and recovery processes on live revetments. The number of live shoots is, alongside the mean shoot length, an important indicator of how an individual stake is performing. Stress periods are usually associated with a decrease in the number of live shoots, but the mean shoot length can still increase. Recovery periods can be recognised by the sprouting of many new young shoots, which will consequently decrease the mean shoot length.

Mean values of the samples in all four cohorts were associated with a standard deviation higher than 0.5 of the mean. This is typical for a non-normal distribution. Therefore the Kruskal-Wallis test has been employed (also known as Mann-Whitney when comparing two groups). This is a non-parametric test that does not assume normal distribution. However, the test does assume an identically-shaped and scaled distribution for each group, except for any difference in medians (Kruskal & Wallis 1952). Various combinations of groups were compared for both mean shoot length and number of live shoots across the monitoring period (Table 5.3.4.)

The results show that there is a significant difference ($p<0.05$) in mean shoot length over the whole monitoring period between the tiers at the non-cohesive site. The upper tier (N1-UT) had the lowest mean ranking, while the lower tier (N1-LT) had the highest. At the cohesive site, both tiers performed similarly. The same tiers at both sites were compared. The upper tier at the non-cohesive site had a significantly lower number of shoots than the same tier at the cohesive site. The lower tier at the non-cohesive site had significantly longer shoots than the tier at the cohesive site, mainly due to the water and grazing stresses that the non-cohesive site was exposed to.

Table 5.3.4 Probability of difference with 95% confidence for mean shoot length and number of shoots obtained from Kruskal-Wallis (Mann-Whitney) test. Pairs of groups were compared as cohorts, sites and tiers.

Group	n	Mean shoot length (cm)		Number of shoots	
		Mean rank	P	Mean rank	P
S1-UT	36	37.99	0.5468	35.54	0.6962
S1-LT	36	35.01		37.46	
N1-UT	114	69.04		80.17	
N1-LT	50	113.18	<0.0001	87.81	0.3412
S1-UT	36	96.85		61.57	
N1-UT	114	68.76	0.0007	79.90	0.0269
S1-LT	36	37.10		35.99	
N1-LT	50	48.11	0.0435	45.91	0.0176
S1	72	132.57		97.53	
N1	164	112.32	0.0357	127.7	0.017
UT	150	103.72		117.31	
LT	86	144.28	<0.0001	120.58	0.723

There was no significant difference in the number of shoots per stake when comparing upper and lower tiers at the same sites. However, when testing the same tiers at different sites, both upper and lower tiers at the cohesive site had significantly less shoots than the same tiers at the non-cohesive site. Overall therefore, the non-cohesive site performed better in terms of number of live shoots (considering the full six month monitoring period) than the cohesive site (Table 5.3.4). The values of means and medians are plotted on Fig. 5.3.14.

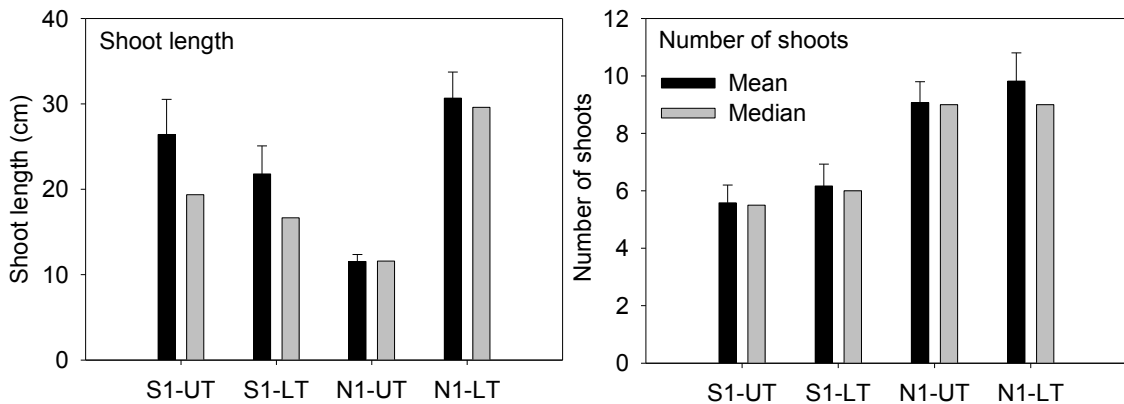


Fig. 5.3.14 Plots of mean and median values for each cohort for mean shoot length and number of shoots per stake. The data taken is for the whole monitoring period. Error bars on mean indicate standard error.

5.3.4(C) NET SEASONAL SHOOT EXTENSION

In biology, the term net seasonal shoot extension (NSSE) is used as a substitute for the net annual above ground production (NAAP), which uses the dried weight of biomass. Two methods have been employed to compare shoot extension in NAAP estimates of a species: increment summation and instantaneous growth. The increment summation method is based on the sum of new production that occurred over a time interval. It is calculated by multiplying the change in individual weight (ΔW) by the average number (\bar{N}) over the time interval (Wetzel & Pickard 1996) and this method expects a linear increase in weight:

$$\sum \bar{N} \times \Delta W + B_0$$

Where N is the mean number of shoots, W is weight and B_0 is the initial biomass.

The instantaneous growth method is based on a multiplication of the growth rate (G) over the time interval ($G = \ln (w_1/w_0)$) by an average biomass (\bar{B}) over that time interval. The initial biomass is added to the production to account for any growth prior to sampling (Wetzel & Pickard 1996).

$$\sum G \bar{B} + B_0$$

Table 5.3.5 shows calculations for the two methods and a final estimation of the net seasonal shoot extension based on shoot length in place of biomass. The biomass sampling would have been destructive and other observations would not be possible.

Table 5.3.5 Values for Net seasonal shoot extension (NSSE) of *Salix* sp. cohorts at S1-UT, S1-LT, N1-UT and N1-LT based on the methods of increment summation and instantaneous growth for each of the monthly observations.

Cohort	Date	N	L	N _{ave}	Δ L	P _S	L _{tot}	L _{tot, ave}	G	P _G
S1-UT	2.5.	19	1.6	30.5	5.5	167.5	30.4	164.1	1.49	244.3
	23.5.	42	7.1	39	15.4	601.4	297.8	554.1	1.2	640.1
	11.7.	36	22.5	35.5	10.3	366.7	810.4	979.9	0.4	370.1
	9.8.	35	32.8	36.5	2.7	100	1149.4	1250.7	0.1	100.2
	5.9.	38	35.6	34.5	7.6	262.6	1352.0	1345.5	0.2	260.8
	13.10.	31	43.2	-	-	-	1338.9	-	-	-
S1-LT	2.5.	26	5.3	48	4.3	207.8	137.3	405	0.6	242.5
	23.5.	70	9.6	48.5	21.7	1051.5	672.7	758.8	1.2	895.7
	11.7.	27	31.3	36	-7.4	0	844.8	960.8	-0.3	0
	9.8.	45	23.9	40	4.6	185.6	1076.9	1038.4	0	184
	5.9.	35	28.6	27	14.3	386.6	999.9	907.4	0.4	368.7
	13.10.	19	42.9	-	-	-	814.9	-	-	-
N1-UT	4.5	177	6.1	215.5	15.3	3293.7	1077.2	3252.6	1.3	4085.3
	14.6.	254	21.4	260	-7.9	0	5428	4506.8	-0.5	0
	12.7.	266	13.5	254	0.6	149.9	3585.7	3495.3	0	149.7
	8.8.	242	14.1	225	-1.3	0	3405	3026.4	-0.1	0
	6.9.	208	12.7	112.5	-5.6	0	2647.8	1384.9	-0.6	0
	1.11.	17	7.2	-	-	-	121.9	-	-	-
N1-LT	4.5	82	3.4	79.5	42.8	3405.1	282	1922.4	2.6	4996.9
	14.6.	77	46.3	99.5	-14.1	0	3562.8	3741.3	-0.4	0
	12.7.	122	32.1	120	4.1	493.2	3919.9	4098.1	0.1	493.3
	8.8.	118	36.2	127	-8.1	0	4276.3	4053.7	-0.3	0
	6.9.	136	28.2	72.5	35.4	2565.8	3831.1	2201.6	0.8	1791.5
	1.11.	9	63.6	-	-	-	572	-	-	-

N - number of all shoots, L - mean length (cm),

N_{ave} - mean number of shoots for 2 consecutive time intervals,

ΔL - change in individual length (cm): (L₂-L₁), P_S - shoot extension by incr. summation: (N_{ave} · ΔL)

L_{tot} - total length of a shoots (cm): (L · N),

L_{tot, ave} - average total length for 2 consecutive time intervals (cm),

G - growth rate over time interval ($\ln(L_1/L_0)$),

P_G - shoot extension by instantaneous growth (G · L_{tot, ave}).

Table 5.3.6 Final values for shoot extension by instantaneous growth (P_G) and by increment summation (P_s) for all the stakes and the values per stake (P_G/N_s and P_s/N_s).

	P_s	P_G	P_s/N_s	P_G/N_s
C-UT	1498.095	1615.699	249.6825	269.2831
C-LT	1831.56	1690.959	305.26	281.8265
G-UT	3443.589	4235.041	171.5	211.07
G-LT	6464.038	7281.678	583.1	610.79

Net seasonal shoot extension (NSSE) by both increment summation and instantaneous growth methods corresponded well when the results from Table 5.3.5 were tested (T-test: $P = 0.43$) and also when the values of shoot extension per stake were tested (T-test: $P = 0.69$). The final values of net seasonal shoot extension by both methods – the increment summation and instantaneous growth per stake, are shown in Fig. 5.3.15.

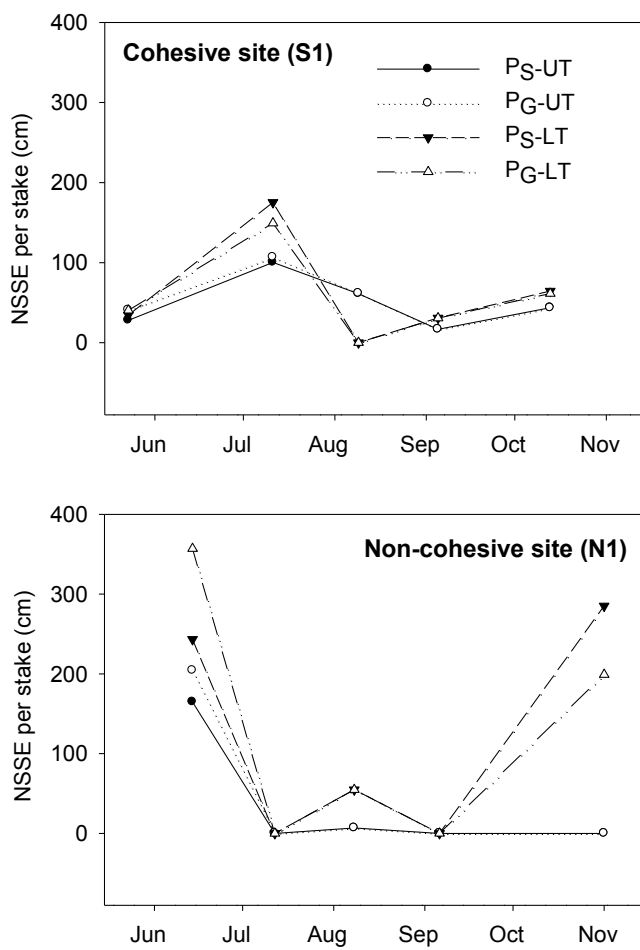


Fig. 5.3.15 Net seasonal shoot extension (NSSE) at cohesive (S1) and non-cohesive (N1) site for monthly intervals based on the two methods for production estimation: increment summation (P_s) and instantaneous growth (P_G). The production values are per stake.

There was a peak in net seasonal shoot extension in the first half of the season (June-July) followed by a decrease in the second half of the season. Production approached zero during August due to various stress conditions (Chapter 5.5). At the non-cohesive site, stress conditions were significant on the upper tier (N1-UT) and resulted in no further shoot extension for the rest of the season. On the remaining cohorts, there was an increase in NSSE towards the end of season (September-October), especially at the lower tier at the non-cohesive site (N1-LT). This increase could, however, be explained by the decreased number of shoots (from 136 at the start of the season to 9) as this had an effect on the mean shoot length that consequently increased from 28.2 cm to 63.6 cm (although the total shoot length of the entire cohort decreased from 3831 to 572 cm). This raises a question about whether NSSE is an appropriate indicator of overall performance of a cohort where shoots have been removed or died.

As an alternative to describe the shoot length dynamics of each cohort, the summed shoot lengths per stake have been plotted (Fig. 5.3.16). The cohesive site cohorts show an increasing trend, with the shoot lengths in the lower tier performing better, but then slowing down towards the end of season. The shoots at the non-cohesive site showed steep growth up to mid-July. Then there was a decline in growth rate that led to a decline in the summed shoot length on both tiers. At the end of season, the summed shoot length per stake at the cohesive site was 223 cm in the upper tier and 135 cm in the lower tier. At the non-cohesive site, the values were considerably lower and the summed shoot length per stake was only 5 cm in the upper tier although it was 63 cm in the lower tier. Mainly grazing and water stress at the non-cohesive site contributed to the low upper tier growth (Chapter 5.5).

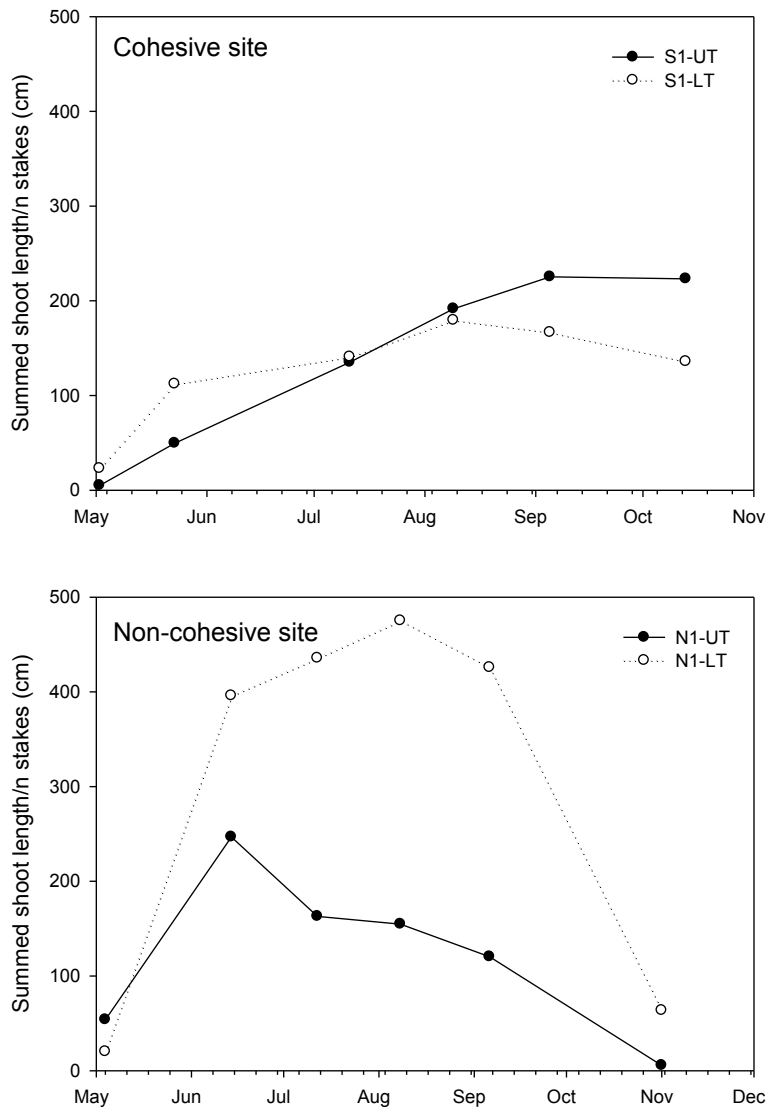


Fig. 5.3.16 Summed shoot length (cm) per stake at the sampling dates for each cohort.

In summary, the summed shoot length proved that the non-cohesive site performed better than cohesive site, initially. However, due to rapid shoot removal and higher mortality later in the season, the final summed shoot length at the non-cohesive site was at around 45-times less in the upper tier and 2-times less in the lower tier than at the cohesive site.

5.4. GEOMORPHOLOGIC PERFORMANCE

The primary aim of the two willow spiling projects was to stabilise the river banks and reduce the rate of retreat. Signs of significant loss of bank material could point to gaps in the design that would gradually lead to partial or complete failure in the project. In the context of Objective 6 of this study, detailed geomorphologic monitoring of the river bank and the adjacent river bed was performed in November 2009 and repeated at the end of March 2010 to record any significant changes to the bank and assess the ability of the two installed spiling projects to control river bank erosion.

5.4.1. METHODS

5.4.1(A) DATA GRIDDING

A Total Station (Nikon DTM 330) was used to measure elevation points chosen at random on the river beds adjacent to the willow spiling and on the backfill of the spiling. Dense data were collected in critical places to record the major surface features of the river bed.

The xyz coordinates were gridded using the Radial Basis Function (RBF) with a Multi-Quadric option. Gridding is a function that enables to extrapolate randomly spaced data to evenly spaced xyz grid nodes that can be shown as a surface plot. There is a range of gridding techniques available but RBF has been shown as the most effective method to reconstruct smooth, manifold surfaces from point data and to repair incomplete meshes. Holes of missing data are smoothly filled and surfaces smoothly extrapolated (Carr *et al.* 2011). The method is used for sophisticated imagining in CAD modelling applied in medicine and manufacturing.

The method, now able to extrapolate millions of data points, uses a single but complicated mathematical function applied to all the data points. The interpolation finds a single complex shape that fits nearly exactly all the surveyed points, and can be used to predict elevation in places where there is no data. Some of the other most commonly used methods require either regularly spaced data or they use the existing data as estimates (R. Kistruck, personal communication, 2011).

Fig. 5.4.1 compares the outcomes from RBF and two other commonly used gridding methods set over randomly spaced xyz data points. The gridding methods agree fairly well over the area with a dense network of elevation points and with the maximum contour displacement approximately 7.00 cm inside the surveyed area. A higher discrepancy

occurs outside the surveyed area. RBF generated contours and the section enclosed by the data points is used for further analysis. Analysis and imaging has been undertaken in Surfer v 9.0 (Golden Software, 2010).

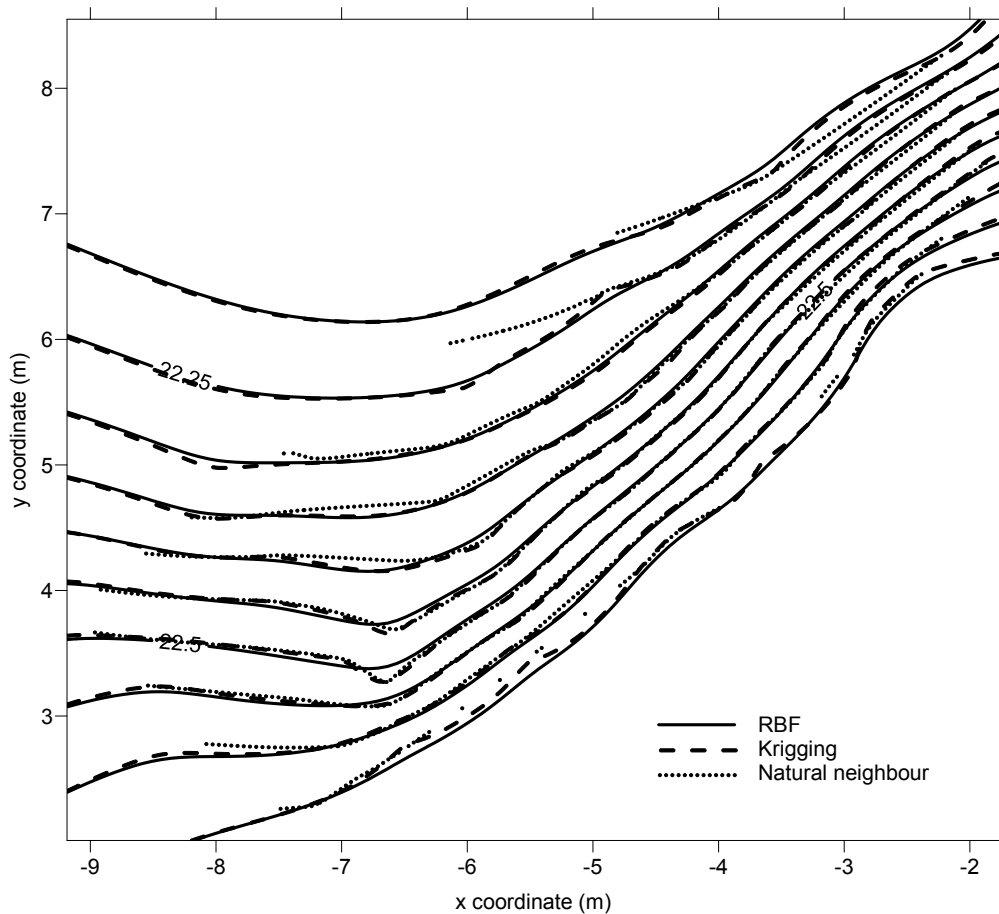


Fig. 5.4.1 Contour plot with three gridding methods overlain of the river bed at S1 site. XY coordinates are in m, elevations are displayed in m A.O.D. The contour interval is 0.05 m. (Please note that the area outside the surveyed zone has not been blanked to demonstrate the extrapolation just beyond the surveyed area).

5.4.1(B) CROSS-SECTIONAL PLOTS OF RIVER BED

Any gridded xyz data can be used to create a cross sectional profile in Surfer. The intersecting vertical line is digitized and used to 'slice' the corresponding grid file. At each point where the boundary line crosses a grid line, a cross section data point is generated (Fig. 5.4.2). Cross section data are written to an ASCII data file (.DAT) that contains five columns of data: XY coordinates of the boundary line and grid line intersection, z value at the boundary line and grid line intersection, accumulated horizontal distance along the boundary line, and boundary number used when more than one boundary line is contained in the file. The Y coordinate and the accumulated horizontal distance are then

saved in a blanking file format (.BLN) and plotted as a cross section (Golden Software, 2010). Eight random river bed cross sections have been sliced through the surveyed area. They were positioned with the 0 distance close to the spiling and directed perpendicular to the flow. The position of cross sections in relation to the surveyed points and lower tier spiling is shown on Fig. 5.4.4.

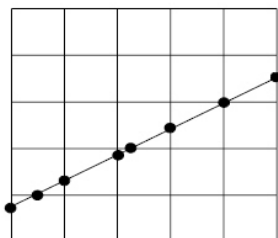


Fig. 5.4.2 Illustration of intersecting points of cross section through a grid file showing locations where data points are created.

To avoid plotting data for the sections outside the surveyed area, the grid data were blanked outside the digitised polygon that contained the surveyed elevation points (ASCII blanked file).

Blanking is a command that removes grid node data from areas not supported by the original data (Fig. 5.4.3). Blanking assigns a blanking value ($1.70141e+38$) to specified groups of grid nodes in a blanked grid file. The blanking file has been modified to allow blanking inside the polygon by setting the blanking flag to 1 (Golden Software, 2010).

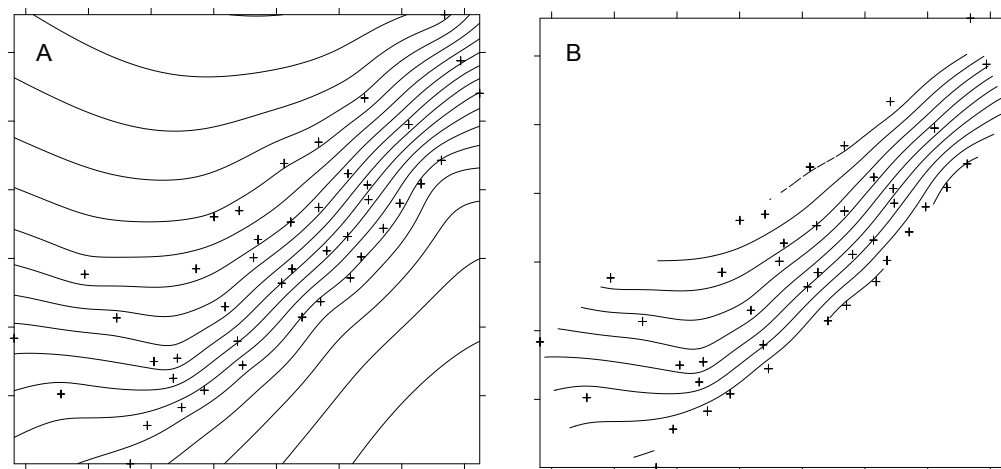


Fig. 5.4.3 Contour plot of full (A) and blanked (B) grid file with location of the surveyed elevation points.

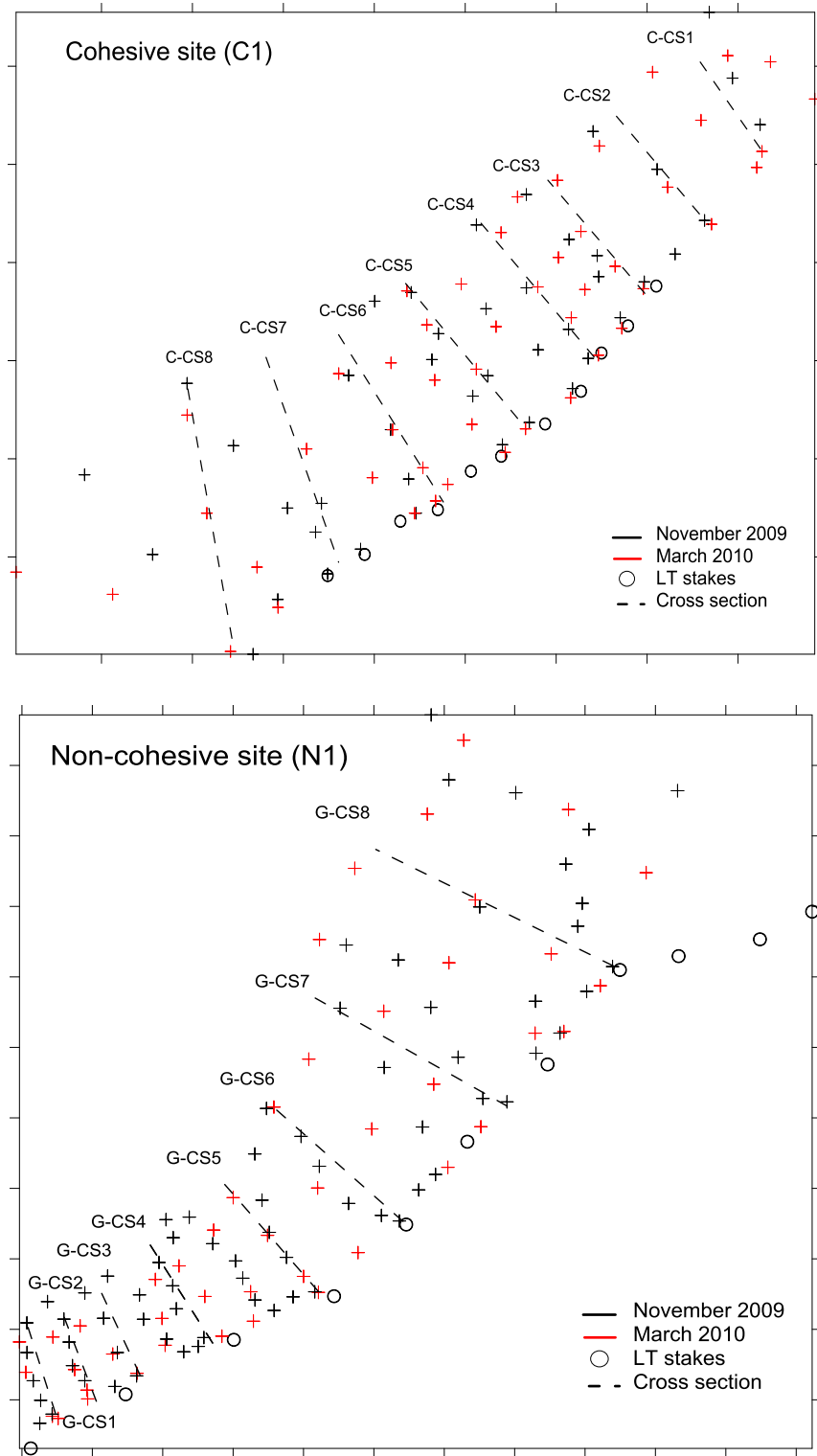


Fig. 5.4.4 The network of surveyed data points in November 2009 (black crosses) and in March 2010 (red crosses) with eight plotted cross sections (dashed lines). The circles indicate the position of the lower tier stakes in relation to the surveyed river bed. The x and y values are in m.

5.4.1(C) THREE-DIMENSIONAL ANALYSIS

The gridding technique is not only useful for plotting random cross sections, but as there are dense data covering the surveyed area, it is a powerful tool for three-dimensional analysis.

The cut off volume between each of the grid surfaces and the horizontal plane given by the z value for the highest rounded contour was calculated. The number of grid nodes used outside the blanked grid for the volume calculations was between 2,000 and 3,000, the blanked regions were excluded from the volume calculations. In principle, in Surfer the volume is generated for each grid cell, and so the more grid cells available, the higher the accuracy of the final volume (Golden Software, 2010). The volume calculation in Surfer computes results using three different methods: Extended trapezoidal rule, Extended Simpson's rule and Extended Simpson's 3/8 rule (Press *et al.* 1988). If the results were close together, the true volume was close to those values. The net volume was then calculated as the mean of the three values. To see where along the elevation ranges the change happened, all elevation data have been used to compute percentiles and for surface plots.

5.4.1(D) MEASUREMENTS FROM STAKE TOPS

In addition to elevation measurements and extrapolation, all of the stakes have been used to reference changes to the backfill immediately behind the spiling. The height from the top of the stake to the top of the backfill was recorded in November 2009 and repeated again in March 2010. It was assumed that there was no vertical growth on stakes during winter months. Where erosion of backfill created hollows and scour, the volume of the eroded soil has been calculated.

5.4.2. RESULTS AND INTERPRETATION

5.4.2(A) CROSS-SECTIONAL PLOTS OF THE RIVER BED

Eight random cross sections at both sites show some significant changes to the river bed. In the case of non-cohesive site N1, these have been of a higher magnitude than those at the cohesive site S1. In both instances the erosion (shown as negative values to demonstrate the material loss) prevailed in the upstream section of the spiling and sedimentation (material gain) occurred within the downstream sections of the lower tiers of spiling. Cross-sectional areas varied in size depending on the width of the surveyed area therefore percentages have been used to indicate the scope of change (Tab 5.4.1).

Table 5.4.1 *Cross-sectional areas of eight random cross-sectional plots of river bed at the cohesive (S1) and non-cohesive (N1) site and the percentage of difference in the cross-sectional area between November 2009 and March 2010.*

	Cohesive site S1 - bed area (m ²)			Non-cohesive site N1 - bed area (m ²)		
	Nov 09	Mar 10	Δ (%)	Nov 09	Mar 10	Δ (%)
CS1	0.2005	0.1671	-16.66	0.7743	0.4524	-41.57
CS2	0.3681	0.3180	-13.60	0.8503	0.5359	-36.98
CS3	0.3737	0.3084	-17.49	0.7555	0.4222	-44.12
CS4	0.3754	0.3376	-10.06	0.8344	0.4838	-42.02
CS5	0.3618	0.3363	-7.05	0.6713	0.5029	-25.09
CS6	0.3134	0.3052	-2.62	0.8255	0.9434	14.28
CS7	0.2979	0.3226	8.27	1.1072	1.3774	24.40
CS8	0.1095	0.4791	-3.36	1.0547	1.3530	28.28

At the cohesive site the change within cross sections fell into an interval from -17% to 8%. At the non-cohesive site the changes were of a higher magnitude and fell into the interval -42% to 28%. The individual cross-sectional plots are shown on Fig. 5.4.5 (S1) and Fig. 5.4.6 (N1). The position of each cross section was shown on Fig. 5.4.4.

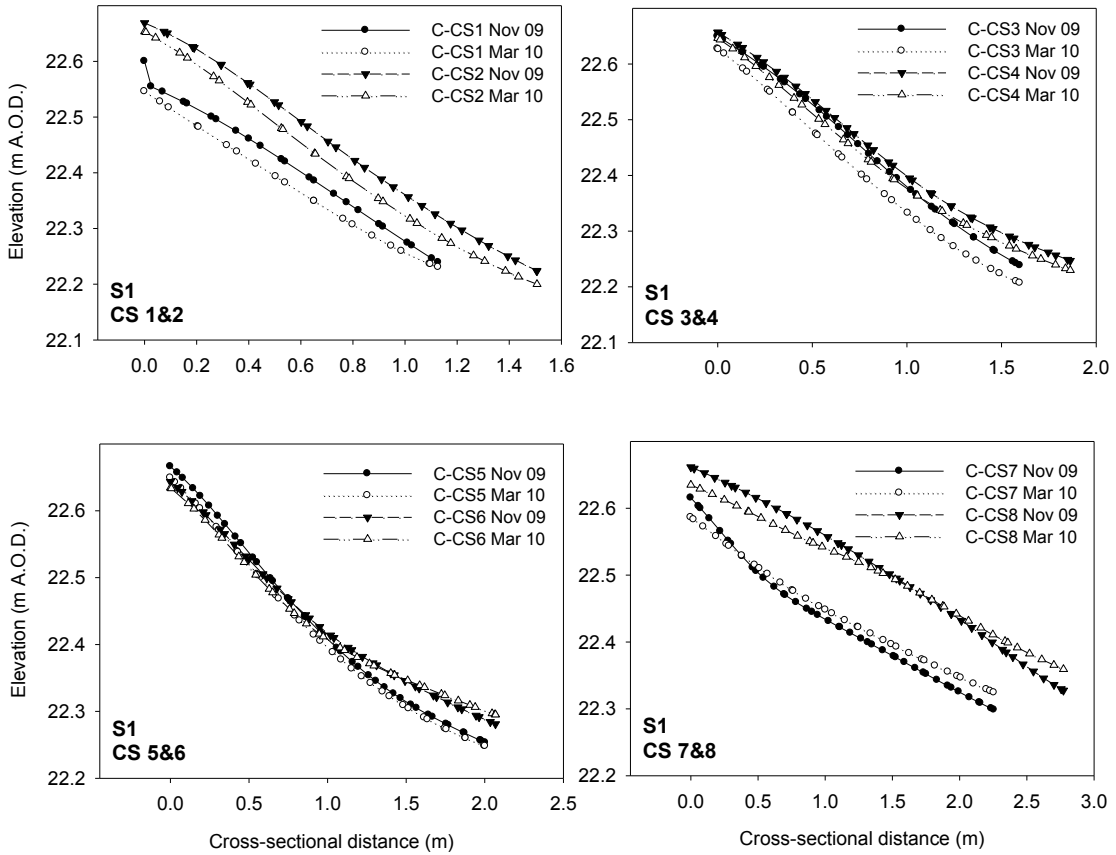


Fig. 5.4.5 Cross section plots of the river bed adjacent to the spiling at the cohesive site S1. The CS1-8 are the codes for the cross sections, as introduced on Fig. 5.4.4. The lines represent each of the elevation data points. Lines with black symbols are for data extrapolated from November 2009 measurement, lines with blank symbols are for measurements taken in March 2010.

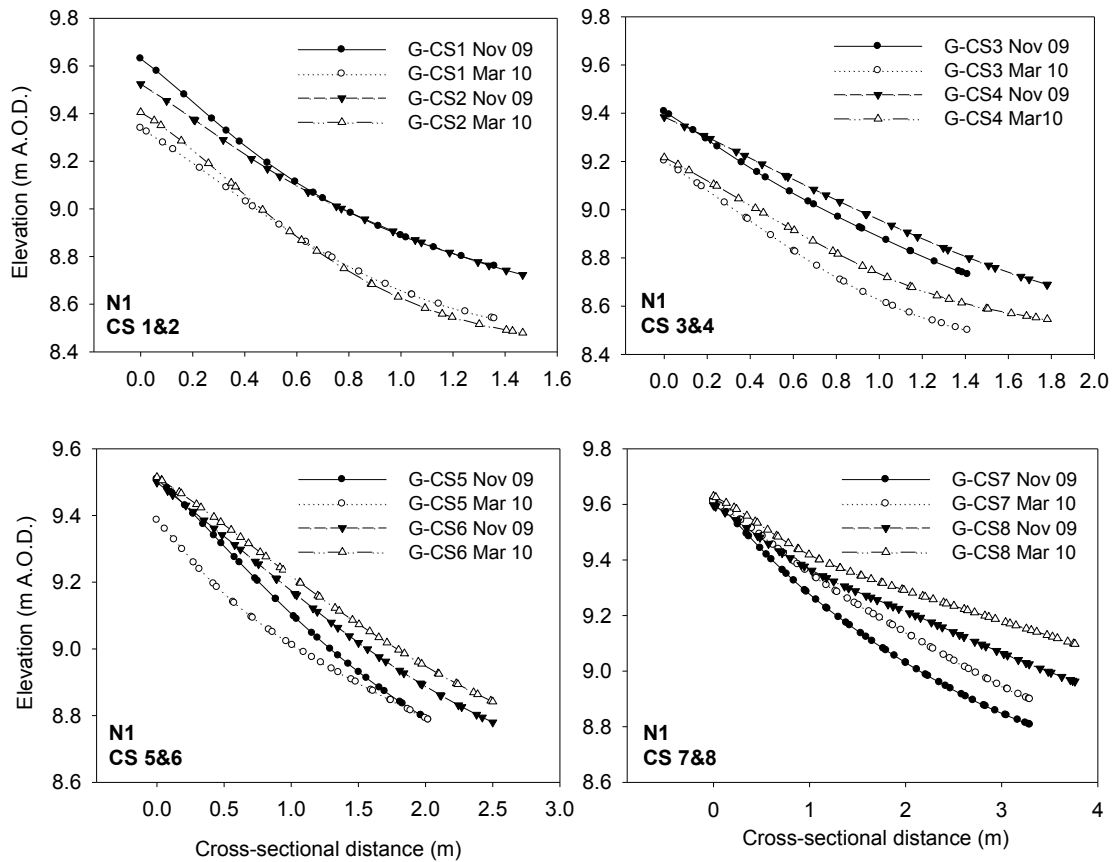


Fig. 5.4.6 Cross-sectional plots of the river bed adjacent to spiling at the non-cohesive site N1. The CS1-8 are the numbered codes for the cross sections, as introduced on Fig. 5.4.6. The lines with black symbols show the November 2009 data while the white symbol lines are data from March 2010.

The percentage of difference in the cross-sectional area for the eight random cross-sections at both sites has been compared. Although there was significant erosion at the non-cohesive site in the upstream section, the mean value has been influenced by the sedimentation in the downstream end. Hence Kruskal-Wallis (resp. Mann-Whitney test) showed no statistical difference between the two sites ($p = 0.442$). Non-linear correlation has been plotted and the values for Pearson's product moment correlation computed. At both sites, there is a growing trend between the percentage of difference in the cross-sectional area and the distance along the spiling, emphasizing that the erosion prevails in the upstream end and sedimentation in the downstream end of the spiling. At the non-cohesive site, the curve is sigmoidal and demonstrates more extreme changes within the middle section of the spiling (Fig. 5.4.7).

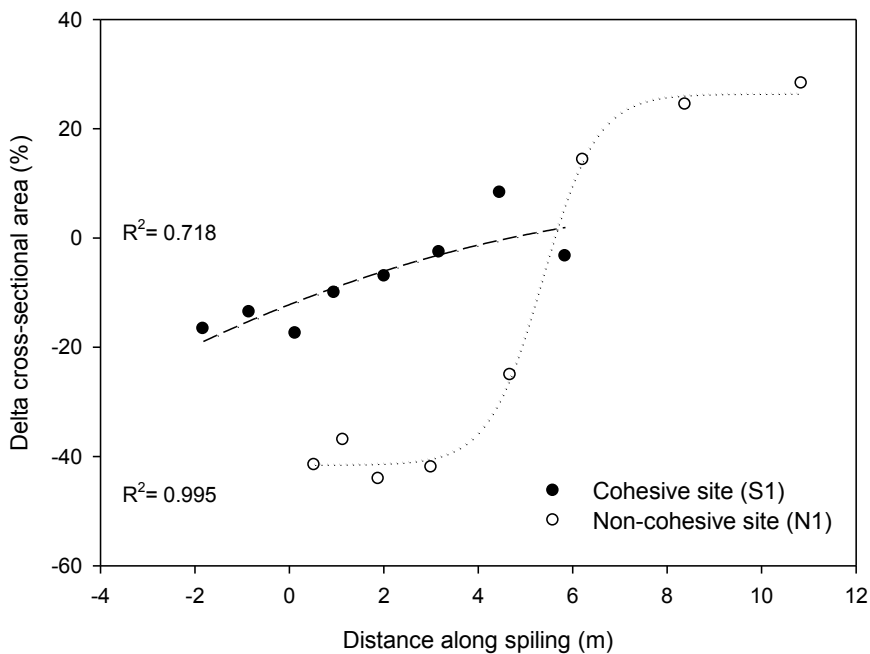


Fig. 5.4.7 Percentage difference of cross-sectional areas at the cohesive (S1) and non-cohesive (N1) site that occurred between November 2009 and March 2010.

Sedimentation in the downstream end may not have a significant adverse effect on the spiling. Erosion in the upstream end at both sites can weaken the structure and, ultimately, can cause it to fail (Chapter 4). Ideally, spiling should extend between sedimentation zones and thus be sufficiently long to prevent any undercutting of the weak ends. The rate and timescale of scouring should be researched prior to installation because the bed scouring process may progress upstream.

To record the immediate effect of the erosion processes on the spiling, the elevation changes at zero distance (closest to the spiling) have been plotted (Fig. 5.4.8). At the cohesive site, some erosion occurred, but it was not significant. The values varied between -1.7 cm and -0.93 cm and the mean value \pm SD was -1.81 ± 0.73 cm. At the non-cohesive site, the toe scour was of significantly higher magnitude and values ranged between -29.14 cm to 3.27 cm. The mean change was $-10.79 (\pm 11.49)$ cm. The linear relationship was less steep at the cohesive site but was steeper at the non-cohesive site, where the erosion rate decreased with increasing distance downstream. Statistically, however, there is no significant difference between the two sites ($p= 0.401$) as again, the more extreme values at either end of the non-cohesive site influenced the position of the mean.

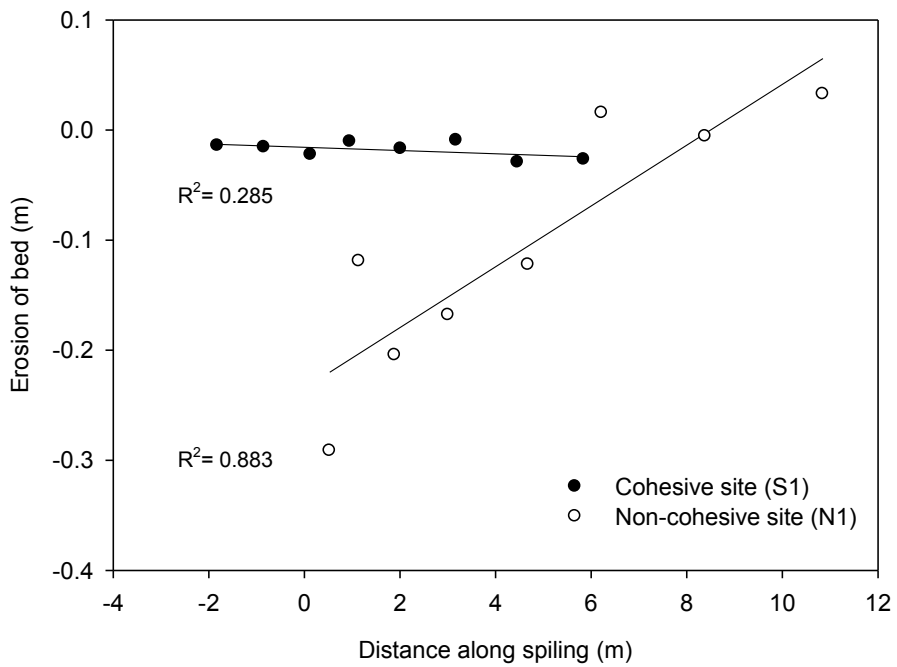


Fig. 5.4.8 Erosion of the river bed adjacent to the spiling that occurred between November 2009 and March 2010 calculated as a difference in elevation at zero cross-sectional area. The negative values on the x axis correspond with the section upstream of the spiling at the cohesive site.

5.4.2(B) THREE-DIMENSIONAL ANALYSIS OF THE RIVER BED

The cut-off plane (a plane taken through the highest common elevation) to determine the upper limit for cut-off (or fill-in) volume was chosen by the highest elevation present within the monitored area (Table 5.4.2) in November 2009 and in March 2010. The mean elevation over the cohesive site has dropped by a small degree (by -1.3 cm) and slightly increased at the non-cohesive site (by 0.78 cm).

Cut-off volumes have been calculated for this plane in Surfer and the mean value has been computed using the three rules described in the methods (Section 5.4.1(C)). Similarly to the mean elevation changes, there has been an increase in the cut-off volume at the cohesive site indicating loss of material of -0.227 m^3 , while there was an overall decrease in cut-off volume at the non-cohesive site indicating 0.204 m^3 of material gain. This means that within the surveyed area of river bed, more material has been deposited on the non-cohesive site than eroded.

Table 5.4.2 Statistical comparison of elevation changes at cohesive (S1) and non-cohesive (N1) sites, including cut-off planes and volumes of river bed.

	Cohesive site (S1)		Non-cohesive site (N1)	
	Nov 09	March 10	Nov 09	March 10
Z statistics (m A.O.D.)				
n	2949	2107	2787	3053
Minimum	22.202	22.185	8.691	8.466
Maximum	22.672	22.665	9.667	9.644
Mean	22.450	22.437	9.142	9.150
Median	22.453	22.443	9.145	9.183
Standard Deviation	0.117	0.114	0.218	0.256
Standard Error	0.002	0.003	0.004	0.005
Cut-off plane	22.700	22.700	9.700	9.700
Volume calculations (m³)				
Trapezoidal Rule	4.162	4.387	16.005	15.788
Simpson's Rule	4.161	4.393	15.988	15.807
Simpson's 3/8 Rule	4.167	4.391	16.017	15.803
Standard deviation	0.003	0.003	0.014	0.009
Mean volume	4.163	4.391	16.003	15.799
Volume difference		-0.227		0.204

To illustrate the changes within the elevation classes, the percentile distributions have been plotted. All elevations for the surveyed area outside the blanked region have been considered, as gridded by Surfer.

Elevations have slightly decreased in all percentile groups at the cohesive site, with more extremes at values lower than 25 and higher than 75 percentile. At the non-cohesive site the decrease occurred only within the 25 percentile of elevation and was very steep within the first 10 per cent of samples. Elevations above 25 percentile value increased slightly (Fig. 5.4.9), meaning that the most extreme changes happened within the lower river bed elevations.

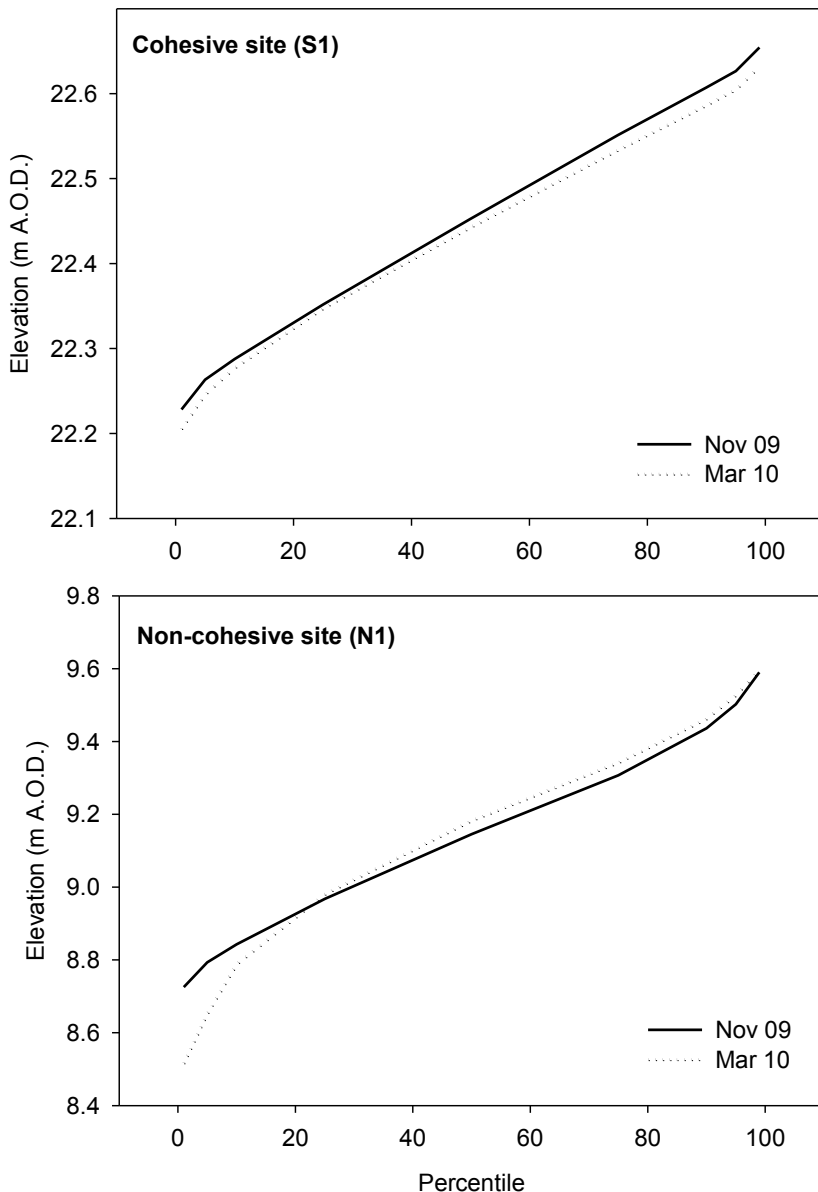


Fig. 5.4.9 Percentile distribution of elevation before and after high flow events at cohesive and non-cohesive site. The values for 1, 5, 10, 25, 50, 75, 90, 95 and 99 percentiles were plotted.

At the cohesive site, the higher elevation range (in red) is slightly shifted down towards the lower elevation range (in blue), (Fig. 5.4.10). At the downstream end there is less graduation, and more space is occupied by the middle range elevation. Although the slight colour shift shows slight erosion, this is not important in terms of undercutting or bank instability caused by bed scouring.

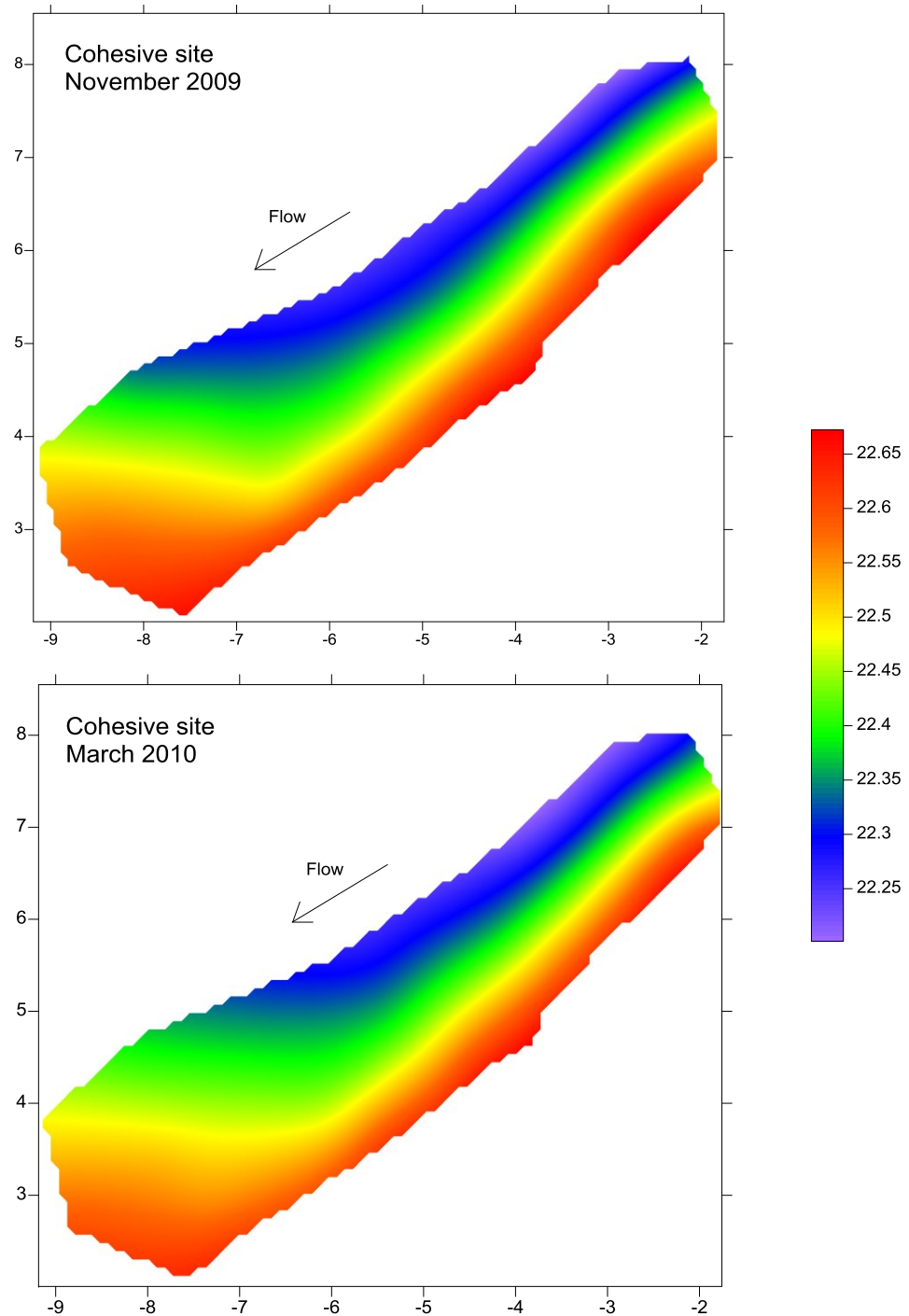


Fig. 5.4.10 Image map of the river bed at the cohesive site (S1) before and after high flow events. The shading is colour coded to represent each of the elevation values, shown by the scale on the right (as m AOD). The axes are coordinates in m.

At the non-cohesive site, the two image plots look different (Fig. 5.4.11). In the upstream section a shift of lower elevation towards the bank indicates some bed scouring. On the other hand, deposition occurred in the middle and downstream section of the surveyed river bed which is illustrated by an increase in elevation. The accumulated material could have either originated from within the same site or from further upstream.

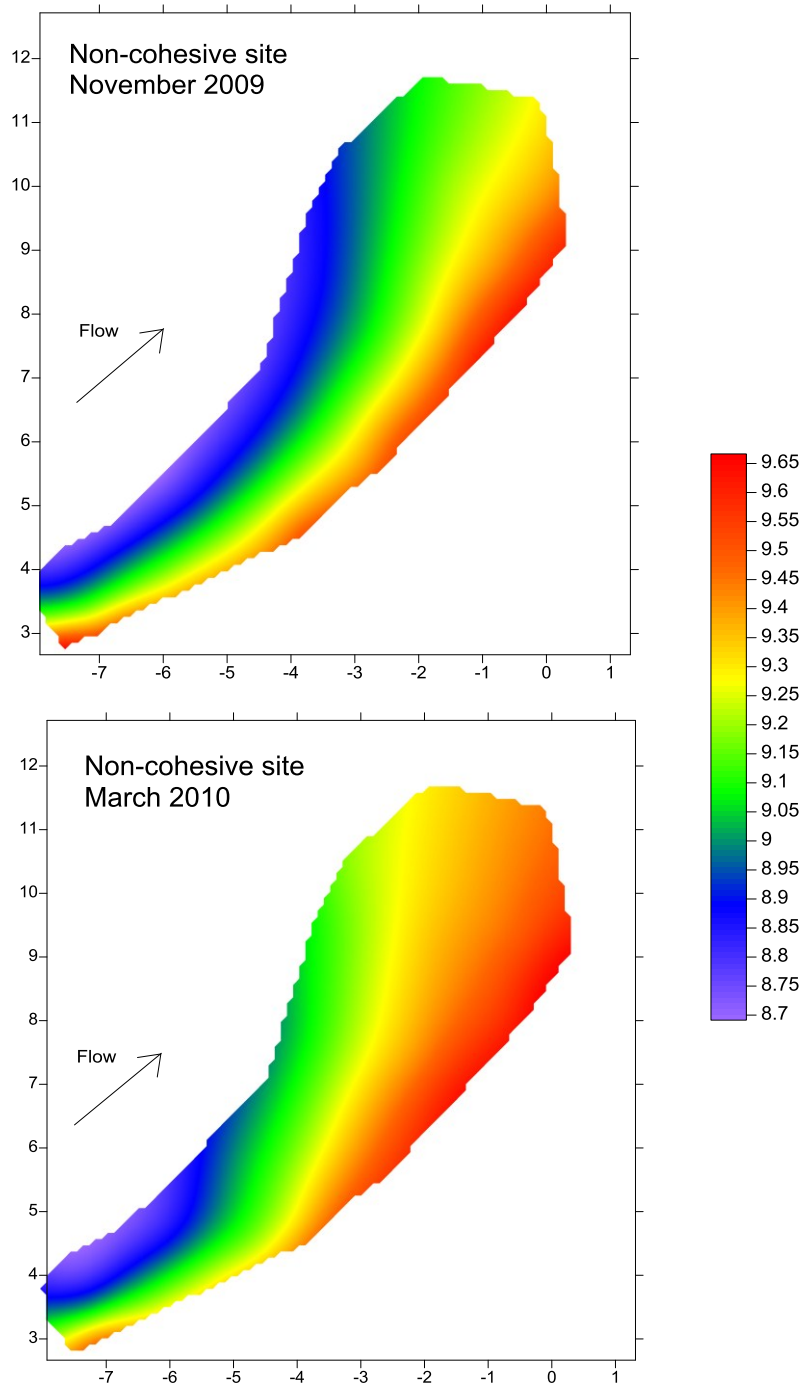


Fig. 5.4.11 Image map of the river bed at the non-cohesive site (N1) before and after high flow events. The shading is colour coded to represent each of the elevation values, shown by the scale on the right (as m AOD). The axes are coordinates in m.

5.4.2(C) THREE-DIMENSIONAL ANALYSIS OF THE BACKFILL

A similar approach to the three-dimensional analysis of the river bed has been employed in observing erosion and consolidation of the lower backfill. The upper cut off plane was used to set the high limit for fill-in volume. The height of the cut-off plane was based on the maximum elevation present within the site dataset for both dates (Table 5.4.3). Between November 2009 and March 2010 the mean elevation \pm SD of the lower backfill at the cohesive site dropped by around 10 cm from 23.63 ± 0.089 m to 23.53 ± 0.051 m AOD. At the non-cohesive site, the lower backfill eroded by around 7 cm from 10.610 ± 0.071 to 10.603 ± 0.097 m AOD.

Cut-off volumes have been calculated using this plane in Surfer and the mean value has been computed using the three rules (Section 5.4.1(C)). As indicated by the decrease in elevation, erosion and consolidation was also expressed as the increase in fill-in volume. At the cohesive site this was -0.156 m³ and at the non-cohesive site it was -0.234 m³ (Table 5.4.3).

Table 5.4.3 Statistical comparison of elevations at cohesive (S1) and non-cohesive (N1) sites, including cut-off planes and volumes of middle backfill.

	Cohesive site (S1) backfill		Non-cohesive site (N1) backfill	
	Nov 09	March 10	Nov 09	March 10
Z statistics (m AOD)				
n	2046	2171	2092	1970
Minimum	23.457	23.345	10.425	10.344
Maximum	23.859	23.627	10.725	10.802
Mean	23.632	23.532	10.610	10.603
Median	23.625	23.537	10.622	10.608
Standard Deviation	0.089	0.051	0.071	0.097
Standard Error	0.002	0.001	0.002	0.002
Cut-off plane	23.860	23.860	10.810	10.810
Volume calculations (m³)				
Trapezoidal Rule:	0.751	0.907	4.435	4.669
Simpson's Rule:	0.752	0.908	4.442	4.677
Simpson's 3/8 Rule:	0.751	0.908	4.438	4.671
Mean	0.752	0.908	4.438	4.672
St deviation	0.001	0.000	0.004	0.004
		-0.156		-0.234

To find out where, within the elevation range, most change occurred, percentiles of elevation were plotted for November 2009 and March 2010. Elevations of backfill have considerably decreased in all percentile groups, with a higher decrease at the upper

elevation end. At the cohesive site, this decrease was more extreme at values lower than 25 and higher than 75 percentile. At the non-cohesive site, the decrease occurred only within the 25 percentile of elevation and was very steep and within the first 10 per cent of samples. Elevations above 60 percentile value increased, which reflects sedimentation in the upper part of the spiling (Fig. 5.4.12). The image maps of lower backfills are shown on Fig. 5.4.13.

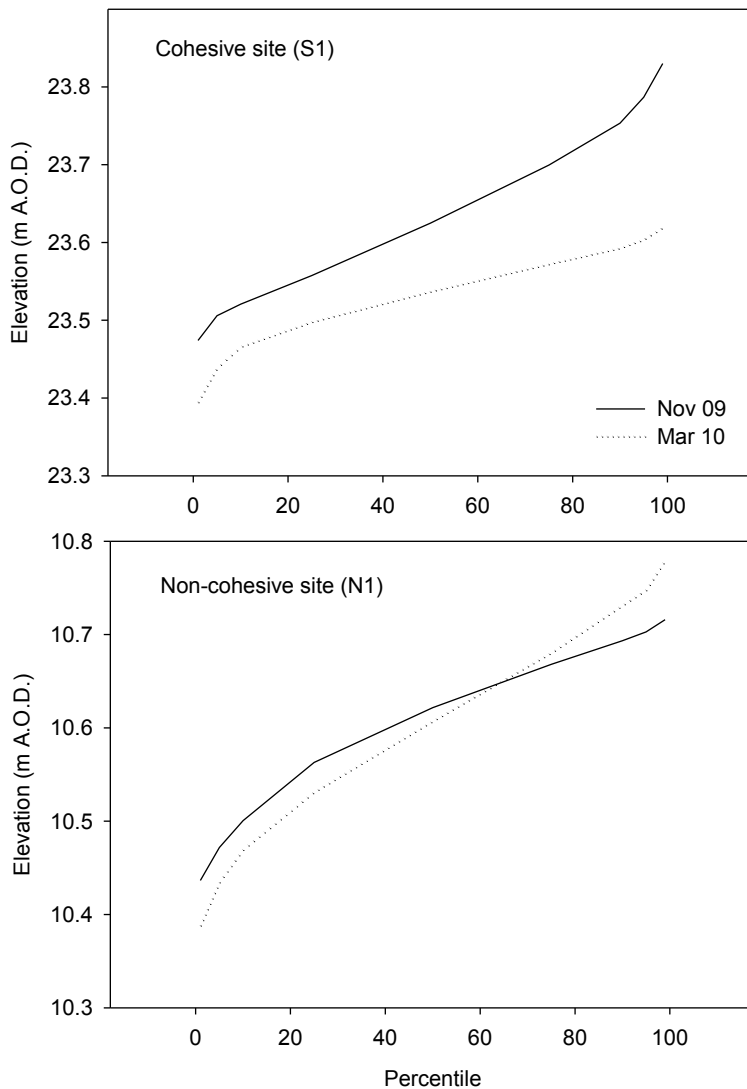


Fig. 5.4.12 Percentile distribution of elevation before and after high flow events at cohesive (S1) and non-cohesive site (N1). The values for 1, 5, 10, 25, 50, 75, 90, 95 and 99 percentiles are plotted.

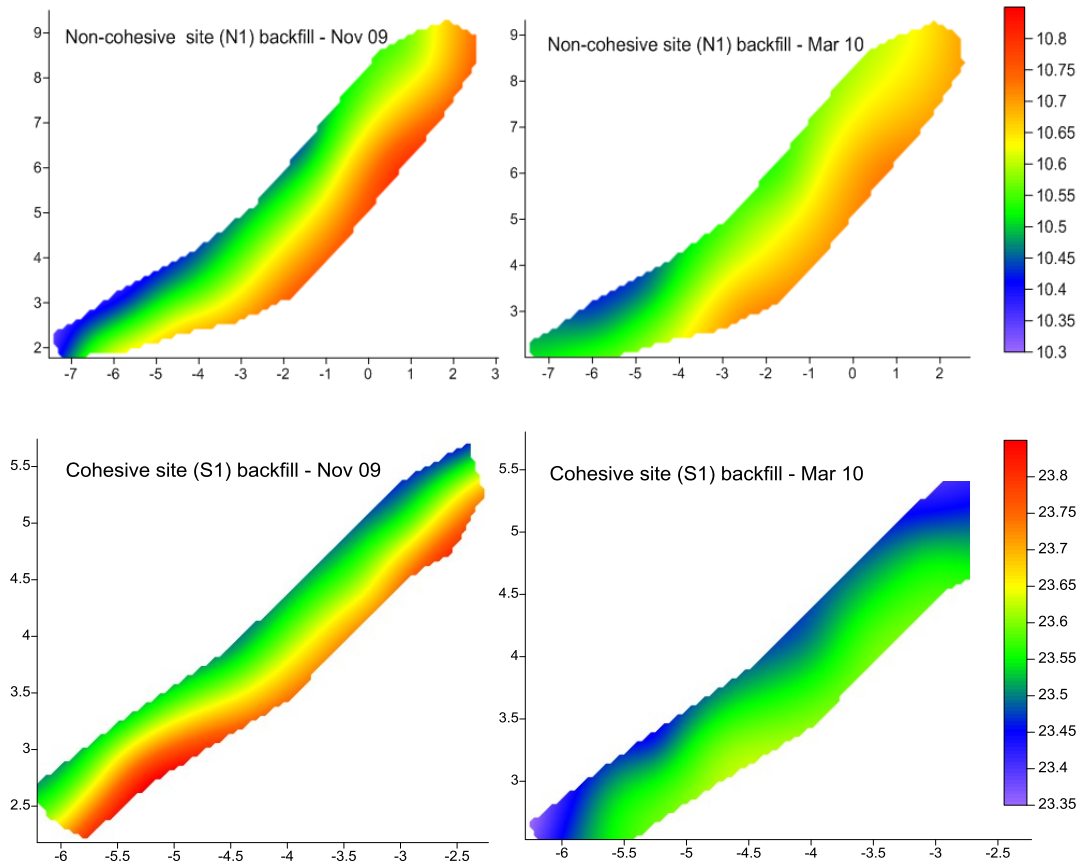


Fig. 5.4.13 Image maps of the backfill at the cohesive (S1) and non-cohesive (N1) sites before and after high flow events. The shading is colour coded to represent each of the elevation values, shown by the scale on the right (as m AOD). The axes are spatial coordinates in m.

5.4.2(D) MEASUREMENTS FROM STAKE TOPS

In addition to the surface analysis, changes to the backfill elevation behind the stakes at both upper and lower tiers were measured. Between November 2009 and March 2010, backfill at the cohesive site dropped by 3 ± 4.6 cm on average at the upper tier and by 6.2 ± 2.9 cm at the lower tier. The maximum eroded depth was 14.5 cm in the upper tier and 11.5 cm in the lower tier. On the other hand, the maximum sedimentation was 1 cm in the upper tier and there was no sedimentation recorded for the period in the lower tier, where backfill from behind all of the stakes eroded by at least 2 cm. In the upper tier, backfill from behind 27% of stakes eroded by at least 5 cm, while in the lower tier this occurred on 63% of the stakes.

During the same period, at the non-cohesive site the backfill retreated on average \pm SD by 0.7 ± 2.6 cm at the upper tier and by 5.9 ± 9.6 cm at the lower tier. The maximum erosion of

the backfill was 11 cm in the upper tier and 35 cm in the lower tier (the upstream entry section of the spiling). Material accretion by up to 9.5 cm in the upper tier and up to 2 cm in the lower tier occurred (Fig. 5.4.14). In the upper tier, backfill behind only 7.3% of stakes eroded more than 5 cm while in the lower tier, retreat over 5 cm was recorded on 31% of stakes.

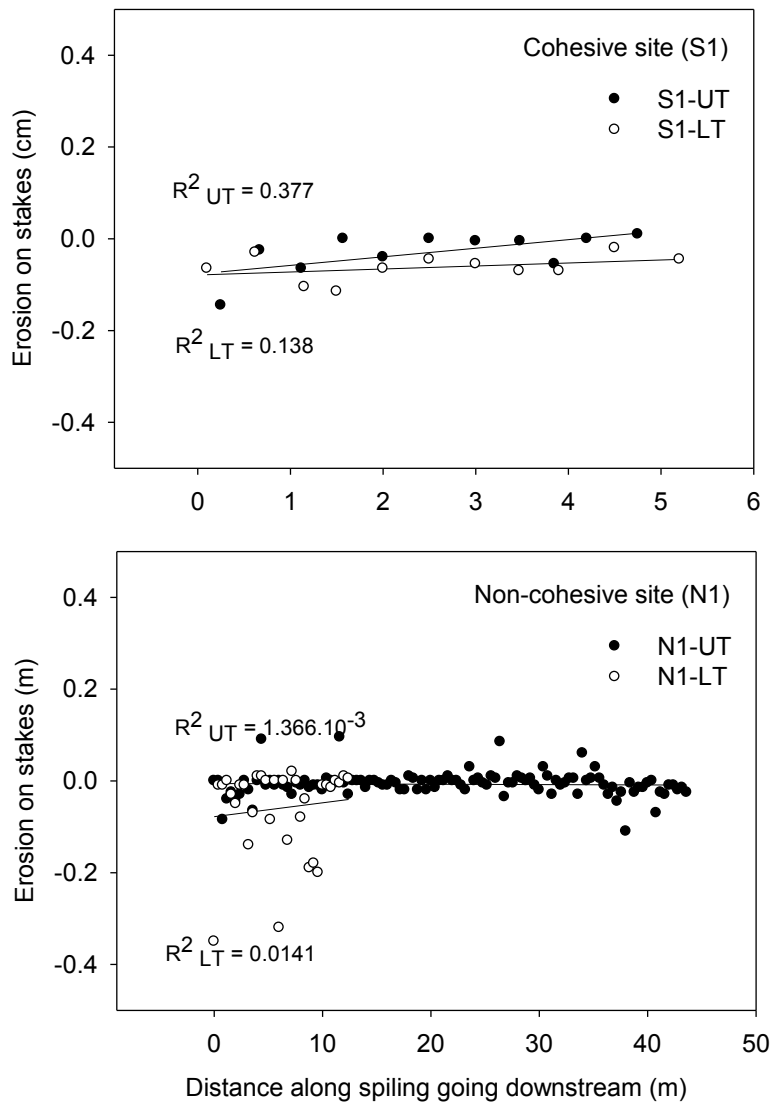


Fig. 5.4.14 Erosion on backfill that occurred on stakes in the upper (UT) and lower tiers (LT) at the cohesive (S1) and at the non-cohesive site (N1) recorded between November 2009 and January 2010.

At the non-cohesive site, scouring behind spiling was observed (Fig. 5.4.15). Again, most material was eroded from the spiling at the upstream end, showing the highest flow forces imposed on this part of the spiling. The total volume of eroded soil at this site in the period between November 2009 and March 2010 was estimated as 0.0257 m^3 .



Fig. 5.4.15 Eroded backfill on the lower tier at the non-cohesive site in March 2010 with visible roots and woven part of spiling that was originally under the backfill.

Factors which influenced the results presented in this chapter and further recommendations on how to eliminate the impact on the spiling from significant scouring of the river bed or to prevent the loss of backfill are discussed in Chapter 5.5.

5.5 PROJECT PERFORMANCE FACTORS AND RECOMMENDATIONS

In a natural environment, every project is subject to natural or anthropogenic factors that can be difficult to predict or control. These may have a significant effect on project performance, especially influences like extensive floods, droughts or intensive grazing and tramping. In this chapter, some of the most critical factors have been selected which might have influenced the ability of the two willow spiling projects to establish and stabilise themselves. These are grouped as abiotic, biotic and anthropogenic factors.

5.5.1. ABIOTIC FACTORS

5.5.1(A) RIVER FLOWS

High river flows influence spiling in three different ways: (1) by removing backfill from behind the spiling; (2) by scouring the river bed adjacent to the spiling and (3) by scouring the bank at either end of the spiling. A loss of soil from in front of and behind the spiling has been mentioned as one of the reasons for potential failure (Chapter 4). Willow canes that have lost contact with the soil are not able to thrive. Removal of soil and undercutting also makes the structures prone to mechanical failures. The entrainment of soil and bed undercutting has been more significant at the non-cohesive site N1 than the cohesive site S1 (Chapter 5.4).

A number of high flow events occurred during winter 2009/2010. The rainfall was well above the average for this season and February was reported as the wettest month in the period, when twice the monthly average rainfall was reached (EA 2011). From November 2009 until February 2010, soil moisture deficits were reduced to zero and the river flows were well above the average. In contrast, the period between March 2009 and October 2009 was extremely dry and soil moisture deficits were well above the average. Fig. 5.5.1 illustrates the discharge from 1 April 2009 until 31 March 2010.

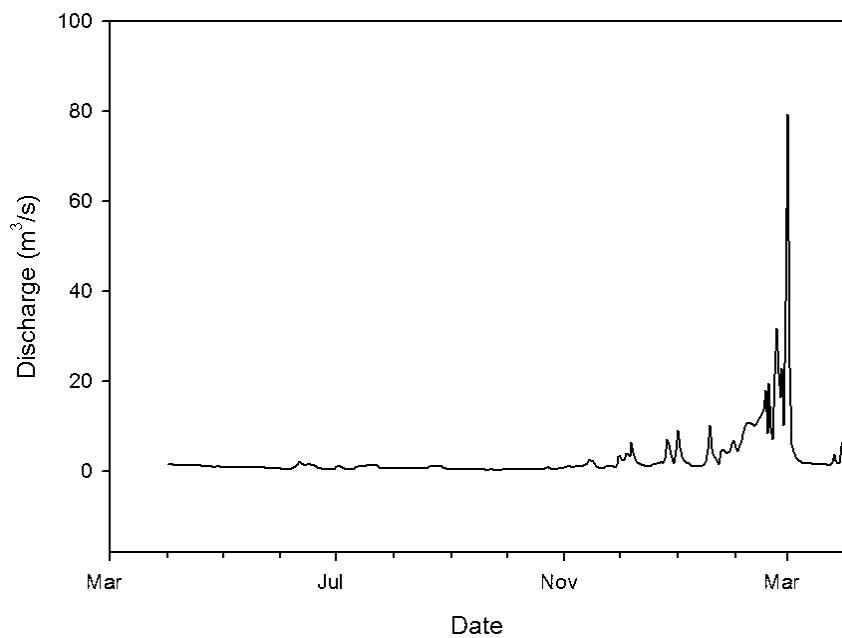


Fig. 5.5.1 Mean daily flows at Lamarsh gauging station between 1 April 2009 and 31 March 2010 (Based on data provided by the Environment Agency).

High flow events had the most significant effect on the river channel during the winter period as the stresses on weak bank and bed materials were high. The spiling had been constructed to withstand the maximum velocities on the river but gradual scouring caused by several events in a row could not be prevented. Between November 2009 and March 2010, the river channel at both sites was at the bankfull stage at four occasions. February 2010 was a month of persistently high flow (Fig. 5.5.2). Effective discharge with velocities able to transport channel boundary material occurred frequently during the winter period (Fig. 3.5.11, Section 3.5.3).

As reflected by the river flows, the winter season between November 2009 and February 2010 saw a lot of rainfall. November had a regional average totalling 104.7 mm making it the seventh wettest November since records began in 1910. February had 82.4 mm and was therefore the fourth wettest February since 1910 (Met Office 2011). Extreme rainfall produced flows that tested both willow structures (Fig. 5.5.3). In addition to the high flows, there were human-made alterations to water levels caused by the opening of flood gates.

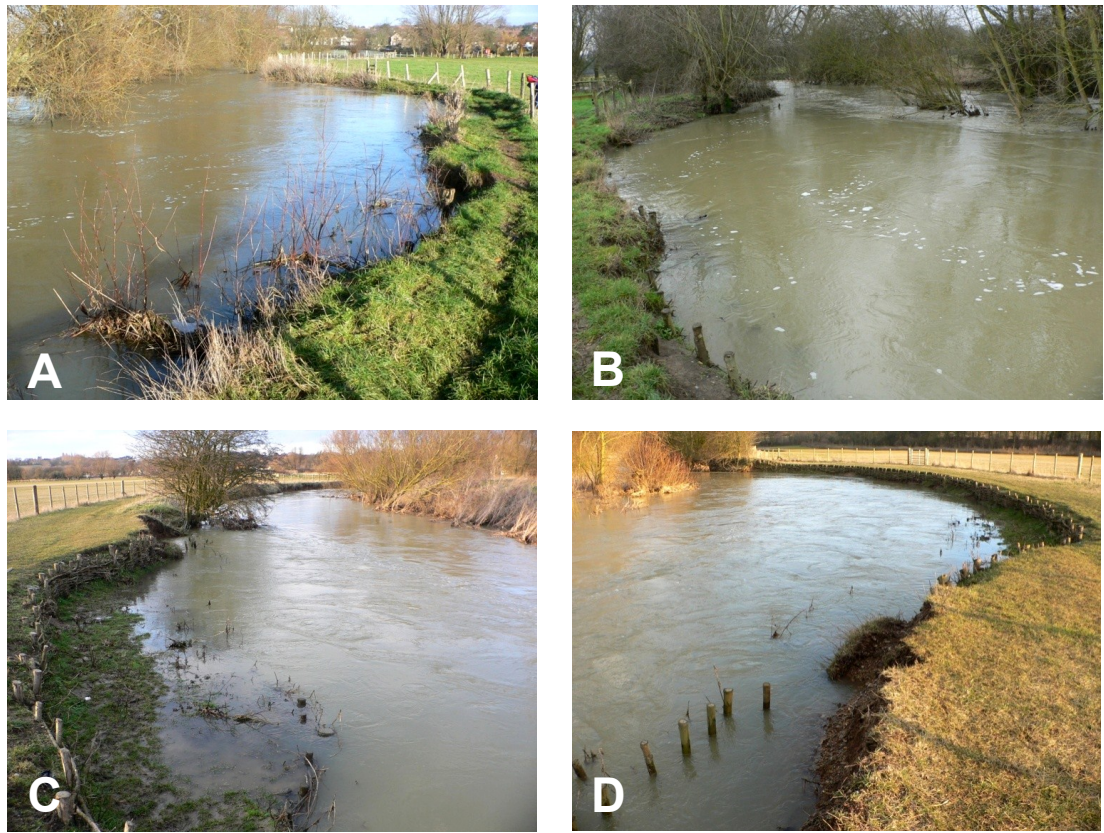


Fig. 5.5.2 High flow events during January and February 2010: (A) Cohesive site on 17 January 2010 before coppicing, looking upstream; (B) Cohesive site on 19 February after coppicing looking downstream; (C) Non-cohesive site on 20 February looking upstream and (D) on the same date looking downstream.

At the cohesive site, for example, the water level dropped from bankfull to minimal stage from 17 to 18 January 2010. The rapid drop in the water level caused some slumping upstream of the spiling which is also shown. Some erosion signs due to flow scouring after the floods occurred also at the non-cohesive site where the upstream end of the spiling was affected by the removal of part of its backfill. This happened because of erosion to the bank immediately upstream of the spiling into which the structure was integrated. The lower spiling should have been set at least 0.5 metres back from its present position.

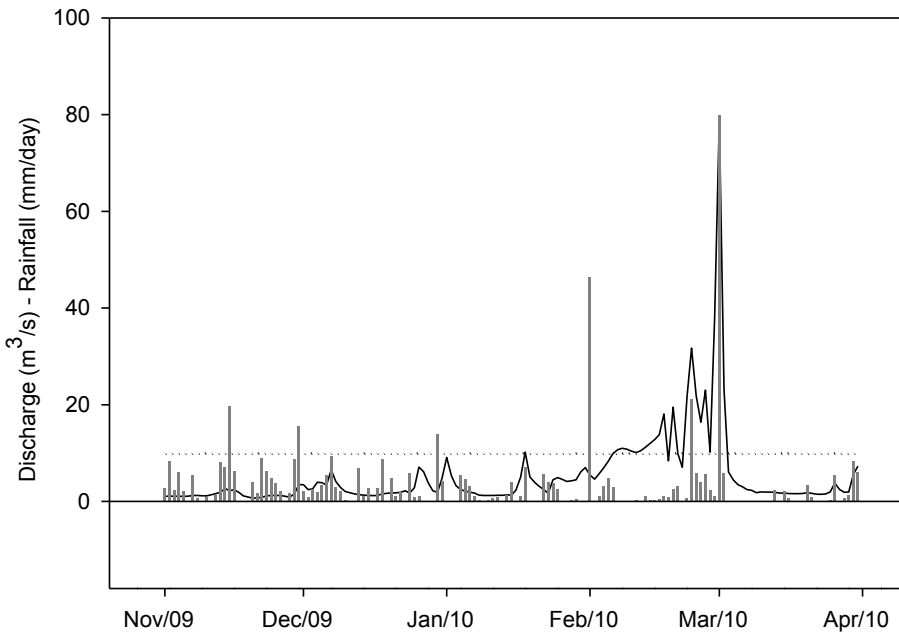


Fig. 5.5.3 River flows during the winter period from November 2009 to March 2010 as gauged at Lammarsh (in m^3/s) and rainfall data as derived from BADC data at surface gage 5106 in Lavenham near Sudbury (in mm/day). (Graph based on data by the Environment Agency and British Atmospheric Data Centre).

A test was undertaken to observe the effect on emergent seasonal willow withies from the spilling on the near bank river flow during a bankfull stage before and after coppicing at the cohesive site. Point flow velocities were taken at 40 cm distance from the bank and at 0.8 of depth (where maximum velocity should occur) on 17 January 2010 (before coppicing) and on 18 February 2010 (after coppicing), Fig. 5.5.2. Flow velocity readings were taken using an ultrasonic current metre SENSA RC2 over 45 second intervals. The readings showed that, prior to coppicing, near bank velocities adjacent to and within a short distance downstream of the spiling were close to zero. However, after this one year growth had been coppiced, near bank velocities increased (Fig. 5.5.4).

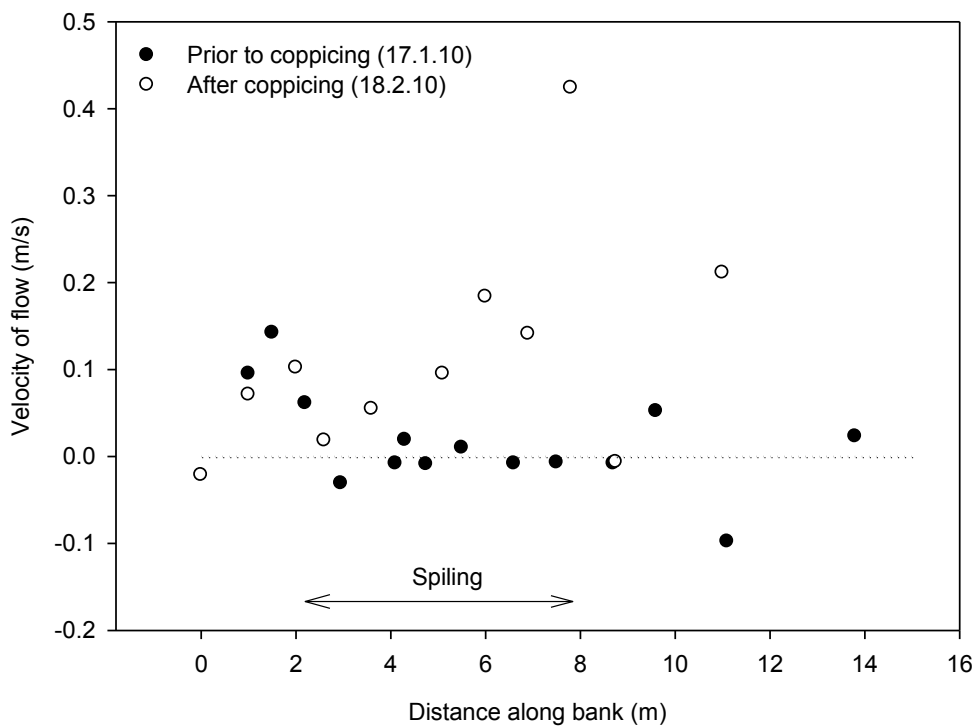


Fig. 5.5.4 Near bank flow velocities at the cohesive site S1 during bankfull events before and after coppicing (in m/s). The negative values are in the opposite direction of flow. The arrow shows the extent of the willow spiling.

This test confirmed the theory that flexible protruding withies from spilling do have an additional river bank protection function by greatly dissipating near bank velocities. The river flow is turbulent and flows in three dimensions. The situation during bankfull is especially complex near the river banks. Although more complex measurements would be needed to exactly quantify the effect of the willow cane on reducing the near bank shear stresses, the difference in speed of flow was visible to the eye. (Before and after flow situations have been captured on video in the Appendix).

Spiling at the two project sites was installed so that it would resist high flow events shortly after installation. However, to avoid the impact of winter high flows in this climatic regime on a newly built structure without roots and shoots, both revetments were installed at the beginning of the vegetation season. As mentioned in Section 4.1.3(E), frequent extreme events and changes in the length of the vegetation season limit the time slot available for installation. It is not possible to predict or control the effect of extreme events, which are becoming more frequent and of higher magnitude. But similar to high river flows, too low river flows are not ideal for installing spiling. Prolonged periods of drought can be as damaging to the living willow spiling, if not more, than extreme high flow events.

5.5.1(B) BED AND BANK MATERIAL PROPERTIES

Contrasting river bed and bank materials was thought to be one of the main reasons for the observed difference in riverbed erosion between the two sites (Chapter 5.4). The river bed at the cohesive site had a less erodible chalk base with sand and silt banks, while the river bed and banks at the non-cohesive site were composed of gravel and sands (Chapter 2.2).

The dissimilarity in bed and bank materials had, in addition to the effect on erodibility, effects on soil moisture and nutrient retention that influenced the growth of willows. The difference in moisture content is of particular importance to willows. As mentioned earlier, rainfall was very low in the first weeks after the willow spiling installation. For example, less than 40% of the average monthly rainfall fell in April 2009 (EA 2011). The initial period immediately after installation was found to be crucial for successful structure establishment as cuttings must maintain constant contact with water (Chapter 4.1). The soil moisture deficit remained high throughout the whole growing period, well above the long-term average, until the end of the vegetation season in November 2009.

The shortage of water was reflected in recorded differences in shoot extension rates, the number of new shoots and stake mortality later in the season. The results in Chapter 5.3 showed that the highest mortality and lowest shoot extension rates occurred on the upper tier at the non-cohesive site N1. This is because gravel differs from cohesive soil in its lower ability to store and chemically bind water (Chapter 2.2).

However, equivalence in water content does not mean that the same volume of water is available to plants as this differs with the soil type. Soil carries water that is available to plants known as available water content (AWC) and also as water that is chemically bound to soil particles. Once the available water in soil is depleted, the threshold moisture content of a plant losing its turgidity is reached. This stage is known as the permanent wilting point (PWP). For sands and gravels, the PWP is up to 7% and for silty loams this is between 9 and 21% (Coppin & Richards 1990).

In situ measurements using Time Domain Reflectometry (TDR) were used to test for differences in the volumetric water content. Available water content at the two sites were estimated based on the silty composition of the backfill. The readings were taken during a period of no rainfall, vertically at random places in the backfill at 20 cm depths on 8 and 9 August 2009. The mean volumetric water content (VWC) and upper and lower estimates of the available water content (AWC) are shown on Fig. 5.5.5.

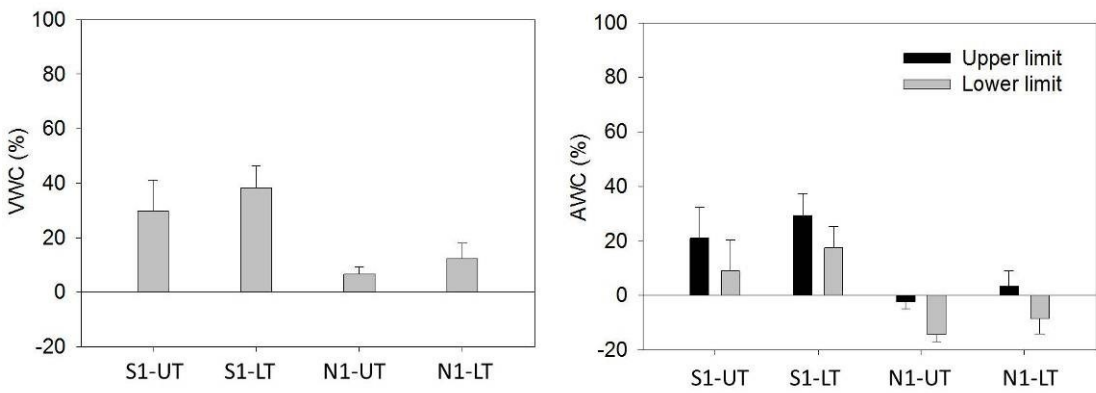


Fig. 5.5.5 Volumetric water content (VWC) and available water content (AWC) in % of soil volume estimated by Time Domain Reflectometry (TDR) on 8 and 9 August 2009. The data show the VWC and AWC on all tiers: Cohesive site – upper tier (S1-UT) where $n=16$ and lower tier (S1-LT) where $n=13$ and non-cohesive site – upper tier (N1-UT) where $n=18$ and lower tier (N1-LT) where $n=7$. The upper and lower limits in AWC show the range based on tabulated values (Coppin & Richards 1990). The error bars are the standard deviations of the mean.

The results show differences in both VWC and AWC within the sites and within the individual tiers. There was a significant difference between the volumetric water content at the two sites ($p=3.69 \times 10^{-4}$) with higher VWC found at the cohesive site. In addition, there was a difference in the water content between the tiers. Lower tiers displayed significantly higher VWC (for cohesive site $p=0.027$ and for non-cohesive site $p=0.034$). Similarly, the available water content would differ with the volumetric water content. There was a clear deficit in the water available to plants in the backfill at the non-cohesive site.

These differences were expected given the nature of the sites. At the non-cohesive site, water drained easily through the adjacent gravel bank. Additionally, the shoots in the upper tier that could contribute shade and slow down the evaporation had been removed by grazing (Section 5.5.3). Higher moisture content in the lower tiers at both sites was a result of (1) capillary rise and (2) soil in the lower tier being more shaded from drying by the wind and sun.

5.5.1(C) LIGHT CONDITIONS

Willows are pioneer species that need sufficient light for successful establishment. Insufficient light availability can have a repressive effect on the growth and survival of the plants (Chapter 4.1).

Both project sites had similar light conditions. They were situated on south banks (facing north) and there were no larger trees or any other objects that would shade any part of the spiling. From field observations, it appears that the most vigorous growth occurred from the top of the stakes. Some shoots growing from the lower parts of stakes that were shaded by the top growth became thin and eventually died. After some of the top growth was removed by grazers, the growth from the lower parts of stakes reappeared.

5.5.2. BIOTIC FACTORS

5.5.2(A) INVERTEBRATES AND FUNGI

Various larvae, aphids and willow weevils were reported to be feeding on the willow shoots during the vegetation period. Top tiers and upper shoots were the most exposed to invertebrates. Willow Redgall Sawfly (*Pontania proxima* LEPELETIER) was abundant in Sudbury (Fig. 5.5.6). The female adult sawfly inserts an egg into leaf tissue in late spring where it hatches and begins to eat the soft leaf tissue. This stimulates the leaf to produce a gall which is bean-shaped, smooth and emerges equally on both sides of the leaf and in which a single larva feeds. There are two generations of sawfly per year (Philip & Mengersen 1989).

Larvae of the Brown Tail Moth (*Euproctis chrysorrhoea* L.) were spotted on the upper tier at the non-cohesive site. They are well-known for their urticating hairs which can cause extreme irritation if in contact with human skin or breathing difficulties in people with asthma. They started to raise concerns in southeast parts of England and they have been recorded spreading further north (Brighton & Hove City Council 2009), (Fig. 5.5.6).



Fig. 5.5.6 Larvae of Willow Redgall Sawfly (*Pontania proxima* LEPELETIER) and Brown Tail Moth caterpillar (*Euproctis Chrysorrhoea* L.), non-cohesive site, August 2009.



Fig. 5.5.7 Fungi (left) and aphids and mosses (right) on dead willow withies, non-cohesive site, November 2009.

Also other butterfly larvae, aphids, lichens, algae, mosses and later in the season also various fungi were found on the spiling. The presence of fungi indicated dead withies (Fig. 5.5.7). Although it is difficult to quantify the impact of the invertebrates and fungi on the shoot growth or stake mortality, they did not influence the biological performance of the structure in a significant way. Willows tend to recover from pests attacks, and fungi or mosses are usually a sign of already dead wood (Section 4.2.4). Only a tree disease or a major infestation by Brown Tail Moth could cause permanent damage to the live willows in the structure. This is more likely to happen in the UK in the future if temperatures continue to rise.

5.5.3. ANTHROPOGENIC FACTORS

5.5.3(A) GRAZING AND MECHANICAL DAMAGE

Both projects were fenced off to prevent cattle grazing on the river banks. However, a small group of goats in Nayland (N1) was able to go under the fence and since July 2009, spiling at the non-cohesive site has been subjected to repeated grazing and trampling by these animals.

Willow stakes responded to the removal and damage to their primary shoots by producing secondary ones (called also the changing of apical dominance), comparable with pollarding and coppicing. As a response to stem damage, 'nodes' were formed where the stem was broken. In spite of the adaptations, repeated grazing and irreversible debarking (the removal of the live cambium layer) on the stakes significantly contributed to increased stake mortality during July and August 2009 because, in combination with drought, the plants were unable to regenerate (Fig. 5.5.8).



Fig. 5.5.8 Stake damaged by grazing at the gravel site (left), September 2009 and a recovery node created in the breakage zone on the stem (right).

5.5.4. RECOMMENDATIONS BASED ON EXPERIENCE FROM THE TWO WILLOW SPILING PROJECTS

During the 12-month post-construction monitoring period both spiling projects fulfilled their geotechnical function and, apart from some (not significant) erosion of the backfill, the previous bank retreat was successfully reduced, as proposed in the second research hypothesis. However, the biological performance of the spiling in one of the cohorts - on the upper tier at the non-cohesive site - was far from successful. The rate of change on the river bed adjacent to the lower tier at this site raises questions about the longevity of the revetment. Despite an attempt to follow the recommendations and case studies reviewed in Chapter 4, further issues arose during the research and a consensus in design has to be achieved that better accounts for factors such as extreme floods and droughts (which are more likely in the light of climate change scenarios) or mechanical damage caused by grazing.

It is necessary to realise that the mechanical performance of willow spiling can be controlled for each project and depends on good design, installation and management of the revetment. The spiling consists of three elements: the stakes, the withies and the backfill. The stakes act as 'pillars', woven withies provide surface protection and mechanical integrity of the revetment and the backfill is the growth medium and holds nutrients, moisture and aids stability. The spiling must be installed at both the upstream and downstream points into a stable bankline to avoid scouring at the ends. All parts must be well installed and remain in a good physical state to avoid failures within, behind or at the ends of the revetment. Growing conditions for willows including sunlight, nutrients and moisture have to be sufficient (Chapter 4.1), (C. Thorne, personal communication 2013).

To maximise the best mechanical integrity and longevity of willow spiling, and further to the suggestions concluded in Chapter 4, the following recommendations are made (related to Objective 7):

- (1) River bed and bank processes should be determined before installing the spiling. If a bank slope is due to fail with a failure plane below the depth of the structure, it will not be an effective revetment. The rate of erosion on the river bed, especially the basal endpoint, should be observed and if there is a danger of the spiling wall being undercut, it should not be placed there. Fast progressing toe scour could quickly undercut the spiling before the tree roots get established. Sufficient effort needs to be given to observing the river bed and bank processes during extreme

events prior to designing a solution. The highest possible velocity should be considered and gradual changes to the river bed should be projected for at least 5 years. If the bed proves unstable, spilling (but also hard engineering) may not be an effective solution.

- (2) Maintenance of the spiling is necessary to manage the vigorous growth that might otherwise cause problems in channel conveyance, especially in channels of smaller width. A well coppiced willow revetment should also live and maintain its function for longer than a non-maintained one. Coppicing should not be undertaken until after the high flow season. The reduction in near bank velocity alongside the uncoppiced spiling was much greater than along the bank without spiling. The flexible willow stems greatly retarded the flow during bankfull events. The effect of flow dissipation would increase with longer, older stems. Conservation objectives should also be considered when planning coppicing or any other management.
- (3) Structure should be retired into the bank. Some ends of the spiling were protruding from the bank and could cause end erosion in the future. Ideally, the spilling should be long enough to extend between sedimentation zones to avoid placing the ends of the spiling in highly erosive zones.
- (4) Stakes should be buried in the soil as much as possible. It has been observed that the upper tier at the cohesive site performed slightly better than the lower tier, even if the stakes were mostly buried with the backfill (protruding by 20-30cm as opposed to the lower tier stakes protruding by 80-100 cm in the lower tier). The burying prevented drying and splitting on the stakes.
- (5) Upper spiling in less cohesive soils should be placed further down the bank, especially on non-cohesive banks. Gravel and sand have lower water holding capacity than silt or clay. Even if the woven part of the spiling does not survive, the growth from the living stakes could be gradually woven in.
- (6) Shade early in the season should be prevented. To prevent the drying of stake tissues, the top of stakes could be protected by horticultural wax to decrease the evapotranspiration from the stake tops.
- (7) Willows can cope with invertebrate predators. Fungi and other decomposers can be a sign of a dead or unhealthy plant suffering from other causes such as drought. Certain types of disease such as the willow watermark disease could have more a serious effect and therefore it should be ensured that the material used is not affected.

- (8) Grazing and trampling should be prevented. Willows are able to recover from grazing pressure but if attacks are repeated and there is damage to the cambium layer on the stake, the chance of stake survival is highly reduced.
- (9) The backfill soil should be surface protected before the winter season. The top of the backfill could be left for natural regrowth, seeded or covered by a geotextile. Surface vegetation would help to minimize soil loss due to erosion by high flows. It may also help to retain moisture near the surface. On the other hand, some plants may compete with the willows so aggressive or invasive species should be avoided by choosing backfill from an area where there is a low risk of contamination by unwanted seeds.
- (10) Backfilling should not be delayed. Willows must be kept in constant contact with soil. Spiling should also be built to allow enough space for easy backfilling to avoid air cavities behind the structure. Any leftover willow material can be used in backfill but should be cut into small pieces and should be well mixed with the soil.

6. CONCLUSION

This chapter draws together the main findings on bank erosion rates, the review of willow spiling in the UK, and the performance of the two implemented projects. It concludes the main research findings in relation to the original research hypotheses and targets, outlining some practical results and observations on a chapter-by-chapter basis. Furthermore, it critically identifies the limitations of the research and lists areas where further work would be beneficial.

6.1. SUMMARY OF THE MAIN CONCEPT

The aim of this research was to determine the magnitude of river bank erosion and retreat rates on the River Stour in East Anglia and what were the main driving forces or properties that caused the erosion. It also intended to examine the soil bioengineering river bank stabilisation method of willow spiling in the UK and to test this method on the River Stour to find out whether it can work effectively in reducing erosion and whether it might be proposed as an ecological alternative in managing river bank instability problems.

River bank erosion has been reviewed as an integral part of complex river processes, but also a phenomenon that is in conflict with human land use and other needs (Chapter 2). The process of bank erosion was often approached in isolation as a threat to land or infrastructure and was commonly treated by hard engineering. Fluvial geomorphologists see bank erosion as a stage in natural channel evolution, apart from situations where erosion rates are unnaturally high. Thorne *et al.* (1996a) highlighted that in most instances, fast progressing erosion rates of typical rivers of UK size and climate are likely to be a result of human activity.

On the River Stour in East Anglia, both historical and recent engineering interventions, intensive river maintenance and artificially pumped water transfer flows have caused an alteration to the river channel's natural processes. Thus firstly, this research tested whether the magnitude of river bank erosion and retreat on the River Stour under these pressures is substantially higher than on other lowland streams of similar size and climate. This was not supported by the data (Section 3.4(G)). Based on previous research that has been reviewed, the author anticipated that additional river flows and engineering

alterations to cross-sectional channel profile dimensions (causing the banks to be steeper and higher) or to channel long profile dimensions (making the water surface slope steeper by installation of weirs or river straightening), would increase the magnitude of river bank erosion to a level that is substantially higher than what is typical for a similar stream (Hypothesis 1). The significance of tackling this issue has grown in the context of increasing water demand (and thus the amount of water necessary to transfer *via* the River Stour) due to population growth and climate change. Increased water transfers are due to start in 2013.

The river channel's adjustment to these changes was exhibited through channel instability at some locations. On the River Stour, these problems have been typically addressed by hard engineering, most often by the installation of gabion baskets. Not only were these of low ecological value, some failures were observed where gabions had collapsed or caused further scouring at the revetment ends (Chapter 2.5). Gabion revetments are increasingly seen as an out-of-date solution in the UK, especially their extensive use in rural areas. From field observations during this research, discussions with conservationists and rangers and by adopting the experience of soil bioengineering methods in the UK and overseas, the author felt that other alternatives to the gabion revetment, and hard engineering in general, would be more suitable on this and similar rivers.

Hence in the second part of this thesis, the research reviewed and tested an ecological alternative to the hard engineering option, a soil bioengineering approach known in the UK as willow spiling. It aimed to prove that if the method is implemented correctly, it can be effective in reducing erosion even on reaches of lowland rivers with a steeper mean water surface slope than is the mean typical for that river reach (Hypothesis 2). The reasons for choosing this method were manifold, but primarily, it was the geotechnical and ecological benefits of utilising live willow material - the flexibility, root function and the natural occurrence along the streams in the UK and with temperate climates overseas (Chapter 4).

The importance of this research lies in the deficiency of studies and post-project monitoring of soil bioengineering projects. The lack of research in this area, especially of data applicable to practical river engineering, has been identified as the most significant drawback that was preventing wider application of soil bioengineering methods. Thorne *et al.* (1998) highlighted a gap in the scientific basis for the application of vegetation-based methods in river management projects and Coppin and Richards (1990) suggested that research should aim to clarify to what extent vegetation approaches can be quantified and

what geotechnical advantages they provide over conventional materials. They suggested that the rate of success from implemented projects should be researched and be made available to practitioners, for example through a national database. To address this problem, the author firstly reviewed all available experience on willow spiling across the UK and with reference to some overseas projects, evaluated the success rate and listed the causes of project failures. Secondly, this experience was used in the implementation of two willow spiling projects on the River Stour. These were monitored in detail for their biological survival rates and growth and assessed geomorphologically to record any erosion on the banks or river bed. Factors such as drought, high river flows or grazing were discussed in relation to the end result, and based on this further recommendations on project procedures were drawn.

6.2. SUMMARY OF RESULTS

This research aimed to test the two research hypotheses by studying problems set out in seven objectives (Chapter 1.2). Based on the nature of the findings, the research results have been divided into three thematic parts:

- (1) Firstly, the magnitude of bank erosion and retreat at nine field sites on the River Stour were quantified. The magnitude of bank erosion and retreat were measured in the field between 2006 and 2010 (Objective 1). Field data were compared to river bank erosion data extracted from historical maps dated since 1880s, and with field studies from some other British streams (Objective 2). The relative influence of some properties of the researched river banks (such as bank material texture, bank height or angle, sinuosity or water surface slopes) were tested against the field erosion rates (Objective 3). The proportions of effective discharges were calculated and transferred flows and their relative influence on the field erosion rates was assessed (Objective 4).
- (2) Secondly, project experience on using willow spiling as the preferred soil bioengineering approach across the UK has been reviewed. Principle conditions, success rates and the most common causes of project failures were concluded (Objective 5).
- (3) Thirdly, the research presented the implementation of model willow spiling projects at two field sites on the River Stour that have relatively high stream power and evaluated them in detail using biological and geomorphological

parameters (Objective 6). It used these observations and discussed them against some of the negative pressures (such as droughts or high flow events) that the projects were exposed to during the 12 month project monitoring period and it concluded the preferred procedures for installing willow spiling and recommendations for its wider application as an alternative to the widely used hard river engineering approaches (Objective 7).

6.2.1 RIVER BANK EROSION RATES

A historical and field based study of river bank erosion rates was presented in Chapter 3. The study area (Chapter 3.1) and field site descriptions (Chapter 3.2) were followed by a study of historical erosion rates (Chapter 3.2) and the field based study (Chapter 3.4).

Nine field sites that had steep and high banks without woody vegetation and that had exposed signs of lateral erosion were established on the river. Nearly all of the sites were composed of cohesive material, with varying silt and sand content but low in the amount of clay. Only one site (N1) was composed of non-cohesive, gravel material. The sites were located within upstream, mid and downstream reaches of the River Stour and were under varying impact from the water transfer scheme. GB1 was a control site carrying only natural flows, GB2, GB3, LB1 and LB2 sites were downstream of the transfer outflow and thus were fully exposed to transfer flows. Sites C1, C2, S1 and N1 were located downstream of the Wixoe intake meaning that the river at these sites carried a reduced amount of water transfer. As the discharges became larger going downstream, the effect of the water transfer on the overall flow was reduced. A common characteristic of the sites was that they were located downstream of a weir which had influenced the water surface slope. The site sinuosity varied between 2.38 at site N1 and 1.02 at site GB2 and the river channel planforms were in different stages of meander development.

Historical maps dating back to 1886 were used in a GIS analysis of river bank erosion. Over this timescale, the mean changes were small and only a minor shift occurred in the channel at the Great Bradley (GB1, GB2, GB3) and Little Bradley (LB1 and LB2) sites. More obvious changes to the lateral shift of the river channel were detected at the Clare (C1 and C2), Sudbury (S1) and Nayland (N1) sites. Maximum retreat varied between 13.5 m (1904-1962) and -6.5 m (1962-2008), both at the N1 site. In the most recent period between 1966 and 2008, the S1 site retreated by 9.5 m. In terms of land loss overall, the S1 site contained the most significant land loss of 0.27 m²/m/year averaged for the length of

observed bank (1886-2008). Over the entire time period, the sinuosity decreased slightly across all sites by -0.045 ± 0.081 m/m, which can be attributed to channel straightening and bank stabilisation measures. The effect of the engineering averaged to all sites was higher than the effect of natural channel migration and adjustment to these changes.

A number of challenges encountered in analysing old maps were discussed, such as the assumption of linearity of change, accuracy of old maps and photographs, changes in channel definition, errors in processing and analysis and the level of human intervention. The last one, in particular, presented a major challenge. The S1 and N1 sites had channels modified during the 1886-2008 period, which resulted in a significant bank accretion at N1 site and a dramatic reduction in sinuosity at S1 site. With administrative changes to the rivers authority, engineering records were lost and thus it was not possible to confidently separate the extent of channel modifications from natural channel migration.

With reference to the assumption of linearity of channel change, Hooke (1979) examined erosion rates both in the field and from old sources and she found that the magnitude of erosion quantified through field monitoring was higher than the values obtained from old map sources. This theory applied to 7 out of 9 of the research field sites. On the remaining two sites the historical and the field erosion rates were both low. It was also demonstrated that the annual bank erosion rates decreased with an increasing time interval of observation.

Chapter 3.4 reported on the field study of erosion rates at nine field sites measured between 2006 and 2010. Three standard methods for field monitoring were adopted: erosion pins, repeated vertical bank profiles and bank edge surveying. In addition, a novel automated system for erosion monitoring (Photo Electronic Erosion Pins) was also tested. The methods were used to compliment or compensate each other and their effectiveness was discussed.

The bank retreat recorded on pins that were installed at eight field sites (all except N1) ranged between 0.30 m/year and -0.03 m/year. The mean annual retreat \pm SD was 0.06 \pm 0.07 m/year. There was no statistically significant difference in erosion retreat amongst the cohesive field sites or sections of the bank. GB1 and C2 sites appeared to erode the most while LB2 and C1 eroded the least. Comparing the three vertical bank zones, bank toes retreated more than bank tops. When account was taken of the channel scale, there was again no statistically significant difference between the sites. Data on site GB1 had shown still the highest annual erosion rate/channel width (0.0167), followed by GB2 and LB2.

A total of 13 vertical profiles were resurveyed at six field sites (all with cohesive bank material). The maximum retreat ranged between 0.326 m/year (at LB1-1 section) and 0.054 m/year (at LB2-2 section). It was found that the magnitude of erosion recorded on the pins, and the retreat calculated from the changes in the vertical bank profile, correlated.

Three field sites with a clear bank top edge were resurveyed on a number of occasions for channel planform changes: LB1, C2 (cohesive) and N1 (non-cohesive). The maximum retreat was 1.32 m/year at site N1 and the mean bank top retreat \pm SD ranged between 0.104 ± 0.304 to 0.208 ± 0.358 m/year. The most land lost per unit of bank length was also from the N1 site, and this was $0.15 \text{ m}^2/\text{m/year}$.

The individual field bank erosion and retreat data demonstrate a great variability between the sites or between the sections within a single site. This variation was also reported by other researchers although a relationship between the erosion rate and the catchment size was determined (Hooke 1980). This trend applied also to the research sites on the River Stour. In relation to Objective 2, the rate of retreat at the field sites did not differ substantially from the data reported by other authors on lowland or other rivers across the UK (Section 3.4.3 (G)).

Field based methods encountered some limitations and these were critically discussed (Section 3.4.3). A summary of these in terms of advantages, disadvantages and further suggestions for their successful implementation were outlined. Erosion pins, although regarded as a method for accurate reading of bank retreat, were, in some instances (GB3, LB2), counter-productive by either accelerating erosion through creation of scour around the pin or by reinforcing the bank. All three standard methods measured bank loss only between two dates and therefore the timing and magnitude of erosion events that contributed to the final recorded retreat was not established. The timing of erosion events during a short test period (November 2009 to March 2010) was determined using Photo Electronic Erosion Pins (PEEPs). Higher electric potential readings appeared to create a response to high flow events. Unfortunately, both erosion pins developed a scour that increased the light input to the photovoltaic cells and therefore did not provide readings of true bank retreat. These observations, together with the erosion rate data, contributed to fulfilling Objectives 1 and 2 of this research.

Chapter 3.5 brought together some of the most critical field site and river flow properties and related them to the field erosion rates. It speculated on how erosion rates were influenced by: (1) soil texture and shear strength, (2) bank and channel geometrical

properties and (3) river flows that contained an effective discharge, with special attention focussed on the transferred flows.

In relation to (1), it was expected, based on the studies reviewed in Chapter 2, that the higher the proportion of cohesive silt and clay, the more resistive the bank would be to erosive forces. However, the relationship between soil texture and erosion rates proved more complex than that. The author reviewed and tested the concept presented by Couper (2003), who suggested that higher silt and clay content could increase erosion in the bank zone where subaerial erosion prevails. This model seemed to fit the data from the River Stour sites.

All three mechanisms of bank erosion cycle, reviewed in Chapter 2, were observed: weathering, fluvial entrainment and mass wasting. Fluvial entrainment prevailed in the lower parts of the bank where shear stresses imposed by river flow were the highest (in magnitude, frequency, duration and efficacy). Weathering and subaerial erosion processes dominated in the middle sections of the bank that were exposed to weather elements as these sections did not contain plant roots and cover, and were wetted only during bankfull events. Mass wasting occurred mostly in the top section of the bank. Typically overhangs were formed with a thickness that corresponded to the rooting depth of grass growing on the top, of around 30 cm. These collapsed when they reached critical dimensions, usually during saturated conditions after a high flow event. A number of failures were observed with failed blocks of 40-50 cm in width.

Based on the erosion processes, the cohesive banks at the research sites were divided into three vertical process dominance zones: (1) top zone, where cantilever failures prevailed due to the added strength of grass roots, (2) middle zone with subaerial processes in dominance and (3) toe zone, where fluvial erosion was the leading erosion mechanism.

The texture of the bank material at the cohesive sites was examined in relation to erosion for each bank zone in isolation. In the top zone, the clay content was too small to be of significance to the erosion pin readings. The clay-silt content in the top zone did not show any correlation, while in the middle and lower bank zone it showed a trend that was in agreement with the theory by Couper (2003).

The bank angles and heights were reviewed as important components of bank stability theory, and determinants of the Factor of Safety. Bank angles and heights were established in close intervals along the two research sites LB1 (cohesive) and N1 (non-cohesive) and the data were related to the bank retreat at each measured point along the bank line. At

both sites regardless of the bank material, the steeper upstream sections of the observed banks (that were adjacent to deeper pools) driven by toe scour, eroded more than the downstream half of the stretch (adjacent to shallower glides and point bars). Because the bank heights were less varied, bank angles that ranged between 37 to 78 degrees at the LB1 site and between 20 to 63 degrees at the N1 site appeared to be the driving component of bank geometry and were critical for the state of basal endpoint control.

Possibly, a stronger correlation would show if the data on the bank top retreat were surveyed over a longer period of time. This is because the retreat at the bank top typically happens at the moment of mass failure. The field planform surveys could not show the preparatory stages of the erosion cycle, which operate over a period of several years.

Other channel properties such as sinuosity and water surface slope, upon which the shear force component depends, were not found to correlate with the field erosion data. Because they were inversely related and would both increase shear stresses, a peak combination of both could mean that an incidence of high retreat was most likely, such as at the S1 site. At locations where the water surface slope and sinuosity were low, the maximum bank retreat was also low. Bank material and geometry, water surface slope and sinuosity (which were tested against the field erosion rates) made only a partial contribution towards answering the Objective 3. This analysis was restricted because only some factors influencing the complex bank processes were considered and these were studied in isolation. Other approaches that account for the interactions of the site parameters, including the channel planform, should be also considered for a fuller explanation of the causes of erosion on the river (Chapter 6.3).

To test the effect of river flows on erosion in relation to Objective 4 of this research, two approaches were used. The first one elaborated flows that were exceeded 10% of the time (Q_{10}). The associated discharges were $2.3 \text{ m}^3/\text{s}$ at the Keddington gauge (indicative of GB1, GB2, GB3, LB1 and LB2 sites) and $2.7 \text{ m}^3/\text{s}$ at Westmill (indicative of river flows at C1, C2 and S1 sites). The second approach was based on a theory that mean velocities over 1 m/s were likely to initiate particle entrainment of the cohesive banks on the River (Chapter 3.1). These velocities were produced by flows greater than $0.6 \text{ m}^3/\text{s}$ at Keddington and $2.3 \text{ m}^3/\text{s}$ at Westmill. This was referred to as the effective discharge for particle entrainment (Q_{Eff}).

Between June 2006 and April 2010 flows of or above Q_{10} threshold occurred at the field sites on up to 63 days and flows of or above Q_{Eff} threshold were present on up to 397 days (depending on the river site). The water transfer represented up to 44% of all effective

flows at the upstream GB and LB sites, while at the downstream sites it created a much smaller fraction of up to 18%. These data demonstrate the downstream decrease in the impact of the water transferred, firstly showed on river flows in Chapter 3.1.

Data from pin readings were used to explore the relationship between the river flows and erosion rates to make an assessment as set out in Objective 4 of this research. A correlation analysis of pin readings and number of days of exposure to these flows did not show any relationship in any of the bank zones. Although high flows and prolonged wet periods have been cited to increase erosion, the number of Q_{10} events or days with Q_{Eff} flows in this test did not appear to influence erosion rates in isolation. Other processes and properties perhaps took dominance or acted in combination with these flows. The only geomorphological evidence of the water transfer that was found was the flat bank area that occurred, most prominently, at sites LB2 and C1 (Fig. 3.5.1). This flat area is the result of flows with steady discharges over longer periods of time that are typical for the water transfer scheme and can be considered as the only positive evidence towards Objective 4. More evidence in relation to the transferred river flows could have been collected by taking a continuous, automated approach as suggested in Chapter 6.3.

To summarise this section, the field erosion rates were not substantially higher than on other comparable rivers and appeared to fit the general trends of variability, relation to the catchment size or the historical decrease of annual erosion rates with an increasing length of study period. However, some effect of past river engineering such as the channel alterations that resulted in an increase in the water surface slope, bank height or bank angle, appeared to have influenced the erosion rates. Engineered banks were higher and steeper than they would be in natural conditions and the presence of weirs or channel straightening increased the water surface slopes and thus the stream power. This demonstrated that the anthropogenic interventions had increased river bank instability, although it is not possible to quantify the extent. One side of the problem lies in the complexity of river bank processes, the other in the lost documentation about the exact position, scale and timing of the engineering interventions on the river. From the field erosion rates and river flow correlation it is also unclear whether the additional flows from the water transfer increased river bank erosion rates, despite the fact that the transferred flows created nearly half of the proportion of discharges effective for particle entrainment at the upstream sites during the study period. And, except the morphological evidence found at some sites, the author is not able to confidently say that the transferred river flows increase the rate of river bank erosion on the River Stour. Propositions on how this could be resolved are suggested in further research (Chapter 6.3).

6.2.2 WILLOW SPILING REVIEW

Chapter 4 reviewed the history, fundamental design considerations and project experience of willow spiling in the UK. A reference has been made also to the use of this method in other countries. Willow spiling was presented as a combination of traditional craft and engineering that involved weaving long willow stems around vertically installed willow poles. The evidence of using willow as a material for river bank protection was tracked as far back as 28 BC. It was reported as currently being the most popular willow-type revetment in the UK.

The author collected information about 139 projects implemented over the last 20 years. Added together, willow spiling projects were used to stabilise 47 km of river banks in the UK. Despite the reports on successful installation, information on post-project performance was available only in 27% of cases. Out of these, 60% were assigned as successful, 30% failed partially and 10% were a complete failure, in which case the spiling was not fulfilling its bank stabilisation function. The most common causes of project failure were undercutting, damage by flood flows, poor growth due to low quality material or the presence of shade. The author believes that most failures were avoidable if the design considerations reviewed (Section 4.1.2) had been carefully considered. Systematic project monitoring should be part of all projects and lessons learned from both successful and failed projects should be made available to river practitioners that are considering using this method.

In relation to Objective 5 of this research, the UK project experience has demonstrated that willow spiling was, in most cases, effective for river bank stabilisation and at the same time it provided numerous other benefits, including habitat enhancement, river restoration and public engagement. If the willow spiling was not sufficient on its own to stabilise the river bank, it was suggested to use it effectively in combination with other biotechnical or hard engineering methods.

6.2.3 PRACTICAL APPLICATIONS AND POST-PROJECT MONITORING OF TWO WILLOW SPILING PROJECTS

Chapter 5 presented two model applications of willow spiling and reported on their biological performance and geomorphologic changes in detail. The most important factors that influenced the spiling were discussed. Recommendations on the implementation procedures were listed, following on the experience from these two projects.

The two sites, cohesive S1 and non-cohesive N1, had both been proposed for hard engineering projects. River bank retreat was significant, at S1 this was up to 0.30 m/year and at N1 the upstream end eroded by up to 1.32 m/year (Chapter 3.4). Both project sites had water surface slopes steeper than the mean water surface slopes typical of their river reach and stream powers, and are comparable to some upland streams in the UK. The mean bankfull velocity was estimated as 1.45 m/s at the cohesive and 2.36 m/s at the non-cohesive site, which was within the permissible velocity range for live willow revetments (Chapter 4.1). Because the maximum recommended height of a willow spiling wall was 1 m, two-tier systems were opted for to protect the >1.5 m high river banks at both sites.

Considering that willow spiling survival and growth was regarded in the review as one of the key criteria to the long term success of the live revetment, much attention was given towards biological growth and survival of the willow stakes 12 month after installation. The early stages of vegetation establishment and survival were regarded as the most critical in terms of surface protection and stability (Jarvis & Richards 2008).

Three parameters have been used to describe the biological growth and survival on both spiling projects: (1) stake survival, (2) shoot length and (3) number of live shoots. These indicators were observed on a monthly basis during the first vegetation season after installation, May–October 2009.

Initially, there was a 100% survival rate on stakes in each tier. Later, this rate dropped slightly at the cohesive site but decreased considerably at the non-cohesive site (down to 17%). Such high mortality was a result of repeated grazing and drought. The energy stored within the stakes was depleted early in the season and without well-developed root systems the plants were unable to resist the imposed water and grazing stress.

Mean shoot lengths were similar throughout the season in both tiers at the cohesive site ($p=0.54$), with the upper tier performing slightly better than the lower tier. At the non-cohesive site, the upper tier displayed fast growth at the start, but after one month, the lower tier took over. Later in the season, there was a decline in the growth on both tiers. Overall, the lower tier at the non-cohesive site performed considerably better than the upper tier ($p<0.0001$).

In contrast, the number of shoots was significantly higher at the non-cohesive site than at the cohesive site ($p=0.017$). Two biological methods were used to combine the number of shoots with shoot extension to obtain an overall picture of the performance on each cohort: (1) Net Seasonal Shoot Extension (NSEE) and (2) summed shoot length per stake. Based on the latter, the non-cohesive site performed better initially, however due to shoot

removal and higher mortality, the resulting summed shoot length was a number of times lower than at the cohesive site.

To evaluate the geomorphological function of the spiling and to make a prognosis of its potential for the future, processes on the river bed and on the backfill were recorded during the first winter after installation (November 2009 and March 2010). River bed elevation data were important for locating and quantifying processes acting on the river bed. The nature of the data collected allowed cross-sections to be cut through any section of the data surface to observe changes at any point on the river bed. Two other data analyses have been employed to supplement the cross-sectional data: the percentile elevation plots and volumetric analysis. The combination of the methods used was a powerful tool in describing elevation and spatial change in river geomorphology.

More significant erosion and sedimentation processes occurred at the non-cohesive site N1 as opposed to the cohesive site S1. At both sites, erosion prevailed in the upper sections of the spiling and the rate decreased downstream. At the non-cohesive site, the sedimentation has been noticeable on the river bed as well as on the backfill. Overall, more material was deposited than was eroded. The downstream end of the spiling was therefore stable while the upstream end had been subjected to high shear stresses. The differences in the river bed elevation immediately adjacent to the spiling revealed substantial toe scour (up to 29.14 cm at the non-cohesive site). This is possibly a rate that the spiling would not be able to compensate for with its roots and without a further human input this part of the structure may fail. This assumption, together with the evaluation of biological survival and growth of the willows, fulfils Objective 6 of this research.

Both projects were tested by a range of factors, some of which were of extreme nature and not planned for in the design stage. The climatic extremes are due to increase with the effect of climate change in this region. An examination of the conditions the projects were exposed to, in order to draw recommendations for future projects, was set out in Objective 7 of the study. The sites were intentionally situated on steep sections of the river with unstable, fast eroding river banks. Because willow spiling demonstrated its geotechnical effectiveness under these conditions 12 months after installation, in what are high stream power river sites, it could, potentially, be applied elsewhere on the River Stour and across lowland East Anglia. However, some general procedures were listed that would have improved the performance of the two spiling projects and that would better accommodate any negative effects the projects were exposed to. Especially they would eliminate the

partial failure later evidenced at the non-cohesive N1 site (Chapter 7 reports on the projects three years after installation). This site suffered more from drought due to the lesser water holding capacity of gravel bank material and from grazing attacks. Considering that the grazing and design problems could have been easily fixed at the N1 site and the fact that the S1 site performed well, the method can be considered as an ecological option to river bank management on banks of rivers with similar climate and properties.

6.3 LESSONS LEARNED AND FURTHER RESEARCH DIRECTIONS

As often happens during the course of this type of research, more research gaps and questions than originally outlined in the introduction were identified and some suggestions for further research are listed below. Furthermore, this study was unable to fully address all the research questions and hypotheses due to a number of challenges that still remain.

Site selection was critical to the study and the sites chosen were, intentionally, not a representative random sample of the bank conditions on the river. Observed banks were high, steep and without vegetation and exhibited signs of erosion. What was not fully considered in the selection process was the channel planform context and the various stages of meander development. These could have been important contributors to the differences in erosion rates that were not explained by other tested properties (in relation to the Objective 3 of this research). Some banks had morphological evidence of the water transfer while others did not, but these had a visibly varied bank stratigraphy. Any evident stratification should have been considered when placing the erosion pins and sampling for bank material textures.

One of the most significant factors, in relation to the first research hypothesis, was the issue of quantifying and separating the influence of the additional river flows due to the water transfer scheme on the river bank erosion rates. No correlation has been found and it proved difficult to state the proportion of erosion caused by human interventions from that caused by natural river processes. It has to be stressed that river bank processes are very complex and the difficulties of separating the individual erosion controls to quantify what effect they are having on river bank erosion had not been appreciated in the initial stages of this study. However, further advances to better address Objectives 3 and 4 could be made by improved investigative design with more intensive observations in the context of transferred flows, both on a spatial and a temporal scale and by elaborating other

approaches that would consider a combined effect of channel dimensions and stream power (Simons *et al.* 1965; Ferguson 1981; Hickin & Nanson 1984; Hudson & Kesel 2000). If funds were available for the equipment, high resolution data for both the temporal and spatial scales could be supplied by thermally-adjusted Photo Electronic Erosion Pins (PEEPs). The results would reflect the responses to the transferred or natural flows. If the drawbacks of this method could be suppressed, the minimal discharge for particle entrainment could be established. The PEEPss could be improved for example by using a flexible photo-array and a wireless device that transferred the voltage output to the data-logger connected to a remote data network. With regards to the classical manual pins, these could be made out of flexible graded tape to eliminate the rigid strength that comes from the solid steel pins. Spatially more complex studies could be carried out by ground-based Li-DAR (O'Neal & Pizzuto 2011). This technology, although expensive as an investment, displays great accuracy, saves cost as it is time effective and provides comprehensive data without any disturbance to the river bank, thus it overcomes most critical challenges encountered by using the standard methods. If used before and after water transfer situations, this approach could highlight some of the less distinctive changes in the river bank morphology. It could point out the main geomorphological effects of the water transfer, for example the occurrence of flat benches that were observed in the vertical profiles at some research sites.

In addition, data on suspended sediment and bed load transport during varying flow conditions would help to establish the new dominant and effective discharge for particle entrainment downstream of the transfer scheme. Data on sediment load at the transfer confluence with the river and at varying points downstream would show the net change in sediment concentration. Because the water transfer is operational during dry periods without much rainfall, any increase in sediment load would be attributable to the bed and bank scour and would thus serve as evidence that the water transfer flows contribute, or not, to river channel erosion (this would directly relate to the Objective 4). These data could be fed to the flow equations proposed in Chapter 3.1 which need further development and analysis using a hydrological model in order to calculate the dominant or effective discharges at each of the sites at any given point in time.

To put the bank erosion results into a direct context with the bank stability analysis (Chapter 2.3) and to make recommendations for further management, it would be worthwhile to establish the threshold bank properties (e.g. maximum bank angles and bank heights) at failure for the research sites. In particular, it would be useful to establish: (1) the new bankfull discharge and corresponding bank height/bankfull height ratios, (2)

Factor of Safety for the vertical bank profiles for varying types of bank failures and (3) bank stability indexes, such as Bank Erosion Hazard Index (BEHI) by Rosgen (2001) or the Channel Instability Index (I_i) by Simon & Downs (1995) by their calibration for the River Stour. These would then allow a quick identification of the potential bank stability problem areas and would be a useful tool for river management.

On willow spiling, a number of recommendations for better implementation and increased success rates were summarised in Section 5.5.4. The issues that these recommendations stem from arose during the installation and post-project monitoring and were not anticipated in the initial planning of this part of the research. Post-project monitoring options reported in Chapter 5 were also not exploited and more sophisticated in-depth analyses should be implemented to strengthen the outcomes in exploring the effects of prime factors, such as the Principle Component Analysis (Abdi & Williams 2010) or Geographically Weighted Logistic Regression (Atkinson *et al.* 2003).

Finally, more research into the biotechnical function of willow spiling needs to be done, as outlined by Thorne *et al.* (1998) or Coppin and Richards (1990) in the Introduction section (Chapter 1.1). Although structural stability was not an issue at the research project sites, it could be with others (Chapter 4). The concept of geotechnical stability analysis for willow spiling immediately after installation and during various flow or soil moisture conditions may need to be developed. As spiling is a retaining wall, in principle it resembles sheet piling and thus similar Factor of Safety relationships can be tested for this method. Stability equations for willow spiling could aid the design stage by establishing the minimal depth of insertion, maximum retaining height of the willow wall or minimum stake spacing. If reliable, this type of approach may put this vegetation-based method in a more favourable position in wider river engineering. The structural stability of the retaining willow wall is an issue especially during the early stages before the root system develops in the first one to two years after installation.

7. FOLLOW UP TO THE TWO WILLOW SPILING PROJECTS THREE YEARS AFTER INSTALLATION

Both willow spiling projects were visited on a few occasions after the biological and geomorphological monitoring had formally ended. The last visits took place in June 2012, over three years after both installations were established. While the revetment in Sudbury, S1 site, remained very much the same (Fig. 7.1) as three years previously, the spiling wall in Nayland, N1 site, had changed considerably (Fig. 7.2). The 50 m long eroding bank edge that was found to be retreating at a rate of up to 1.3 m per year before installing the revetment (see Chapter 3.4) has become stable, apart from two locations close to each other where the river flow reached behind the spiling and started to erode the bank edge. The total length of these failures was 4.5 m and the bank retreat rate there was 0.5 m. The upper tier on this stretch, apart from one stake, had failed to survive, the withies had dried out and disintegrated, and dead stakes had started to decompose. Without any vital root system, willow spiling is short lived (Chapter 4). Two stakes had already been removed from the revetment by the river flow. However, the lower tier had survived well, shoots were in abundance and it has been successful in protecting the bank from erosion. The shorter lower tier was expected to be undercut in the years immediately following installation (Chapter 5.4) as it was exposed to the highest flow velocities, yet this now appeared stable and well growing, with shoots around 4 m high.

Changes to the river geomorphology at both sites were interesting and unexpected. At the Sudbury site the point gravel bar adjacent to the bank opposite to the spiling was entrained and some signs of early undercutting were noted on this bank. At the Nayland site the situation was more complex. Here, the bank was eroding upstream of the spiling and the intention had originally been to extend the revetment. This did not happen and the reed bed, which was increasing in size on the opposite bank, continued to deflect the flow to the right bank upstream of the spiling causing significant instability. The thalweg was imposed on the spiling yet the spiling itself dissipated the flow's energy but at the same time contributed to back-eddying upstream of the structure. The lower tier, that was initially expected to be undercut and fail, is now vital and is accumulating sediment. Downstream of the lower tier, the bank for a stretch of 10 metres appears relatively stable with some grass cover, but then there is another pool section that has deepened since the spiling was installed and the banks on both sides of the river have become steeper. At this

downstream section the channel bed and banks have started to erode and, over a small distance, the upper tier revetment has failed and the bank edge retreated (Fig. 7.2).



Fig. 7.1 Willow spiling in Sudbury at the S1 site on the River Stour, during a high flow event, looking upstream in March 2012. The spiling acts as a flow deflector and a trap for small floating debris and sediment.



Fig. 7.2 Willow spiling at N1 site in Nayland on the River Stour in June 2012, looking upstream. Some dead stakes and scouring are visible on the left (right bank) and there is no growth from the revetment in the upper tier. On the other hand, a vigorous growth is seen from the shorter lower tier, in the top middle of the picture.

This situation raises some interesting questions that were not discussed earlier in the thesis. Firstly, what role has the spiling had on these 'side effects' and what would the river geomorphology have looked like if nothing had been installed? Secondly, if the answer was that the spiling actually contributes to the erosion somewhere else, fully or

partially, should any measures for river bank stabilisation be used in rural areas, unless they are absolutely crucial (i.e. access, property or infrastructure is in danger)?

Further research is needed to answer these questions categorically and find out what effect does the spiling have on post-installation river processes. It would be necessary to determine the extent that the spiling caused the changes and what other factors contributed. For example, was it the result of flow deflection or the locking of the sediment in the bank, so that the flow had more capacity for entraining the sediment from somewhere else? It would be interesting to explore what role does the channel width (or w/d ratio) play in this. The wider the channel, the less likely it would be for spiling to deflect the flow to the opposite bank so what is the minimum 'ideal' channel width for spiling implementation? This should be considered in a channel planform context too. Another approach would be to find the maximum gross stream power (Chapter 5.1) that does not have any significant effects on channel form such as bed and bank scour at the ends of an installed revetment or does not initiate erosion on the opposite bank.

Overall, the spiling, for the purpose it was built, could be regarded as successful at the S1 site in Sudbury and partially successful at the N1 site in Nayland, but only time will tell and it is therefore important to keep visiting these case study sites and record major changes alongside any future management practices. The S1 site will be managed and the ranger is exploring different ways of doing it. It has been extended upstream and the ranger is testing a natural sedimentation instead of backfill to slow down the plant competition that colonises a newly backfilled structure. The site in Nayland has a more questionable future as the land is for sale and there is no management of it in the interim period between owners, with the site left to the river's processes. If no management takes place, some of the willow stakes that have survived will grow into trees and will continue to protect the river bank, while the erosion of the loose bank upstream will continue and the large, over 200 m long, meander will migrate, leaving some of the spiling in place or taking it all down eventually.

To close, some written comments on the project made in November 2012 by Adrian Walters, the Chair of Sudbury Common Lands Charity, who has been looking after the Sudbury river meadows for decades:

I am extremely pleased at the effectiveness of the willow spiling. It costs us nothing to install providing we have volunteer labour. Erosion to the bank where we had previously lost approximately 2.5 metres was stopped with immediate effect although we may need to continue upstream with some further extension works. The most interesting and, for me, surprising result is that it appears that the processes of erosion might be reversing. Whether this is entirely attributable to the willow spiling I cannot say but there does appear to be some indication of erosion to the opposite bank where deposition was formerly taking place.

We have another small willow spiling project for the Mill Stream next spring so this technique is one that we have very much 'taken on board'.

REFERENCES

Abdi, H. & Williams, L.J. (2010). Principal component analysis. *Wiley Interdisciplinary Reviews: Computational Statistics* **2**, 433–459.

Abernethy, B. & Rutherford, I.D. (1998). Where along a river's length will vegetation most effectively stabilise stream banks? *Geomorphology* **23**, 55–75.

Abernethy, B. & Rutherford, I.D. (2000a). Does the weight of riparian trees destabilize riverbanks? *Regulated Rivers-Research & Management* **16**, 565–576.

Abernethy, B. & Rutherford, I.D. (2000b). The effect of riparian tree roots on the mass-stability of riverbanks. *Earth Surface Processes and Landforms* **25**, 921–937.

Abernethy, B. & Rutherford, I.D. (2001). The distribution and strength of riparian tree roots in relation to riverbank reinforcement. *Hydrological Processes* **15**, 63–79.

Agate, E. & Brooks, A. (2001). *Waterways and Wetlands: A Practical Conservation Handbook*, British Trust for Conservation Volunteers, Reading, UK. 170pp.

Akridge, A., Eigel, J. D. & Athanasakes, J. G. (1999). Stream restoration and soil bioengineering. *Public Works*, 48–51.

Allen, H.H. & Leech, J.R. (1997). *Bioengineering for Streambank Erosion Control. Report 1 – Guidelines*. Technical Report EL-97-8. US Army Corps of Engineers, Waterways Experiment Station, Vicksburg, Mississippi. 105 pp. Available online in March 2010 at:
http://www.engr.colostate.edu/~bbledsoe/CIVE413/Bioengineering_for_Streambank_Erosion_Control_report1.pdf

Amlin, N.A. & Rood, S.B. (2001). Inundation tolerances of riparian willows and cottonwoods. *Journal of the American Water Resources Association* **37**, 1709–1720.

Andrews, E.D. (1984). Bed-material entrainment and hydraulic geometry of gravel-bed rivers in Colorado. *Geological Society of America Bulletin* **95**, 371–378.

Anstead, L. & Boar, R.R. (2010). Willow spiling: Review of streambank stabilisation projects in the UK, *Freshwater Reviews* **3**, 33–47.

Ashmore, P. & Day, T. (1988). Effective discharge for suspended sediment transport in streams of the Saskatchewan River basin. *Water Resources Research* **24**, 864–870.

Atkins, W.S. (2000). *River Stour and Pant/Blackwater PHABSIM Studies*. Epsom, Surrey, Atkins Consultants Ltd., UK. 160 pp.

Atkinson, J. & Springman, S. (2000). *Soil Mechanics: Soil Description and Classification*. 42 pp. Available online in March 2012 at:
<http://environment.uwe.ac.uk/geocal/SoilMech/classification/soilclas.htm>

Atkinson, P.M., German, S.E., Sear, D.A. (2003). Exploring the relations between riverbank erosion and geomorphological controls using geographically weighted logistic regression. *Geographical Analysis* **35**, 58–82.

Bathurst, J.C., Hey, R.D. & Thorne, C.R. (1979). Secondary flow and shear stress at river bends. *Journal of the Hydraulics Division* **105**, 1277–1295.

Baver, L.D., Gardner, W.H. & Gardner, W.R. (1972). *Soil physics*. Cambridge University Press, Cambridge, UK.

Begon, M., Harper, J.L. & Townsend, C.R. (1996). *Ecology: individuals, populations, and communities*, Blackwell Science, Oxford, UK. 1068 pp.

Benson, M.A. & Thomas, D.M. (1966). A definition of dominant discharge. *International Association of Scientific Hydrology Bulletin* **11**, 76–80.

Bentrup, G. & Hoag, J.C. (1998). *The Practical Streambank Bioengineering Guide. User's Guide for Natural Streambank Stabilization Techniques in the Arid and Semi-arid Great Basin and Intermountain West*. US Department of Agriculture, Natural Resources Conservation Service, Plant Materials Center, Aberdeen, Idaho. 150 p.

Bischetti, G.B., Chiaradia, E.A., Simonato, T., Speziali, B., Vitali, B., Vullo, P. & Zocco, A. (2005). Root strength and root area ratio of forest species in Lombardy (Northern Italy). *Plant and Soil* **278**, 11–22.

Bouassida, M. & Boussetta, S. (1999). On the determination of vane shear strength of soft soils. In: *Geotechnics for Developing Africa* (eds.: R.R. Wordle & G.E. Blight), Taylor and Francis, Oxford, UK. 698 pp.

Brighton and Hove City Council (2009). *Brown Tailed Moth Caterpillars (Euproctis chrysorrhoea L.)*. 8pp. Available online in March 2012 at: http://www.brighton-hove.gov.uk/downloads/bhcc/trees/Brown_Tail_Moth.pdf

Brooks, A. & Agate, E. (1981). *Waterways and Wetlands. A Practical Conservation Handbook*. British Trust for Conservation Volunteers, Reading, UK. 169 pp.

BSI (1975). BS 1377 - Methods of Test for Soils for Civil Engineering Purposes, British Standards Institution, London, UK. 68 pp.

BSI (1999). BS 5930 - The code of practice for site investigations, British Standards Institution, London, UK. 152 pp.

Burton, R. (2006). *Texture Triangle 01*. Available online in March 2012 at: <http://www.soil-net.com/album/slides/Texture%20Triangle%2001.html>

Cadling, L. & Odenstad, S. (1950). *The Vane Borer*. Swedish Geotechnical Institute Proceedings, Stockholm, Sweden. 87 pp. Available online in March 2012 at: <http://trid.trb.org/view.aspx?id=121160>

Carlson, M.C. (1950). Nodal adventitious roots in willow stems of different ages. *American Journal of Botany* **37**, 555–561.

Carr, J.C., Beatson, R.K., Cherrie, J.B., Mitchell, T.J., Fright, W.R., McCallum, B.C. & Evans, T.R. (2011). Reconstruction and Representation of 3D Objects with Radial Basis Functions, *SIGGRAPH Computer Graphics 2001 Conference Proceedings* ACM SIGGRAPH, Springer 67–76.

Carson, M.A. & Kirkby, M.J. (1972). *Hillslope form and process*. Geographical Studies No. 3, Cambridge University Press, Cambridge, UK. viii+475 pp.

Casagli, N., Rinaldi, M., Gargini, A. & Curini, A. (1999). Pore water pressure and streambank stability: Results from a monitoring site on the Sieve River, Italy. *Earth Surface Processes and Landforms* **24**, 1095–1114.

CEH (2005). *Catchment Spatial Statistics: 36001 Stratford St Mary*. Centre for Ecology and Hydrology, UK.

Chow, V.-T. (1959). *Open-channel hydraulics*. McGraw-Hill College, New York. 680 pp.

Chu-Agor, M.L., Wilson, G.V. & Fox, G.A. (2008a). Numerical Modeling of Bank Instability by Seepage Erosion Undercutting of Layered Streambanks. *Journal of Hydrologic Engineering* **13**, 1133–1145.

Chu-Agor, M.L., Fox, G.A., Cancienne, R.M., & Wilson, G.V. (2008b). Seepage caused tension failures and erosion undercutting of hillslopes. *Journal of Hydrology* **359**, 247–259.

Conroy, S.D. & Svejcar, T.J. (1991). Willow planting success as influenced by site factors and cattle grazing in north eastern California. *Journal of Range Management* **44**, 59-63.

Copeland, R., Soar, P. & Thorne, C. (2005). Channel-forming discharge and hydraulic geometry width predictors in meandering sand-bed rivers. *2005 World Water and Environmental Resources Congress Proceedings: Impacts of Global Change*. Anchorage, Alaska, United States, May 15-19, 2005. Available online in December 2012 at: [http://ascelibrary.org/doi/pdf/10.1061/40792\(173\)568](http://ascelibrary.org/doi/pdf/10.1061/40792(173)568)

Coppin, N.J. & Richards, I.G. (1990). *Use of Vegetation in Civil Engineering*. Butterworths, London, UK. 312 pp.

Couper, P.R. (2003). Effects of silt-clay content on the susceptibility of river banks to subaerial erosion. *Geomorphology* **56**, 95–108.

Couper, P.R. & Maddock, I.P. (2001). Subaerial river bank erosion processes and their interaction with other bank erosion mechanisms on the River Arrow, Warwickshire, UK. *Earth Surface Processes and Landforms* **26**, 631–646.

Craig, R.F. (2004). *Craig's soil mechanics*. Taylor & Francis, Abingdon, UK. 485 pp.

Crowder, W. & Pullman, P.M.C. (1995). *Collecting Willow, Poplar and Redosier Dogwood Hardwood Cuttings for Riparian Site Plantings*. Technical Note: Plant Materials 29. US Department of Agriculture, Natural Resources Conservation Service, Spokane, Washington. 5 pp. Available online in March 2010 at: <http://plant-materials.nrcs.usda.gov/pubs/wapmctn290195.pdf>

Dapporto, S., Rinaldi, M., Casagli, N. & Vannocci, P. (2003). Mechanisms of riverbank failure along the Arno River, central Italy. *Earth Surface Processes and Landforms* **28**, 1303–1323.

Darby, S.E. & Thorne, C.R. (1995). Fluvial maintenance operations in managed alluvial rivers. *Aquatic Conservation: Marine and Freshwater Ecosystems* **5**, 37–54.

Das, B.M. (2006). *Principles of Geotechnical Engineering*. Thomson, Canada. 666 pp.

Dietrich, W.E. & Gallinatti, J.D. (1991). *Fluvial geomorphology*. In: Field Experiments and Measurement Programs in Geomorphology (ed: O. Slaymaker), A.A. Balkema, Rotterdam, 169-229.

Downward, S.R., Gurnell, A.M. & Brookes, A. (1994). A methodology for quantifying river channel planform change using GIS. *IAHS Publications, Series of Proceedings and Reports, International Association of Hydrological Sciences* **224**, 449–456.

EA (1998). *The Denver Complex. The Story of the Drainage of the Fens, the Ouse Flood Protection Scheme and the Ely-Ouse to Essex Water Transfer Scheme*. Environment Agency, Bristol, UK.

EA (2008). *Climate Change and the River Flows on 2050s: Science Summary*. SC070079/SS1. Environment Agency, Peterborough, UK. Available online in March 2012 at: <http://publications.environment-agency.gov.uk/PDF/SCHO1008BOSS-E-E.pdf>

EA (2009). *Water for People and the Environment: Water Resources Strategy for England and Wales*. Environment Agency, Bristol, UK. Available online in March 2012 at: <http://publications.environment-agency.gov.uk/PDF/GEHO0309BPKX-E-E.pdf>

EA (2011). *The State of our Environment: Water - East of England 2010*. Environment Agency, Peterborough, UK. Available online in November 2011 at: http://www.environment-agency.gov.uk/static/documents/Business/SOE_Water.pdf

EC (2000). Directive 2000/60. *EC of the European Parliament and of the Council of Ministers*, European Parliament & Council, Article 175(1), Journal OJL 327. 23 pp.

EERA SDRT (2004). *Living with Climate Change in the East of England*. East of England Regional Assembly and Sustainable Development Roundtable. Available online in November 2011 at: <http://www.hef.org.uk/news/climate-change.pdf>

Eliasson, L. & Brunes, L. (1980). Light effects on root formation in aspen and willow cuttings. *Physiologia Plantarum* **48**, 261-265.

Elowson, S. (1999). Willow as a vegetation filter for cleaning of polluted drainage water from agricultural land. *Biomass & Bioenergy* **16**, 281-290.

Entec (1998a). *Assessment of the Impact of the Ely Ouse - Essex Transfer Scheme: Land Use & Socio-Economic Aspects*. Environment Agency, Bristol, UK.

Entec (1998b). *Assessment of the Impact of the Ely Ouse - Essex Transfer Scheme: River & River Corridor Biology*. Entec & Environment Agency, Bristol, UK.

Entec (2007). *The Abberton Scheme Environmental Impact Assessment*. Entec & Environment Agency, Bristol, UK.

ESRI (2009). *ArcGIS 9.3.1*. Environmental Systems Research Institute, Redlands, United States.

ESW (2005). *PR 09 Water Resources Management Plan: Strategic Environmental Assessment Report - Non-Technical Summary*. Essex and Suffolk Water, Chelmsford. Available online in November 2011 at: http://www.eswater.co.uk/PR09_WRMP_SEA_Non-technical_Summary_for_Web_Site.pdf

ESW (2011). *The Abberton Scheme*. Essex & Suffolk Water, Chelmsford, UK. Available online in March 2012 at: <http://www.eswater.co.uk/Abbertonreservoirscheme.aspx>.

Evette, A., Labonne, S., Rey, F., Liebault, F., Jancke, O. & Girel, J. (2009). History of bioengineering techniques for erosion control in rivers in Western Europe. *Environmental Management* **43**, 972-984.

Ferguson, R. I. (1981). *Channel form and channel changes*. In: Lewin J. (Ed) British Rivers, George Allen and Unwin, London, 90–125.

Fischchenich, C. (2001). *Stability Thresholds for Stream Restoration Materials*. EMRRP (Ecosystem Management and Restoration Research Program), Technical Notes Collection (ERDC TN-EMRRP-SR-29), US Army Engineer Research and Development Center, Vicksburg, Mississippi. 10 pp. Available online in March 2010 at: <http://el.erdc.usace.army.mil/elpubs/pdf/sr29.pdf>

Fox, G.A., Wilson, G.V., Simon, A., Langendoen, E.J., Akay, O. & Fuchs, J.W. (2007). Measuring streambank erosion due to ground water seepage: correlation to bank pore water pressure, precipitation and stream stage. *Earth Surface Processes and Landforms* **32**, 1558–1573.

Freudlund, D.G., Rahardjo, H. & Gan J.K.-M. (1987). Non-linearity of strength envelope for unsaturated soils. *6th International Conference on Expansive Soils*. New Delhi, India, 49–54.

Gerstgraser, C. (2000). *Ingenieurbiologische Bauweisen an Fliessgewässern. Grundlagen zu Bau, Belastbarkeit und Wirkungsweisen*. Dissertationen der Universität für Bodenkultur Wien 52, Österreichischer Kunst-und Kulturverlag, Wien.

Glenz, C., Schlaepfer, R., Lorgulescu, I. & Kienast, F. (2006). Flooding tolerance of Central European tree and shrub species. *Forest Ecology and Management* **235**, 1-13.

Golden Software (2010). *Surfer 9.11.947*, Golden Software Inc., Colorado.

Goodson, J.M. (2002). *Environmental controls on the colonisation and establishment of vegetation on river banks under varying grazing pressure*. PhD thesis, Oxford Brookes University, UK (unpublished).

Google Inc. (2009). *Google Earth 5.2*. Available online in March 2009 at: <http://earth.google.com>

Google Inc. (2011). *Google Earth 6.1*. Available online in March 2011 at: <http://earth.google.com>

Graf, W. (1978). Fluvial adjustments to the spread of tamarisk in the Colorado Plateau region. *Geological Society of America Bulletin* **89**, 1491-1501.

Graf, W. (1984). A Probabilistic Approach to the Spatial Assessment of River Channel Instability. *Water Resources Research* **20**, 953–962.

Gray, D. H. & Leiser, A.T. (1982). *Biotechnical Slope Protection and Erosion Control*, Van Nostrand Reinhold Co., USA. 271 pp.

Gray, D.H. & Sotir, R.B. (1996). *Biotechnical and Soil Bioengineering Slope Stabilization: A Practical Guide for Erosion Control*. John Wiley & Sons, New York. 400 pp.

Greenway, D.R. (1987). *Slope Stability: Geotechnical Engineering and Geomorphology*. John Wiley & Sons, New York. 230 pp.

Gregory, K.J. & Gurnell, A.M. (1988). Vegetation and river channel form and process. In: *Biogeomorphology* (ed.: H.A. Viles), Oxford: Basil Blackwell, 11–42. Available online in August 2011 at: <http://www.sciencedirect.com/science/article/pii/S0169555X96000281>

Hagerty, D.J., Spoor, M.F. & Ullrich, C.R. (1981). Bank failure and erosion on the Ohio River. *Engineering Geology* **17**, 141–158.

Haque, C.H. (1988). Human adjustments to river bank erosion hazard in the Jamuna floodplain, Bangladesh. *Human Ecology* **16**, 421-437.

Hauben, L., Steenackers, M. & Swings, J. (1998). PCR-based detection of the casual agent of watermark disease in willows (*Salix* spp.). *Applied and Environmental Microbiology* **64**, 3966-3971.

Hemphill, R.W. & Bramley, M.E. (1989). *Protection of River and Canal Banks: Guide to Selection and Design*. Butterworths, London, UK. 216 pp.

Hey, R.D. (1975). Design discharges for natural channels. In: *Science and Technology in Environmental Management* (eds.: R. D Hey & J. D. Davies), Saxon House, Farnborough, UK, 73–88.

Hey, R.D. (1986). River Mechanics. *Institution of Water Engineers and Scientists* **40**, 139–158.

Hey, R.D. (1994). Environmentally sensitive river engineering. In: *The Rivers Handbook* (eds.: P. Calow & G.E. Petts), Volume 2, Wiley-Blackwell, Oxford, UK, 337-362.

Hey, R.D. (2006). Fluvial geomorphological methodology for natural stable channel design. *Journal of the American Water Resources Association* **42**, 357-386.

Hey, R.D. & Thorne, C.R. (1986). Stable channels with mobile gravel beds. *Journal of Hydraulic Engineering* **112**, 671–689.

Hey, R.D & Tovey, N.K. (1989). Processes of bank failure. In: *Protection of River and Canal Banks* (eds.: R. W. Hemphill & M.E. Bramley), CIRIA/Butterworths, London, UK, 7–39.

Hickin, E.J. (1984). Vegetation and river channel dynamics. *Canadian Geographer / Le Géographe canadien* **28**, 111–126.

Hickin, E.J. & Nanson, G. (1975). The character of channel migration on the Beatton River, Northeast British Columbia, Canada. *Geological Society of America Bulletin*, **86**, 487-494.

Hickin, E.J. & Nanson, G. (1984). Lateral Migration Rates of River Bends. *Journal of Hydraulic Engineering* **110**, 1557–1567.

Hill, A.R. (1973). Erosion of river banks composed of glacial till near Belfast, Northern Ireland. *Zeitschrift für Geomorphologie* **17**, 428–442.

Hjulstrom, F. (1935). *Studies of the Morphological Activity of Rivers as illustrated by the River Fyris*. Almqvist & Wiksell, Uppsala, Sweden. 527 pp.

Hoag, C.J. & Fripp, J. (2005). *Streambank Soil Bioengineering Considerations for Semi-arid Climates*. Riparian/Wetland Project Information Series No. 18, US Department of Agriculture, Washington D.C. 15 pp. Available online in March 2010 at: <http://plant-materials.nrcs.usda.gov/pubs/idpmcar5981.pdf>

Hoag, J.C. & Short, H. (1993). *Use of Willow and Cottonwood Pole Cuttings for Vegetating Shorelines and Riparian Areas*. Popular Report of the Aberdeen Plant Materials

Center. US Department of Agriculture, Soil Conservation Service, Aberdeen, Idaho, 12 pp.

Hooke, J.M. (1979). An analysis of the processes of river bank erosion. *Journal of Hydrology* **42**, 39–62.

Hooke, J.M. (1980). Magnitude and distribution of rates of river bank erosion. *Earth Surface Processes* **5**, 143–157.

Hooke, J.M. (1995). River channel adjustment to meander cut-offs on the River Bollin and River Dane, northwest England. *Geomorphology* **14**, 235–253.

H.R. Wallingford (1992). *Standards of Service for Flood Defence: Reach Specification Methodology*. National Rivers Authority, Hydraulics Research, UK.

Hudson, P. F. & Kesel, R. H. (2000). Channel migration and meander-bend curvature in the lower Mississippi River prior to major human modification. *Geology* **28**, 531–534.

Hulme M., Jenkins G. J., Lu X., Turnpenny J. R., Mitchell T. D., Jones R. G., Lowe J., Murphy J. M., Hassel D., Boorman P., Mc Donald R. and Hill S. (2002). *Climate Change Scenarios for the United Kingdom: The UKCIP02 Scientific Report*. Tyndall Centre for Climate Change Research, School of Environmental Sciences, University of East Anglia, Norwich, 2002. Available online in July 2012 at: http://www.ukcip.org.uk/wordpress/wp-content/PDFs/UKCIP02_briefing.pdf

Huntington, R. & Armstrong, R.B. (1974). Operation of the Ely Ouse-Essex Scheme. *Journal of Institution of Water Engineers* **28**, 387–401.

Hupp, C.R. (1986). Upstream Variation in Bottomland Vegetation Patterns, Northwestern Virginia. *Bulletin of the Torrey Botanical Club* **113**, 421–430.

Hupp, C.R & Simon A. (1986). Vegetation and bank-slope development. *Proceedings of 4th Federal Interagency Sedimentation Conference, Las Vegas* **2**, 83- 91.

Hupp, C.R., Schenk, E.R., Richter, J.M., Peet, R.K. & Townsend, P.A. (2009). Bank erosion along the dam-regulated lower Roanoke River, North Carolina. *Geological Society of America Special Papers* **451**, 97–108.

Jackson, M.B. & Attwood, P.A. (1996). Roots of willow (*Salix viminalis* L.) showed marked tolerance to oxygen shortage in flooded soils and in solution culture. *Plant and Soil* **187**, 37–45.

Jarvis, R. & Richards, I.G. (2008). *Engineering and the Environment – Perfect Partners? The use of Willows in Bioengineering*. Meeting report, CIWEM, Birmingham, UK. 10 pp. Available online in February 2010 at: http://www.ciwem.org/groups/rivers/04_willow_in_bioeng_paper.pdf

Karrenberg, S., Edwards, P.J. & Kollmann, J. (2002). The life history of *Salicaceae* living in the active zone of floodplains. *Freshwater Biology* **47**, 733–748.

Keller, E.A. & Swanson, F.J. (1979). Effects of large organic material on channel form and fluvial processes. *Earth Surface Processes* **4**, 361–380.

Kesel, R.H., Dunne, K.C., McDonald, R.C., Allison, K.R. & Spicer, B.E. (1974). Lateral erosion and overbank deposition on the Mississippi River in Louisiana caused by 1973 flooding. *Geology* **2**, 461–464.

Knighton, A.D. (1973). Streambank erosion in relation to streamflow conditions, River Bollin-Dean, Cheshire. *East Midland Geographer* **5**, 416–426.

Knighton, A.D. (1988). The impact of the Parangana Dam on the River Mersey, Tasmania. *Geomorphology* **1**, 221–237.

Knox, J.C. (1985). Responses of floods to Holocene climatic change in the upper Mississippi Valley. *Quaternary Research* **23**, 287–300.

Knox, J.C. (1988). Climatic influence on upper Mississippi Valley floods. *Flood Geomorphology*, 279–300.

Kruskal, W. & Wallis, W.A. (1952). Use of ranks in one-criterion variance analysis. *Journal of the American Statistical Association* **47**, 583–621.

Kuzovkina, Y.A. & Quigley, M.F. (2005). Willows beyond wetlands: Uses of *Salix* L. species for environmental projects. *Water, Air and Soil Pollution* **162**, 183–204.

Laing, S. (2003). *Investigating the Application and long-term Performance of 'soft' Riverbank Protection Techniques: 30 Case Studies from the Thames Region*. Internal Report, Environment Agency, UK (unpublished: available from the Environment Agency, Thames Region).

Lawler, D.M. (1986). River bank erosion and the influence of frost - a statistical examination. *Transactions of the Institute of British Geographers* **11**, 227–242.

Lawler, D.M. (1992a). Design and installation of a novel automatic erosion monitoring-system. *Earth Surface Processes and Landforms* **17**, 455–463.

Lawler, D.M. (1992b). Process dominance in bank erosion systems. In: *Lowland Floodplain Rivers: Geomorphological Perspectives*, (eds.: P. Carling & G. E. Petts), John Wiley & Sons, Chichester, UK. 117–143.

Lawler, D.M. (1993a). The measurement of river bank erosion and lateral channel change: A review. *Earth Surface Processes and Landforms* **18**, 777–821.

Lawler, D.M. (1993b). Needle ice processes and sediment mobilization on river banks - the river Ilston, West-Glamorgan, UK. *Journal of Hydrology* **150**, 81–114.

Lawler, D.M. (2005a). Defining the moment of erosion: the principle of thermal consonance timing. *Earth Surface Processes and Landforms* **30**, 1597–1615.

Lawler, D.M. (2005b). The importance of high-resolution monitoring in erosion and deposition dynamics studies: examples from estuarine and fluvial systems. *Geomorphology* **64**, 1–23.

Lawler, D.M. & Bull, P.A. (1977). Erosion in the valley of the Pennard Pill, *Journal of the Gower Society* **28**, 46–54.

Lee, K.L. & Seed, H.B. (1967). Drained strength characteristics of sands. *Journal of Soil Mechanics and Foundations Division*. ASCE 93, No. SM6, pp 117–141. Available online in March 2012 at: <http://trid.trb.org/view.aspx?id=126865>

Lawler, D.M., Thorne, C.R & Hooke, J.M (1997). Bank erosion and stability. In: *Applied Fluvial Geomorphology for River Engineering and Management* (eds.: C.R. Thorne, R.D. Hey & M.D. Newson), John Wiley & Sons, Chichester, UK, 137–172.

Lawler, D.M., Grove, J.R., Couperthwaite, J.S. & Leeks, G.J. (1999). Downstream change in river bank erosion rates in the Swale–Ouse system, northern England. *Hydrological Processes* **13**, 977–992.

Lawler, D.M., West, J.R., Couperthwaite, J.S. & Mitchell, S.B. (2001). Application of a novel automatic erosion and deposition monitoring system at a channel bank site on the tidal river Trent, UK. *Estuarine Coastal and Shelf Science* **53**, 237–247.

Leeks, G.J., Lewin, J. & Newson, M.D. (1988). Channel change, fluvial geomorphology and river engineering: The case of the Afon Trannon, Mid-Wales. *Earth Surface Processes and Landforms* **13**, 207–223.

Leopold, L.B. (1973). River channel change with time: An example: Address as retiring President of the Geological Society of America, Minneapolis, Minnesota, November 1972. *Geological Society of America Bulletin* **84**, 1845–1860.

Leopold, L.B. & Wolman, M.G. (1957). *River Channel Patterns: Braided, Meandering and Straight*. Physiographic and Hydraulic Studies of Rivers. Geological Survey Professional Paper 282-B, US Government Printing Office, Washington, USA. 85 pp.

Leopold, L.B., Wolman, M.G. & Miller, J.P. (1995). *Fluvial Processes in Geomorphology*, Courier Dover Publications, New York, USA. 522 pp.

Lewin, J. (1976). Initiation of bed forms and meanders in coarse-grained sediment. *Bulletin of the Geological Society of America* **87**, 281.

Lewin, J. (1987). Historical river channel changes. In: *Palaeohydrology in Practice* (eds: K.J. Gregory, J. Lewin, J.B. Thornes), International Geological Correlation Programme, Volume 158, John Wiley & Sons, New York, USA. 161–175.

Lewin, J. & Hughes, D. (1976). Assessing channel change on Welsh rivers. *Cambria* **3**, 1–10.

Li, M.-H. & Eddleman, K.E. (2002). Biotechnical engineering as an alternative to traditional engineering methods. A biotechnical streambank stabilization design approach. *Landscape and Urban Planning* **60**, 225–242.

Li, M.-H., Landphair, H.C., Arnold, M.A., Mullin, K. & Eddleman, K.E. (2005). A dormancy extension technique for biotechnical streambank stabilization in warm regions. *Landscape and Urban Planning* **71**, 223–231.

Li, X., Zhang, L. & Zhang, Z. (2006). Soil bioengineering and the ecological restoration of riverbanks at the Airport Town, Shanghai, China. *Ecological Engineering* **26**, 304–314.

Malvern (2000). *Mastersizer 5.60*. Malvern Instruments Ltd., Worcestershire, UK.

Marriage, J. (2001). *The Essex & Suffolk River Stour Navigation*. 1st Auflage. The History Press Ltd., UK. 128 pp.

MathWorks (2011). *MathLab R2011a*. The MathWorks Inc., Natick, Massachusetts, USA.

McCulloch, I. (2000). Willow Spiling – the use of willow spilings (stems) to control riverbank erosion. *Enact – Peterborough* **8**, 19–20.

Menzel, A. (2000). Trends in phenological phases in Europe between 1951 and 1996. *International Journal of Biometeorology* **44**, 76–81.

Met Office (2011). *2010 Weather Summaries*. Available online in November 2011 at: <http://www.metoffice.gov.uk/climate/uk/2011/october/averages.html>

Micheli, E.R. & Kirchner, J.W. (2002). Effects of wet meadow riparian vegetation on streambank erosion. 1. Remote sensing measurements of streambank migration and erodibility. *Earth Surface Processes and Landforms* **27**, 627–639.

Mills, A.D. (2003). *Oxford Dictionary of British Place Names*. Oxford University Press, UK. 576 pp.

Mitchell, S.B., Couperthwaite, J.S., West, J.R. & Lawler, D.M. (1999). Dynamics of erosion and deposition events on an intertidal mudbank at Burringham, River Trent, UK. *Hydrological Processes* **13**, 1155–1166.

Morgan, R.P.C., Collins, A.J., Hann, M.J. & Morris, J. (1999). *Waterway Bank Protection: A Guide to Erosion Assessment and Management*. Environment Agency R&D Publication 11, Environment Agency & Cranfield University, Bristol, UK. 251 pp.

Murphy, D. & Vivash, R. (1998). *Revetment Techniques used on the River Skerne Restoration Project*. Environment Agency R&D Technical Report W83, Environment Agency, Bristol, UK. 75 pp.

Newsholme, C. (1992). *Willows: the genus Salix*. B.T. Batsford Ltd., London. 224 p.

Newson, M.D. & Block, C. (2002). *Fluvial Audit of the Upper Stour*. Environment Agency, Ipswich, UK.

NSRI (2007). *National Soil Map, NATMAP*. National Soil Resources Institute, Cranfield University. Available online in March 2012 at: www.cranfield.ac.uk/nsri

NSRI (2010a). *Academic Soils Site Report for location 566959E, 253835N (Great Bradley) 2km x 2km*. National Soil Resource Institute, Cranfield University. Available online in March 2012 at: www.cranfield.ac.uk/nsri

NSRI (2010b). *Academic Soils Site Report for location 567928E, 252034N (Little Bradley), 2km x 2km*. National Soil Resource Institute, Cranfield University. Available online in March 2012 at: www.cranfield.ac.uk/nsri

NSRI (2010c). *Academic Soils Site Report for location 577571E, 244979N (Clare), 2km x 2km*. National Soil Resource Institute, Cranfield University. Available online in March 2012 at: www.cranfield.ac.uk/nsri

NSRI (2010d). *Academic Soils Site Report for location 586598E, 241750N (Sudbury), 2km x 2km*. National Soil Resource Institute, Cranfield University. Available online in March 2012 at: www.cranfield.ac.uk/nsri

NSRI (2010e). *Academic Soils Site Report for location 597467E, 233715N (Nayland), 2km x 2km*. National Soil Resource Institute, Cranfield University. Available online in March 2012 at: www.cranfield.ac.uk/nsri

ONS (2011). *2011 Census Home*. Office for National Statistics, Census Demography and Regional Statistics. Available online in March 2012 at: <http://www.ons.gov.uk/ons/guide-method/census/2011/index.html>

OJC (2000). Directive 2000/60/EC of the European Parliament and of the council of 23 October 2000 establishing a framework for Community action in the field of water policy. *Official Journal of the European Communities* **60**, 1–72.

O'Neal, M.A. & Pizzuto, J.E. (2011). The rates and spatial patterns of annual riverbank erosion revealed through terrestrial laser-scanner surveys of the South River, Virginia. *Earth Surface Processes and Landforms* **36**, 695-701.

Osman, A.M. & Thorne, C.R. (1988). Riverbank Stability Analysis I: Theory. *Journal of Hydraulic Engineering*, **114**, 134-150.

Parsons, D.A., Apmann, R.P. & Decker, G.H. (1963). The determination of sediment yields from flood water sampling. *International Association Scientific Hydrology Publication* **65**, 7-15.

Payne, P.C.J. & Fountaine, E.R. (1952). A Field Method of Measuring the Shear Strength of Soils. *Journal of Soil Science* **3**, 136-144.

Pezeshki, S.R., Shields, F.D. & Anderson, P.H. (1998). The relationships between soil conditions and growth of willow posts on streambanks. In: *Proceedings of the International Conference on Water Resources Engineering* (eds S.R. Abt, J. Young-Pezeshki & C.C. Watson). American Society of Civil Engineers. Memphis, Tennessee, 447-452.

Pezeshki, S.R., Li, S., Shields, J.F.D. & Martin, L.T. (2007). Factors governing survival of black willow (*Salix nigra*) cuttings in a streambank restoration project. *Ecological Engineering* **29**, 56-65.

Philip, H.G. & Mengersen, E. (1989). *Insect Pests of the Prairies*. Faculty of Extension, University of Alberta, Edmonton, AB. 122 pp.

Pickup, G. & Warner, R. (1976). Effects of hydrologic regime on magnitude and frequency of dominant discharge. *Journal of Hydrology* **29**, 51-75.

Pollen, N. (2004). *The effects of riparian vegetation on streambank stability: Mechanical and hydrological interaction*. PhD Thesis, King's College, University of London. 320 pp (unpublished).

Pollen, N. (2007). Temporal and spatial variability in root reinforcement of streambanks: accounting for soil shear strength and moisture. *Catena* **69**, 197-205.

Pollen, N. & Simon, A. (2005). *Estimating the mechanical effects of riparian vegetation on streambank stability using a fibre bundle model*. WaTer Resources Research 41, W07025, [doi:10.1029/2004WR003801](https://doi.org/10.1029/2004WR003801)

Pollen, N., Simon, A. & Collinson, A.J.C. (2004). *Advances in assessing the mechanical and hydrological effects of riparian vegetation on streambank stability*. In: Bennett, S., Simon, A. (Eds.), Riparian vegetation and fluvial geomorphology: Water Science and Applications, vol. 8, pp. 125-139.

Polster, D.F. (2002). Soil bioengineering techniques for riparian restoration. *Proceedings of the 26th Annual British Columbia Mine Reclamation Symposium*, The Technical and Research Committee on Reclamation, Dawson Creek, BC, 230-239. Available online in March 2012 at: <http://www.trcr.bc.ca/docs/2002-polster.pdf>

Potere, D. (2008). Horizontal Positional Accuracy of Google Earth's High-Resolution Imagery Archive. *Sensors* **8**, 7973-7981.

Press, W.H., Flannery, B.P., Teukolsky, S.A. & Vetterling, W.T. (1988). Numerical recipes in C: the art of scientific computation. *Cambridge University Press* **31**, 109.

Prosser, I.P., Hughes, A.O. & Rutherford, I.D. (2000). Bank erosion of an incised upland channel by subaerial processes: Tasmania, Australia. *Earth Surface Processes and Landforms* **25**, 1085–1101.

Purseglove, J. (1988). *Taming the Flood: A History and Natural History of Rivers and Wetlands*. Oxford University Press, Oxford, UK. 307 pp.

Ree, W.O. & Palmer, V.J. (1949). *Flow of Water in Channels Protected by Vegetative Linings*, U.S. Department of Agriculture. University of Michigan. 115 pp.

Rey, F. (2009). A strategy for fine sediment retention with bioengineering works in eroded catchments in a mountainous mediterranean climate (Southern Alps, France). *Land Degradation & Development* **20**, 210–216.

Rinaldi, M. & Casagli, N. (1999). Stability of streambanks formed in partially saturated soils and effects of negative pore water pressures: the Sieve River (Italy). *Geomorphology* **26**, 253–277.

Rinaldi, M., Casagli N., Dapporto S. & Gargini A (2004). Monitoring and modelling of pore water pressure changes and riverbank stability during flow events. *Earth Surface Processes and Landforms* **29**, 237–254.

Rosgen, D.L. (2001). A practical method of computing streambank erosion rate. *Proceedings of the Seventh Federal Interagency Sedimentation Conference*, March 25-29, 2001, Reno, Vol. 2, NV, 9–15.

Rowntree, K.M. (1991). An assessment of the potential impact of alien invasive vegetation on the geomorphology of river channels in South Africa. *South African Journal of Aquatic Science* **17**, 28–43.

Rowntree, K.M. & Dollar, E.S.J. (1999). Vegetation controls on channel stability in the Bell River, Eastern Cape, South Africa. *Earth Surface Processes and Landforms* **24**, 127–134.

RRC (2002). *Manual of River Restoration Techniques*. The River Restoration Centre (RRC), Silsoe, UK. 168 pp. Available online in March 2012 at: http://www.therrc.co.uk/rrc_manual_pdf.php

RST (2012). *The River Stour Navigation Guide*. River Stour Trust, UK. Available online in September 2012 at: <http://www.riverstourtrust.org/>

Saynor, P. (2005). *Abberton Scheme: Denver and Wash Aspects*. Essex & Suffolk Water, Chelmsford, UK.

Schaff, S.D., Pezeshki, S.R. & Shields, F.D. (2002). Effects of pre-planting soaking on growth and survival of black willow cuttings. *Restoration Ecology* **10**, 267–274.

Schiechtl, H.M. (1992). *Weiden in der Praxis: Die Weiden Mitteleuropas, ihre Verwendung und Bestimmung*. Patzer-Verlag, Berlin. 132 pp.

Schiechtl, H.M. & Horstmann, N.K. (1980). *Bioengineering for Land Reclamation and Conservation*, University of Alberta Press, Edmonton. 404 pp.

Schiechtl, H.M. & Stern, R. (1996). *Ground Bioengineering Techniques for Slope Protection and Erosion Control*. Blackwell, Oxford. 146 pp.

Schiechtl, H.M. & Stern, R. (1997). *Water Bioengineering Techniques: for Watercourse, Bank and Shoreline Protection*. Wiley-Blackwell, Oxford. 186 pp.

Schlüter, U. (1984). Zur Geschichte Ingenieurbiologie. *Landschaft & Stadt* **16**, 2-9.

Schofield, W. & Breach, M. (2007). *Engineering Surveying*. Butterworth-Heinemann, UK. 640 pp.

Schofield, A.N. & Wroth, P. (1968). *Critical State Soil Mechanics*. Cambridge University, UK. 228 pp.

Schumm, S.A. (1961). *Sediment Sources and Drainage Basin Characteristics in upper Cheyenne River Basin*. U.S. Geological Survey, Water Supply Paper, 137-196.

Schumm, S.A. (1977). *The Fluvial System*, John Wiley & Sons, New York. 338 pp.

Sear, D.A. & Newson, M.D. (2003). Environmental change in river channels: a neglected element. Towards geomorphological typologies, standards and monitoring. *The Science of the Total Environment* **310**, 17 – 23.

Sear, D.A., Thorne, C.R. & Newson, M.D. (2004). *Guidebook of Applied Fluvial Geomorphology*. R&D Technical Report FD1914. Defra Flood management Division. Available online in March 2012:
<http://www.restorerivers.eu/LinkClick.aspx?fileticket=o2ghg%2FI4DzQ%3D&tabid=2624>

Serota, S. & Jangle, A. (1972). A direct-reading pocket shear Vane. *Civil Engineering* **42**, 73-74.

Shields, A., Ott, W.P. & van Uchelen, J.C. (1936). *Application of similarity principles and turbulence research to bed-load movement*. Hydrodynamics Laboratory Publication 167. Available in August 2011 at:
<http://caltechkhr.library.caltech.edu/56/>

Shields, F.D., Cooper, C.M. & Knight, S.S. (1995). Experiment in Stream Restoration. *Journal of Hydraulic Engineering* **121**, 494-502.

Simon, A. (1989a). A model of channel response in disturbed alluvial channels. *Earth Surface Processes and Landforms* **14**, 11-26.

Simon, A. (1989b). The discharge of sediment in channelized alluvial streams. *Journal of the American Water Resources Association* **25**, 1177-1188.

Simon, A. (1992). Energy, time and channel evolution in catastrophically disturbed fluvial systems. In: *Geomorphologic Systems, Binghamton Symposia in Geomorphology International Series* (eds.: J. D. Phillips & W. H. Renwick), Elsevier Science, UK, 345-372.

Simon, A. & Collison, A. J.C. (2002). Quantifying the mechanical and hydrologic effects of riparian vegetation on streambank stability. *Earth Surface Processes and Landforms* **27**, 527-546.

Simon, A. & Downs, P.W. (1995). An inter-disciplinary approach to evaluation of potential instability in alluvial channels. *Geomorphology* **12**, 215-232.

Simon, K. & Steinemann, A. (2000). Soil bioengineering challenges for planning and engineering. *Journal of Urban Planning and Development* **126**, 89-102.

Simon, A. & Thorne, C.R. (1996). Channel adjustment of an unstable coarse-grained stream: opposing trends of boundary and critical shear stress, and the applicability of extreme hypotheses. *Earth Surface Processes and Landforms* **21**, 155–180.

Simon, A., Curini, A., Darby, S.E. & Langendoen, E.J. (1999). Streambank Mechanics and the Role of Bank and Near-bank Processes. In: *Incised Channels: Processes, Forms, Engineering and Management* (eds.: A. Simon, S.E. Darby), John Wiley & Sons, Chichester, UK, 123-152.

Simon, A., Curini A., Darby S.E. & Langendoen E.J. (2000). Bank and near-bank processes in an incised channel. *Geomorphology* **35**, 193–217.

Simons, D. B, Richardson E. V & Nordin C. F. (1965). Sedimentary structures generated by flow in alluvial channels. *Socio-Economic Mineral Petrology Special Publication* **12**, 34-52.

SkillCrest (2008). *VistaMetrix v 1.38*. Skillcrest LLC, Tucson, USA.

Soar, P.J. & Thorne, C.R. (2001). *Channel restoration design for meandering rivers*. ERDC, HL CR-01-1. US Army Engineer Research and Development Center, Coastal and Hydraulics Laboratory, Vicksburg, MS. 454 pp.

Sotir, R.B. & Fischenich, J.C. (2001). *Live and Inert Fascine Streambank Erosion Control*. EMRRP (Ecosystem Management and Restoration Research Program), Technical Notes Collection (ERDC TN-EMRRP-SR-31), US Army Engineer Research and Development Center, Vicksburg, Mississippi. 8 pp. Available online at: <http://el.erdc.usace.army.mil/elpubs/pdf/sr31.pdf>

Sotir, R.B. & Fischenich, J.C. (2007). *Live Stake and Joint Planting for Streambank Erosion Control*. EMRRP (Ecosystem Management and Restoration Research Program), Technical Notes Collection (ERDC TN-EMRRP-SR-35). US Army Engineer Research and Development Center, Vicksburg, Mississippi. 9 pp. Available online in March 2010 at: <http://www.dtic.mil/cgi-bin/GetTRDoc?AD=ADA474067&Location=U2&doc=GetTRDoc.pdf>

Spoor, G., Leeds-Harrison, P.B. & Godwin, R.J. (1982). Potential role of soil density and clay mineralogy in assessing the suitability of soils for mole drainage. *Journal of Soil Science* **33**, 427–441.

Starkel, L., Gregory, K.J. & Thorne, J.B. (1991). *Temperate Palaeohydrology: Fluvial Processes in the Temperate Zone during the last 15,000 years*. Wiley, Chichester, England & Toronto, Canada. xviii + 548 pp.

Strachan, R. (2004). Conserving water voles: Britain's fastest declining mammal. *Water and Environment Journal* **18**, 33-47.

Taylor, D.W. (1948). *Fundamentals of Soil Mechanics*. John Wiley & Sons, New York, USA. 700 pp.

Tengbeh, T. (1989). *The Effect of Grass Cover on Bank Erosion*. PhD thesis, Cranfield University, Cranfield, UK (unpublished).

Thorne, C.R. (1978). *Processes of Bank Erosion in River Channels*. PhD thesis, 2 vols., University of East Anglia, Norwich, UK (unpublished).

Thorne, C.R. (1981). Field measurements of rates of bank erosion and bank material strength. *Erosion and Sediment Transport Measurement, Proceedings of the Florence Symposium, June 1981*. IAHS **133**, 503–512.

Thorne, C.R. (1982). Processes and mechanisms of river bank erosion. In: *Gravel-bed Rivers*, (eds.: R. D. Hey, J. C. Bathurst & C. R. Thorne), Chichester, Wiley, 227–259.

Thorne, C.R. (1990). Processes and mechanisms of river bank erosion. In: *Vegetation and Erosion* (ed.: J.B. Thorne), John Wiley & Sons, Chichester, UK, 125–144.

Thorne, C.R. (1992). Bend scour and bank erosion on the meandering Red River, Louisiana. In: *Lowland Floodplain Rivers: Geomorphological Perspectives* (eds.: P. Carling, G. E. Petts), John Wiley & Sons, Chichester, UK, 95–116.

Thorne, C.R. & Lewin, J. (1979). Bank processes, bed material movement and planform development in a meandering river. *Adjustments of the Fluvial System, Proceedings of the 10th Annual Geomorphology Symposia, Series No. 10*, September 21-22, 1979, Binghamton, New York, USA, Allen & Unwin, Australia, 117–138.

Thorne, C.R. & Osman, A.M. (1988). The influence of bank stability on regime geometry of natural channels. *International Conference on River Regime*, John Wiley & Sons, Chichester, UK, 18-22.

Thorne, C.R. & Tovey, N.K. (1981). Stability of composite river banks. *Earth Surface Processes and Landforms* **6**, 469–484.

Thorne, C.R., Hey, R.D. & Newson, M.D. (1997). *Applied Fluvial Geomorphology for River Engineering and Management*, John Wiley & Sons, Chichester, UK. 376 pp.

Thorne, C.R., Reed, S. & Doornkamp, J.C. (1996a). *A Procedure for Assessing River Bank Erosion Problems and Solutions*. R&D Report, National Rivers Authority, UK.

Thorne, C.R., Allen, R.G. & Simon, A. (1996b). Geomorphological river channel reconnaissance for river analysis, engineering and management. *Transactions of the Institute of British Geographers, The Royal Geographical Society* **21**, 469-483

Thorne, C.R., Amarasinghe, I., Gardiner, J., Perala-Gardiner, C. & Sellin, R. (1998). *Riverbank Protection using Willows*. Scoping Study. Environment Agency R&D Technical Report W154, Environment Agency, Bristol. 125 pp.

Tilley, D. & Hoag, J.C. (2008). *Evaluation of Fall versus Spring Planting of Dormant Hardwood Willow Cuttings with and without Soaking Treatment*. Riparian/Wetland Project Information Series No. 25. US Department of Agriculture, Natural Resources Conservation Service, Plant Materials Center, Aberdeen, Idaho. 9 pp. Available online in March 2010 at: <http://www.plant-materials.nrcs.usda.gov/pubs/idpmcar8305.pdf>

Tosi, M. (2007). Root tensile strength relationships and their slope stability implications of three shrub species in the Northern Apennines (Italy). *Geomorphology* **87**, 268–283.

UK TAG WFD (2008). *Environmental Standards and Conditions (Phase 2)*. UK Technical Advisory Board on the Water Framework. Available online in November 2011 at: http://www.wfd.uk.org/tag_guidance/Article%20_11/POMEnvStds/sw_07

USGS (2008). *Probability Flows for Streams in Eastern WA - Project Summaries*. U.S. Geological Survey. Available online in March 2012 at: http://wa.water.usgs.gov/projects/prob_flow/summary.htm

Veihe, A., Jensen, N.H., Schiøtz, I.G. & Nielsen, S.L. (2011). Magnitude and processes of bank erosion at a small stream in Denmark. *Hydrological Processes* **25**, 1597–1613.

Waldron, L.J. (1977). The shear resistance of root-permeated homogeneous and stratified soil. *Soil Science Society of America Journal* **41**, 843–849.

Waldron, L.J. & Dakessian, S. (1981). Soil reinforcement by roots: Calculations of increased soil shear resistance from root properties. *Soil Science* **132**, 427-435.

Ward, R. C. & Robinson, M. (1990). *Principles of Hydrology*. McGraw-Hill Book Company, London, UK. 403 pp.

Ward, D., Holmes, N., & José, P. (1994). *The New Rivers & Wildlife Handbook*. Royal Society for the Protection of Birds, Sandy, Bedfordshire, UK. 438 pp.

Watson, C.C., Abt, S.R. & Derrick, D. (1997). Willow posts bank stabilization. *Journal of the American Water Resources Association* **33**, 293-300.

Werritty, A. (1997). Short-term changes in channel stability. In: *Applied Fluvial Geomorphology for River Engineering and Management* (eds.: Thorne, C. R., Hey, R. D. & Newson, M. D.), John Wiley & Sons, Chichester, UK, 47–65.

Wetzel, R.G. & Pickard, D. (1996). Application of secondary production methods to estimates of net aboveground primary production of emergent aquatic macrophytes. *Aquatic Botany* **53**, 109-120.

Wilby, R.L., Orr, H.G., Hedger, M., Forrow, D. & Blackmore, M. (2006). Risks posed by climate change to the delivery of Water Framework Directive objectives in the UK. *Environment International* **32**, 1043-1055.

Wilkinson, A.G. (1999). Poplars and willows for soil erosion control in New Zealand. *Biomass and Bioenergy* **16**, 263-274.

Williams, G.P. & Wolman, M.G. (1984). Downstream effects of dams on alluvial rivers. *U.S. Geological Survey Professional Paper* **1286**, 83.

Wilson, G.V., Periketi, R.K., Fox, G.A., Dabney, S.M., Shields, F.D. & Cullum, R.F. (2007). Soil properties controlling seepage erosion contributions to streambank failure. *Earth Surface Processes and Landforms* **32**, 447–459.

Wolman, M.G. (1955). *The Natural Channel of Brandywine Creek, Pennsylvania*. U.S. Government Printing Office. 56 pp.

Wolman, M.G. (1959). Factors influencing erosion of cohesive river bank. *American Journal of Science* **257**, 204–216.

Wolman, M.G. & Miller, J.P. (1960). Magnitude and frequency of forces in geomorphic processes. *The Journal of Geology* **68**, 54–74.

Wood, D.M. (1990). *Soil Behaviour and Critical State Soil Mechanics*. Cambridge University Press, Cambridge, UK. 462 pp.

Wu, T.H. (1976). *Investigation of Landslides on Prince of Wales Island*. Columbus, Ohio State University, USA. 94 pp.

Wu, T.H, McKinnell, W.P. & Swanston, D.N. (1979). Strength of tree roots and landslides on Prince of Wales Island, Alaska. *Canadian Geotechnical Journal* **16**, 19–33.

Wynn, T.M. & Utley, B.C. (2011). Quantifying fluvial erosion over short time-scales. *International Symposium on Erosion and Landscape Evolution (ISELE)*, 18-21 September 2011, Anchorage, Alaska.

Young, A. (1975). *Slopes*. Longman Inc., New York, USA. 288 pp.

APPENDIX

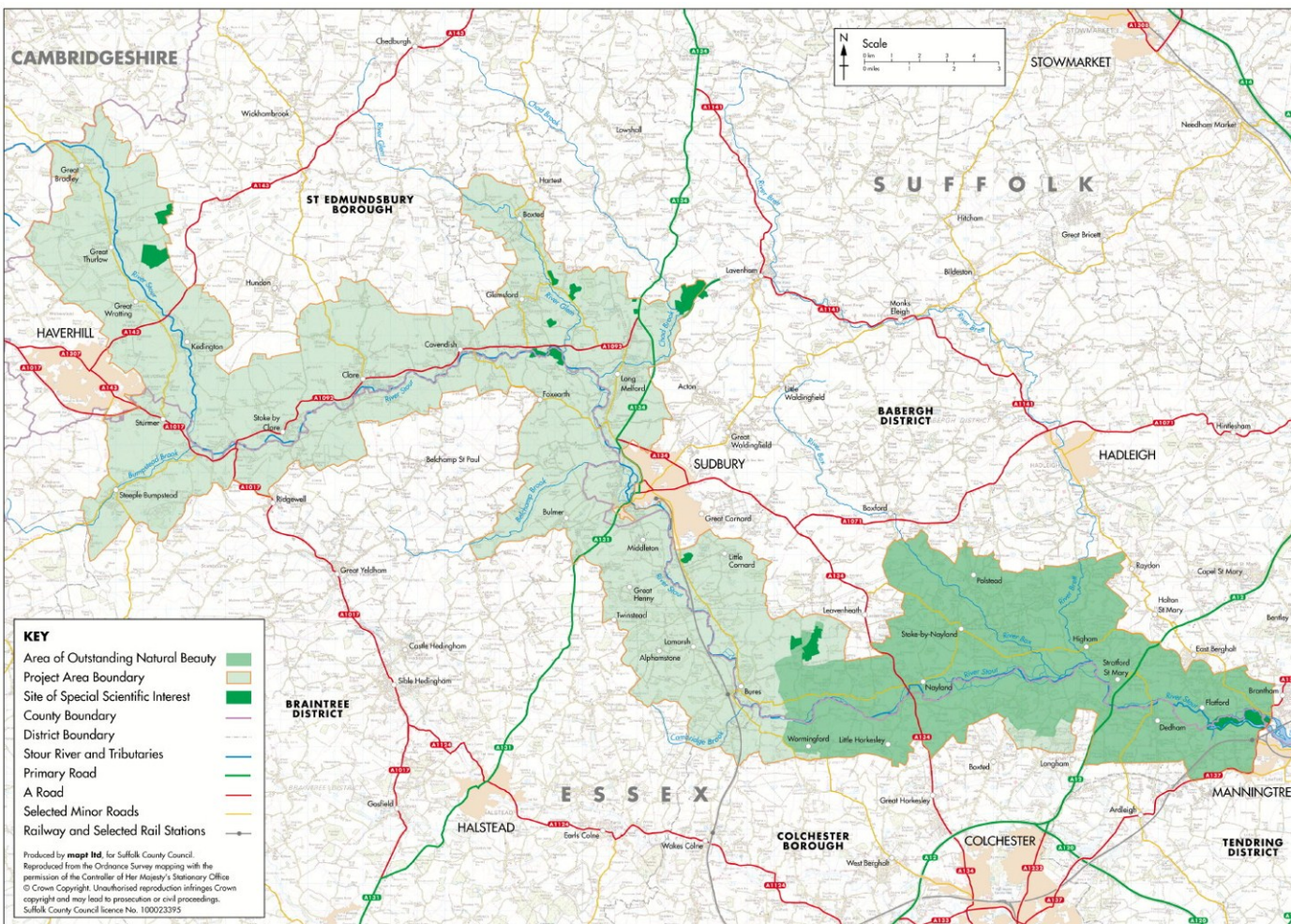


Fig. 3.1.A Stour Valley Map picturing the protected areas and the main settlements along the River Stour (© Map Ltd., Suffolk County Council and Ordnance Survey, Crown copyright).

Table 3.2(A) *Texture type, specific surface area (g/m²), percentile readings (μm) and percentage of clay, silt and sand particles.*

Field site	Texture type	Spec. surface area	d (0.1)	d (0.5)	d (0.9)	Clay (%)	Silt (%)	Sand (%)
GB1-1A	Sandy silt loam	0.17	4.80	34.82	252.47	0.63	60.35	39.02
GB1-1B	Sandy loam	0.11	6.41	215.62	667.53	0.60	36.40	62.99
GB1-1C	Sandy silt loam	0.17	4.31	42.70	263.75	1.84	57.03	41.13
GB1-2A	Sandy loam	0.13	5.48	106.08	465.84	0.85	43.31	55.84
GB1-2B	Sand	0.03	53.82	352.02	640.15	0.12	10.38	89.49
GB1-2C	Loamy sand	0.09	7.37	370.01	883.85	0.89	23.63	75.48
GB1-3A	Sandy loam	0.08	9.09	190.72	534.10	0.45	30.26	69.29
GB1-3B	Sandy loam	0.11	6.52	97.33	415.36	0.49	42.57	56.94
GB1-3C	Sandy loam	0.08	9.81	102.09	416.18	0.09	41.65	58.26
GB2-1A	Sandy silt loam	0.30	2.98	12.19	213.12	2.97	75.55	21.48
GB2-1B	Sandy silt loam	0.16	4.52	52.46	415.15	1.56	51.34	47.09
GB2-1C	Sandy silt loam	1.32	1.22	7.73	341.31	16.28	60.82	22.90
GB2-2A	Sandy loam	0.11	6.04	145.03	615.10	0.83	36.73	62.45
GB2-2B	Sandy silt loam	0.18	4.21	34.58	288.86	1.59	62.43	35.98
GB2-2C	Sandy silt loam	0.22	3.58	24.74	232.45	2.51	73.58	23.91
GB2-3A	Sandy silt loam	0.24	3.37	19.29	247.41	2.31	68.41	29.28
GB2-3B	Silt loam	0.30	3.05	12.04	252.52	2.84	77.78	19.38
GB2-3C	Sandy silt loam	0.83	1.71	8.91	283.25	12.59	61.74	25.67
GB3-1A	Sandy loam	0.11	7.05	93.37	519.70	0.55	42.20	57.25
GB3-1B	Sandy loam	0.14	5.40	65.74	689.66	0.73	48.56	50.71
GB3-1C	Sandy loam	0.10	7.21	118.37	678.00	0.65	36.77	62.59
GB3-2A	Sandy loam	0.11	6.86	94.61	713.07	0.59	42.27	57.14
GB3-2B	Sandy silt loam	0.15	4.88	58.91	371.37	1.27	49.59	49.14
GB3-2C	Sandy loam	0.12	5.86	116.62	427.32	0.81	40.08	59.10
GB3-3A	Silt loam	0.31	2.92	11.43	148.05	3.24	79.30	17.45
GB3-3B	Sandy silt loam	0.16	4.62	46.37	317.45	1.22	54.54	44.24
GB3-3C	Sand	0.04	34.56	303.41	597.05	0.15	13.46	86.39
LB1-1A	Silt loam	0.35	2.73	8.99	61.01	3.61	86.61	9.78
LB1-1B	Sandy silt loam	0.20	3.59	54.11	360.61	2.30	48.99	48.71
LB1-1C	Sandy silt loam	2.28	0.30	60.87	355.66	13.03	37.35	49.62
LB1-2A	Sandy silt loam	0.15	5.11	40.23	321.69	0.73	58.89	40.38
LB1-2B	Sandy silt loam	0.29	2.96	14.36	223.70	3.25	69.02	27.73
LB1-2C	Sandy silt loam	0.12	5.76	134.39	424.68	1.21	38.93	59.86
LB1-3A	Sandy silt loam	0.18	4.27	35.46	300.90	1.13	57.48	41.40
LB1-3B	Silt loam	0.35	2.69	9.29	96.10	3.96	83.09	12.95
LB1-3C	Sandy silt loam	0.21	3.69	23.82	364.30	1.70	63.97	34.33

Table 3.2(A) - Continued

Field site	Texture type	Spec. surface area	d (0.1)	d (0.5)	d (0.9)	Clay (%)	Silt (%)	Sand (%)
LB2-1A	Sandy loam	0.10	7.38	147.68	450.56	0.55	34.92	64.53
LB2-1B	Sandy loam	0.10	6.89	155.66	431.59	0.55	35.68	63.77
LB2-1C	Sandy loam	0.12	5.63	138.98	422.31	0.80	38.73	60.48
LB2-2A	Sandy silt loam	0.10	7.18	155.17	453.55	0.62	34.78	64.59
LB2-2B	Sandy silt loam	0.11	6.74	95.66	402.68	0.68	41.47	57.84
LB2-2C	Loamy sand	0.06	16.53	137.59	376.56	0.30	27.63	72.07
LB2-3A	Loamy sand	0.05	18.68	163.22	426.75	0.16	23.51	76.33
LB2-3B	Loamy sand	0.06	15.20	199.24	492.57	0.33	22.09	77.58
LB2-3C	Sand	0.04	28.22	209.47	413.18	0.16	13.41	86.43
C1-1A	Sandy silt loam	0.12	6.97	41.95	265.06	0.17	59.29	40.54
C1-1B	Sandy silt loam	0.14	5.33	60.75	345.60	0.76	49.69	49.55
C1-1C	Sandy silt loam	0.21	3.90	24.57	258.97	1.54	66.21	32.25
C1-2A	Sandy loam	0.10	7.78	69.65	322.71	0.21	47.95	51.84
C1-2B	Sandy silt loam	0.20	4.16	23.11	238.51	1.20	68.40	30.39
C1-2C	Sandy silt loam	0.20	4.07	28.70	187.30	1.60	66.86	31.55
C1-3A	Loamy sand	0.05	21.66	211.24	523.62	0.16	18.57	81.27
C1-3B	Loamy sand	0.06	12.98	237.21	527.22	0.32	22.82	76.86
C1-3C	Sandy silt loam	0.19	3.96	32.31	266.63	1.55	60.65	37.79
C2-1A	Sandy loam	0.10	7.66	123.78	527.59	0.53	38.41	61.06
C2-1B	Silt loam	0.27	3.19	15.24	81.23	2.68	83.05	14.27
C2-1C	Sandy loam	0.11	7.03	109.81	436.87	0.65	40.09	59.26
C2-2A	Sandy silt loam	0.13	6.01	53.28	293.25	0.62	52.88	46.50
C2-2B	Loamy sand	0.24	3.57	18.95	95.68	2.03	80.22	17.76
C2-2C	Sandy silt loam	0.20	4.17	25.12	249.32	1.22	68.94	29.84
C2-3A	Sandy loam	0.09	8.51	118.20	398.94	0.41	37.68	61.91
C2-3B	Silt loam	0.30	2.96	13.04	78.91	3.36	83.50	13.14
C2-3C	Sandy silt loam	0.14	5.28	47.55	534.94	0.71	54.18	45.11
S1-1A	Sandy silt loam	0.18	4.88	24.71	132.18	0.42	74.08	25.50
S1-1B	Sandy silt loam	0.21	3.88	22.20	168.69	1.43	70.86	27.71
S1-1C	Sandy silt loam	0.24	3.52	19.23	202.10	2.07	71.89	26.04
S1-1D	Loamy sand	0.07	15.35	209.73	502.61	0.61	25.13	74.26
S1-2A	Sandy silt loam	0.15	5.92	28.74	140.30	0.20	72.41	27.39
S1-2B	Sandy silt loam	0.13	6.11	49.13	291.34	0.43	55.46	44.11
S1-2C	Sandy loam	0.16	4.60	65.41	205.41	1.37	47.70	50.94
S1-2D	Sandy loam	0.09	9.19	177.79	604.92	0.87	32.52	66.61

Fig. 3.3(A) Historical maps sequences (Maps downloaded from ©Crown Copyright/database right 2008. An Ordnance Survey/EDINA supplied service.)

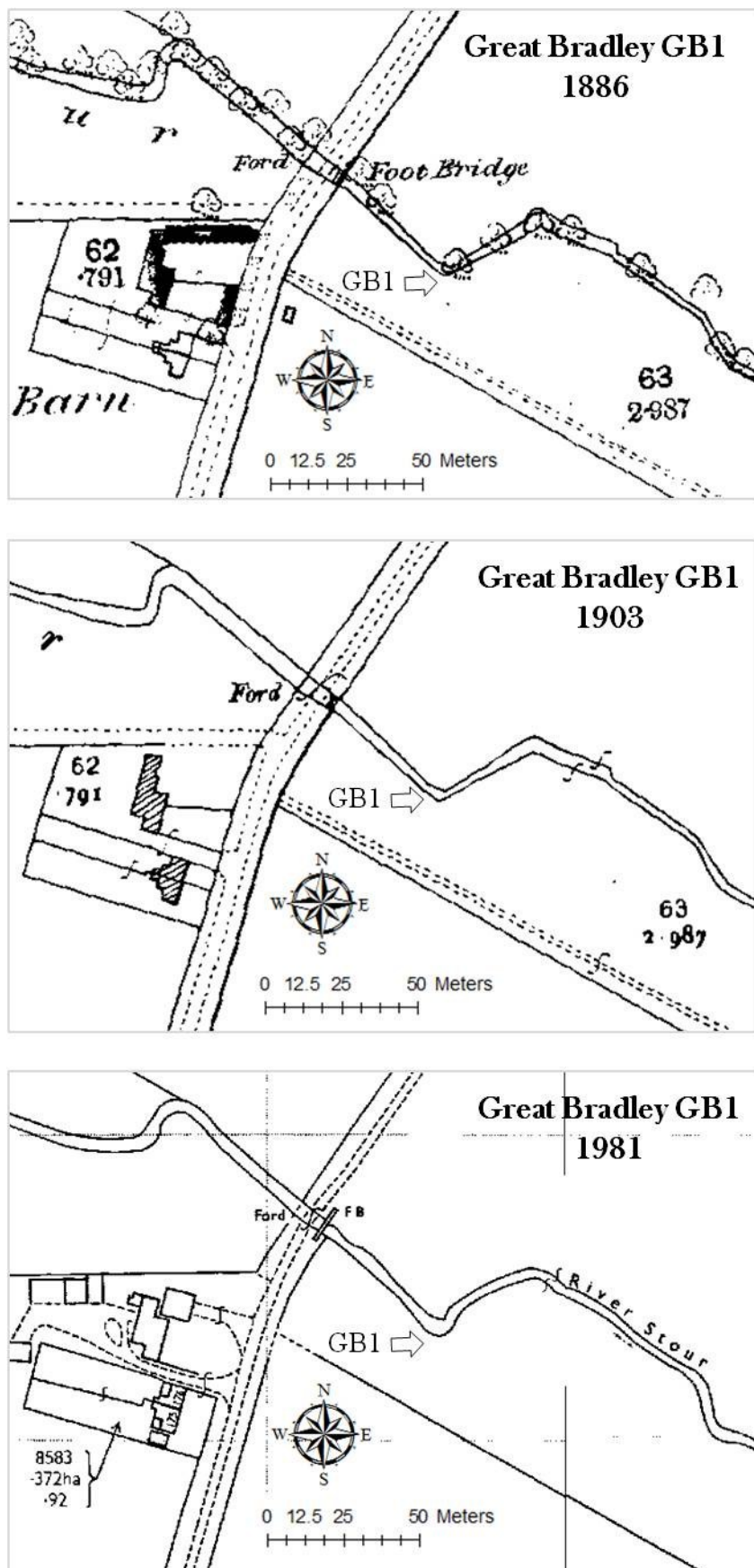


Fig. 3.3(A) *Continued*

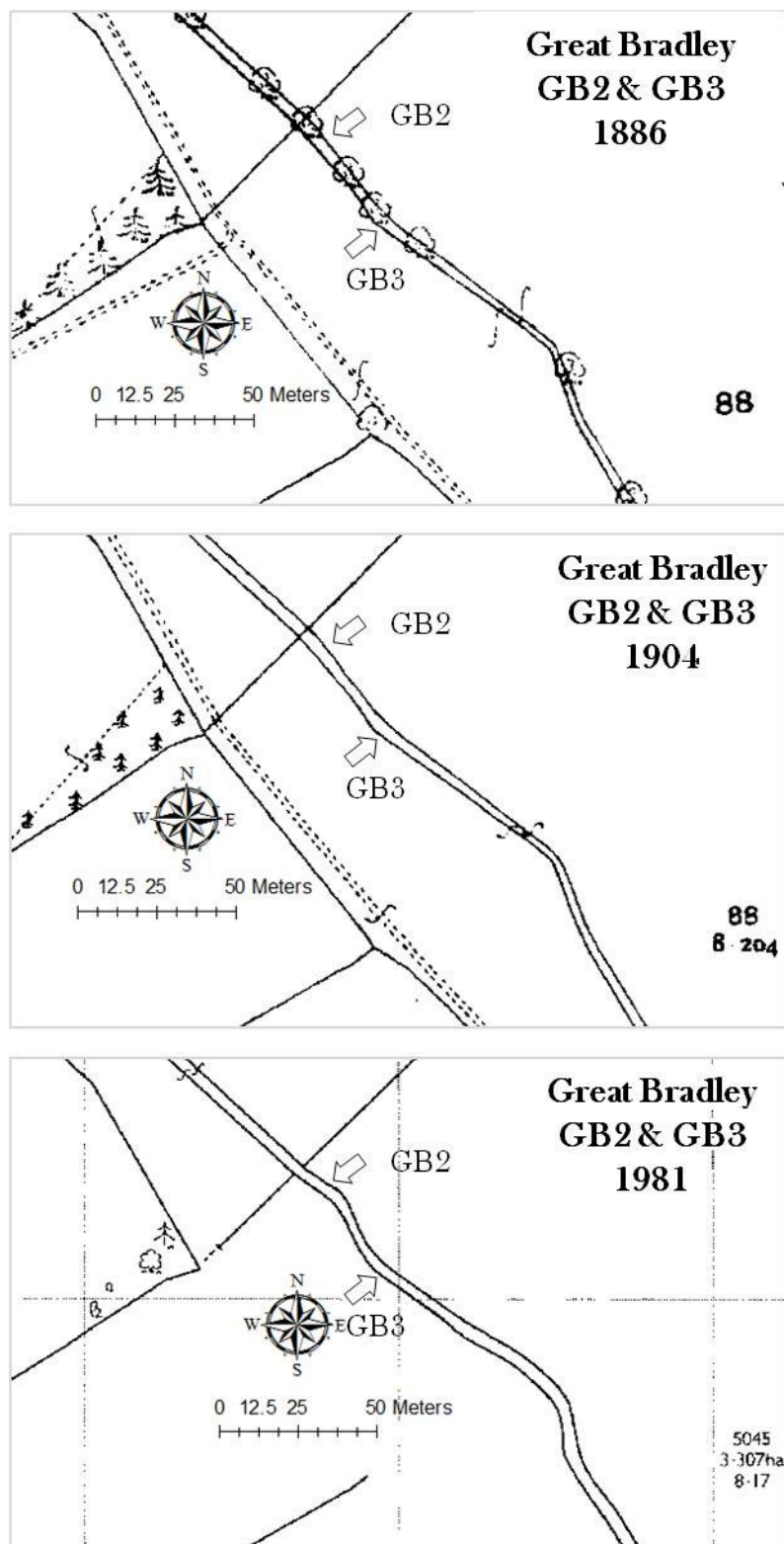


Fig. 3.3(A) *Continued*

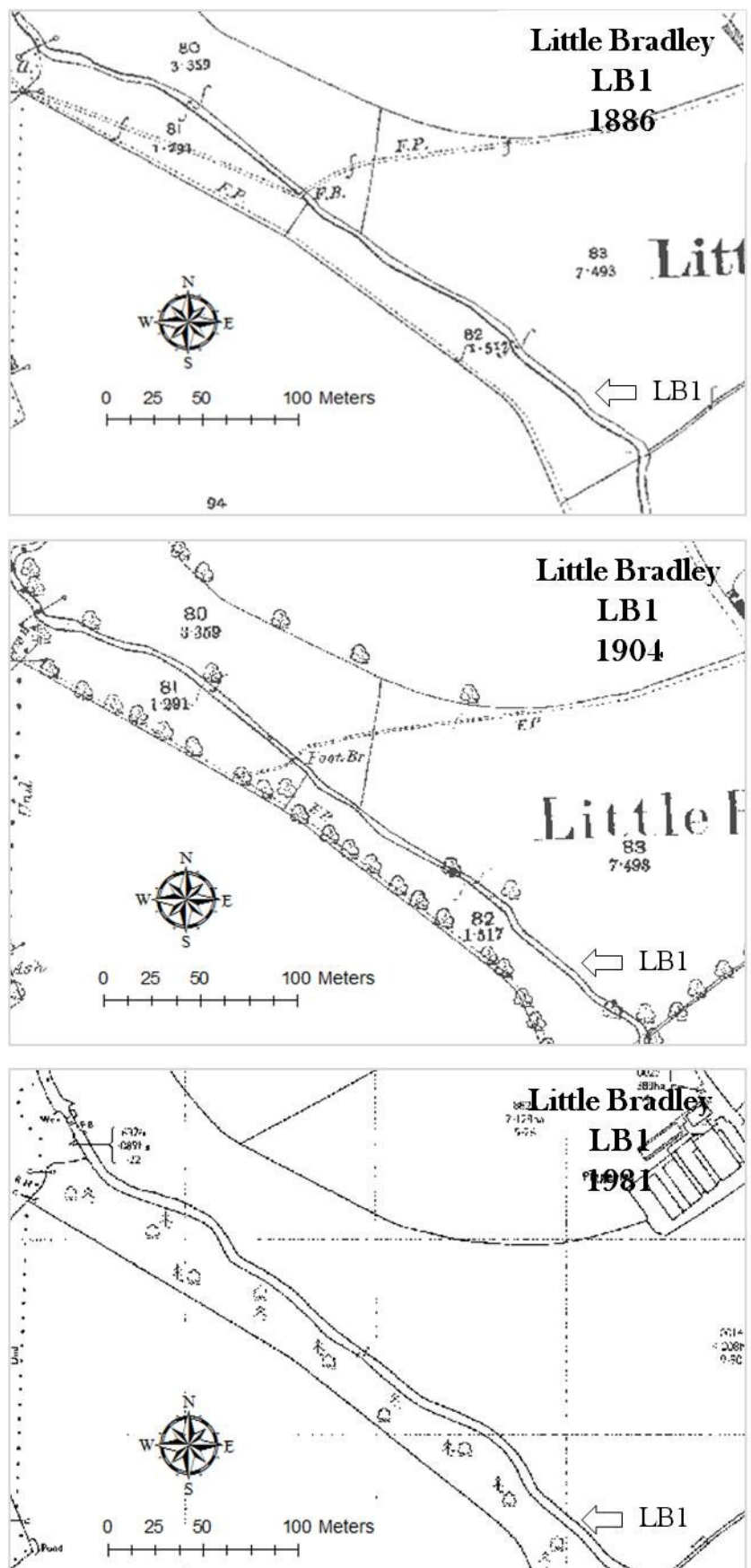


Fig. 3.3(A) *Continued*

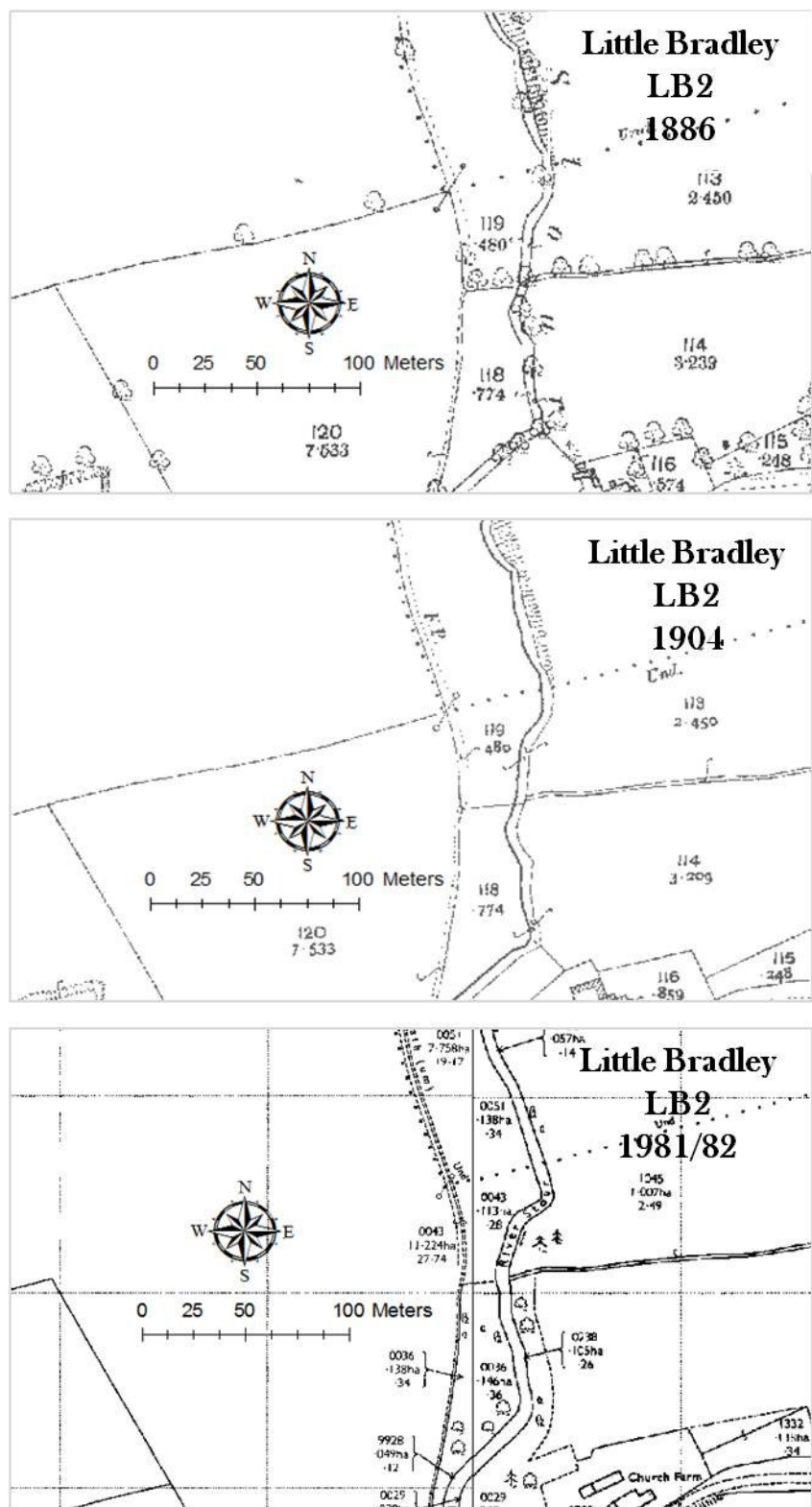


Fig. 3.3(A) *Continued*

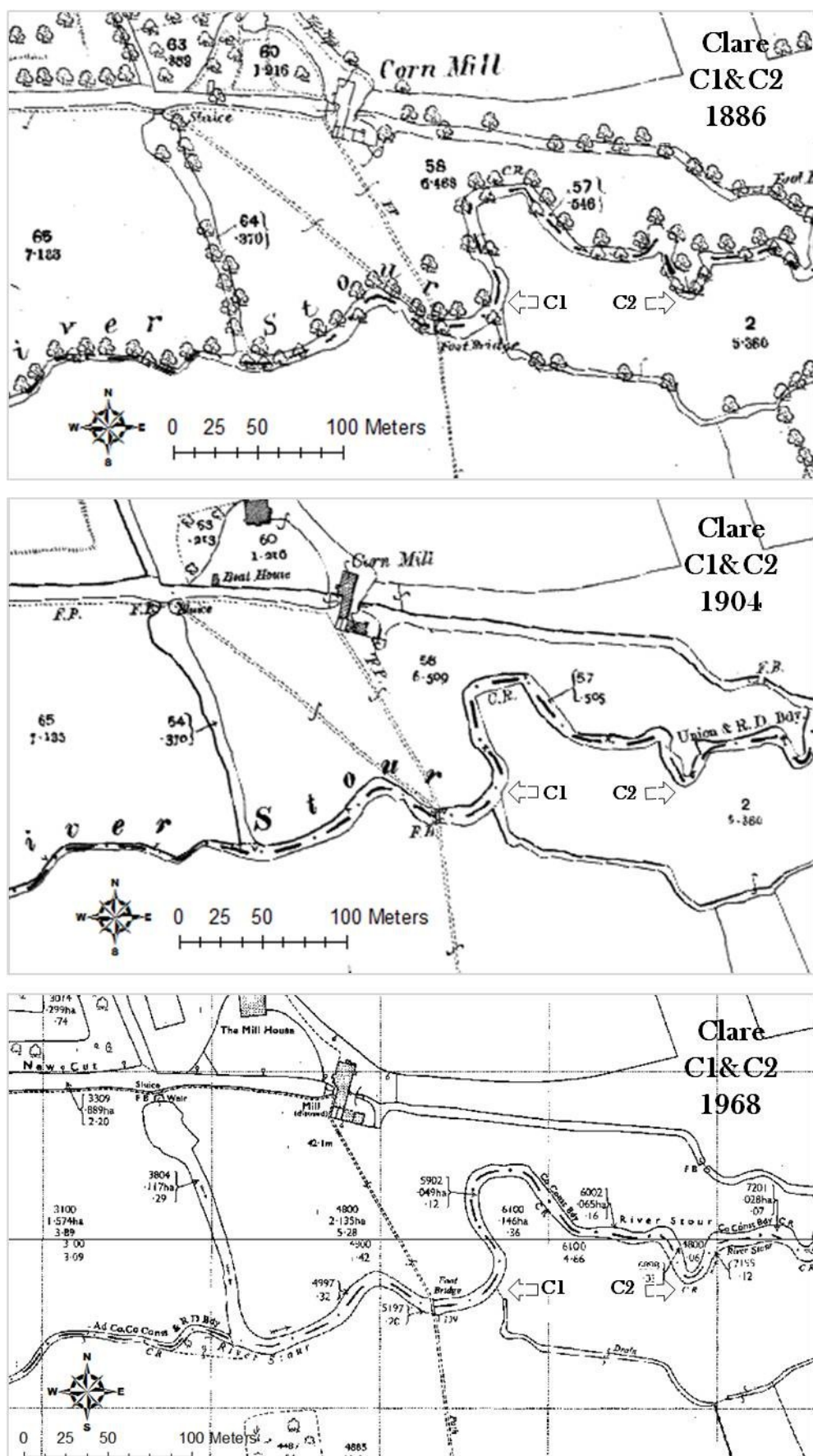


Fig. 3.3(A) *Continued*

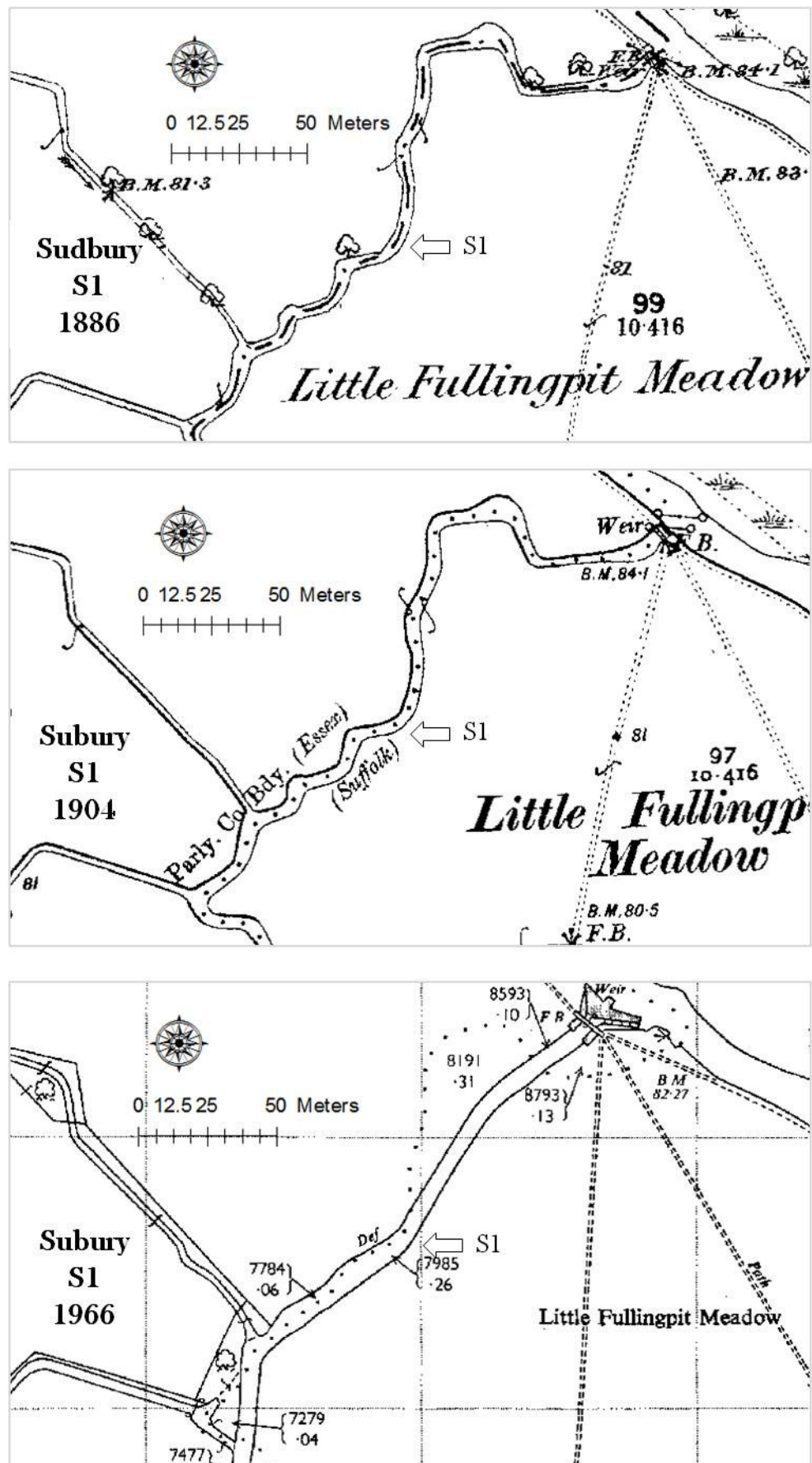


Fig. 3.3(A) *Continued*

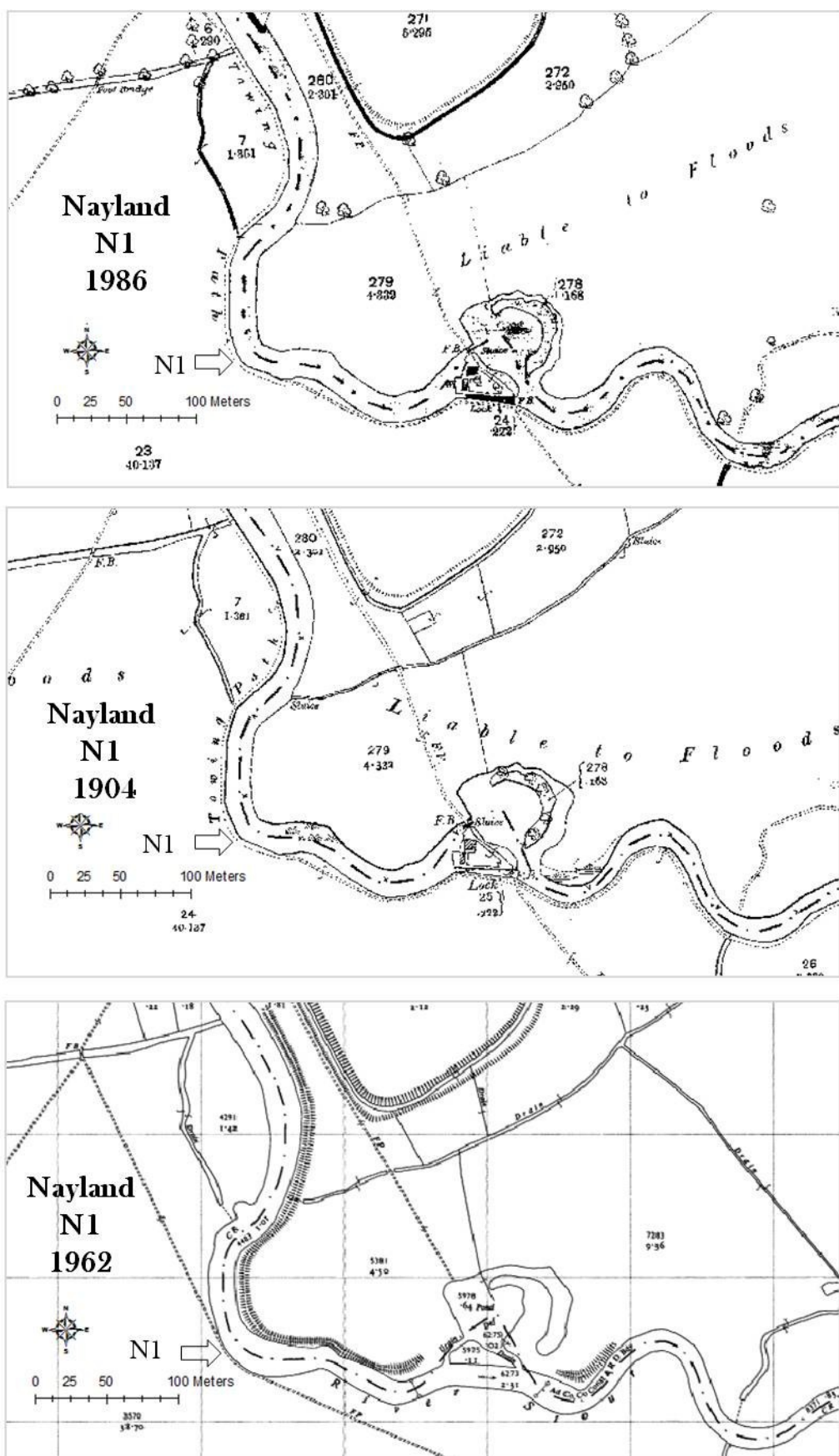


Table 3.4(A) Pin readings, the length of the measurement period in days, total cumulative erosion and ratios of cumulative erosion/number of days and cumulative erosion/years. A, B and C are the sections of the bank where A is the top of the bank face, B is the mid part and C is the lower part/bank foot. Negative readings indicate sedimentation or accumulation of material fallen from above.

Site	Pin	Section of the bank	Days with data	Total cumulative erosion (cm)	Cumulative erosion/number of days (mm)	Cumulative erosion/number of years (cm)
GB1	GB1-1A	A	673	25.7	0.38	13.94
	GB1-1B	B	673	12.8	0.19	6.94
	GB1-1C	C	673	8.5	0.13	4.61
	GB1-2A	A	791	-1	-0.01	-0.46
	GB1-2B	B	791	54	0.68	24.92
	GB1-2C	C	1247	49.5	0.40	14.49
	GB1-3A	A	1247	3	0.02	0.88
	GB1-3B	B	Lost	-	-	-
	GB1-3C	C	Lost	-	-	-
GB2	GB2-1B	B	911	5.64	0.06	2.26
	GB2-1C	C	911	10.35	0.11	4.15
	GB2-1/2B	B	911	8.98	0.10	3.60
	GB2-1/2C	C	911	12.7	0.14	5.09
	GB2-2A	A	553	3	0.05	1.98
	GB2-2B	B	315	5	0.16	5.79
	GB2-2C	C	911	8.7	0.10	3.49
	GB2-2Cex	C	553	21.7	0.39	14.32
	GB2-2/3B	B	553	13.4	0.24	8.91
	GB2-2/3C	C	673	11.7	0.17	6.35
	GB2-3B	B	673	18.4	0.27	9.98
	GB2-3C	C	673	10.5	0.16	5.69
GB3	GB3-1A	A	1023	31	0.30	11.06
	GB3-1B	B	350	0	0.00	0.00
	GB3-1C	C	350	5	0.14	5.21
	GB3-2A	A	1226	3	0.02	0.89
	GB3-2B	B	1226	9.5	0.08	2.83
	GB3-2C	C	1226	9.5	0.08	2.83
	GB3-3A	A	Lost	-	-	-
	GB3-3B	B	673	-1.4	-0.02	-0.76
	GB3-3C	C	673	39.5	0.59	21.42

Table 3.4(A) *Continued*

Site	Pin	Section of the bank	Days with data	Total cumulative erosion (cm)	Cumulative erosion/number of days (mm)	Cumulative erosion/number of years (cm)
LB1	LB1-1A	A	1050	25.5	0.24	8.86
	LB1-1B	B	1050	10.6	0.10	3.68
	LB1-1C	C	1050	-2.4	-0.02	-0.83
	LB1-1Cex	C	1050	-0.2	0.00	-0.07
	LB1-2A	A	1050	19.7	0.19	6.85
	LB1-2B	B	1050	17.9	0.17	6.22
	LB1-2C	C	1050	16.2	0.15	5.63
	LB1-3B	B	1050	28.2	0.27	9.80
	LB1-3C	C	1050	26.5	0.25	9.21
	LB1-4B	B	1050	19.2	0.18	6.67
	LB1-4C	C	1050	27.8	0.26	9.66
	LB1-5B	B	1050	25	0.24	8.69
	LB1-5C	C	1050	35	0.33	12.17
LB2	LB2-1A	A	1050	17	0.16	5.91
	LB2-1B	B	619	-1	-0.02	-0.59
	LB2-1C	C	1050	21.5	0.20	7.47
	LB2-2A	A	1050	4	0.04	1.39
	GB2-2B	B	619	-0.5	-0.01	-0.29
	GB2-2C	C	619	11	0.18	6.49
C1	C1-1A	A	287	0.5	0.02	0.64
	C1-1B	B	987	12.4	0.13	4.59
	C1-1C	C	952	11.15	0.12	4.27
	C1-1D	C	952	9.95	0.10	3.81
	C1-1E	C	643	10.95	0.17	6.22
	C1-2A	A	610	1	0.02	0.60
	C1-2B	B	994	10.9	0.11	4.00
	C1-2C	C	994	14.65	0.15	5.38
	C1-2D	C	952	9.5	0.10	3.64
	C1-2E	C	776	7.6	0.10	3.57
	C1-3A	A	1099	17.45	0.16	5.80
	C1-3B	B	1099	15.35	0.14	5.10
	C1-3C	C	1099	13.2	0.12	4.38
	C1-3D	C	952	4.35	0.05	1.67
	C1-4A	A	1155	28.1	0.24	8.88
	C1-4R	B	959	16.7	0.17	6.36
	C1-4B	B	1155	21.3	0.18	6.73
	C1-4C	C	1155	16.7	0.14	5.28
	C1-4D	C	959	9.6	0.10	3.65

Table 3.4(A) *Continued*

Site	Pin	Section of the bank	Days with data	Total cumulative erosion (cm)	Cumulative erosion/number of days (mm)	Cumulative erosion/number of years (cm)
C1	C1-5A	A	1155	21.5	0.19	6.79
	C1-5R	B	959	12.4	0.13	4.72
	C1-5B	B	1155	16.7	0.14	5.28
	C1-5C	C	1155	17.9	0.15	5.66
	C1-5D	C	Lost	-	-	-
	C1-6A	A	1155	11.15	0.10	3.42
	C1-6R	B	959	5	0.05	1.90
	C1-6B	B	1155	7.8	0.07	2.46
	C1-6C	C	1155	27.6	0.24	8.72
	C1-6D	C	Lost	-	-	-
C2	C2-1A	A	206	0.5	0.02	0.89
	C2-1B	B	470	23	0.49	17.86
	C2-1C	C	525	-3	-0.06	-2.09
	C2-2A	A	729	17	0.23	8.51
	C2-2B	B	729	1	0.01	0.50
	C2-2C	C	Lost	-	-	-
	C2-3A	A	Lost	-	-	-
	C2-3B	B	319	18	0.56	20.60
	C2-3C	C	319	26	0.82	29.75
	C2-3D	C	319	-3	-0.09	-3.43
	C2-4A	A	207	6	0.29	10.58
	C2-4B	B	319	21	0.66	24.03
S1	C2-4C	C	207	10	0.48	17.63
	C2-4D	C	188	-1	-0.05	-1.94
	S1-1A	A	241	1.5	0.06	2.27
	S1-1B	B	241	8.9	0.37	13.48
	S1-1C	C	241	4.4	0.18	6.66
	S1-1D	C	241	2.8	0.12	4.24
	S1-2A	A	78	0	0.00	0.00
	S1-2B	B	78	0.14	0.02	0.66
	S1-2C	C	78	0.55	0.07	2.57
	S1-2D	C	78	6.5	0.83	30.42

Table 3.5(A) The length of monitoring period at each pin and number of days the field site was exposed to discharges higher than Q_{10} and higher than effective discharges. Q_{Eff} was for GB and LB sites $0.53 \text{ m}^3/\text{s}$, for C sites $1.73 \text{ m}^3/\text{s}$ and for S1 $2.672 \text{ m}^3/\text{s}$.

Pin	Start	Q_{10} (days)	Q_{10} (%)	Q_{Eff} (days)	Q_{Eff} (%)	$T_{E>Q_{Eff}}$ m^3/s (days)	$T_{E>Q_{Eff}}$ (%)
GB1-1A	17/5/08	31	4.61	255	37.89	-	-
GB1-1B	17/5/08	31	4.61	255	37.89	-	-
GB1-1C	17/5/08	31	4.61	255	37.89	-	-
GB1-2A	21/10/06	63	5.05	397	31.84	-	-
GB1-2B	21/10/06	63	5.05	397	31.84	-	-
GB1-2C	21/10/06	63	5.05	397	31.84	-	-
GB1-3A	21/10/06	63	5.05	397	31.84	-	-
GB1-3B	21/10/06	63	5.05	397	31.84	-	-
GB1-3C	21/10/06	63	5.05	397	31.84	-	-
GB2-1B	22/9/07	43	4.72	305	33.48	116	12.73
GB2-1C	22/9/07	43	4.72	305	33.48	116	12.73
GB2-1/2B	22/9/07	43	4.72	305	33.48	116	12.73
GB2-1/2C	22/9/07	43	4.72	305	33.48	116	12.73
GB2-2A	11/11/06	63	5.14	396	32.30	127	10.36
GB2-2B	11/11/06	63	5.14	396	32.30	127	10.36
GB2-2C	22/9/07	43	4.72	305	33.48	116	12.73
GB2-2Cex	11/11/06	63	5.14	396	32.30	127	10.36
GB2-2/3B	17/5/08	31	4.61	255	37.89	113	16.79
GB2-2/3C	17/5/08	31	4.61	255	37.89	113	16.79
GB2-3B	17/5/08	31	4.61	255	37.89	113	16.79
GB2-3C	17/5/08	31	4.61	255	37.89	113	16.79
GB3-1A	2/6/07	46	4.50	317	30.99	116	11.34
GB3-1B	2/6/07	46	4.50	317	30.99	116	11.34
GB3-1C	2/6/07	46	4.50	317	30.99	116	11.34
GB3-2A	11/11/06	63	5.14	396	32.30	127	10.36
GB3-2B	11/11/06	63	5.14	396	32.30	127	10.36
GB3-2C	11/11/06	63	5.14	396	32.30	127	10.36
GB3-3A	17/5/08	31	4.61	255	37.89	113	16.79
GB3-3B	17/5/08	31	4.61	255	37.89	113	16.79

Table 3.5(A) *Continued*

Pin	Start	Q ₁₀ (days)	Q ₁₀ (%)	Q _{Eff} (days)	Q _{Eff} (%)	T _{E>Qeff} m ³ /s (days)	T _{E>Qeff} (%)
GB3-3C	17/5/08	31	4.61	255	37.89	113	16.79
LB1-1A	2/6/07	46	4.38	317	30.19	116	11.05
LB1-1B	2/6/07	46	4.38	317	30.19	116	11.05
LB1-1C	2/6/07	46	4.38	317	30.19	116	11.05
LB1-1Cex	2/6/07	46	4.38	317	30.19	116	11.05
LB1-2A	2/6/07	46	4.38	317	30.19	116	11.05
LB1-2B	2/6/07	46	4.38	317	30.19	116	11.05
LB1-2C	2/6/07	46	4.38	317	30.19	116	11.05
LB1-3B	2/6/07	46	4.38	317	30.19	116	11.05
LB1-3C	2/6/07	46	4.38	317	30.19	116	11.05
LB1-4B	2/6/07	46	4.38	317	30.19	116	11.05
LB1-4C	2/6/07	46	4.38	317	30.19	116	11.05
LB1-5B	2/6/07	46	4.38	317	30.19	116	11.05
LB1-5C	2/6/07	46	4.38	317	30.19	116	11.05
LB1-6B	2/6/07	46	4.38	317	30.19	116	11.05
LB1-6C	2/6/07	46	4.38	317	30.19	116	11.05
LB2-1A	2/6/07	46	4.38	317	30.19	116	11.05
LB2-1B	2/6/07	46	4.38	317	30.19	116	11.05
LB2-1C	2/6/07	46	4.38	317	30.19	116	11.05
LB2-2A	2/6/07	46	4.38	317	30.19	116	11.05
LB2-2B	2/6/07	46	4.38	317	30.19	116	11.05
LB2-2C	2/6/07	46	4.38	317	30.19	116	11.05
C1-1A	23/9/06	131	12.56	211	20.23	0	0.00
C1-1B	23/9/06	131	12.56	211	20.23	0	0.00
C1-1C	28/10/06	130	12.90	209	20.73	0	0.00
C1-1D	28/10/06	130	12.90	209	20.73	0	0.00
C1-1E	2/9/07	130	18.60	209	29.90	0	0.00
C1-2A	16/9/06	131	12.48	211	20.10	0	0.00
C1-2B	16/9/06	131	12.48	211	20.10	0	0.00
C1-2C	16/9/06	131	12.48	211	20.10	0	0.00
C1-2D	28/10/06	130	12.90	209	20.73	0	0.00
C1-2E	22/4/07	90	10.82	148	17.79	0	0.00
C1-3A	3/6/06	131	11.34	213	18.44	11	0.95
C1-3B	3/6/06	131	11.34	213	18.44	11	0.95
C1-3C	3/6/06	131	11.34	213	18.44	11	0.95
C1-3D	28/10/06	130	12.90	209	20.73	0	0.00
C1-4A	3/6/06	131	11.34	213	18.44	11	0.95
C1-4R	16/12/06	121	12.62	191	19.92	0	0.00
C1-4B	3/6/06	131	11.34	213	18.44	11	0.95
C1-4C	3/6/06	131	11.34	213	18.44	11	0.95
C1-4D	16/12/06	131	13.66	213	22.21	11	1.15

Table 3.5(A) *Continued*

Pin	Start	Q ₁₀ (days)	Q ₁₀ (%)	Q _{Eff} (days)	Q _{Eff} (%)	T _{E>Qeff} m ³ /s (days)	T _{E>Qeff} (%)
C1-5A	3/6/06	131	11.34	213	18.44	11	0.95
C1-5R	16/12/06	131	13.66	213	22.21	11	1.15
C1-5B	3/6/06	131	11.34	213	18.44	11	0.95
C1-5C	3/6/06	131	11.34	213	18.44	11	0.95
C1-5D	16/12/06	131	13.66	213	22.21	11	1.15
C1-6A	3/6/06	131	11.34	213	18.44	11	0.95
C1-6R	16/12/06	131	13.66	213	22.21	11	1.15
C1-6B	3/6/06	131	11.34	213	18.44	11	0.95
C1-6C	3/6/06	131	11.34	213	18.44	11	0.95
C1-6D	16/12/06	131	13.66	213	22.21	11	1.15
C2-1A	2/5/06	85	11.38	137	18.34	11	1.47
C2-1B	2/5/06	85	11.38	137	18.34	11	1.47
C2-1C	2/5/06	85	11.38	137	18.34	11	1.47
C2-2A	2/5/06	85	11.38	137	18.34	11	1.47
C2-2B	2/5/06	85	11.38	137	18.34	11	1.47
C2-2C	2/5/06	85	11.38	137	18.34	11	1.47
C2-3A	12/12/06	74	14.15	112	21.41	0	0.00
C2-3B	12/12/06	74	14.15	112	21.41	0	0.00
C2-3C	12/12/06	74	14.15	112	21.41	0	0.00
C2-3D	12/12/06	74	14.15	112	21.41	0	0.00
C2-4A	12/12/06	74	14.15	112	21.41	0	0.00
C2-4B	12/12/06	74	14.15	112	21.41	0	0.00
C2-4C	12/12/06	74	14.15	112	21.41	0	0.00
C2-4D	22/4/07	43	10.97	67	17.09	0	0.00
S1-1A	23/5/09	15	6.22	16	6.64	0	0.00
S1-1B	23/5/09	15	6.22	16	6.64	0	0.00
S1-1C	23/5/09	15	6.22	16	6.64	0	0.00
S1-1D	23/5/09	15	6.22	16	6.64	0	0.00
S1-2A	23/5/09	15	6.22	16	6.64	0	0.00
S1-2B	23/5/09	15	6.22	16	6.64	0	0.00
S1-2C	23/5/09	15	6.22	16	6.64	0	0.00
S1-2D	23/5/09	15	6.22	16	6.64	0	0.00